Distribution, identity and putative function of fibroblast growth factor 10 expressing cells in the developing and adult mouse brain

A thesis submitted to the University of East Anglia for the degree of Doctor of Philosophy

by

Niels Haan

April 2012

Abstract

Neural stem cells in the adult mammalian brain have been extensively studied and well characterised. However, apart from the classical stem cell niches of the lateral ventricle and the hippocampus, other brain areas, including the hypothalamus and amygdala, are potential novel stem cell niches. These areas have previously been found to express fibroblast growth factor 10 (Fgf10), known to maintain stem cell niches in other tissues. Here the hypothalamus and amygdala are investigated as potential novel neural stem cell niches, and the possibility of the olfactory bulb as the target of a putative migratory stream from the amygdala is assessed. Using a combination of immunohistochemistry, BrdU incorporation assays, genetic lineage tracing and in vitro cultures, the properties of Fgf10 expressing cells were examined. The Fgf10 expressing cells of the hypothalamus, the tanycytes, were found to express stem cell markers, and are capable of division in vivo. This stem cell niche was found to be generated during development and continues to be present into adulthood. Although proliferation is highest in the early post-natal period, it continues into later life. The $Fgf10^{+}$ lineage is able to generate neurons and glia both in vivo and in vitro. Given the location of newly generated $Fgf10^{+}$ lineage derived neurons in the hypothalamus, a function in control of energy balance seems likely. In contrast, in the amygdala $Fgf10^{+}$ cells do not appear to be stem cells, but mostly mature neurons. These do not express neural stem cell markers or incorporate BrdU. In the olfactory bulb, the majority of $Fgf10^{+}$ cells, which are found in all layers, are mature neurons, of both a glutamatergic and GABAergic phenotype. Although the function of Fgf10 in these brain areas is as yet unknown, it marks a diverse population of cells, and is a candidate molecule to fulfil a number of different functions in these cells.

Acknowledgements

First and foremost I must thank my supervisor, Mohammad K Hajihosseini for continued advice and support and for pushing me to achieve a great deal in my three years in Norwich. My secondary supervisors, Grant Wheeler and Uli Mayer, provided much useful input to my project.

I am grateful to the Anatomical Society of Great Britain and Ireland for providing the funding for this project.

In the lab, I must thank my Alaleh Najdi-Samiei for trustworthy and speedy genotyping and for making sure we always had ample supplies of anything we could think off, Christina Stratford and Irina Djacova for always being fun to be with and always willing to listen to me rant. Special thanks goes out to Timothy Goodman for being a good colleague, sounding board and for injecting what must at times have seemed millions of mice. Both in and out of the lab you have been great people to be with. I couldn't have asked for better people to work with.

Outside the UEA I sincerely thank Dr Saverio Bellusci for the $Fgf10^{CreERT2}$ mouse line, and Dr Natalie Bronstein for the custom Fgf10 antibody.

I would like to thank the Wheeler and Münsterberg lab members for never looking too bored during my lab meetings, and for always being fun company outside of the lab. The microscope support received from Paul Thomas and Alba Warn has always been useful. Special thanks goes out to the staff of the DMU, present and former, Simon Deakin, Rich Croft and Donna Hinds, for animal maintenance.

In the BMRC I would like to single out the Mogensen lab for special thanks, for putting up with me continuously using their Western equipment and for much help, support and company. The rest of the people in the BMRC, former and present, have always been good friends and colleagues, and always put up with me asking to 'borrow' things or annoying them with small talk and gossip when trying to avoid doing work. I hope I have on occasion been useful in return as well.

I must thank my parents and grandfather for financial support and apologize for seriously neglecting them whilst being all too busy in distant England.

My greatest thanks go out to Jenny, Rob and Sally, for being the best friends, drinking buddies, and support group I could have wished for. I couldn't have done it without you guys.

Index

List of figures

List of tables

Chapter 1

Introduction

1.1 - Adult neural stem cells

The adult brain is characterised by a large proportion of terminally differentiated cells, the neurons. These cells are incapable of cell division, and as such the adult brain is highly sensitive to insults causing cell death, such as neurodegenerative diseases such as Alzheimers and Parkinsons, or traumatic injuries such as ischemic stroke. For many years, the accepted view was that no stem cells exist in the adult brain, and that any cell loss was irreversible. However, as early as the 1960s this view began to change with the work of Robert Altman. In a series of experiments with radioactively labelled thymidine (^{3}H-thymidine) he undertook a search for dividing cells in the adult rodent brain. The first study to show cell division in the brain showed incorporation of ^{3}H-thymidine in the rat brain, indicative of cell division, following electrolytic lesions (Altman, 1962). Later, he showed constitutive cell division in the hippocampus (Altman and Das, 1965), cerebral cortex (Altman and Das, 1966) and olfactory bulb (Gould et al., 1999). An electron-microscopic analysis of these cells showed a neuronal morphology (Kaplan and Hinds, 1977). Apart from neurogenesis, adult formation of oligodendrocytes was reported by Paterson in 1973 (Paterson et al., 1973) and new astrocytes in the post-natal brain were found by Schmechel and Rakic in 1979 (Schmechel and Rakic, 1979). These findings were not widely accepted. It was only after the detection of seasonal adult neurogenesis in songbirds (Barnea and Nottebohm, 1994), (Alvarez-Buylla et al., 1988) that the question of adult stem cells in rodents came to the forefront again.

1.2 – Origin of adult neural stem cells

Current understanding of the adult neural stem cells suggest their origin is in fact during development. The formation of the subventricular zone (SVZ) is a prime example (fig 1.1). During embryonic neurogenesis, the primitive neuroepithelium forms the earliest

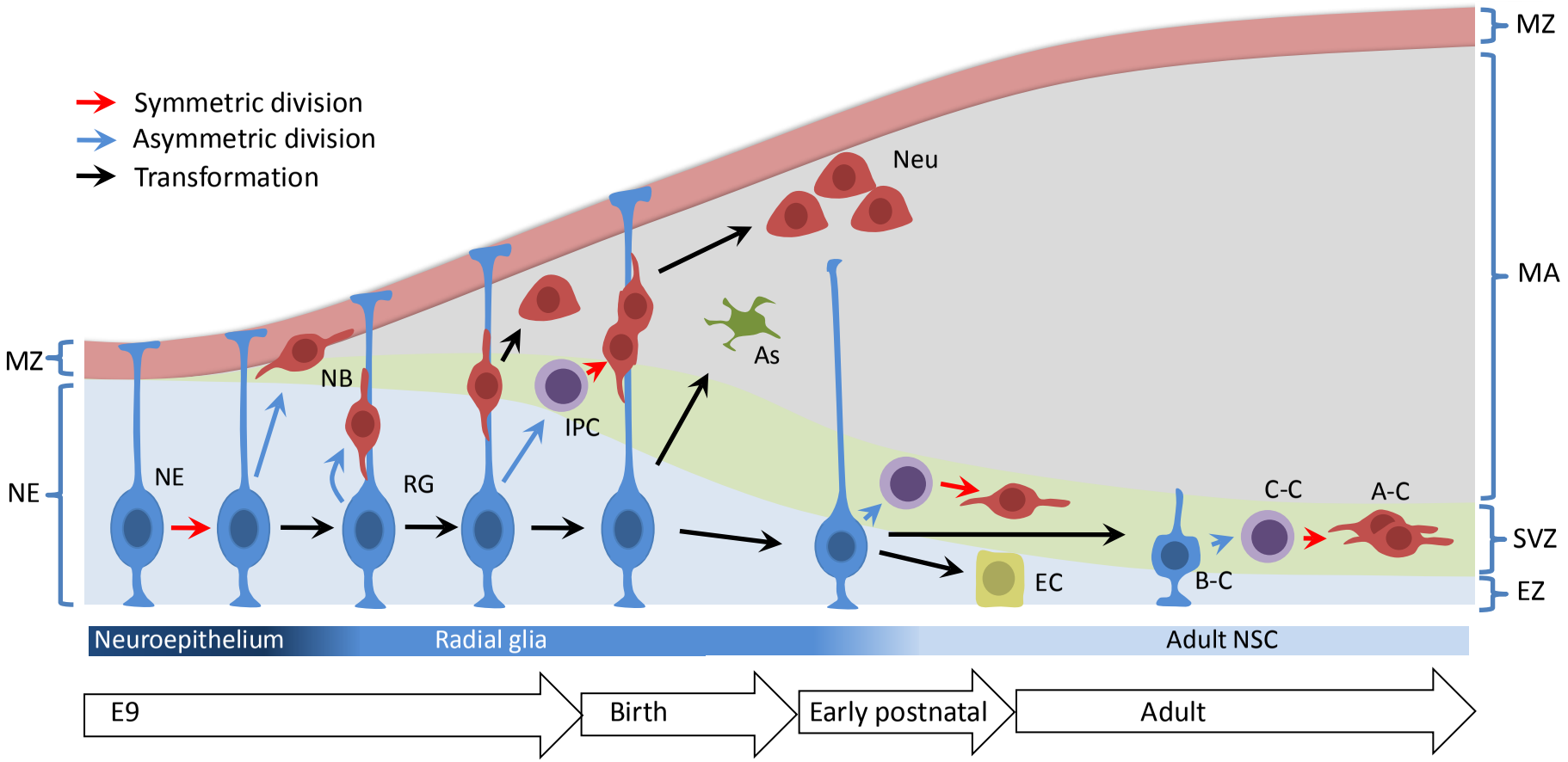

Fig 1.1- Development of the adult NSC lineage in the SVZ. Starting at E9 to E10, the neuroepithelial cells (NE) span the developing brain from ventricle to the marginal zone (MZ). They divide mostly symmetrically, greatly increasing number and area of future cortical cells. During this phase, early neuroblasts (NB) are produced by asymmetric division. By E11 to E12 the NE have transformed into radial glia, still spanning the width of the brain, which continue to generate neuroblasts, which then differentiate into mature neurons (NeuN). Later in development, rather than directly forming from the radial glia, neuroblasts are generated through intermediate progenitor cells (IPC). Around birth, a subset of the radial glia transforms into terminally differentiated astrocytes (As), some transform into ependymal cells (EC) and the remainder retract their processes to form the adult NCS, the B-cell (B-C). These continue to produce an intermediate progenitor, here named the transit amplifying cells, or C-cell. These then give rise to neuroblasts, or A-cells. Based on Kriegstein et al 2009

precursor population, these will then from the ventricular zone directly abutting the developing ventricles (fig 1.1), and later generate the subventricular zone cells. In these layers, the neuroepithelium has transformed into several cell types including radial glia. These cells, characterised by expression of both stem cells markers such as nestin and BLBP and glial markers such as GLAST are the neural stem cells during development. Their highly characteristic morphology consists of a cell body in the ventricular zone, with a small basal foot on the ventricular surface, and a long radial projection touching the outer, or marginal zone of the developing brain (see fig 1.1). Late during gestation and in the perinatal period, the ventricular zone is transformed into the ependymal surface layer which, at least in the SVZ, does not have stem cell potential (Charrier et al., 2006), and only the SVZ of the lateral ventricle and the dentate gyrus of the hippocampus remain as stem cell niches into adulthood. Although many of the embryonic radial glia transform into terminally differentiated astrocytes, it has been shown by viral lineage tracing the these cells are indeed the source of the adult neural stem cell, as they are capable in later life of generating all neural lineages (Merkle et al., 2004)

1.3. – Canonical niches for adult neural stem cells

Two well-described niches for adult neural stem cells are the subventricular zone (SVZ) of the lateral ventricle, and the subgranular zone (SGZ) of the hippocampal dentate gyrus.

1.3.1 Subventricular zone of the lateral ventricle

In the SVZ, the NSC niche is closely associated with the ventricular wall. The ventricle is lined with a single cell layer of ciliated ependymal cells, which form the barrier between the lumen of ventricle and the surrounding tissue. While it was known for a long time that

this area contained neural stem cells, for many years it was unknown whether these were the ependymal cells or some other cell type. However, most evidence now points to the fact that the ependymal cells themselves are not stem cells, but that the stem cells are closely associated with the ependyma. The actual stem cells are located in the cell layers directly adjacent to the ependymal layer and can have apical processes that extend to the lumen and contain a single cilium (Zhao et al., 2003). Three main cell types interact to make the SVZ NSC niche (see fig 1.2). The actual glial stem cells, usually called 'B-cells', are $GFAP^{+}$/$nestin^{+}$/$BLBP^{+}$ slowly dividing cells. These stem cells generate a more rapidly dividing transit amplifying cell, the 'C-cells' which are $GFAP^{-}$/$Dlx2^{+}$. These populations are not mutually exclusive, transit amplifying cells can be 'regressed' into multipotent stem cells by stimulation with EGF (Doetsch et al., 2002). The 'C-cells' then in turn produce the migratory neuroblasts, the $GFAP^{-}$/$Dlx2^{+}$/$doublecortin^{+}$ 'A-cells' which migrate to their destination to form new neurons.

The non-neurogenic terminally differentiated astrocytes in the niche are vital for niche maintenance. They envelop and contact all cell types in the niche (Seri et al 2004), stimulate neurogenesis (Lim and Alvarez-Buylla, 1999), and may facilitate signalling throughout the niche via gap junction coupling (Giaume and Venance, 1998). The ependymal cells, although not the stem cells they were once thought to be (Johansson et al., 1999), do play an important role in maintaining the stem cells niche by secreting the BMP antagonist noggin, preventing premature differentiation (Peretto et al., 2004), and the growth factor Fgf2 (Hayamizu et al., 2001). The entire niche is connected by specialised basal laminae known as fractones, extending from the local blood vessels,

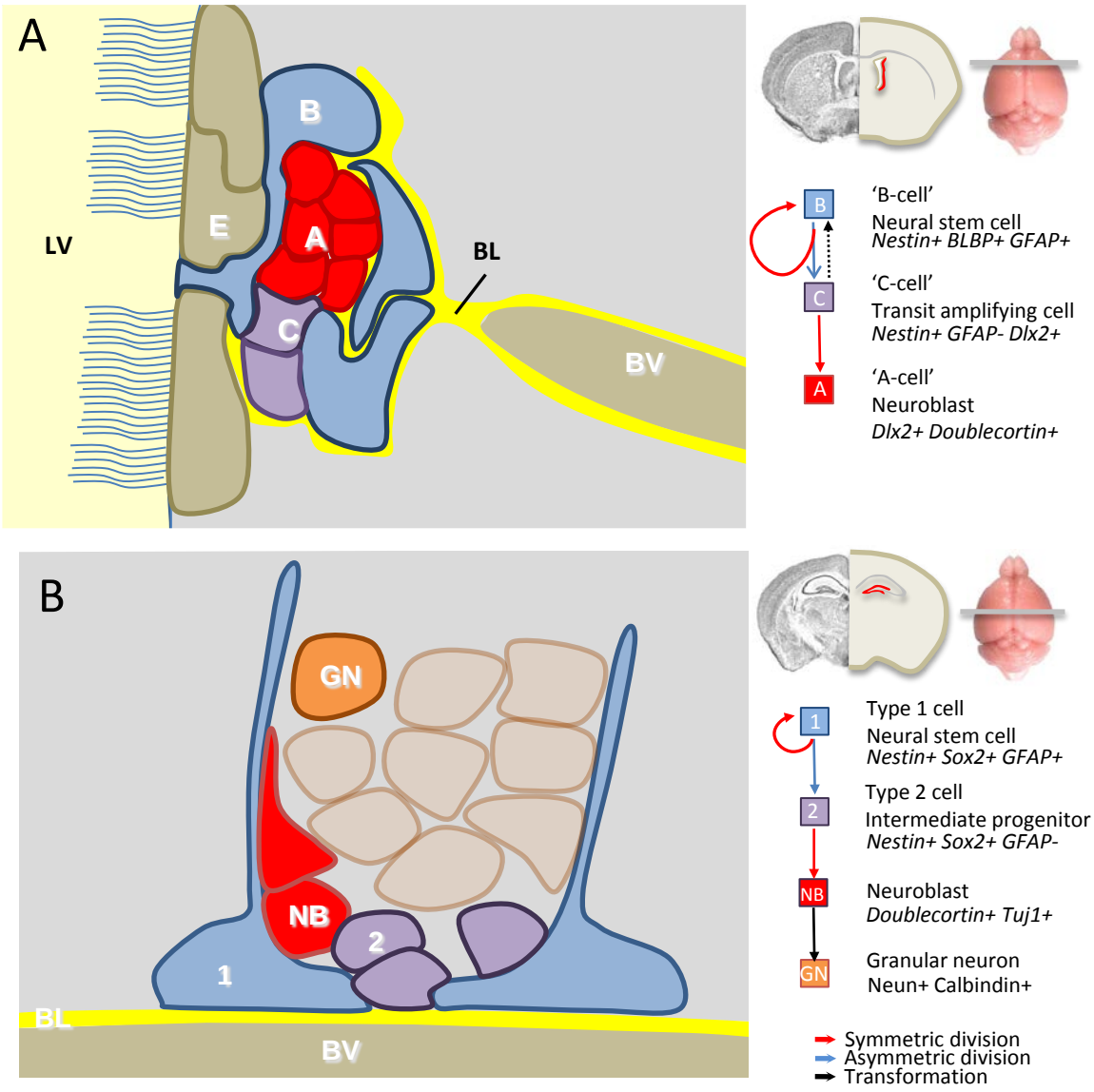

Fig 1.2 – Cytoarchitechture of the canonical neural stem cell niches. (A) The stem cell niche of the SVZ is closely connected to the lateral ventricle (LV). The B-cells are in close proximity to the ependymal cells, and some extend small end-feet to the ventricular surface itself. The B-cells either generate the transit amplifying C-cell, or selfrenew. The C-cells, which under certain conditions can revert into B-cells, normally generate migratory neuroblasts, A-cells, which leave the SVZ toward the olfactory bulb. The whole niche is invested by a specialised basal lamina (BL), extending from local bloodvessels (BV).
(B) In the hippocampus, the type 1 cells are anchored on bloodvessel (BV) derived basal lamina (BL). The type 1 cells generate the intermediate type 2 cells, which are neuronal precursors migrating along the radial fibers. Type 2 cells have a limited proliferative capacity and generate migratory neuroblasts. The neuroblasts then mature into granular neurons locally.

which are thought to bind and concentrate growth factors in the niche (Kerever et al., 2007). These fractones extend from perivascular macrophages through the SVZ before terminating at the ependymal cells. Neural stem cells are in fact clustered around, and neuroblasts migrate along, blood vessels, in a laminin/integrin mediated processes (Kokovay et al., 2010), (Shen et al., 2008). Apart from laminin-integrin interactions, the adhesion protein E-cadherin is required for self-renewal of adult neural stem cells both in vivo and in vitro (Karpowicz et al., 2009), indicating the importance of direct cell-cell interaction in niche-maintenance. The neuroblasts generated in the SVZ eventually go on to form interneurons in the olfactory bulb, which are important to olfactory discrimination and memory (Imayoshi et al., 2008).

1.3.2 Subgranular zone of the dentate gyrus

Many of the basic concepts of the SVZ niche also hold true in the in the subgranular zone (SGZ) in the hippocampus, but there are also notable differences. The niche here is not associated with a ventricular surface, as the SGZ is not in the vicinity of any ventricles (see Fig 1.2b). The stem cells of the SGZ niche are the $GFAP^{+}$/$nestin^{+}$/$S100\beta^{-}$ Type 1 cells, which are closely associated with the local vasculature (Gerdes et al., 1983). The Type 1 cells produce a Type 2 $GFAP^{-}$ intermediate progenitor cell capable of one or a limited number of divisions. These Type2 cells then produce $doublecortin^{+}$ neuroblasts that migrate along the radial fibers of the Type 1 cells to locally form granular neurons (Mu et al., 2010). It is still somewhat unclear what the function of the newly generated cells is, but they do seem to be required for dentate gyrus dependant learning tasks (Deng et al., 2010).

1.4 – Potential new niches for adult neural stem cells

Although the SVZ and SGZ niches have been well studied and thoroughly characterised, they may not be the only stem cell niches in the adult mammalian brain (Fig 1.4). The hypothalamus and the amygdala as potential stem cell niches will be discussed in detail in chapters 3 and 6, respectively. The neocortex, one of the largest areas of the brain, has been suggested to contain stem cells. Several areas of the cortex of the primate *Macaca fascicularies* show cells incorporating BrdU, indicating cell division (Sauer and Henderson, 1988), (Orban et al., 1992). These cells expressed either NeuN or GFAP, indicating formation of neurons or glia. The striatum has been found to contain diving cells generating neurons in rabbits and primates (Metzger et al., 1995); (Feil et al., 1996). The olfactory tubercle sees neurogenesis in primates, but this may be derived from the rostral migratory stream originating in the SVZ (Feil et al., 1997). The substantia nigra has been observed as a target of migration in the adult mouse (Kellendonk et al., 1996). The vagus nucleus of the brain stem of the rat shows cell division and can give rise to neurospheres in vitro (Kellendonk et al., 1999). However, in most of these areas there are conflicting reports on the presence of neurogenesis or stem cells, and much research remains to be done to confirm these areas as neurogenic niches.

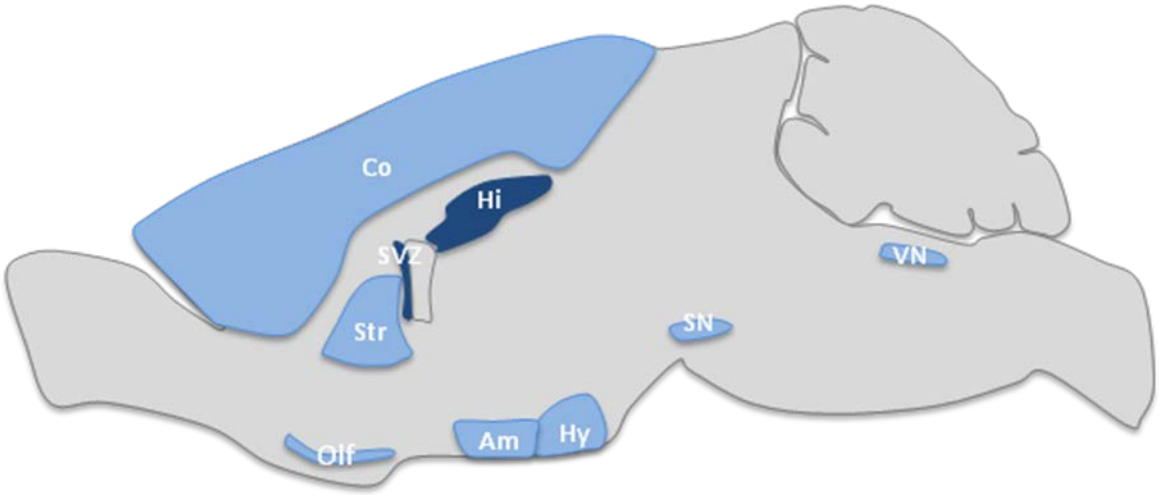

Fig 1.3 - Schematic location of canonical and potential novel neural stem cell niches in the adult brain. In dark blue, the hippocampus (Hi) and subventricular zone (SVZ) are known to contain neural stem cells. Other areas that potentially contain neural stem cells include the neocortex (Co), striatum (Str), olfactory tubercle (Olf), amygdala (Am), hypothalamus (Hy), substantia nigra (SN) and vagus nucleus (VN)

1.5 - Selfrenewal of adult neural stem cells

As with any stem cell population, neural stem cells need to undergo selfrenewal through either symmetric or asymmetric division, to maintain the number of the progenitor pool. A number of factors are required to maintain this selfrenewing capacity. Notch1 is required for the maintenance of the adult neural stem cell pools in the SVZ (Aguirre et al., 2010) and SGZ (Ables et al., 2010). Conditional deletion of Rbpj, an intracellular signalling molecule for notch receptors, causes complete loss of stem cell selfrenewal and differentiation of the complete population to transit amplifying cells and neuroblasts (Imayoshi et al., 2010). Infusion of the notch ligand Dil4 into the brain leads to

increased proliferation (Androutsellis-Theotokis et al., 2006). Also involved in the notch mediated selfrenewal is the presenilin 1 gene, known to be involved in the pathology of Alzheimer's disease, which is thought to be involved in notch cleavage (Veeraraghavalu et al., 2010). The fact that notch is required for stem cell selfrenewal can also explain the link between the vasculature and stem cell niches, as vascular derived PEDF induces Notch expression in neural stem cells (Andreu-Agullo et al., 2009). The main intracellular effectors of Notch signalling are the basic helix-loop-helix transcription factors of the Hes family, Hes 1, 3 and 5, which are known to be key repressors of neurogenesis during development, preserving the stem cell state (Hatakeyama et al., 2004), (Kageyama et al., 2005). Other cell-extrinsic factors promoting self-renewal are LIF and CNTF, which use the JAK/STAT pathway to promote cell proliferation (Bauer, 2009).

Sonic hedgehog is expressed selectively in the ventral lateral ventricle ependyma, and promotes proliferation of these cells (Palma et al., 2005), as well as specifiying neuronal fates in these cells (Ihrie et al., 2011).

The orphan nuclear receptor TLX has long been known to be important for selfrenewal (Shi et al., 2004), as cells deficient in TLX have greatly reduced proliferation potential in vitro (Zhang et al., 2008). Inducible knockouts of TLX show a complete loss of neurogenesis from the SVZ (Lie et al., 2005), and are impaired in learning tasks (Zhang et al., 2008). The effect of TLX in neural stem cells may be mediated by activation of the Wnt/β-catenin pathway (Qu et al., 2010), but at least part of the mechanism seems to be the histone deacetylase mediated silencing of p21 and PTEN (Sun et al., 2007). The ligand for TLX is still unknown, although it is known to be targeted by microRNAs, specifically 7b (Zhao et al., 2010) and 9 (Zhao et al., 2009).

The transcription factor Sox2 is crucial for stem cell maintenance, as low levels of Sox2 in the adult lead to a loss of neural stem cells (Ferri et al., 2004). Sox2 maintains neural stem cells through a Shh dependant pathway (Favaro et al., 2009). Another factor that is required for stem cell maintenance is BMI1, which promotes selfrenewal in vivo and in vitro (Yadirgi et al., 2011).

Wnt signalling is strongly involved in the neural stem cell biology. Enhancing Wnt signalling increases proliferation in the hippocampus (Lie et al., 2005), and blocking Wnt signalling decreases proliferation (Qu et al., 2010). Wnt is required for maintenance of the stem cell niche, inhibition of Wnt in vivo leads to progenitor depletion followed by overproduction of neurons (Wexler et al., 2009). Wnt signalling has been found to promote symmetric over asymmetric division (Piccin and Morshead, 2010).

1.6 - Neuroblast migration

The immature progeny of the adult neural stem cell, the neuroblast, is characterised by its migratory behaviour, both in the SVZ and in the hippocampus. From the SVZ, neuroblasts migrate towards the olfactory bulb, the rostral migratory stream (RMS) (Luskin, 1993), (Lois and Alvarez-Buylla, 1994), while in the hippocampus cells only migrate short distances locally.

The RMS starts at the subventricular wall, from which the immature neuroblasts (A-cells) align in a chain migration, where cells migrate along each other in direct cell-cell contact (fig 1.4). The initiation of the RMS, the departure of neuroblasts from the ventricular wall niche, is mediated by a combination of cytoarchitecture and cell signalling

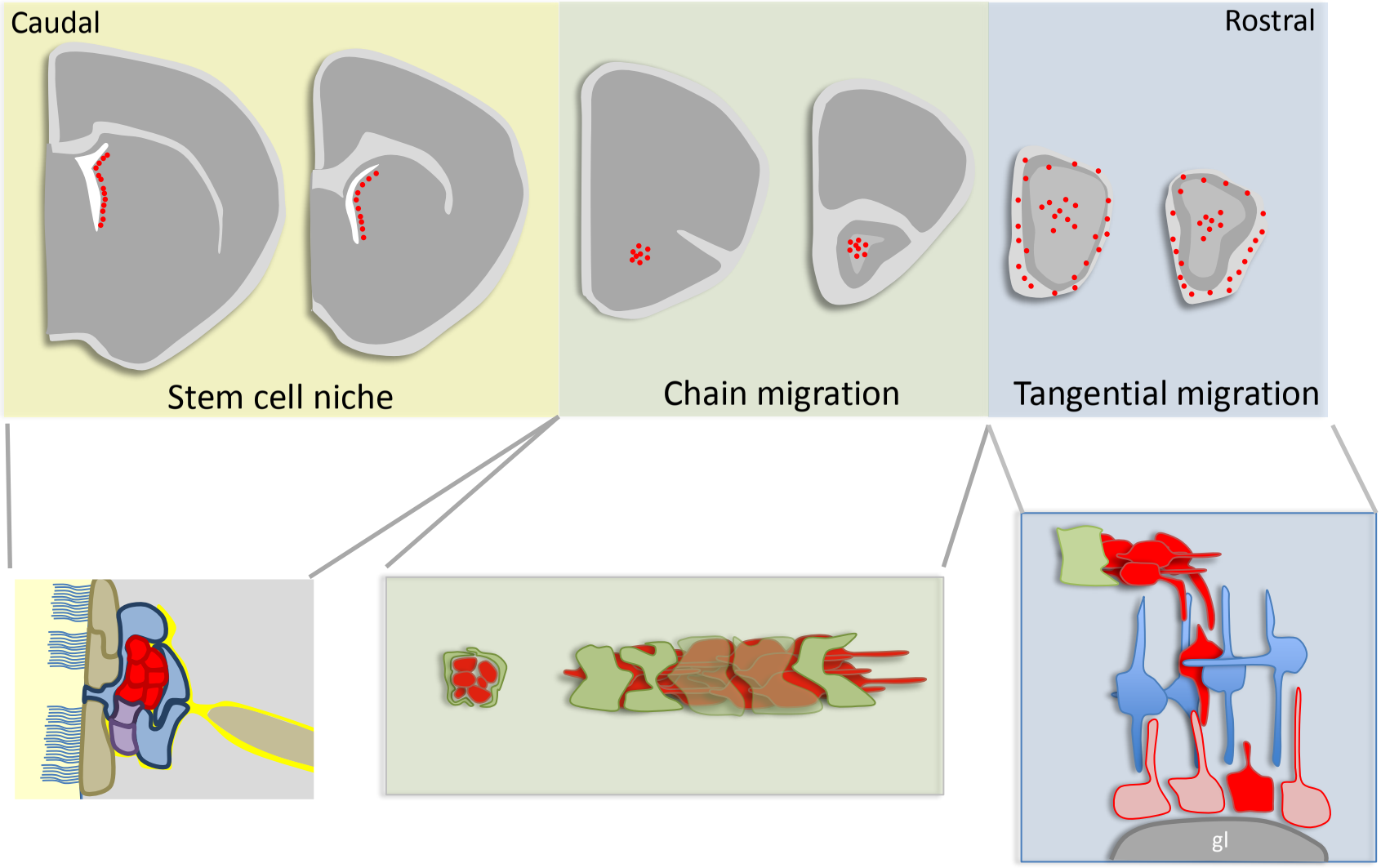

Fig 1.4 - The rostral migratory stream (RMS). Neuroblasts (red) depart from the subventricular zone stem cell niche, from where they join a chain migration stream moving rostrally, where they are ensheathed by a tunnel of glia (green). Upon reaching the olfactory bulb, neuroblasts leave the RMS and migrate tangentially before integrating themselves into the local neuronal structure.

events. The direction of the radial glia fibres from which the neuroblasts are born imparts the initial direction of migration, which is crucial for the initialisation of the RMS (Ghashghaei et al., 2007). The departure of neuroblasts from the SVZ is further promoted by repulsive signalling through ROBO/Slit interactions (Perez-Martin et al., 2010), (Nam et al., 2007).

The stream of chain migrating neuroblasts is contained and given directionality by a surrounding layer of astrocytes, forming a glial tunnel through which the neuroblasts migrate. Although the overall direction of migration is rostrally from the SVZ to the OB, an individual neuroblast may undergo a more complex motion, including stops and temporary reversals of direction (Nam et al., 2007). Cell-cell contacts are crucial for maintaining the migration, as gap junctions between the neuroblasts are required (Marins et al., 2009). Other cell-cell contacts required for the formation and maintenance of the chain migration are mediated by integrin/laminin interactions, especially β1 integrins (Belvindrah et al., 2007). Other important adhesion molecules are the neural adhesion molecules NCAMs, specifically the polysialated form PSA-NCAM. Enzymatic removal of the PSA moieties from NCAM in vivo leads to a disturbed RMS morphology and ectopic neuroblast migration (Battista and Rutishauser, 2010).

The glial tunnel also speeds up neuroblast migration, by up to 20% compared to the neonatal RMS, where the glial tunnel is not yet formed (Bovetti et al., 2007). The presence of the glial tunnel also seems to ease migration by providing a permissible extracellular matrix environment, as blocking of MMP activity with a broad spectrum inhibitor did not inhibit chain migration in the glial tunnel, but did negatively affect migration of individual neuroblasts. (Bovetti et al., 2007). As in the actual stem cell niches, the local vasculature plays an important role in migration, many migrating neuroblasts

directly contact blood vessels and release of BDNF from the vascular endothelium modulates their migration (Whitman et al., 2009), (Snapyan et al., 2009).

During migration, neuroblasts undergo a characteristic cell morphology change cycle. At the initiation of the migration, a leading process forms, the cytoskeletal centrosome translocates to the process, and the nucleus translocates in the direction of the migration, after which the cycle repeats. This process is mediated by GSK3β and PKCζ controlled dynamic microtubule remodelling (Higginbotham et al., 2006). One of the most widely used markers for migrating neuroblasts, doublecortin, is required for these cell morphology changes (Koizumi et al., 2006). In the olfactory bulb, the end of the RMS, the neuroblasts are induced to break from the chain migration stream, and individually migrate to their final destination. The main signal that neuroblasts encounter that drives them out of the RMS is reelin (Hack et al., 2002), when reelin is ectopically administered, the chain migration of the RMS breaks down (Courtes et al., 2010). Once out of the RMS, local cues direct the final localisation and differentiation of the new neurons, see chapter 6 for further details.

1.7 - Differentiation of neural stem cells

The exact fate a neural stem cell will adopt is dependant both on cell-intrinsic and extrinsic cues. The neuronal differentiation potential of SVZ stem cells is dependent on their location within the SVZ, different spatial populations preferentially form specific types of neurons through some form of cell-intrinsic programming (Merkle et al., 2007). For instance, dopaminergic interneurons are generated mainly from the dorsal SVZ, while GABAergic ones mostly originate ventrally. These populations are derived from different embryonic origins (Young et al., 2007). Initial neuronal differentiation is induced by the

transcription factors NeuroD (Boutin et al., 2010) and Mash1 (Parras et al., 2004). Differentiation into glutamatergic neurons is driven by Neurog2 and Tbr2 (Brill et al., 2009). Differentiation into calretinin positive interneurons is driven by the transcription factor Sp8 (Waclaw et al., 2006), and dopaminergic differentiation is driven by Sal3 (Harrison et al., 2008) and Pax6 (Hack et al., 2005). Following commitment to a neuronal fate and arrival at their final destination, the new neurons receive a number of cues to start forming dendritic networks and synapses, these include neurotransmitters such as glutamate and GABA (Tashiro et al., 2006), (Gascon et al., 2006), and growth factors such as BDNF (Bergami et al., 2008). Gradients of these factors may lead neuroblasts to their final destination.

In contrast to neuronal differentiation, little is known about glial differentiation from adult neural stem cells. Differentiated glial cells are readily generated from cultured neural stem cells, but it seems the majority of progeny in vivo is neuronal. The transition from glial stem cell to mature astrocytes is marked by the onset of S100β expression (Raponi et al., 2007), and is promoted by BMP4 (Bonaguidi et al., 2005). Oligodendrocytes can also be generated from the SVZ cells in vivo. A subset of stem cells already expresses the oligodendrocyte transcription factor Olig2 at an early stage of differentiation (Menn et al., 2006). In response to experimental demyelination, increased activity of the RMS is seen, with an increase in cells expressing Sox9 and Sox 10, transcription factors that are associated with oligodendrocyte formation (Nait-Oumesmar et al., 2007).

In both the SVZ and hippocampus, 50 to 80% of newly generated cells will fail to integrate and eventually die (Petreanu and Alvarez-Buylla, 2002; Sun et al., 2004).

1.8 Fibroblast growth factors

Fibroblast growth factors were named after the properties of the first two described members of the family, Fgfs 1 and 2 (also known as aFGF and bFGF respectively) which act as mitogens for fibroblasts (Thomas et al., 1984); (Bohlen et al., 1984). Currently, 22 members of the Fgf family are known, and given the high homology between members, and the fully sequenced genomes of model organisms, it is unlikely the number will increase. Fgf23 does exist, but this is due to a naming inconsistency, with human Fgf19 being the same as mouse Fgf15. A phylogenetic overview of all Fgfs clearly shows multiple subfamilies of Fgfs, based on protein homology (see figure 1.5). Members of subfamilies often show similar localisations and biological effects. Fgfs are relatively small proteins, ranging from 17-29 kDa molecular weight, and have between 13 to 71% homology on the protein level. The main conserved regions are in two core regions of 10 amino acids each, which are responsible for interactions with Fgf receptors (Ornitz and Itoh, 2001).

The majority of Fgfs (1, 3-8, 10, 15, 17-19 and 21-23) contain signal peptides and are secreted (Ornitz and Itoh, 2001), while Fgf2 and members of the Fgf9 subfamily (Fgfs 9, 16 and 20) lack a signal peptide, but are still secreted (Miyamoto et al., 1993), (Miyake et al., 1998), (Ohmachi et al., 2000). Fgfs 11-14 are retained in the cell.

1.9 – Fgf receptors

Fgfs, with the notable exception of the intracellular Fgfs 11-14, exert their effect through the Fgf receptors (FgfR). Five FgfRs have been described so far, although FgfR5 lacks an intracellular signalling domain, and is thus not capable of signal transduction (Sleeman et al., 2001). FgfRs belong to the immunoglobulin family of receptors, with their

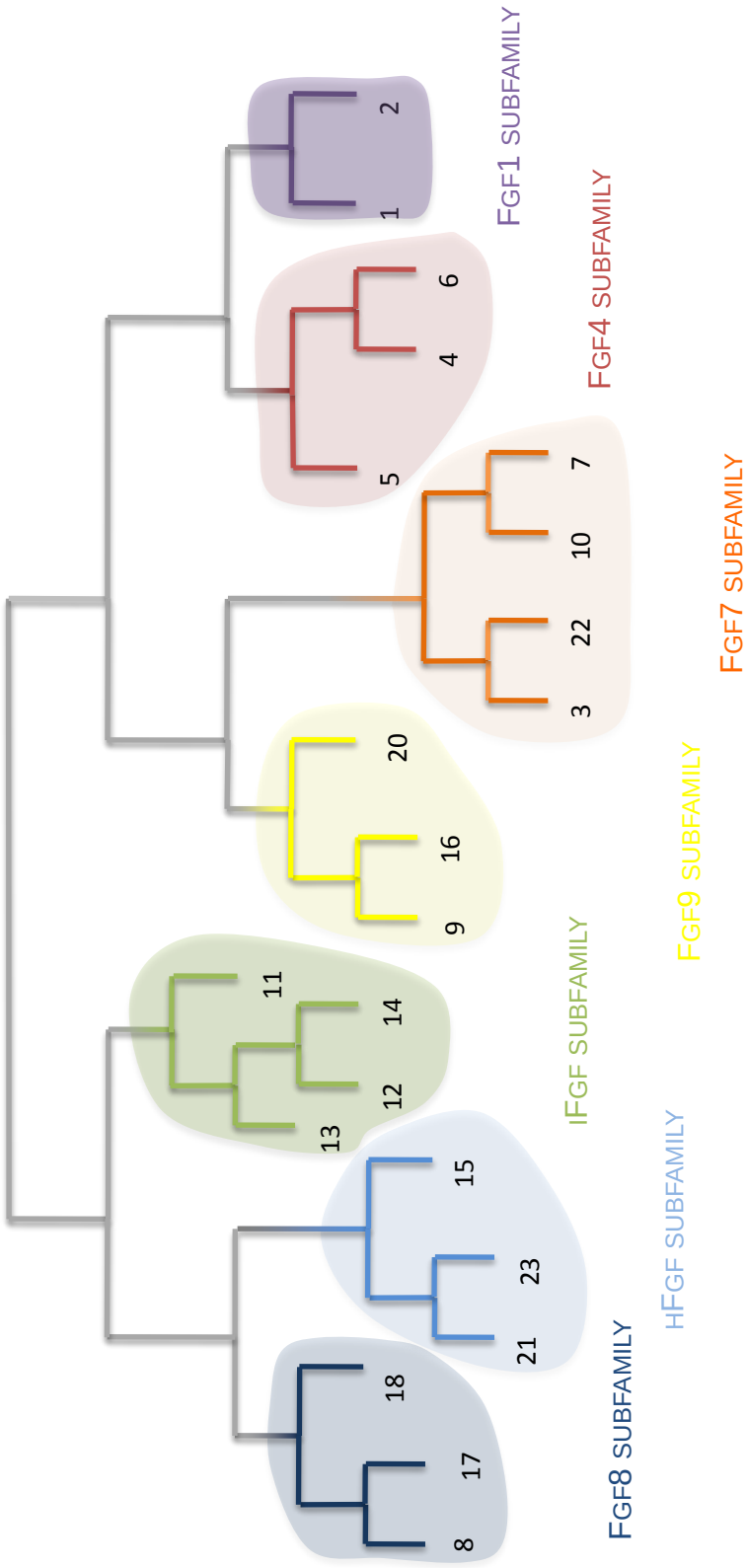

Fig 1.5 - Phylogenetic tree of the Fgf family. The grouping of the different members in a number of subfamilies is clear.

extracellular domains containing two or three immunoglobulin domains, the second and third of which comprise the ligand binding domain, a single-pass transmembrane domain and an intracellular split tyrosine kinase domain (figure 1.6a).

Upon ligand binding, FgfRs form a homodimers (figure 1.6b), in a complex which requires sulphate proteoglycans such as heparin as a cofactor (Mohammadi et al., 2005). Upon complex formation, several tyrosine residues in the intracellular domain of the FgfR are auto-phosporylated, leading to the recruitment of scaffolding and adaptor proteins, most prominently fibroblast growth factor substrate 2 (FRS2), which is required for, and coordinates further protein binding, leading to the activation a number of possible pathways (Gotoh et al., 2005). Binding of a complex with Grb2 and Gab1 activates the PI3 signalling cascade (Ong et al., 2001), whist binding of Shp2 and SOS activates Ras/MAPK/Erk signalling (Hadari et al., 1998)

In the extracellular domain, the second and third Ig loops bind Fgfs and determine ligand specificity. Apart from the four different receptors, further variety is introduced in the FgfRs by alternate splicing variants of FgfRs 1-3 (figure 1.6c). Part of the last IgG loop can be encoded by a sequence of exons using either exon 8 or exon 9, leading to the FgfR-IIIb or IIIc isoforms, respectively (Eswarakumar et al 2005). These forms are generally shortened to FgfRb/FgfRc. FgfR4 does not undergo alternate splicing, and exists only in the IIIc form. The IIIb vs IIIc splice variants different effects on ligand specificity, see table 1.1. Also, different isoforms have different tissue localisations.

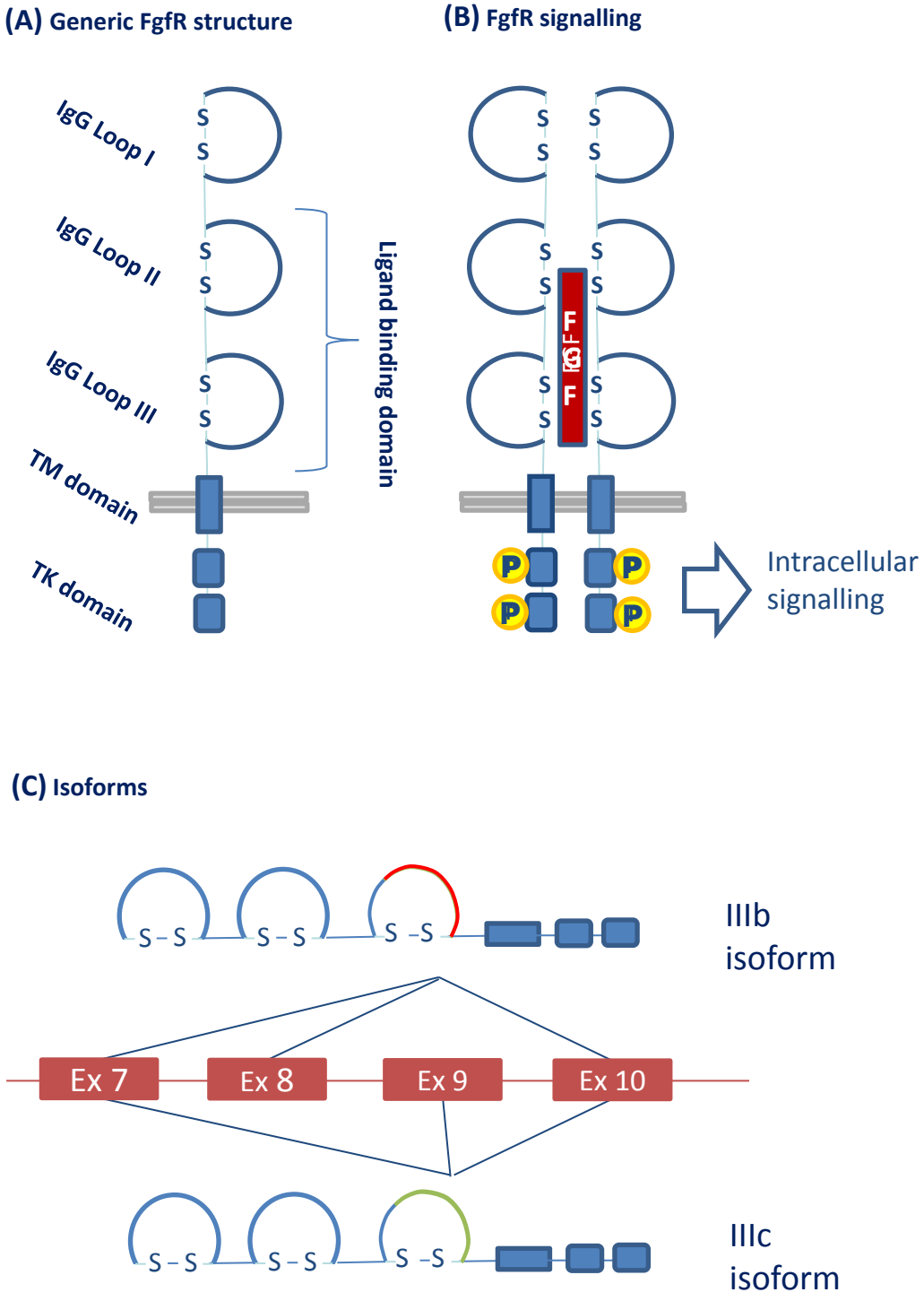

Figure 1.6 - Structure, signaling and diversity of the Fgf receptors. The FgfRs consist of 3 extracellular IgG loops, the two closest to the membrane being the ligand binding domain. A transmembrane domain (TM) crosses the membrane and is followed by an intracellular tyrosine kinase domain (TK). Upon ligand binding, a homodimer is formed, and the tyrosine kinase domains are phosphorylated, leading to further downstream signaling. The ligand binding domain of FgfRs 1-3 exists in 2 isoforms, dependant on alternative splicing of the receptor mRNA.

Table 1.1 – Ligand specificities of the Fgf receptors

	FgfR1		FgfR2		FgfR3		FgfR4
Fgf	IIIb	IIIc	IIIb	IIIc	IIIb	IIIc	IIIc
1							
2							
3							
4							
5							
6							
7							
8							
9							
10							
16							
17							
18							
19							
20							
21*							
22							
23*							

This table show the ligand specificity for each of the FgfR isoforms. Red strong binding, , yellow moderate (less than 50% of a strong binding), and green low affinity (less than 10% of a strong response). Data from (Ornitz et al., 1996) and (Zhang et al., 2006). * Fgf21 and Fgf23 require an accessory protein, β-klotho, for receptor activation

1.10 Fgf expression and function in developing and adult nervous system

1.10.1 Fgf1 subfamily (Fgf1 and 2)

Fgf2 is expressed in selected astrocytes and neurons during development (Xu et al., 2005) and adulthood (Gomez-Pinilla et al., 1992). It is also the best known mitogen for both embryonic and adult neural stem cells, and is widely used in conjection with EGF in culture to promote proliferation and prevent differentiation (Weiss et al., 1996). Fgf2 knockout animals have been shown to have a reduction in the number of GFAP-positive astrocytes, and show blood-brain-barrier defects (Reuss et al., 2003).

1.10.2 Fgf4 subfamily (Fgf 4, 5 and 6)

Fgf4 expression is found in the early notocord, where it is likely involved in setting up neural patterning (Shamim et al., 1999). Fgf4 signalling also promotes neurogenesis in embryonic stem cells in vitro (Chen et al., 2010). In the adult, Fgf4 expression is seen in adult neurogenic niches, including the hippocampus, SVZ and RMS, and was found to both increase proliferation of neural stem cells and promote neuronal differentiation in vitro (Kosaka et al., 2006). Fgf5 expression was found in both the developing (Goldfarb et al., 1991) and adult (Haub et al., 1990) nervous system. In adult mouse and human brain, it was found to be expressed in neurons in the cortex, hippocampus and thalamus and induced neuronal differentiation in PC-12 cells (Ozawa et al., 1998). Prominent expression of Fgf5 in the adult brain is seen in the hypothalamus, and is reduced following food deprivation, strongly suggesting a role in feeding behaviour (Li et al., 1999).

1.10.3 Fgf7 subfamily (Fgf 3, 7, 10 and 22)

(Note: Fgf10 will be discussed in detail later)

Fgf3 is expressed in the developing hindbrain (Mahmood et al., 1996), and is thought to be important for patterning during development. It is also expressed in the developing forebiran, but is not required for correct forebrain development (Theil et al., 2008). Fgf7 is expressed in the forebrain ventricular zone, but its function was not known at this time (Mason et al., 1994). In the adult, Fgfs 7 and 22 are both expressed in the hippocampus (Terauchi et al., 2010). Members of the Fgf7 subfamily Fgfs 7, 10 and 22 promote neurite outgrowth in culture chick motorneurons, and postnatal inactivation of FgfR2, or sequestering of Fgf7 family members by antibodies in the brain disturbs synapse formation (Umemori et al., 2004). Fgf7 is involved in formation of inhibitory synapses,

while Fgf22 is involved in excitatory synapse formation (Terauchi et al., 2010). The importance of these factors is illustrated by the fact that Fgf7 knockouts are more prone to epileptic seizures, while Fgf22 knockouts are resistant to induced seizures (Terauchi et al., 2010).

1.10.4 Fgf8 subfamily (Fgfs 8, 17 and 18)

Fgf8 is a crucial organiser in embryonic brain development. It is expressed in the isthmic organiser, which induces polarisation and development of the frontal cortex and midline cerebellar structures (Xu et al., 2000), (Cholfin and Rubenstein, 2008). These are 8 different isoforms of Fgf8, the Fgf8b containing isoforms are required for patterning, whereas the Fgf8a forms are not (Guo et al., 2010). The other members of the subfamily have similar roles; Fgf17 induces midline and cerebellar patterning and neuronal differentiation during neural tube organisation (Cholfin and Rubenstein, 2008), Fgf17 knockouts have reduced amounts of midline and cerebellar tissues (Xu et al., 2000). Fgf18 has a comparable, but more widespread expression pattern as Fgf8, and in addition to mideline patterning, is also involved in cortical patterning (Liu et al., 2003).

1.10.5 Fgf9 subfamily (Fgfs 9, 16 and 20)

Fgf9 is required for correct development of the cerebellum, as Fgf9 knockout mice have a disrupted radial glia formation and neuronal migration, leading to severe ataxia (Lin et al., 2009). Fgf9 also promotes survival of embryonic cholinergic forebrain neurons in an autocrine or paracrine manner (Kanda et al., 2000), and promotes survival and inhibits astrocytic differentiation from cultured adult neural stem cells (Lum et al., 2009). Fgf16 does not seem to be expressed in nervous tissue. Fgf20 in the adult brain is

expressed in the substantia nigra, where it has promotes differentiation (Grothe et al., 2004) and survival of domapinergic neurons (Ohmachi et al., 2000), and in the hippocampus, where it may affect hippocampal size (Lemaitre et al., 2010).

1.10.6 iFGF subfamily (Fgfs 11-14)

The iFGF subfamily, also known as fibroblast homologous factors, are not secreted as classical Fgfs and do not interact with Fgf receptors (Olsen et al., 2003). They are generally not considered canonical Fgfs, but are expressed in the nervous system, where they play a role in neuronal signalling through ion channel modulation (Goldfarb, 2005). Fgf14 has been shown to be involved in dopamine signaling, and Fgf14 knockout mice show movement disorders such as ataxia and dyskinesia (Wang et al., 2002).

1.10.7 hFGF subfamily (Fgfs 15/19, 21 and 23)

Fgf15, known as Fgf19 in human and rat, influences forebrain development, through interactions with Fgf8 and Shh at the isthmic organiser (Gimeno et al., 2003), (Gimeno and Martinez, 2007), and is required for progenitor cells to exit the cell cycle to generate neurons (Fischer et al., 2011). Fgf21 acts as a circulating hormone, which is induced by fasting and can cross the blood-brain-barrier (Hsuchou et al., 2007), where it can increase both food intake and energy expenditure (Sarruf et al., 2010). Fgf23 is preferentially expressed in the thalamus (Yamashita et al., 2000), but its function in the brain is currently unknown.

1.11 - Fgf10

Fgf10 was first indentified in 1996 by the Itoh group (Yamasaki et al., 1996), who cloned a novel Fgf mRNA from rat brain and found it coded for a 251 aa, 24-26 kDa protein. It was found to have high homology with Fgfs 3 and 7, with which it shared a hydrophobic N-terminal region that serves as a secretory signal. By northern blot expression was found predominantly in the heart and lungs. Cloning of the human (Emoto et al., 1997) and mouse (Tagashira et al., 1997), (Beer et al., 1997) homologues quickly followed. Initial study of the role of Fgf10 focussed on lung and limb development. It is important to note the field has been greatly hindered by the lack of a working antibody for immunohistochemistry. Although numerous commercial vendors offer antibodies for Fgf10, these are not capable of detecting endogenous levels of Fgf10 in tissue. The study of Fgf10 was greatly advanced by the generation of Fgf10 knockout mouse lines.

1.12 - Fgf10 knockout mice

The first knockout line was produced in the Simonet lab in 1998, by replacing the translation initiation site with a neomycin cassette, to disrupt translation (Min et al., 1998). It was found that homozygous Fgf10 knockouts were not viable, while surviving gestation, the knockout animals died at birth. The obvious feature of these animals was a complete lack of limbs. Cause of death was found to be an absence of lungs, confirming the crucial role already described of Fgf10 in lung and limb formation. Heterozygous mutants were found to be viable, and without obvious phenotype. A second knockout line was generated in 1999, confirming these findings (Sekine et al., 1999). Further effects of knocking out Fgf10 include absence of the thyroid, pituitary and saliva glands, and defects in the stomach, teeth, kidneys, hair follicles and digestive tract (Ohuchi et al., 2000). As a

parallel, knockouts of the receptor for Fgf10, FgfR2IIIb, show a similar phenotype (De Moerlooze et al., 2000).

1.13 – Mutations in Fgf10 and disease in humans

The phenotype of Fgf10 knockout mice led to comparisons with human congenital disorders with similar phenotypes. Two syndromes, aplasia of the lacrimal and salivary glands (ALSG) and lacrimo-auriculo-dento-digital syndrome (LADD) have been associated with Fgf10 mutations. For ALSG, which is characterised by reduced development of the lacrimal and salivary glands, a number of mutations including several SNPs and a truncation of Fgf10 were described in two Swedish families (Entesarian et al., 2005). As inheritance of ALSG is dominant, indicating one affected copy of Fgf10 is sufficient to cause symptoms, heterozygous Fgf10 knockout mouse were re-examined, and found to have a similar hypoplastic glandular phenotype (Entesarian et al., 2005). In a different affected family, a mutation causing a splice defect in Fgf10 was found (Scheckenbach et al., 2008). In LADD, a syndrome with similar presentation as ALSG with the addition of defects in teeth and digits, two affected families were found to have mutations in exons 2 or 3 of the Fgf10 gene (Milunsky et al., 2006), leading to a loss-of-function for Fgf10 (Shams et al., 2007).

1.14 Roles of Fgf10 in tissue development

Little data exists on the role of Fgf10 in the adult, due to the lethality of knocking out Fgf10, and the lack of antibodies for Fgf10. However, the functions of Fgf10 during the development of many tissues have been studied in detail. In these systems, Fgf10 is

generally expressed in mesenchymal cells, signalling to FgfR2IIIb receptors expressed on the adjacent epithelial cells.

1.14.1 Lung

Analysis of Fgf10 expression in the developing lung by both RT-PCR and in situ hybridization has shown that Fgf10 is expressed from the start of lung development at E9.5 in the mouse, and is maintained through to E11.5, with strongest expression seen in the most distal end of the developing lung, largely restricted to the mesenchyme (Bellusci et al., 1997). Addition of Fgf10, but not of Fgf7, to cultured E11.5 lung buds embedded in a Matrigel substrate elicits extensive budding (Bellusci et al., 1997). Addition of Fgf10 soaked beads to cultured mesenchyme-free E11 mouse lung explants, showed chemoattractant effect of Fgf10 on the distal developing lung (Park et al., 1998). The requirement for Fgf10 during lung development was shown conclusively when it was found that lung formation in Fgf10 knock-out mouse does not progress past the initial formation of the trachea (Sekine et al., 1999). The chemoattractive and proliferative effects of Fgf10 in the lung are controlled by a negative feedback of BMP4 in the underlying lung endoderm (Weaver et al., 2000). In a gene expression study of embryonic lung explants stimulated with Fgf10, it was found that BMP receptor type I and Wnt pathway component β-catenin were upregulated by Fgf10, as well as genes involved in cytoskeleton remodeling and migration, lipid synthesis and a number of cell cycle genes (Lu et al., 2005). Using limited lineage tracing, it was found that Fgf10 positive cells in the developing lungs can form parabronchial smooth muscle cells, formation of which is reduced in an Fgf10 hypomorphic mouse model (Mailleux et al., 2005). Fgf10 hypomorphic mice also show a simplified lung architecture, along with a reduction in both

epithelial and smooth muscle cell numbers (Ramasamy et al., 2007). In contrast, genetic overexpression of Fgf10 leads to epithelial hyperplasia and attenuated differentiation (Nyeng et al., 2008). Conditional knock-out of Fgf10 during late lung branching (E12.5) causes increased apotosis throughout the lung, and reduces Shh and Patched1 expression, both also known to be involved in lung morphogenesis (Abler et al., 2009). Disturbing the levels of Fgf10 in vivo has clearly indicated Fgf10 has both a mitogenic effect and maintains undifferentiated lung progenitors.

1.14.2 Stomach

Fgf10 null mice have morphogenic defects in the stomach, with the smooth muscle cell layer being absent (Ohuchi et al., 2000). Closer analysis of Fgf10 knockouts has shown a reduced stomach size, particularly of the glandular stomach, along with a simplified mucosal architecture (Spencer-Dene et al., 2006). In the developing stomach, Fgf10 is expressed from at least E11.5 (prior to cell fate specification), and ectopic expression of Fgf10 throughout the stomach leads to epithelial hyperplasia at the cost of endocrine differentiation, along with an increased proliferative index and disruption of normal Notch and Wnt signaling (Nyeng et al., 2007)

1.14.3 - Pancreas

In the pancreas, Fgf10 expression is detectable by RT-PCR at E12, and is expressed throughout development. In culture, a mesenchyme free pancreatic preparation exposed to exogenous Fgf10 shows a mitogenic response, along with a more branched morphology and a shift in differentiation pattern to favour the exocrine over the endocrine lineage (Miralles et al., 1999). In Fgf10 knock-outs a marked reduction in

pancreatic epithelium is seen, due to reduced progenitor cell proliferation, which can be rescued in vitro by addition of Fgf10 (Bhushan et al., 2001). Ectopic constitutive Fgf10 expression leads to hyperprofileration of undifferentiated cells, characterised by expression of Notch (Norgaard et al., 2003); (Hart et al., 2003). The effect of Fgf10 on pancreatic precursors was found to be mediated through the Notch pathways, in a Hes1 dependant mechanism (Miralles et al., 2006).

1.14.4 Limbs

The most striking feature of Fgf10 knock-outs is the complete lack of limb development, indicating the crucial role of Fgf10. Formation of limbs starts with the induction of the limb bud from the apical ectodermal ridge (AER), where Fgf10 signalling from the lateral plate mesoderm induces reciprocal Fgf8 signalling from the AER, reinforcing the Fgf10 signal (Ohuchi et al., 1997).

1.14.5 Adipose tissue

Fgf10 was found to be highly expressed in the white adipose tissue, specifically in the pre-adipocytes, the precursors to mature adipocytes, and acted as a mitogen for the pre-adipocytes (Yamasaki et al., 1999), Fgf10 is required for the differentiation of pre-adipocytes into mature adipocytes (Sakaue et al., 2002), which is clearly illustrated by the fact that Fgf10 knockouts have disturbed fat morphogenesis through the downregulation of transcription factors C/EBPβ and PPARγ (Asaki et al., 2004). The proliferative effect of Fgf10 on pre-adipocytes is mediated through a Ras/MAPK dependant expression of cell cycle protein cyclin D2 (Konishi et al., 2006).

1.14.6 Teeth

Defects in tooth morphogenesis were noted in Fgf10 knock-out mice (Ohuchi et al., 2000). Fgf10 is required to maintain the stem cells compartment of the growing incisor, with Fgf10 knockouts, or animals in which Fgf10 was sequestered with antibodies showing premature growth arrest, which can be rescued with exogenous Fgf10 (Harada et al., 2002)

1.14.7 Small intestine

The developing duodenum expresses Fgf10 at an early stage (E8.5 in the mouse), and loss of Fgf10 leads to duodenal atresia, where the lumen of the duodenum fails to form (Kanard et al., 2005). Close examination of the role of Fgf10 by comparison of knockouts and animals overexpressing Fgf10 in the small intestine showed that Fgf10 is required for maintenance of the intestinal stem cell niche, as overexpression caused an expanded and ectopic stem cell compartment, whereas loss of Fgf10 caused premature differentiation (Nyeng et al., 2011).

1.14.8 Liver

Livers of Fgf10 knockout mice showed a significantly reduced size and number of proliferating cells, while analysis in vitro showed that the effect of Fgf10 is mediated via β-catenin dependent mechanism (Berg et al., 2007).

1.15 – Expression and functions of Fgf10 in the brain.

During development, Fgf10 has an important role in controlling the size of the cortex. In the cortex, Fgf10 is expressed at E10.5 and E11.5, although expression in the hypothalamus is seen as early as E9.5. In Fgf10 knockouts, the initial transition from neuroepithelium to radial glia is delayed. Once the glia are formed, they undergo more symmetric divisions, and eventually overproduce neuroblasts, leading to a larger than normal cortex (Sahara et al 2009). In the adult brain, Fgf10 expression has been studied using in situ hybridisation, with expression reported in the hippocampus, thalamus, midbrain, brainstem and the oculomotor, dorsal motor trigeminal facical and hypoglossal nuclei (Hattori et al., 1997). However, a more complete description of the expression of Fgf10 was performed by Hajihosseini et al, using a lacZ reporter mouse for Fgf10 ($Fgf10^{nlacZ}$) (Hajihosseini et al., 2008). This particular reporter strain has a nuclear targeted lacZ insert upstream of the Fgf10 promoter, which is produced as a separate protein. Owing to the high stability of the β-galactosidase reporter protein, this particular reporter strain is also suitable for short term lineage tracing (Fowler et al., 2002).

During development, Fgf10-lacZ was found to be expressed in the developing hypothalamus, and several brain stem nuclei at E14, while at E18 the expression pattern had expanded to also include the cerebellum and dorsal midbrain. The expression range of Fgf10-lacZ continues to expand after birth, with the final expression pattern not being fully developed until post-natal day 30 to 60 (P30-60). At this stage, areas expressing Fgf10-lacZ are the cerebellum, brain stem, ventral telencephalon (including amygdala), thalamus, hypothalamus, hippocampus, neocortex and olfactory bulb. It is of interest to note that some of these areas are also areas that have recently been implicated to contain putative stem cell niches (Gould, 2007).

The hypothalamus has in the past been suggested as a potential neural stem cell niche, and dividing cells have been detected in this area (Kokoeva et al., 2005). However, the specific cells that form the putative stem cells population in the hypothalamus has yet to be characterised. Similar to the SVZ, this potential niche is associated with a ventricle, in this case the 3rd ventricle. The specialised ependymal cells lining the ventral 3rd ventricle, termed tanycytes, have in the past been suggested to be a potential stem cell population (Rodriguez et al., 2005). The distribution of Fgf10 and its lacZ reporter in the hypotahalamus is suggestive of a stem or progenitor population. An in situ hybridisation for Fgf10 mRNA shows Fgf10 transcript exclusively in the ventricle wall, in the tanycytes (Fig 1.7a). This is faithfully recapitulated by the reporter lacZ mRNA (Fig 1.7b). However, the presence of the reporter protein, which is retained in cells for some time, is found far more widespread, with cells located throughout the surrounding hypothalamic tissue, the parenchyma (Fig 1.7c). This, coupled with a migratory 'trailing speck' phenotype of some of the cells located in the parenchyma, has led to the hypothesis that Fgf10 expressing progenitors in the ependyma generate progeny that migrates into the surrounding hypothalamic parenchyma.

The amygdala, also a putative neurogenic niche, also shows considerable Fgf10 expression, starting after birth (Fig 1.7D). From the amygdala, Fgf10-lacZ expressing cells can be seen in a trail through the frontal cortex towards the olfactory bulb (Fig 1.7E-I). In the olfactory bulb, Fgf10-lacZ expressing cells are found in multiple layers. RT-PCR for Fgf10 has shown active Fgf10 expression in both amygdala and olfactory bulb (Fig 1.7J). Given that the olfactory bulb is a known target for migrating neuroblasts, and the amygdala may contain neural stem cells, the hypothesis is that Fgf10 expressing cells in

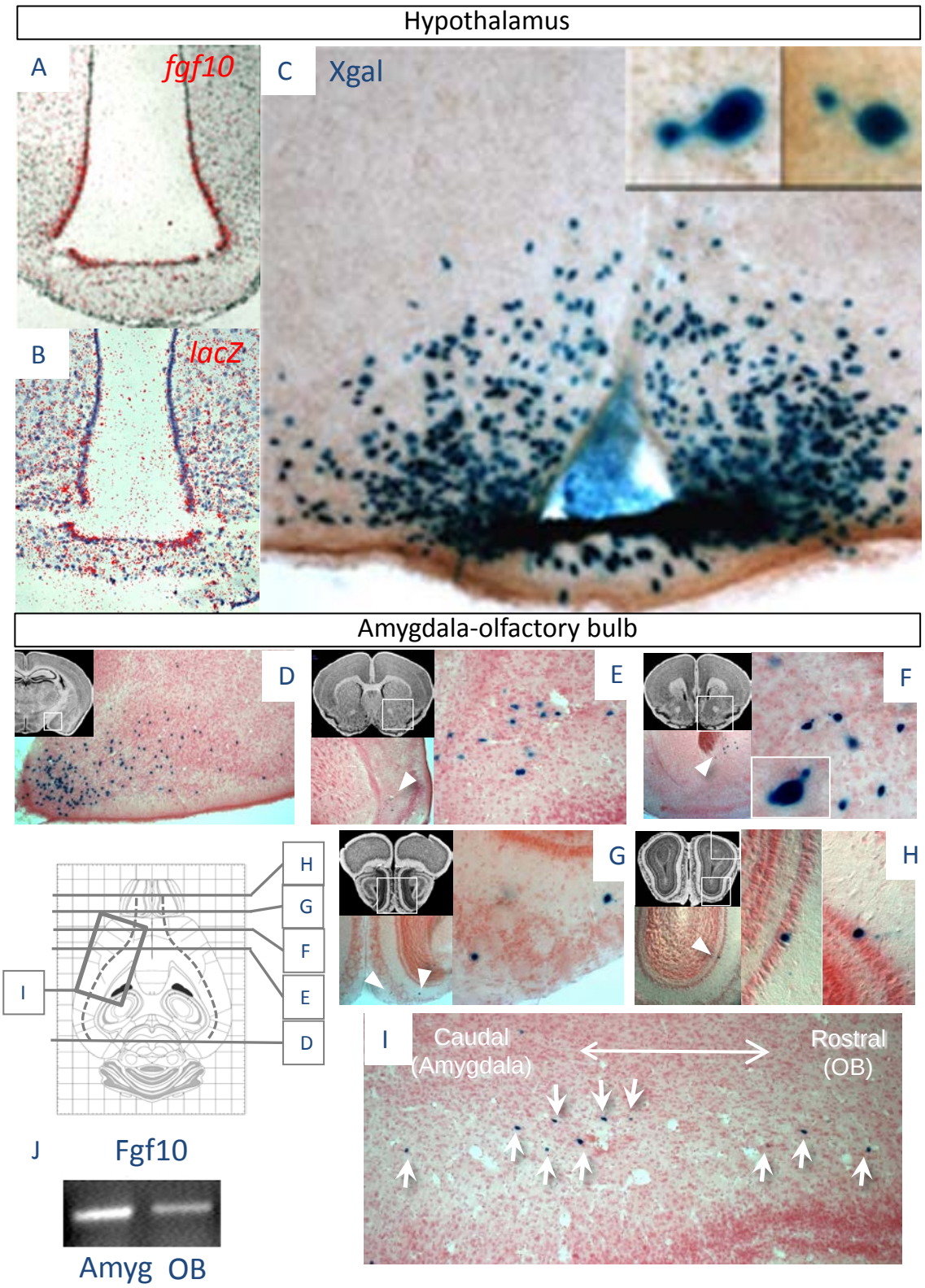

Fig 1.7 - Fgf10 in the adult brain as shown by the Fgf10^{nlacZ} mouse. (A) In the hypothalamus, Fgf10 mRNA is found exclusively in the ventricle wall, the ependyma. (B) This is faithfully repoduced by the LacZ reproter, the mRNA of which is found in the same location. (C) The protein product of the reporter is found far more widespread. Some of these cells show a migratory 'trailing speck' morphology (inset). (D) A strong reporter expression is seen in the amygdala. (E-I) A trainl of Fgf10-lacZ expressing cells connects the amygdala with the olfactory bulb, seen in both coronal (E-H) and horizontal (I) sections. (J) RT-PCR for Fgf10 shows active expression in both amygdala and olfactory bulb bob (OB). Adapted from Hajihosseini et al, 2008

the amygdala generate neuroblasts that migrate towards the olfactory bulb, where they differentiate.

1.16 - Aims

In both the hypothalamus and amygdala, the expression patterns of Fgf10 are suggestive of a possible neural stem cell or progenitor role for Fgf10 expression cells. Both of these areas have previously been shown to contain dividing cells, but the exact identity of these cells, and the progeny they generate has yet to be characterised. In this project, the putative Fgf10 expressing stem cells in the hypothalamus and amygdala, and their putative progeny in the hypothalamus and olfactory bulb, were examined. The main aims, and the methods used to investigate them, were as follows:

(1) Improve detection methods for Fgf10

- Optimisation of both known commercial and novel custom antibodies for Fgf10 in Western blot and immunohistochemistry, in order to be able to directly detect Fgf10 without the need for transgenic animals

(2) To characterise the putative stem cells in the hypothalamus and amygdala

- Immunohistochemistry and Xgal staining in $Fgf10^{nlacZ}$ mice during different developmental stages and throughout adulthood to show the development and fate of the Fgf10 expressing cells throughout life.
- Immunohistochemistry for known neural stem cell markers and the β-galactosidase reporter in $Fgf10^{nlacZ}$ mice to study whether Fgf10 expressing cells are neural stem cells.

- Neural stem cell culture from adult hypothalamus to confirm presence of stem / progenitor cells and investigate their differentiation potential

(3) To characterise and quantify the putative descendants of Fgf10 expressing progenitors in the hypothalamus and amygdala

- Immunohistochemistry for differentiated neuronal and glial cell markers and β-galactosidase in $Fgf10^{nlacZ}$ mice at various ages in hypothalamus and amygdala/olfactory bulb to study the identity and number of differentiated cells derived from the Fgf10 expressing lineage.
- Inducible genetic lineage tracing using $Fgf10^{CreERT2}$ mice, to study descendants from Fgf10 expressing cells generated during specific periods.

(4) To investigate the proliferative capacity of $Fgf10^{+}$ cells

- Long term BrdU administration at different ages to investigate the capacity of Fgf10 expressing cells to divide.
- Use of inducible lineage tracing models to search for expansion of the Fgf10 expressing population during life.

(5) To investigate the properties of $Fgf10^{+}$ cells in vitro in a number of culture models

- Setting up of culture protocols for primary neurons and astrocytes from the postnatal hypothalamus
- Culture of primary cells from Fgf10lacZ mice to assess the capability of the Fgf10 expressing lineage to generate these differentiated cell types in vitro.
- To study the potential of FACS as a method of enriching Fgf10-lacZ expressing cells

Chapter 2

Materials and methods

2.1 - Mouse lines

Unless specified otherwise, all mouse lines were bred and maintained as heterozygots on a mixed genetic background, according to local regulation for use of transgenic animals.

2.1.1 Fgf10$^{nlacZ/+}$

Reporter strain for Fgf10. A lacZ cDNA containing a nuclear localization signal is located downstream of the Fgf10 promotor, but upstream to the first exon of Fgf10 (Kelly et al., 2001). As this generates two separate transcripts, rather than a fusion protein, and the β-galactosidase protein is highly stable in mammalian environment, this allows for temporary lineage tracing. This line has been used for lineage tracing experiment in the developing heart (Kelly et al., 2001) and lung (Mailleux et al., 2005). The line was normally kept on a heterozygous background, but is also viable as homozygotes (Fgf10$^{nlacZ/nlacZ}$). The insertion of the lacZ cDNA causes a slightly hypomorphic phenotype for Fgf10 (Mailleux et al., 2005).

2.1.2 Nestin^{creERT2}

In order to perform inducible genetic lineage tracing on neural stem cells, a CreERT2 cDNA was inserted after the nestin promotor. The cDNA was followed by the second intron of the nestin gene, which contains a transcriptional enhancer required for strong transcription (Imayoshi et al., 2006).

2.1.3 Fgf10^{creERT2}

Part of the first exon and downstream intronic sequences of the Fgf10 gene has been replaced with a construct containing cDNA for the CreERT2 gene, followed by an independent ribosomal entry site (IRES) and a YFP reporter gene. It is important to note that since the transgene renders the first exon of the Fgf10 gene dysfunctional, this allele is also an Fgf10 knockout, and cannot be bred homozygously.

Fgf10 lines

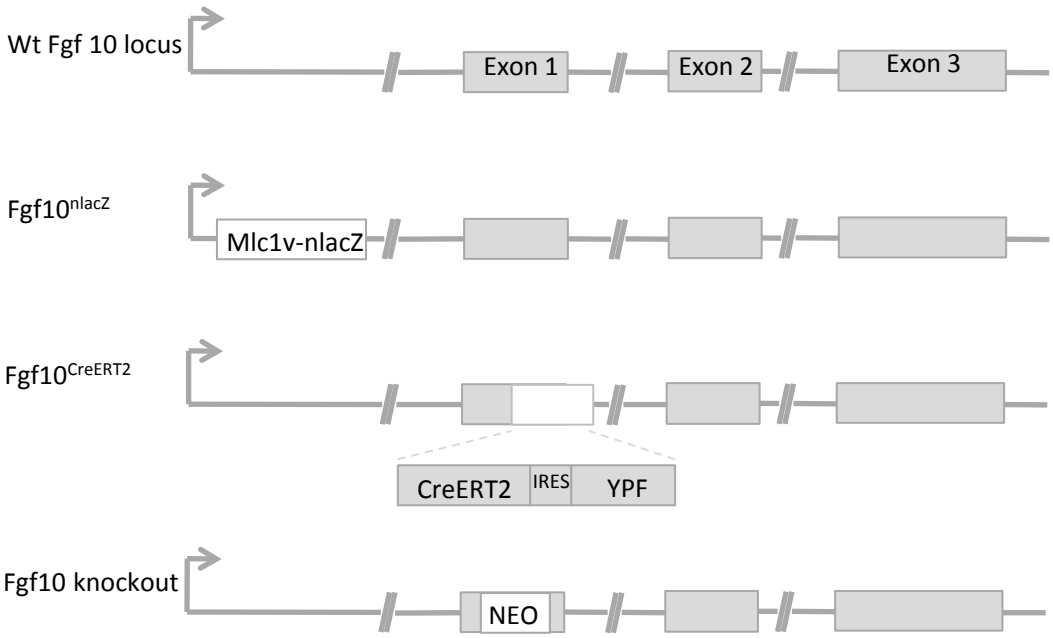

Nestin lines

Reporter lines

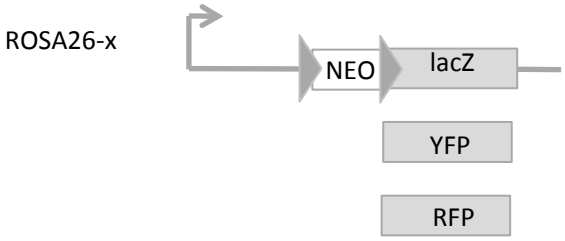

Fig 2.1 Transgenic mouse lines used. The normal Fgf10 locus contains a promoter followed by three coding exons. In the Fgf10^{nlacZ} reporter mouse, a nuclear targeted lacZ has been inserted downstream of the promoter, upstream of the first exon. In the Fgf10^{CreERT2} line, a construct containing CreER2 and a YFP reported separated from each other by a IRES site has been inserted in the first exon, replacing the Fgf10 gene product with separate CreERT2 and YFP products. The Fgf10 knockout line was generated by disrupting transcription of the first exon of Fgf10 by insertion of a neomicin cassette. The Nestin^{CreER} line carries a CreER cDNA after the nestin promoter, which is followed by the second intron of the nestin gene, which contains an important transcriptional enhancer. The ROSA26 reporter lines contain a floxed neomicin followed by a lacZ, YFP or RFP cDNA, all under control of the ubiquitous ROSA26 promotor

2.1.4 ROSA26^{YFP}/ROSA26^{RFP}/ROSA26^{LacZ}

In these generic reporter strains, yellow or red fluorescent protein (YFP or RFP) or a lacZ reporter is inserted in the ubiquitously expressed ROSA26 locus. A loxP flanked neomycin cassette preceding the reporter cDNA prevent this from being expressed except in the presence of Cre recombinase, upon which it will act as a reporter for recombinase activity. These lines are also viable both heterozygously and homozygously

2.1.5 Fgf10 KO

A neomycin cassette was inserted into the first exon of the Fgf10 locus, effectively stopping transcription and forming a Fgf10 knockout (Min et al 1999). The heterozygous mouse has minor phenotypes in glandular development (Entesarian et al 2005), but is viable, the homozygous knock-out is lethal at birth.

2.1.6 Fgf10^{CreERT2}::Rosa26^{Tomato}

These lineage tracing mice were not bred locally, but tissues were obtained from Dr Saverio Belluci at the Justus Leibig Universität, Giessen, Germany.

2.1.7 Breeding and genotyping

The genotypes used, and the matings done to generate them are detailed in table 3.1

Tailsnips were taken from transgenic litters following weaning. The tissue was digested in proteinase K at 55°C overnight and spun down to remove undigested tissue, after which the genomic DNA was precipitated with isopropanol, and resuspended in 30% TE buffer (3 mM Tris, 0.3 mM EDTA). The DNA was then used for genotyping by PCR, using the Expand Long Template System (Roche).

Table 2.1: Crosses used to generate required genotypes				
Parent 1	**Parent 2**	**Resulting genotypes**	**Viable**	**Purpose**
$Fgf10^{lacZ/+}$	Wt	$Fgf10^{lacZ/+}$	y	IM
$Fgf10^{lacZ/+}$	$Fgf10^{lacZ/+}$	$Fgf10^{+/+}$ (wt) $Fgf10^{lacZ/+}$ $Fgf10^{lacZ/lacZ}$	y y y	Western
$Fgf10^{+/-}$	$Fgf10^{+/-}$	$Fgf10^{+/+}$ (wt) $Fgf10^{+/-}$ $Fgf10^{-/-}$	y y n	Western
$Nestin^{cre-ER}$	$ROSA26^{YFP}$	$Nestin^{cre-ER}$::$ROSA26^{YFP}$	y	Genetic linage tracing, IM
$Nestin^{cre-ER}$	$ROSA26^{RFP}$	$Nestin^{cre-ER}$::$ROSA26^{RFP}$	y	Genetic linage tracing, IM
$Fgf10^{cre-ERT2}$	$ROSA26^{lacZ}$	$Fgf10^{cre-ERT2}$::$ROSA26^{lacZ}$	y	Genetic linage tracing, IM

(note: not all possible resulting genotypes are shown, only those that were used)

The primers used for genotyping are detailed in table 3

Table 2.2 – Genotyping primers (5'-3')		
Allele	**Primers**	**Product**
$Fgf10^{lacZ}$	GCA TCG AGC TGG GTA ATA AGC GTT GGC AAT	LacZ: 0.8 kb WT: 0.5 kb
	GAC ACC GAC ACA ACT GGT AAC GGT AGC GAC	
	CGA GFG GAG CAT GTA CTT CCG TGT CCT GAA	
	TCC CTA CCC AGT CAC AGT CAC AGC TGC ATA	
$Nestin^{CreER}$	GGC GGA TCC GAA AAG AAA A	Cre:0.5 kb
	CAG GGC GCG AGT TAG TAG	
$Fgf10^{CreERT2}$	AGC AGG TCT TAC CCT TCC AGT ATG TTC C	Cre: 0.5 kb WT:0.3 kb
	TCC ATG AGT GAA CGA ACC TGG TCG	
	CTC CTT GGA GGT GAT TGT AGC TCC G	
$ROSA26^{YFP}$	AAG ACC GCG AAG AGT TTG TC	WT: 0.6 kb YFP: 0.3 kb
	AAA GTC GCT CTG AGT TGT TAT	
	GGA GCG GGA GAA ATG GAT ATG	
$ROSA26^{RFP}$	AAG ACC GCG AAG AGT TTG TC	WT: 0.2 kb RFP: 0.3 kb
	TAA GCC TGC CCA GAA GAC TCC	
	AAG GGA GCT GCA TGT GAG TA	
$ROSA26^{lacZ}$	AAG ACC GCG AAG AGT TTG TC	WT: 0.2 kb lacZ: 0.3 kb
	TAA GCC TGC CCA GAA GAC TCC	
	AAG GGA GCT GCA TGT GAG TA	
Fgf10 ko	CAC CAA AGA ACG GAG CCG GTTG	KO: 0.9 kb
	ACT CTT TGG CCT CTA TCT AG	

2.2 - Animal treatments

2.2.1 Time mating

Males and females were housed in separate breeding pairs, and checked daily for vaginal plugs. The morning of observation of vaginal plug was taken as E0.5.

2.2.2 BrdU administration

Animals were given ad libitum access to drinking water, slightly acidified with 25 mM HCl to improve BrdU solubility, containing 1 mg/ml of BrdU (sigma Aldrich) and 0.25 mg/ml glucose to mask the bitter flavour of the BrdU and facilitate uptake by the animals. BrdU was administered for a total of 21 days, replacing the BrdU solution every 3 days.

2.2.3 Tamoxifen administration

Tamoxifen (Sigma Aldrich) was administered either as an intraperitoneal (IP) injection, or via food. For injection, tamoxifen was dissolved at 20 mg/ml in corn oil containing 10% ethanol. The injection volume per mouse was 100 µl, resulting in an approximate dose of 80-100 mg per kg bodyweight. Food pellets contained 0.4 g of tamoxifen per kg dry weight. A number of different dosage regimes were used, these are specified in chapter 5.

2.3 - Tissue processing

Unless otherwise noted, animals used for immunohistochemistry were sacrificed with CO_2 asphyxiation, followed by transcardial perfusion with 4% paraformaldehyde (PFA) in PBS and removal of the brain from the skull. If required, wholemount Xgal staining was preformed at this point, with the brain being incubated in 0.5 µg/ml Xgal (from a 20 mg/ml stock in DMF) in Xgal staining buffer (2 mM $MgCl_2$, 5 mM $K_4Fe(CN)_6$, 5 mM $K_3Fe(CN)_6$ in PBS) at 37°C overnight.

Following perfusion, the brain was postfixed in 4% PFA overnight or for 1 hour if following Xgal staining. For vibratome sectioning, the following day the tissue was dehydrated in a graded ethanol series to absolute ethanol, allowing 1 hour for each step, and stored at 4°C until used. For cryostat sectioning, the brain was transferred from the post-fix to a cryopotective solution of 30% sucrose in PBS for 3d, embedded in OCT (Tissue-Tek), and stored at –80°C until used. For some antibodies, brains were removed from the skull without prior fixation, and embedded directly in OCT and frozen, this is referred to as 'fresh frozen'.

To isolate embryonic tissue, time-mated mothers were sacrificed by CO_2 asphyxiation, followed by cervical dislocation. For embryos younger than E14.5, whole embryos were fixed in 4% PFA for 2-3 hours and incubated in Xgal until the staining reached sufficient intensity. At E14.5 and over, the embryos were decapitated, brains were removed from the embryos and fixed and Xgal stained separately. Embryonic tissue destined for immunohistochemistry was treated identically with the exception of the omission of the Xgal staining.

2.4 - Sectioning

For vibratome sectioning, tissues were rehydrated through a graded ethanol series, and embedded in 3% agar in dH_2O at 80°C for 25 minutes, before being set in the desired orientation. 60 µm thick sections were taken on a vibrating microtome (Leica), and stored in sequence in well of 48 well plates in PBS.

Cryostat sections were collected onto slide previously coated with TESPA (3-aminopropyl-triethoxy silane). To coat, slides were dipped 10 times in acetone, 10 times in a 4% TESPA in actone solution, 10 times in actetone, and rinsed under running dH_2O

before being air-dried overnight. 12 µm sections were generated on a freezing microtome (Microm HM560), collected at 2-3 sections per slide, and stored at -80°C.

When serial sections were used for experiments where exact location is of importance, the coordinates of the section in mm from bregma was determined by comparing gross morphology to a stereotactic atlas (Franklin and Paxinos, 2008). For embryonic sections, an embryonic rat brain for comparable stages was used (Altman and Bayer, 1995). Coordinates of sections are given in the distance in mm from the bregma, the standard reference point on the skull where the coronal suture meets the saggital suture.

2.5 - Immunohistochemistry

2.5.1 Antigen retrievals

HCl pre-treatment

Sections were incubated with 1 M HCl in dH_2O at 47°C for 30 minutes, before being thoroughly rinsed in PBS.

Heat mediated (citrate)

Sections were incubated at 80°C with prewarmed 20 mM sodium citrate containing 0.01% Tween 20 at pH 6.0, for 20 minutes, allowed to cool to room temperature, and washed several times in PBS.

Methanol (MeOH)

Sections were incubated for 20 minutes at room temperature in absolute methanol, precooled to -20°C, and washed several times in PBS.

Acid/alcohol (Acid/OH)

Sections were incubated for 20 minutes at room temperature in 5% acetic acid in ethanol, precooled to -20°C, and washed several times in PBS.

Pepsin

Pepsin was dissolved at 10 mg/ml in 10 mM HCl and diluted to a final concentration of 200 μg/ml in PBS. Sections were incubated for 35 minutes (vibratome) or 5 minutes (cryostat) at room temperature, and washed several times with PBS.

Trypsin

Sections were incubated at 37°C for 15 minutes (vibratome) or 3 minutes (cryostat) in 0.05% Trypsin, 0.1% $CaCl_2$ in dH_2O at pH 7.4.

2.5.2 Cryostat section staining

Depending on the primary antibody, different post-fixes of sections were required. Sections were either (1) not post-fixed, (2) fixed in 4% paraformaldehyde at room temperature for 20 minutes, (3) in a 1:1 mixture of methanol and acetone at -20°C for 2 minutes followed by air-drying, or (4) absolute methanol at -20°C for 20 minutes. Following fixation, sections were washed three times, each wash being 5 minutes in PBS. If required, antigen retrieval was preformed at this stage. Nonspecific binding was blocked with 10% normal goat serum (NGS) and 1% Triton X-100 in PBS for 1h at room temperature. Antibodies were diluted in 0.2% normal goat serum (NGS), 0.1% Triton in PBS, and (except where noted otherwise) incubated overnight at 4°C in a humidified chamber. Sections were then washed 3 times 5 minutes in 0.2% NGS and 0.1% Triton, before being incubated for 1h at room temperature in 0.2% NGS and 0.5% NP-40 with the relevant secondary antibodies conjugated to Alexa 488 or 568 or biotin if further signal

amplification was required. For the latter, a second series of 3 washes in 0.2% NGS, 0.1% Triton in PBS was followed with 1h at room temperature in stratavidin conjugated to Cy2 or Texas Red. Sections were then washed 2 times 5 minutes in PBS and counterstained with 5 μg/ml Hoescht in PBS for 10 minutes, before being mounted using Vectashield (Vector Laboratories)

2.5.3 Vibratome staining

If required, antigen retrieval was preformed prior to blocking. Nonspecific binding was blocked with 20% NGS and 1% Triton in PBS for 2 hours at room temperature. All antibody incubations, except where noted otherwise, were at 4°C overnight, in 0.2% NGS and 0.1% Triton in PBS. After primary and seconday/teriary antibody incubations, sections were washed 5 times 1 hour in 0.2% NGS and 0.1% Triton in PBS. Secondary antibodies were used as described in the previous section. Prior to mounting, sections were washed 6 time 30 minutes in PBS, and counterstained with 5 μg/ml Hoescht in PBS for 10 minutes. On Xgal stained sections, peroxidase labeling was preformed. Prior to blocking, endogenous peroxidases were quenched with 6% H_2O_2 in PBS for 90 minutes at room temperature. Sections were stained as above, using HRP conjugated secondaries. Following the last wash, sectioned were further washed in 50 mM Tris, pH 8.0 for 3 times 20 minutes, before the staining was visualised using 3,3' diaminobezidine (DAB). Sections were mounted in glycerol gelly (5% gelatin in 50% glycerol).

Antibodies used for both cryostat and vibratome sectioning are detailed in tables 2.3 and 2.4

Table 2.3 Primary antibodies used

Antibody	Host	Manufacturer	Cat No	Tissue processing	Fix	AR	Dilution	Biotin
Cryostat								
β-gal	Rb	Millipore	AB1211	multiple[1]	multiple[1]	multiple[1]	1:300/1:1000[2]	No
β-gal	Ms	Abcam	ab1047	multiple[1]	multiple[1]	multiple[1]	1:100/1:500[2]	No
Nestin	Ms	Millipore	MAB353	Perfused	Ac/MeOH	-	1:100	Yes
Musashi	Ms	Abcam	AB5977	Perfused	Ac/MeOH	-	1:300	Yes
BLBP	Rb	Abcam	ab32423	Perfused	MeOH	-	1:300	Yes
Ki67	Ms	NovoCastra	NCL-Ki67-P	Fresh frozen	-	Citrate	1:50	Yes
Fgf10	Rb	Pacific Immunology	custom	mutiple	mutiple	multiple	1:10 1:25-1:50[3]	Yes
FgfR1[4]	Hu			Fresh frozen	-	-	1:500	No
FgfR2[4]	Rb	Sigma	F0300	Fresh frozen	-	-	1:500	No
FgfR3[4]	Hu			Fresh frozen	-	-	1:500	No
GAD67	Ms	Millipore	MAB54066	Fresh frozen	Ac/MeOH	-	1:1000	Yes
β-actin	Rb	Abcam	ab8227	n/a	n/a	n/a	1:10000[3]	
Vibratome								
β-gal	Rb	Millipore	AB1211	Perfused	n/a	multiple	1:1000 1:3000[3]	No
β-gal	Ms	Abcam	ab1047	Perfused	n/a	multiple	1:300	No
BrdU	Rb	Sigma	B2531	Perfused	n/a	HCl	1:200	Yes
GFAP	Ms	Millipore	MAB360	Perfused	n/a	-	1:800	No
GFP	Rb	Abcam	ab290	Perfused	n/a	-	1:1000	No
GFP	Rb	Invitrogen	A11122	Perfused	n/a	-	1:300	Yes
NeuN	Ms	Millipore	MAB377	Perfused	n/a	-	1:1500	No
TH[5]	Rb	Millipore	Ab152	Perfused	n/a	Methanol	1:250	Yes

[1] β-gal antibodies are compatible with most protocols, exact protocol is dependant on which other antibody is labeled with
[2] Higher concentrations of antibody are required for fresh-frozen tissue
[3] Dilution for Western blot
[4] A non-standard protocol was used for FgfR stains, where a permeabilisation step with 1% Triton took place prior to blocking, and no further Triton was included in subsequent steps. Primary antibody incubation was for 2h at room temperature.
[5] A 3 day primary incubation was used to detect TH

Table 2.4 Secondary antibodies used					
Host	**Target**	**Conjugation**	**Manufacturer**	**Cat No**	**Dilution**
Gt	Rb	Alexa 350	Invitrogen	A11046	1:1000
Gt	Rb	DyLight 488	Stratech	111-485-003	1:1000
Gt	Rb	Alexa 568	Invitrogen	A11011	1:1000
Gt	Rb	Biotin	Novus	NB7169	1:800
Gt	Rb	HRP	Vector Labs	PI-1000	1:800 1:3000[1]
Gt	Ms	Alexa 488	Invitrogen	A11001	1:1000
Gt	Ms	Alexa 568	Invitrogen	A11004	1:1000
Gt	Ms	Biotin	Stratech	115-065-205	1:300
Gt	Ms	HRP	Sigma	A4416	1:300 1:3000[1]
Gt	Hu	568	Invitrogen	A-21091	1:1000
n/a	n/a	Streptavidin-Tx Red	Stratech	016-070-084	1:800
n/a	n/a	Streptavidin-Cy2	Stratech	016-220-084	1:800

[1] Dilution for western blot

2.6 - Cell culture

2.6.1 Culture surface coatings

For certain cell types, coating of the tissue culture surface was required. Flasks, wells or coverslips were coated with poly-D-lysine (PDL) by incubating in a 20 μg/ml PDL solution in ddH_2O at 37°C overnight. After removal of the coating solution, the surfaces were allowed to dry to the air at room temperature for several hours. In some cases, the procedure was repeated to make double-coated surfaces. For primary neuron cultures, laminin coating was then preformed onto PDL coated surfaces, approximately 1 h prior to plating of the neurons. Previously PDL coated surfaces were coated with 1 μg/ml laminin 1 in DMEM/F12 medium at 37°C. The coating solution was removed immediately prior to plating cells, and not allowed to dry at any time. For some neurosphere differentiation experiments, poly-L-ornithin (PORN) coating was used. Coverslips were coated with 40, 100 or 150 μg/ml PORN in ddH_2O for 1.5h at room temperature, diluted from a 1 mg/ml stock in 150 mM boric acid, pH 8.4.

2.6.2 Neurosphere culture

To establish a neurosphere culture protocol, a number of different protocols were assessed. In all cases, animals were sacrificed by CO_2 asphyxiation and the brains removed from the skull. The subventricular zone and the median eminence of the hypothalamus were dissected out in ice-cold PIPES buffered saline or DMEM/F12. Four different methods of dissociation were tried (Wachs et al., 2003), prior to all of these the tissue was triturated into smaller chunks with a P1000 pipette.

1. Accutase solution (a proprietary protease solution, Invitrogen) at 37°C for 30 minutes
2. 0.05% trypsin in DMEM/F12 at 37°C for 30 minutes
3. 3 mg/ml Papain in PIPES buffered saline, containing 12 mM NaCl, 5 mM KCl, 1 mM L-cysteine, 0.2 mM EDTA at 37°C for 30 minutes
4. Mechanical dissociation by tritrurating using a syringe and 19G, 21G and 23G needles followed by filtration through a 60 µm mesh

Following dissociation, cells were spun down at 1000 rpm for 5 minutes, washed in PBS, spun down again at 1000 rpm for 5 minutes, resuspended in medium and counted before being cultured in a T25 flask in 5% CO_2 at 37°C. In some cases, a density gradient purification using Percoll was preformed by loading the cell suspension after dissociation on top of a 22% or 11% solution of Percoll in PBS, and centrifugating this for 10 minutes at 1800 RPM, before resuspending the cell pellet in the usual manner.

NSC were cultured either in Neurobasal or DMEM/F12 1:1 basal media. All media were supplemented with 2% B27 supplement, 2 mM glutamine, 100 µg/ml Primocin, 2 µg/ml heparin, 20 ng/ml EGF, 10 ng/ml Fgf2. Additionally, for some experiments the basal DMEM/D12 medium was further supplemented with 0.6% extra glucose, 0.1% $NaHCO_3$

and 50 mM HEPES. This is noted as DMEM/F12 (mod). The exact combinations of condition used are detailed in table 2.5.

Table 2.5 - Conditions used for neurosphere culture

Dissociation	**Culture medium**	**Percoll**
Accutase	Neurobasal + B27	-
Mechanical	Neurobasal + B27	-
	DMEM/F12 + B27	-
Trypsin	DMEM/F12 + B27	-
Papain	DMEM/F12 + B27	-
	DMEM/F12 (mod) + B27	22%
	DMEM/F12 (mod) + B27	11%

All NSC were cultured with 5% CO2 at 37°C. Fresh growth factors (FGF2 and EGF) were added two times per week. When monitoring growth rates, 10 randomly selected neuropsheres were imaged regularly to measure their diameter. Growth rate was calculated using $i = \left(\frac{d_n}{d_0}\right)^{\frac{1}{n}} - 1$, where i is growth rate in %, d_0 initial diameter and d_n diameter after *n* days in culture. Three weeks after isolation, and every second week subsequently, neurospheres were dissociated using the same method as they were originally isolated with, spun down at 1000 rmp, and resuspended in fresh medium.

To asses the differentiation potential of cultured neurospheres, cells were plated on a variety of substrates (single or double coats of 20 μg/ml PDL, or 40, 100 or 250 μg/ml PORN) in proliferation medium without growth factor and 2 or 10% added heat inactivated fetal bovine serum. To promote attachment, 5 to 10 neurospheres were plated in the centre of coverslips in an 80 μl drop for 2h, before 500 μl medium was added. The spheres were then cultured for 4 more days, before being fixed in 4% paraformaldehyde for 15 minutes, and stained for differentiation markers (Tuj1, GFAP and Olig2).

2.6.3 Primary neurons

Under aseptic conditions, brains were removed from adult (P60-P90) animals following CO2 asphyxiation, and placed in ice-cold DMEM/F12 medium. The hypothalamus was dissected out, taking care to include the parenchyma. The tissue was transferred to 0.05% trypsin/1 mM EDTA prewarmed to 37°C, broken up by triturating with a P1000 pipette and incubated at 37°C for 40 minutes, with regular trituration. Cells were then spun down at 1000 RPM for 10 minutes, resuspended in medium (DMEM/F12 containing 10% FBS, 1% L-glut, 1% Na Pyruvate, 1% Pen/Strep and 10 ng/ml Fgf2) and plated at 250.000 cells per well onto PDL and laminin coated 24 well plates, plating directly onto the well plastic. 48 hours after plating half the medium wass replaced with fresh medium. 3-5 days after plating, differentiated were observed, and cultures were fixed for X-gal staining or immunohistochemistry.

2.6.4 Primary astrocytes

Brains were removed from pups at post-natal day 1-3, and placed into ice-cold DMEM. 4 to 6 brains were pooled and transferred to 0.25% trypsin/1 mM EDTA containing 1 mg/ml DNAseI, prewarmed to 37°C, broken up by triturating with a P1000 pipette and incubated at 37°C for 25 minutes, with regular trituration. Cells were then spun down at 800 rpm for 5 minutes before being resuspended in medium (DMEM containing 10% FBS and 1% Pen/Strep) and plated in T75 flasks with a single PDL coating at a density of 1.5 whole brains per flask. Medium was replaced with fresh medium twice per week, until cells were confluent, at which point they were be passaged by incubating with 0.25% trypsin/1mM EDTA until all astrocytes were detached, as which points cells were diluted with fresh medium to obtain a 1:3 split. Alternatively, cells were plated onto

13 mm glass coverslips, previously coated with PDL. 24-48 hours after plating onto coverslips, cultures were fixed for immunohistochemistry.

2.6.5 Cell lines

Cell lines used were the mouse embryonic fibroblast line NIH3T3, and the ψ2 line, a mouse embryonic fibroblast line stably transfected with a cytoplasmic lacZ (Mann et al., 1983). Both lines were maintained in T75 flasks. Medium for the 3T3 cells consisted of DMEM with 10% FBS, 1% L-glut and 1% Pen/Strep, for the ψ2 cells DMEM with 10% NCS, 1% L-glut and 1% Pen/Strep was used. Both lines were passaged using 0.25% trypsin/1 mM EDTA at a 1:30 dilution two times per week.

2.6.6 - Xgal staining on cells

Cultures were rinsed with PBS, fixed with 0.5% gluteraldehyde in PBS at room temperature for 15 minutes, and rinsed thoroughly with PBS, before being incubated in X-gal staining solution at 37°C until positive cells were observed, typically approximately 30-90 minutes.

2.7 - Immunocytochemistry

Cells were rinsed in PBS and fixed in 4% PFA at room temperature for 15 minutes. Following fix, cells were washed 5 minutes in PBS, permeabilised with 1% Triton in PBS for 5 minutes, and washed again with PBS for 5 minutes. The staining protocol is identical to that for cryostat sections, with the exception that no detergents were used after permeabilisation.

2.8 - Microscopy

Fluorescently stained sections or cells were imaged on a Zeiss Axioimager M2 with an Apotome attachment, allowing for optical sectioning and three-dimensional reconstructions through the use of structured illumination. Imaged were acquired and processed using Axiovision 3.8. Where vibratome sections were used to quantify cell numbers, three-dimensional reconstructions were used to avoid double-counting cells. Primary cultures grown directly in 24 well plates were imaged using an inverted fluorencent microscope. Xgal stained sections were imaged on an upright microscope using differential interference contrast (DIC).

2.9 - Flow cytometry

In order to be able to enrich $lacZ^+$ cells in culture, a flow cytometry method for detection was developed based on the β-galactosidase substrate fluorescein-di-β-D-galactopyranoside (FDG). Cleavage of this substrate by β-galactosidase liberates fluorescein, giving a fluorescent signal. Stock solutions of FDG were prepared at 2 mM in DMSO or at 20 mM in a 1:1:8 mixture of DMSO:ethanol:ddH_2O. Ψ2 cells (positive control) and 3T3 cells (negative control) were trypsinised, spun down at 800 rpm for 5 minutes, and resuspended at $1x10^7$ cells per ml. The cell suspensions were then mixed in a 1:1 ratio with FDG substrate, diluted in ddH_2O to the appropriate concentration, to obtain a hypotonic loading solution. FDG concentration varied from 40 µM to 2 mM, and loading times of 1-5 minutes were used. Following loading, the hypotonic mixture was diluted 10-fold in ice-cold medium, after which the cells were kept on ice for 15-30 minutes, during which the substrate was metabolized to fluorescein in cells expressing β-galactosidase. The cell suspensions were then measured for fluorescence on an Accuri C6 flow

cytometer, with at least 20.000 events per sample measured with appropriate gating in forward- and side-scatter to exclude cell debris. After flow cytometry, the remaining cells were counterstained with Hoescht, and observed microscopically to asses substrate specificity. In parallel, cells grown on coverslips were also loaded with FDG and observed microscopically.

2.10 – Reverse transcriptase PCR

2.10.1 Sample preparation

Wildtype C57Bl6 mice were sacrificed by CO_2 asphyxiation followed by cervical dislocation. Brains were removed from the skull, and the hypothalamus removed, snapfrozen on dry ice, and stored at -80°C until use. 3 to 4 hypothalami were pooled for RNA isolation. Frozen tissue was thawed on ice in 500 μl Tri reagent for 10 minutes, before being dissociated by repeated trituration with a 19G, 21G and 25G needle and syringe. 100 μl of chlorophorm was added, and the resulting mixture was incubated at room temperature for 3 minutes before being spun at 13000 rpm for 15 minutes at 4°C. The aqueous upper phases was transferred to a new tube, 500 μl of isopropanol was added, and the RNA precipitate was pelleted by centifugation at 13000 rpm for 15 minutes at 4°C. The supernatant was removed, and the pellet was washed in 70% ethanol and spun again at 13000 rpm for 10 minutes. The supernatant was removed, and the RNA pellet was airdried briefly before being resuspended in ddH_2O. Concentration and purity of RNA was assessed using a Nanodrop spectrophotometer.

2.10.2 RT-PCR

2 step RT-PCR was preformed using Illustra Ready-to-go RT-PCR beads (GE Healthsciences), according to manufacturers instructions, using 1 μg of template RNA. Primers used are detailed in table 2.6

Table 2.6: Primers (5'-3') and product sizes for different FgfR isoforms

Receptor	Primers	Product size (bp)
FgfR1IIIb	GCA GGG CTG CCT GCC AAC GAG ACA GTG	300
	GGT CTG GTG CAG TGA GCC ACG CAG ACT G	
FgfR1IIIc	GCA GGG CTG CCT GCC AAC GAG ACA GTG	306
	GAA CGG TCA ACC ATG CAG AGT GAT GG	
FgfR2IIIb	CCC ATC CTC CAA GCT GGA CTG CCT	317
	CTG TTT GGG CAG GAC AGT GAG CCA	
FgfR2IIIc	CCC ATC CTC CAA GCT GGA CTG CCT	310
	CAG AAC TGT CAA CAA TGC AGA GTG	
FgfR3IIIb	GAC AGA CAC ACG GAT GTG CTG GA	350
	GTG AAC ACG CAG CAA AAG GCT TT	
FgfR3IIIc	GAC AGA CAC ACG GAT GTG CTG GA	348
	AGC ACC ACC AGC CAC GCA GAG	
FgfR4	TAC AGC TAT CTC CTG GAT GTG CTG	195
	GAA ACC GTC GGC GCC GAA GCT GCT	

The following cycles were used:

Reverse transciptase
42°C 15 min
95°C 5 min

PCR
95°C 30 sec
56°C 30 sec
72°C 1 min
35 cycles

Following RT-PCR, samples were resolved on a 1.8% agarose in TBE gel and visualized using ethidium bromide under UV illumination.

2.11 - Western blot

2.11.1 Sample preparation

Samples for western blotting were prepared from snap-frozen whole brains (E14.5) or isolated hypothalami (adults). To obtain embryonic tissue, time-mated mothers were sacrificed by CO_2 asphyxiation at E14.5, with day of finding plug being E0.5. The embryos were removed from the uterus, and heads were removed and snap-frozen on dry ice. For adult tissue, processing was identical to that for RT-PCR. Embryonic tissue was used in case of $Fgf10^{-/-}$ animals and their littermate controls, as the knockouts are not viable. The genotypes of the animals used are detailed in table 2.1.

For lysis, samples were thawed on ice in ice-cold RIPA buffer (150 mM NaCl, 50 mM Tris, 1.25 mM EDTA, 1% Triton, 1% sodium deoxicholate, 0.1% SDS) for 10 minutes, before being dissociated with a 1 ml syringe using a 19G, 21G and 23G needle. Unlysed material was removed from the lysate by centrifugation at 13.000 rpm at 4°C for 10 minutes, after which the supernatant was transferred to a fresh centrifuge tube and spun again to ensure full clearing of the lysate. Protein concentration of the lysates was measured by spectrophotometry. Lysates were stored at -80°C until use.

2.11.2 SDS-PAGE and transfer

45 μg of total protein was prepared for western blotting by mixing with 6X loading buffer and ddH_2O for a total sample volume of 25 μl. Samples were heated to 100°C for 1 minute to ensure full denaturation of proteins. In order to probe for Fgf10 (23 kDa) and β-actin (42 kDa), an 18% resolving gel (18% acylamide, 375 mM Tris, 0.1% ammonium persulphate, 0.25% TEMED) with a 5% stacking gel (5% acrylamide, 125 mM Tris, 0.15% ammonium persulphate, 0.4% TEMED) was run, to optimize separation of lower

molecular weight proteins. Samples were loaded in sample buffer containing 60 mM Tris-Cl pH 6.8, 2% SDS, 10% glycerol, 5% β-mercaptoethanol and 0.01% bromophenol blue, along with a protein ladder. Gels were run at 35 mA per gel in running buffer (25 mM glycine, 250 mM Tris, 0.2% SDS) until the 10 kDa marker reached the bottom of the gel (approx 90 minutes). The resolving gel and sufficient filterpaper were soaked in transfer buffer (192 mM glycine, 25 mM Tris, 20% methanol) for 20 minutes, while the PDVF membrane was activated by rinsing in absolute methanol for 1 minute, after which this was also soaked in transfer buffer for 20 minutes. Protein was transferred using the semi-dry method, at 15V for 45 minutes.

2.11.3 Detection

Different protocols were used to optimize the detection of Fgf10. This included blocking in the traditional milk, or using Millipore BlØk-CH noise canceling reagent. Processing was done either using the traditional method, or using the vacuum driven Millipore snapID system. Following transfer, membranes were blocked in either 5% non-fat milk powder in PBST (PBS containing 0.5% Tween-20) or in Millipore BlØk-CH noise canceling reagent for 3 hours at room temperature. Antibodies were diluted in 0.5% milk in PBST or BlØk-Ch, with anti-Fgf10 at a 1:50 dilution, anti-β-gal at 1:3000 and anti-β-actin at 1:10.000. The membranes were incubated with antibody overnight at 4°C (Fgf10, β-gal) or 2 h at room temperature (β actin). Membranes were then washed 3 times 30 minutes in 0.5% milk in PBST (when blocked in milk) or PBST alone (when blocked in BlØk-Ch), and incubated with 1:3.000 HRP conjugated anti-rabbit secondary antibody in the same buffer for 1 h at room temperature. Following secondary antibody incubation, all membranes were washed in PBST for 3 times 30 minutes, before proceeding to ECL detection. When

using the snapID system, antibody incubations were identical, but membranes were washed using 3 times 10 ml of PBST, pulled through the membrane under mild vacuum.

2.11.4 ECL detection

Membranes were incubated in ECL solution, consisting of 100 mM Tris, pH8, containing 1.25 mM luminol, 0.2 mM coumaric acid and 0.01% H_2O_2 for 1 minute and exposed to the film (Hyperfilm ECL). Typical exposure times were 1-2 minutes for Fgf10, and 5-10 seconds for β-actin, when processing using snapID exposures 3-4 times this were required.

2.11.5 Quantification

Densitometry was preformed in ImageJ. Values are represented as the ratio of FGF10 to β-actin.

2.12 Statistical analysis

When comparing two groups, Student's t-test was preformed in Microsoft Excel 2008. For experiments containing multiple different groups, an ANOVA with Tukey post-hoc test was preformed in SPSS 16.0. Values were expressed as averages with standard error of the mean.

Chapter 3

Optimisation of detection of FGF10 protein in immunohistochemistry and Western blot

3.1 – Introduction

In order to study Fgf10, detection of the expression of this factor is required. Although a number of methods already exist, these each have their advantages and disadvantages. In situ hybridisation for Fgf10 gives clear expression patterns but does not give direct information about the protein product of the Fgf10 mRNA. A number of reporter strains, as also used in this project, come with their own sets of complications. The $Fgf10^{nlacZ}$ line provides a convenient way of detecting the Fgf10 expressing lineage. However, due to the fact the lacZ reporter is expressed as a separate mRNA and the β-galactosidase protein is very long lived, temporal dynamics of Fgf10 expression cannot be determined with this line. While this property does allow for limited lineage tracing in this line, it also complicates interpretation of results.

This novel $Fgf10^{CreERT2}$ line, as validated in this report, represents an alternative to the $Fgf10^{nlacZ}$ line, but suffers from the same limitations regarding timing of expression. Although the start of reporter expression can be controlled by administration of tamoxifen, the recombination event makes reporter expression permanent, and independent of Fgf10 promoter activity. Additionally, in these transgenic strains, the reporter is expressed as a separate protein in Fgf10 expressing cells, thus not providing any information on the subcellular localisation of Fgf10. As Fgf10 is both secreted, and possibly has a nuclear role (Kosman et al., 2007), the subcellular localisation of Fgf10 may have functional consequences.

These limitations could be overcome by the use of a suitable anti-Fgf10 antibody for use in immunohistochemistry and Western blotting. A number of companies offer antibodies against Fgf10, including Abcam, R&D Systems, Abnova and Santa Cruz. Although many of these claim to be able to detect Fgf10 in immunohistochemistry, this does not seem to be reliable, as Western blots shown for these antibodies frequently show a band of 40 to 50 kDa, whereas Fgf10 is 21-23 kDa (depending on species). Although over-expressed exogenous Fgf10 may be

detected using anti-FGF10 antibodies in cells (Kosman et al., 2007), endogenous levels of FGF10 have yet to be detected in a reliable manner using commercial antibodies.

Through collaborators, a novel custom antibody against FGF10 was obtained. This antibody was raised in rabbits against a peptide from the sequence of chicken FGF10 conjugated to keyhole limpet hemocyanin. The immunisation and production protocol is in fig 3.1. Availability of this novel antibody represents a new possibility of detecting FGF10 in both Western blots and immunohistochemistry.

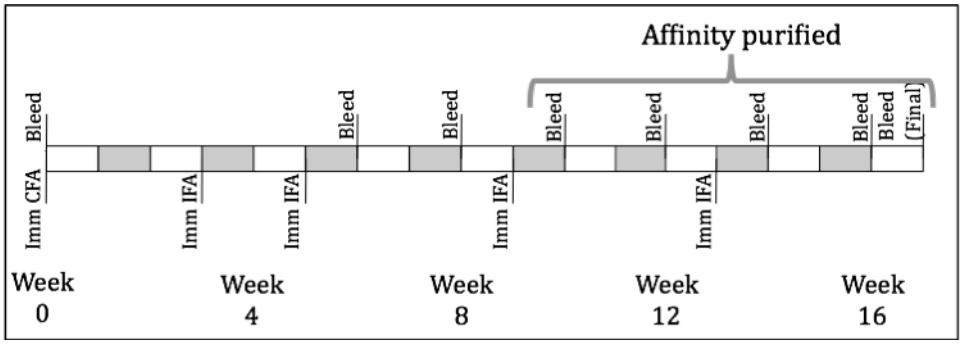

Fig 3.1: Immunisation and production schedule for production of anti-Fgf10 antibody. At the start of the protocol, a pre-immunisation bleed was taken, and the animals were immunized with the Fgf10 peptide in Complete Freund's Adjuvant ("Imm CFA"). Further immunizations in Incomplete Freund's Adjuvant took place at weeks 3, 5, 9 and 13. ("Imm IFA"). Production bleeds took place at weeks 6, 8, 10, 12, 14, 16 and 17. Apart from weeks 6 and 8, these bleeds were further processed by column affinity purification.

Aims

In order to develop a working protocol for the detection of FGF10 in both immunohistochemistry and Western blots, a thorough optimisation of conditions for immunohistochemistry for both a number of commercial and the novel custom anti-FGF10 antibody were preformed. Additionally, the specificity of the novel antibody was analysed with Western blotting.

3.2 – Results

3.2.1 Commercial anti-FGF10 antibodies do not work in immunohistochemistry

In order to optimise staining for FGF10 with three commercially available antibodies in a number of different conditions and antigen retrieval techniques were used, these are detailed in table 3.1.

Table 3.1 – Conditions and results of optimisation of commercial anti-FGF10 antibodies in IHC

	Post-fix	**Antigen retrieval**	**Antibodies**		
			Santa Cruz		Abnova
			Sc-7917	Sc-7375	H00002255-A01
Vibratome sections	n/a	-	-	-	-
		Citrate	-	-	-
		MeOH	-	-	-
		Acid/OH	-	-	-
		Pepsin	-	nd	-
		Trypsin	-	nd	-
Cryostat sections	PFA	-	-	-	-
	MeOH		-	-	nd
	PFA	Citrate	-	-	-
	MeOH		-	-	nd
	PFA	Acid/OH	-	-	-
	MeOH		-	-	nd
	PFA	Pepsin	nd	-	-
	MeOH		nd	-	nd
	PFA	Trypsin	nd	-	-
	MeOH		nd	-	nd

Many different conditions for immunohistochemistry were tried for three commercially available anti-FGF10 antibodies, and are detailed in the above table. "-" signifies no observed stain, "nd" is not determined. Abbreviations: MeOH: methanol, Acid/OH: acid/alcohol, PFA: paraformaldehyde

None of the tested conditions resulted in any staining in the brain.

3.2.2 Custom anti-FGF10 does not appear to be specific for FGF10.

An affinity purified polyclonal rabbit antibody raised against a chicken FGF10 peptide was used in immunohistochemistry. A number of conditions were tried including different blocking agents in order to obtain immunoreactivity and improve specificity of any label.

Table 3.2 – Conditions and results of optimisation of custom anti-FGF10 antibody in IHC				
	Post-fix	**Antigen retrieval**	**Blocking**	**Result**
Vibratome	n/a	-	20% NGS	-
		Citrate	20% NGS	-
		MeOH	20% NGS	-
		Acid/OH	20% NGS	-
Cryostat	PFA	-	10% NGS	-
		Citrate	10% NGS	-
		Pepsin	10% NGS	-
	Ac/MeOH	-	10% NGS	++
			5% BSA	+
			2% Milk/2% BSA	+/-
		Citrate	10% NGS	-
		Pepsin	10% NGS	-

Many different conditions for immunohistochemistry were tried for three commercially available anti-FGF10 antibodies, and are detailed in the above table. "-" signifies no observed stain, "++" strong stain and "+" and "+/-" progressively weaker stains.

Immunoreactvity was seen in a number of the above conditions (fig 3.1). Staining was observed across both the ependyma and the parenchyma in many cells, in a pattern more widespread than seen with Fgf10 in situ hybridisation or in the $Fgf10^{nlacZ}$ line. In the ependyma, staining was observed in many, but not all, cells and was located in a distinct subcellular concentration, generally facing the ventricular space. In the ependyma, the staining was more punctate, and located mostly perinuclear. In the rest of the brain, widespread immunoreactivity was observed (figure 3.2). Pre-immune serum does not show any immunoreactivity (data not shown). In the Fgf10 expressing hippocampus, staining was observed in most cells, in a punctate pattern similar to that seen in the hypothalamic parenchyma. In the neocortex, not known to express Fgf10, sparse staining was seen, with a relatively large portion of the cytoplasm of cells filled with punctate labelling.

3.2.3 Custom anti-FGF10 does detect FGF10 in western blot, but is not specific

When probing adult hypothalamus lysate with the custom anti-FGF10 antibody as unpurified serum, a band of 23 kDa, corresponding to the predicted size for mouse FGF10 is observed (fig 3.4). However, many higher molecular weight bands are also seen. These are not protein complexes, as they are still present in stronger reducing conditions using DTT or TCEP.

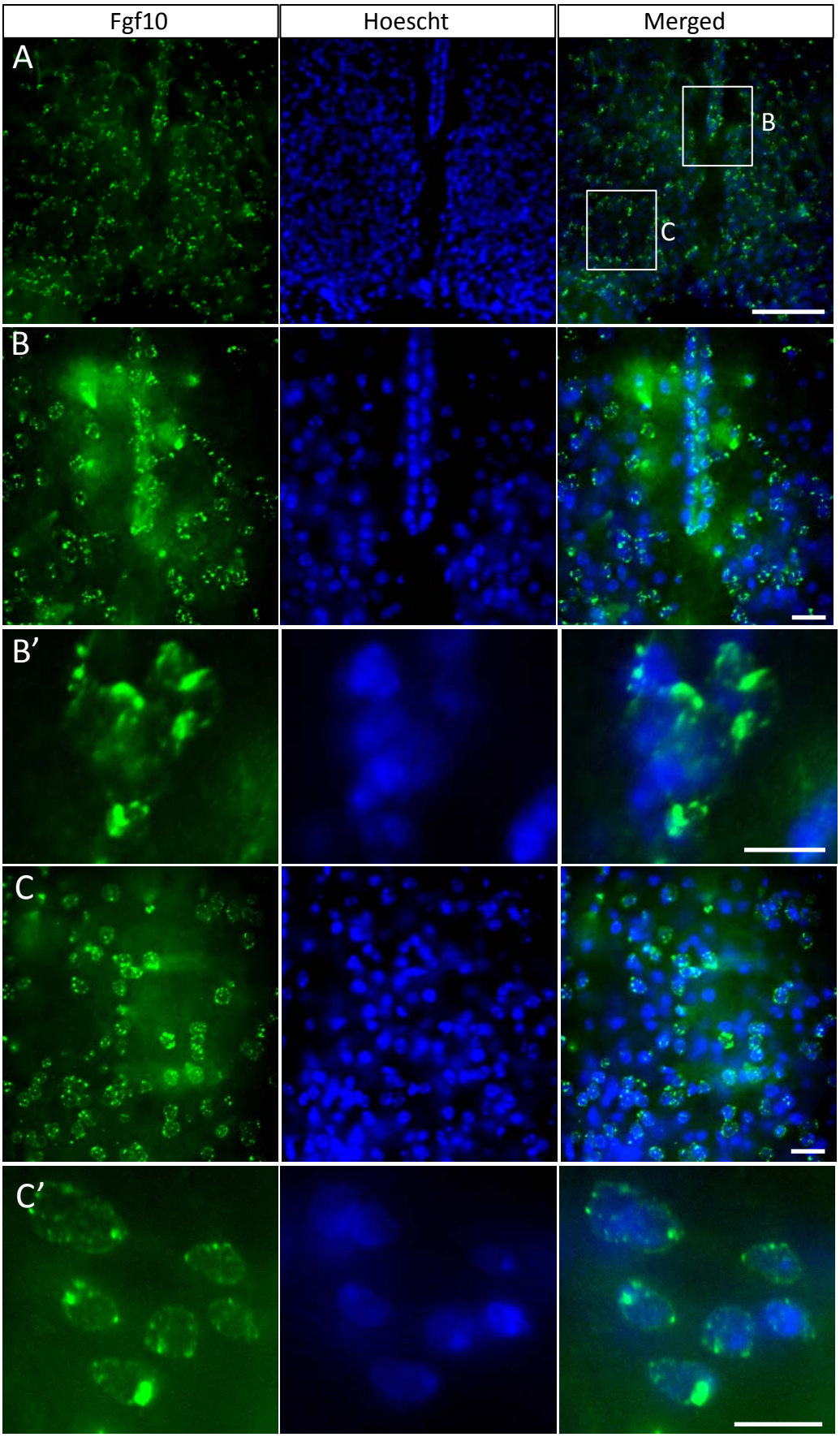

Figure 3.2 – Immunohistochemistry with custom anti-Fgf10 antibody in the hypothalamus. (A) The antibody shows immunoreactivity throughout the hypothalamus. (B) The ventricle wall contains many immunoreactive cells. (B') The staining is no located uniformly throughout the cells, but seems to be in clusters. (C) In the parenchyma, a heterogeneous expression pattern is seen. (C') Here, the localisation of the immunoreactivity is cytoplasmic and predominantly perinuclear. Scalebars: A: 100 µm, B-C': 10 µm

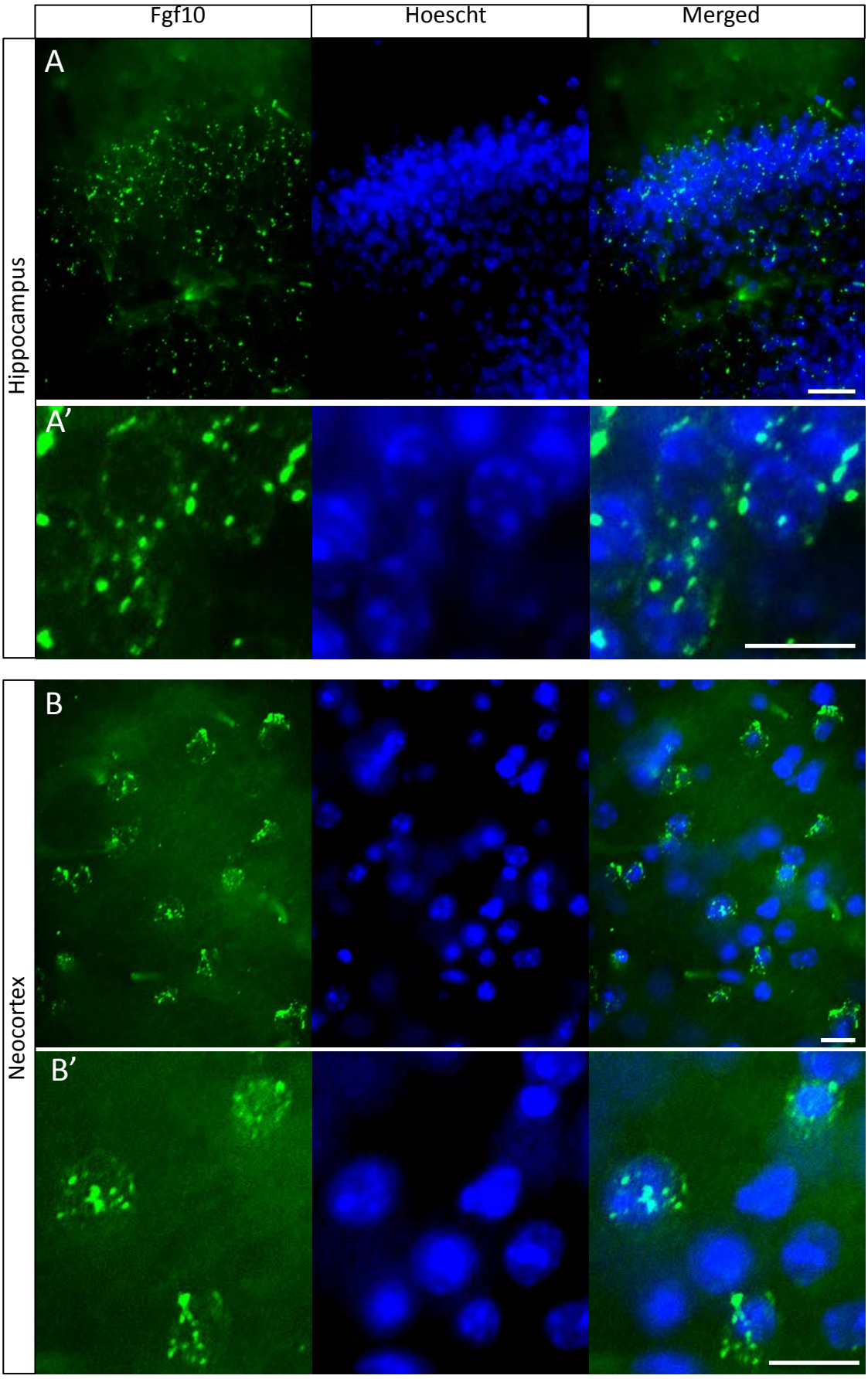

Figure 3.3 – Immunohistochemistry with custom anti-Fgf10 antibody in the hippocampus and neocortex. (A, A') Most cells in the hippocampus show immunoreactivity for the custom anti-Fgf10 antibody, in a characteristic cytoplasmic punctate pattern. (B, B') Many cells in the neocortex also show immunoreactivity. Scalebars : A: 25 µm, A'-B': 10 µm

The latter causes an overall decrease of band intensity, but does not improve specificity. The pre-immune serum form the same animal does not show any bands (fig 3.4b). When using affinity purified serum, bands are both stronger and the detection is somewhat more specific as fewer bands are observed. The banding pattern is identical between adult hypothalamus lystate and embryonic (E14.5) whole brain lystate, where Fgf10 is highly expressed in the developing hypotahlamus. The 23kDa band is not visible in lysates for Fgf10 KO embryonic brains, confirming this band is indeed FGF10 (fig 3.4c), but the higher molecular weight bands are still present. Specificity is not improved by titrating down antibody concentration, as only the strongest bands remain in lower dilutions, which do not include the 23 kDa FGF10 band (fig 3.4d)

3.2.4 Specificity can be somewhat improved using unconventional blotting techniques

In a further attempt to improve specificity different blocking reagents and blotting methods were tried. Use of the proprietary non-protein BlØk blocking reagent does decrease background, and blocks some of the higher molecular weight bands, but does not make the antibody fully specific. Combining this buffer with the vacuum-driven SnapID blotting system decreases background somewhat, but also decreases general band intensity, which can be compensated for by doubling primary antibody concentration. This leads to a similar blot as using BlØk in a conventional western.

Table 3.3 Band patterns and strengths in different methods for blotting for FGF10

Blotting method / Band size	Conventional	SnapID		
	Milk	BlØk		
	1:50	1:50	1:50	1:25
23	++	++	+	++
34	+/-	++	+/-	++
42	-	+/-	+/-	+
45	++	-	-	-
50	++	+	+/-	+/-
60	+	++	+	+
75	++	-	-	-

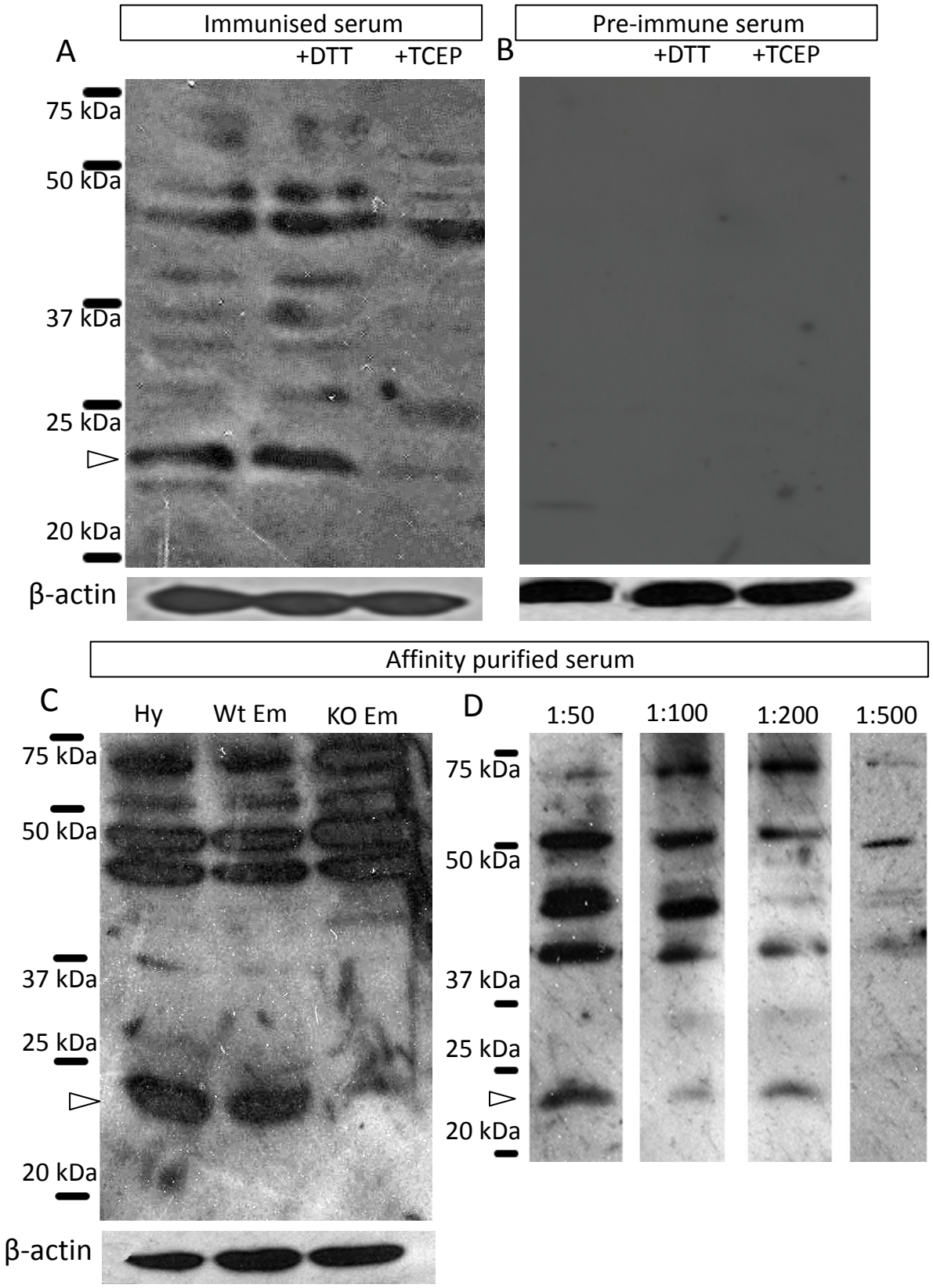

Figure 3.4 – Western blotting for Fgf10. (A) Using unpurified immunised serum results in many weak bands, including one of the appropriate size for mouse Fgf10 (23 kDa, arrowhead). Using harsher reducing conditions (DTT or TCEP) removed some of these bands. (B) Pre-immune serum from the same animal does not show any significant bands. (C) Affinity purification leads to a cleaner blot, but higher molecular weight bands are still present. Fgf10 is detected at 23 kDa in adult hypothalamus (Hy) and Wt embryonic brain (Wt Em), but is absent from Fgf10 KO embryonic brain (KO Em). (D) Titrating down the antibody concentration does not improve specificity.

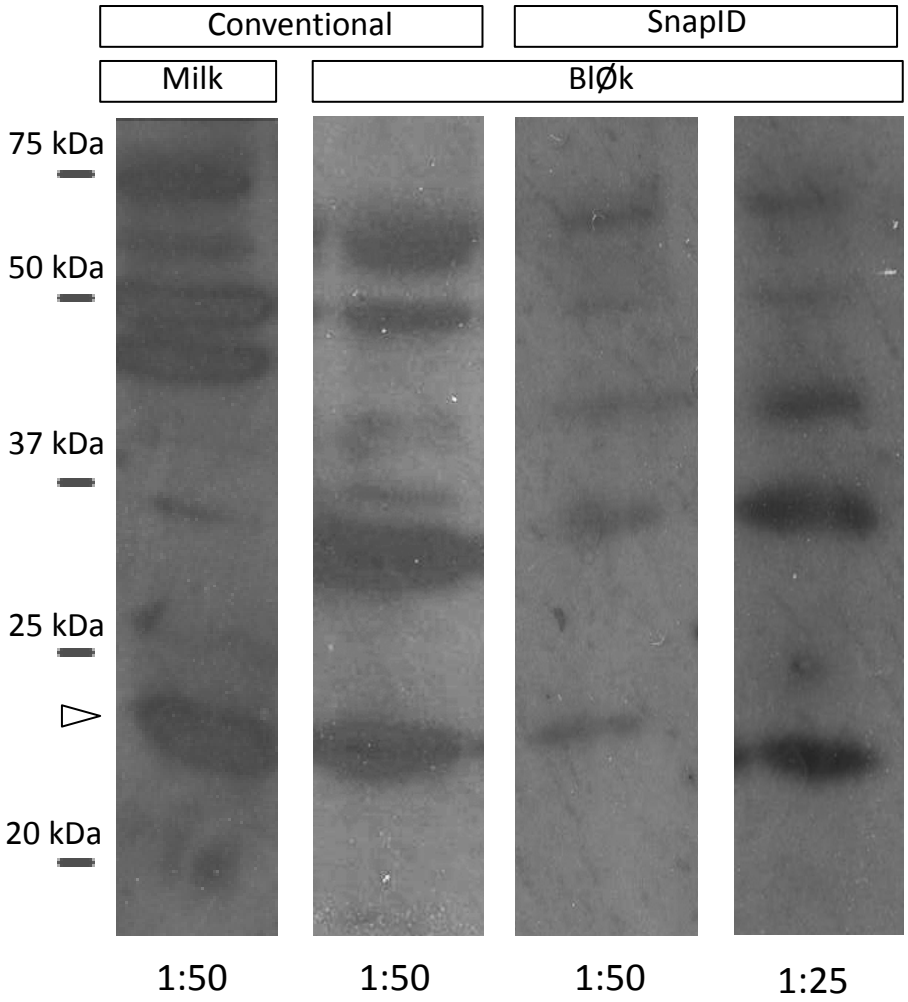

Figure 3.5 – Optimisation of Western blotting for Fgf10 with different blotting methods. Compared to the baseline western, blocked in milk, the use of the BlØk reagent improves the background, and gives fewer bands. When this buffer is used on the SnapID blotting system, background is low as wel, but overall band intensity is reduced. This can be remedied by using higher primary antibody concentrations.

3.2.5 Custom antibody may be used for quantification of FGF10 protein levels

To test whether this antibody can be used quantitatively, hypothalamic lysates from $Fgf10^{+/+}$, $Fgf10^{+/lacZ}$ and $Fgf10^{lacZ/lacZ}$ animals were compared. It is known that the lacZ allele slightly decreases FGF10 levels, creating a mild hypomorph. When blotting for FGF10, a slight decrease in FGF10 levels is seen in the transgenic animals (fig 3.6). Their transgenic nature is confimed by blotting for β-galactosidase. When the levels of FGF10 as a ratio of β-actin levels are compared, is can be seen that the presence of the transgene decreases the levels of FGF10 by 35% to 43% for heterozygous and homozygous, respectively.

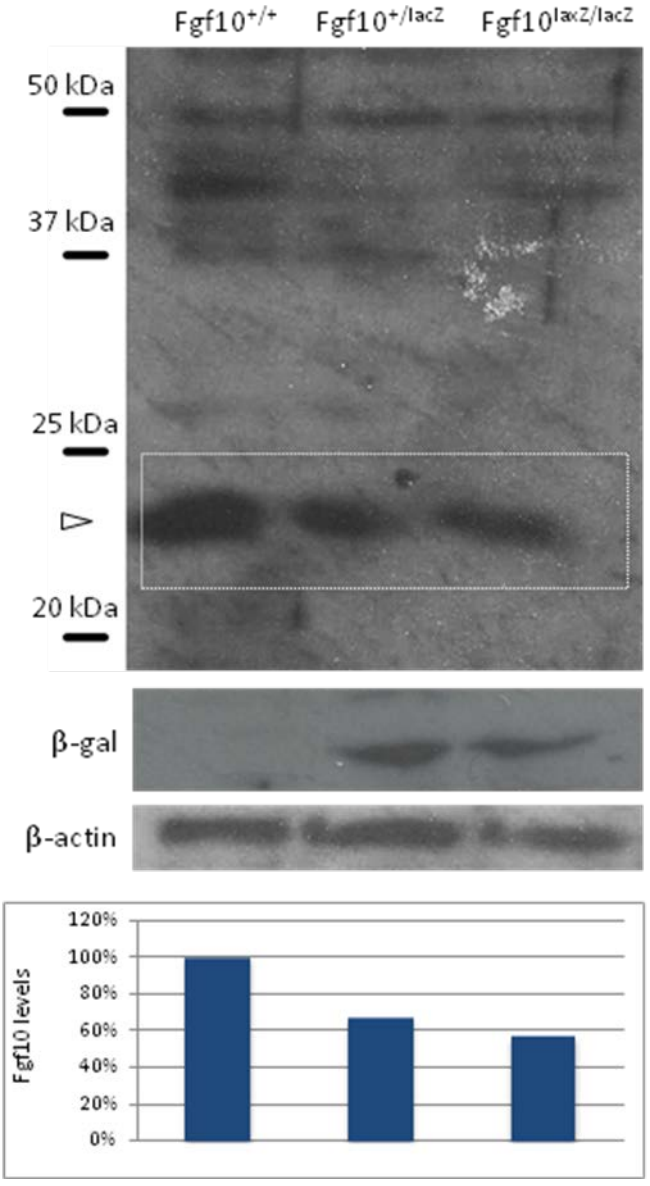

Figure 3.6 – Quantitative use of the anti-Fgf10 antibody. Fgf10 levels (arrowhead) are decreased in heterozygous and homozygous transgenic animals. Expression of the transgene is confirmed by the presence of β-gal protein. When quantified, it is clear that the transgenic animals do have lower Fgf10 protein levels. The region of the gel used for quantification is indicated by the dotted box

3.3 Discussion

The current inability to detect endogenous FGF10 in tissue or western blots limits the options to elucidate the role of FGF10 in the adult brain. Detecting endogenous FGF10 by immunohistochemistry would provide an accurate read-out of protein location in time, which is not possible with current means.

Contrary to any tested commercial antibody, the novel anti-FGF10 antibody does produce staining in adult brain sections. However, the staining is far more widespread than expression of FGF10 as seen by in situ hybridisation or in the $Fgf10^{nlacZ}$ or $Fgf10^{CreERT2}$ lines. The expression throughout the hypothalamus and hippocampus is at odds with the established expression pattern, as in situ data has shown the Fgf10 transcript is limited to the epenymda of the hypothalamus and a thin layer of the dentate gyrus of the hippocampus. Additionally, widespread expression in the neocortex and other brain areas that are not known to express Fgf10 makes this expression pattern suspect. Given the large mismatch in immunoreactivity seen with this antibody and the established expression domains of Fgf10 makes it unlikely it is actually specifically picking up Fgf10.

This lack of specificity is confirmed by Western blot, where apart from FGF10, a number of higher molecular weight bands are also observed. The observed 23 kDa band is FGF10, as it is not present in lystates from Fgf10 knockout embryos. Although the higher molecular weight bands were generated as a result of the immunisation, as they are not present in the pre-immunisation serum, these are not directly related to FGF10 as they are still present in the knockout lystate. These also do not represent protein complexes, as strongly denaturing sample buffers containing DTT or TCEP do not remove these bands.

Although the background of the Western can be improved with different blotting techniques, the band pattern remains virtually identical, indicating that it is not a result of poor blocking or processing. Neither are they a result of aspecific secondary antibody binding, as

secondary-only control blots do not show any bands (data not shown). The higher molecular weight bands represent crossreactivity of the antibody. The identity of these proteins is unknown, the only other proteins to have significant homology with FGF10 are different Fgfs, which are all too small to be causing bands at 35+ kDa.

Despite the aspecificity of the antibody, it can still be used for quantification, as the comparison of the different Fgf10 transgenic mice shows. It has long been known that the $Fgf10^{nlacZ}$ line is somewhat hypomorphic for Fgf10 (Mailleux et al., 2005). When comparing $Fgf10^{+/+}$, $Fgf10^{lacZ/+}$ and $Fgf10^{lacZ/lacZ}$ adult hypothalamus lysates, the decrease in FGF10 protein levels is clear, confirming the capability for quantification of FGF10 levels of the novel anti-FGF10 antibody.

Although it is not capable of reliable detection of FGF10 in immunohistochemistry, the new anti-FGF10 antibody does represent a step forward. A reliable way of detecting endogenous FGF10 in tissue remains elusive. Ultimately, the best way of detecting FGF10 in/ex vivo may be to make a mouse which expresses FGF10 fused to a small peptide tag, such as FLAG or HA. An $Fgf10^{FLAG}$ overexpression construct has already been used to study embryonic intestine formation (Nyeng et al., 2011).

Chapter 4

Distribution and phenotype of Fgf10-lacZ expressing cells in the developing and adult hypothalamus

4.1 – Introduction

The hypothalamus, a brain area crucial in the regulation of many homeostatic processes such as blood pressure and energy balance regulation, is located on the ventral surface of the brain. It surrounds, and is in close contact with the third ventricle. Ventral to the hypothalamus is the pituitary gland, which is closely linked with the homeostatic functions of the hypothalamus. The hypothalamus can be further subdivided into a number of areas. The single cell layer forming the boundary between the hypothalamus and the ventricle is the ependyma. Ventral to the ventricle is the median eminence, while the remainder of the hypothalamus is known as the parenchyma. The parchenchyma can be further divided (Garcia et al., 2003) into a number (up to several dozen depending on definitions) of anatomically distinct nuclei. Major nuclei include the venteromedial and arcuate nuclei. See figure 4.1 for schematic locations of major nuclei.

The cells forming the boundary between the ventral hypothalamus and the 3rd ventricle are a specialized ependymal cell type, termed tanycytes (Horstman, 1954). These Tanycytes, which are of a glial linage, can be further subdivided into four subtypes based on localisation and immunoreactivity. From dorsal to ventral, respectively, these are the α1, α2, β1 and β2 types. The α1,2 subtypes are distinguished by their expression of GFAP and S100β, which are absent from the β1,2 tanycytes (see Fig 4.2f for their distribution)

The nucleus and cell body of the tanycytes form the ventricular wall of the ventral hypothalamus, but they also project a single long process into the surrounding hypothalamic parenchyma. The direct contact with the cerebrospinal fluid (CSF) in the 3rd ventricle gives tanycytes a unique position to monitor many metabolic parameters. Particularly the β1,2 tanycytes, which through their processes link the CSF with the local vasculature, express glucose transporters (Garcia et al., 2003) and receptors for circulating hormones such as estrogen (Langub and Watson, 1992) and prolactin (Lerant and Freeman, 1998).

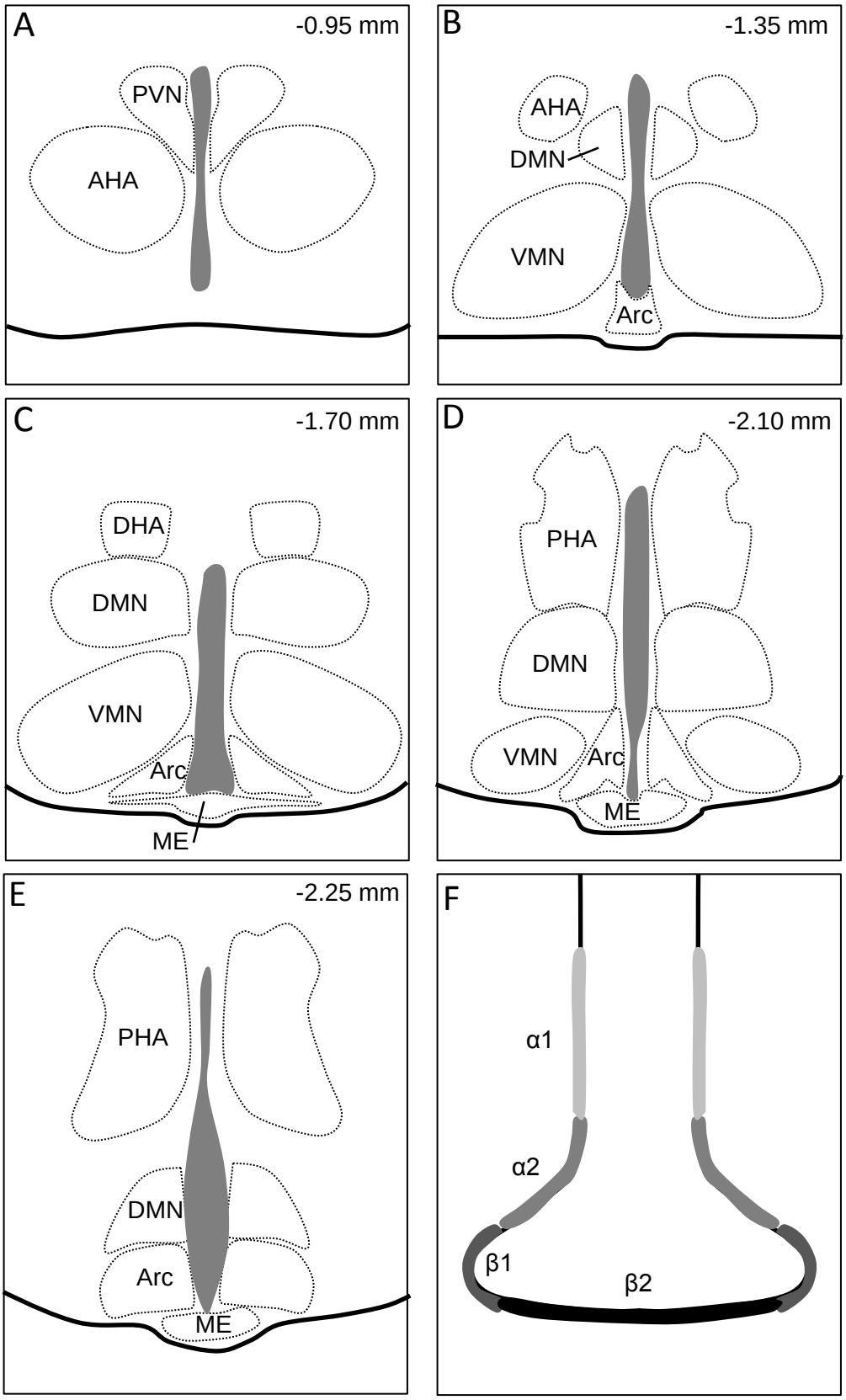

Fig 4.1 – Anatomy of the adult mouse hypothalamus. (A-E) Nuclei of the hypothalamus, rostral to caudal with approximate location from bregma. PVN: paraventricular nucleus, AHA: anterior hypothalamic area, DMN: dorsomedial nucleus, VMN: ventromedial nucleus, Arc: arcuate nucleus, DHA: dorsal hypothalamic area, ME: median eminence, PHA: posterior hypothalamic area. All based on Paxinos and Franklin, 2004 (F) Location of different tanycyte subtypes.

The development of the hypothalamus in the mouse starts at E10 and lasts through to E16, with the bulk of cells being generated between E11 and E14 (Shimada and Nakamura, 1973). The sequence of formation is conserved between mice, rats and humans, and follows a latero-medial outside-in gradient, with the lateral-most nuclei being generated before more central nuclei such as the arcuate and paraventricular nuclei (Ifft, 1972; Koutcherov et al., 2002; Shimada and Nakamura, 1973). The normal cilated epithelium of the dorsal ventricle differentiates at E16 to E18 in the rat (E14-E16 in the mouse), while the specialised tanycytes appear around the ventral ventricle after E19 in rat (E17 in mouse) and mature in the perinatal period, up to two weeks after birth (Altman and Bayer, 1978; Rutzel and Schiebler, 1980).

As tanycytes are radial glia-like cells which share many characteristics with the neurogenic radial glia of the hippocampus, and other putative neurogenic glia such as the Müller glia of the retina (Das et al., 2006) and Bergmann glia of the cerebellum (Sottile et al., 2006), the notion of a possible progenitor/stem cell role for these cells has long been suggested (Rodriguez et al., 2005). The mouse hypothalamus has been found to contain a relatively quiescent resident stem cell population in mice, which has been implicated in the control of feeding behaviour and energy balance (Bennett et al., 2009; Kokoeva et al., 2005; Kokoeva et al., 2007; Pierce and Xu, 2010; Yamauchi et al., 2010). Cell proliferation has also been seen in the hypothalamus of rats (Perez-Martin et al., 2010; Xu et al., 2005) and voles (Fowler et al., 2003; Fowler et al., 2005). Hypothalamic proliferation can be stimulated by a number of factors, including growth factors such as BDNF (Pencea et al., 2001), CNTF (Kokoeva et al., 2005), and IGF1 (Perez-Martin et al., 2010), exogenous drugs such as the antipsychotic olanzepine (Yamauchi et al., 2010), neuronal damage (Pierce and Xu, 2010) and neurodegenerative disease (Haan and Eisel, unpublished observations). However, none of the aforementioned studies has indentified the exact cell type that is the local stem cell or the niche cytoarchitecture of the hypothalamus. The factors controlling this putative stem cells niche are unknown, but recent evidence suggests that Fgf10 may be involved.

Fgf10 is expressed in a specific pattern in the hypothalamus, both during development at E14.5 and during adulthood at P60, Fgf10 mRNA expression can be found by in situ hybridisation in the ventral ependyma of the third ventricle, which in the adult contains tanycytes (Hajihosseini et al., 2008). Given the important role of Fgf10 in maintaining stem cell identity in other tissues during development, and the similarities between tanycytes and other neurogenic radial glia, the possibility that Fgf10 expressing tanycytes act as progenitor cells is tantalising.

Aims

To investigate whether Fgf10 expressing tanycytes act as stem cells in the hypothalamus, the development of this population in the embryo and the dynamics of the population during adulthood were examined. The phenotype of both ependymal and parenhcymal Fgf10-lacZ^{+} cells during development and adulthood was investigated with immunohistochemistry for neural stem cell and mature neural markers.

4.2 – Results

4.2.1 Fgf10-lacZ positive cell population is dynamic over time.

Serial sectioning of $Fgf10^{nlacZ}$ animals at postnatal ages P4 (n=3), P60 (n=5), P150 (n=4) and P400 (n=3) and staining for β-galactosidase allowed for an examination of the temporal dynamics of Fgf10-lacZ expression in the ependyma/ME and the parenchyma. Despite the lack of Fgf10 mRNA expression the parenchyma, the lineage tracing made possible by the $Fgf10^{nlacZ}$ line allows for the study of the Fgf10 derived population in this area too. In the ependyma and ME, cell number increases from P4, reaching a significantly higher number at P60 ($p=0.04$), before then gradually declining and dropping significantly below the neonatal baseline at P400 ($p=0.03$) (Fig 4.2a). The postnatal increase in ependymal Fgf10-$lacZ^+$ cells is reflected in the distribution of the total positive population, with the fraction of ependymal cells significantly increasing up to P60 ($p=0.01$), before stabilising at later ages (Fig 4.2b). In the parenchyma a different pattern was seen, with the highest number of $lacZ^+$ cells directly after birth, and a drop in cell number by P150 ($p=0.04$) and a further decrease by P400 ($p=0.002$) (Fig 4.2c). Not only the total cell number in the parenchyma changes with time, but also their distribution. At P4, cells are more densely packed in the parenchyma, located close to the ventricle, during maturation, the number of cells drops, and they spread more laterally, leading to a lower cell density from P60 onwards ($p<0.01$) (Fig 4.2d,e)

4.2.2 Fgf10-lacZ positive cells are located across the adult hypothalamus

Using serial sectioning and anti-β-gal labelling, the distribution of Fgf10-lacZ positive cells over the adult hypothalamus was investigated at P60 (n=5) and P150 (n=4). The number of β-gal positive cells was counted in the ependymal zone, median eminence and parenchyma over the rostral-caudal axis and animals at P60 and P150. In the ependyma, cells are widespread, but primarily located around -2.0 to -2.2 mm from bregma, in both P60 and P150

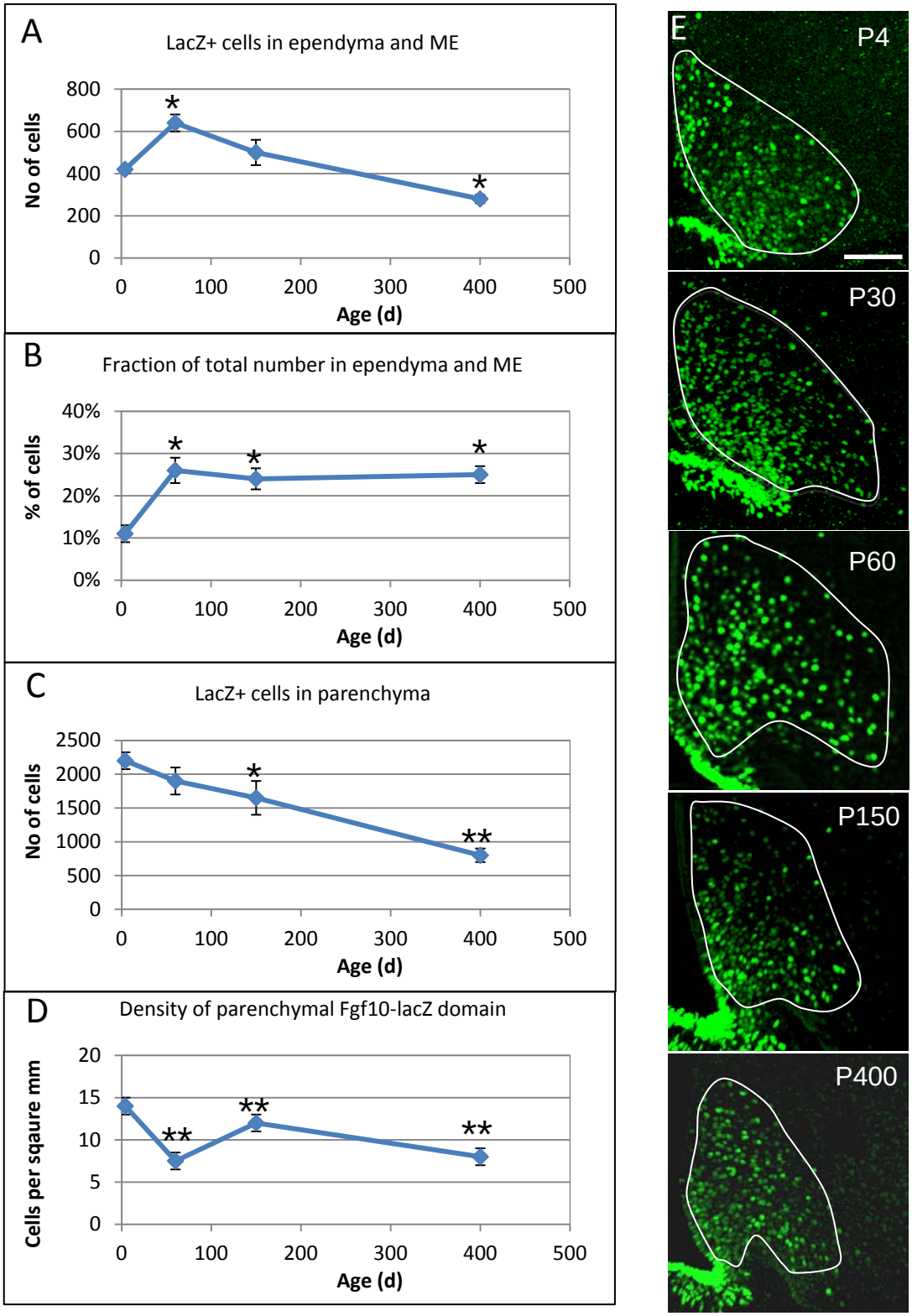

Fig 4.2 – Fgf10-lacZ expression throughout life. (A) In the ependyma, the Fgf10-lacZ$^+$ population increases up to postnatal day 60, before gradually decreasing over time, dropping significantly below the level at P4 by P400. (B) These dynamics affect the distribution of Fgf10-lacZ$^+$ cells, with the percentage of total cells in the ependyma increasing significantly up to P60, before stabilising for the rest of the lifetime. (C) In the parenchyma, the highest number of Fgf10-lacZ$^+$ cells is found directly after birth, at P4 and decreases with time, becoming significantly lower at P150. (D) The drop in total cell number is accompanied by a drop in Fgf10-lacZ$^+$ cell density in the parenchyma. (E) Representative images of density and extent of the Fgf10-lacZ domain in the parenchyma, visualised with anti-β-gal immunohistochemistry. Scale bar represents 50 µm.

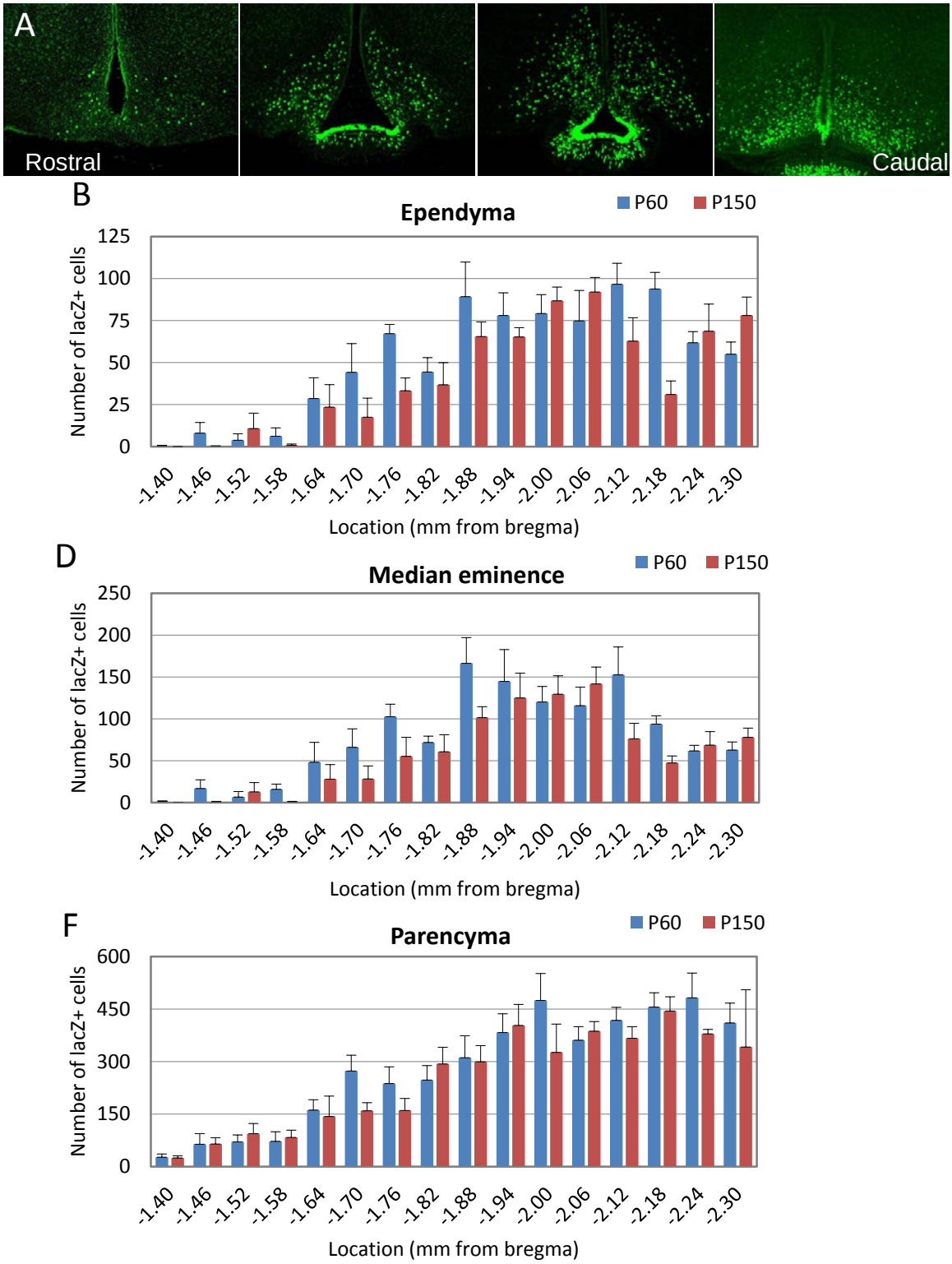

Figure 4.3 – Distribution pattern of Fgf10-lacZ in the adult hypothalamus. (A) Anti-β-gal immunohistochemistry illustrates the different expression patterns of Fgf10-lacZ over the rostral-caudal axis. (B) Fgf10-lacZ^{+} cells are seen throughout the hypothalamus, with the majority of cells located between -1.88 and -2.12 mm from bregma, no difference is seen in distribution between P60 and P150. (D) Number of Fgf10-lacZ^{+} cells in the ME peak at the same location as in the ependyma, but there is a clear drop-off at the caudal end. (F) Two foci of expression are seen in the parenchyma, at -1.94 to -2.00 mm from bregma and further rostral at -2.24 mm from bregma.

(Fig 4.3b). For the median eminence, the focus of expression is located further rostral, peaking around -2.0 mm (Fig 4.3c). In the parenchyma, cell number shows a distinct and reproducible two-peaked pattern, with the peaks located at -2.0 mm from bregma and at -2.2 mm (Fig 4.3d). In all areas, no significant difference in distribution was seen between ages.

4.2.3 Fgf10-lacZ expressing cells are located mostly in the arcuate nucleus

At P60, the distribution of Fgf10-lacZ expressing cells over the different hypothalamic nuclei was examined (Fig 4.4). Rostral-most expression is mostly limited to the dorsomedial and arcuate nuclei. Further caudal, expression in the ventromedial nucleus decreases, but is maintained in the arcuate nucleus. Around bregma -1.8 to -1.9 mm some expression can be seen in the dorsomedial nucleus as well as the median eminence. Towards the caudal end of the hypothalamus, expression becomes more restricted to the arcuate nucleus and the pituitary gland, ventral of the hypothalamus.

4.2.4 A heterogeneous population of tanycytes express neural stem cell markers

In order to ascertain whether the tanycytes of the hypothalamus are progenitors or stem cells, immunohistochemistry for known stem cell markers was preformed on cryostat sections. Double-labelling of BLBP and β-gal reveals that a large proportion of tanycytes express both markers (Fig 4.5). These cells show a typical elongated radial glia like morphology shown by BLBP. When located in or immediate adjacent the ependyma, the nuclei of these cells show a rounded or oval shape, while those nuclei that are located further out from the ventricle show a more elongated morphology. The expression of nestin is more widespread (Fig 4.5b), with a comparable tanycyte stain as seen with BLBP, but is also seen in more rounded cells located further outward from the ventricle. These more rounded cells also express musashi (Fig 4.5c), which is absent in the tanycytes.

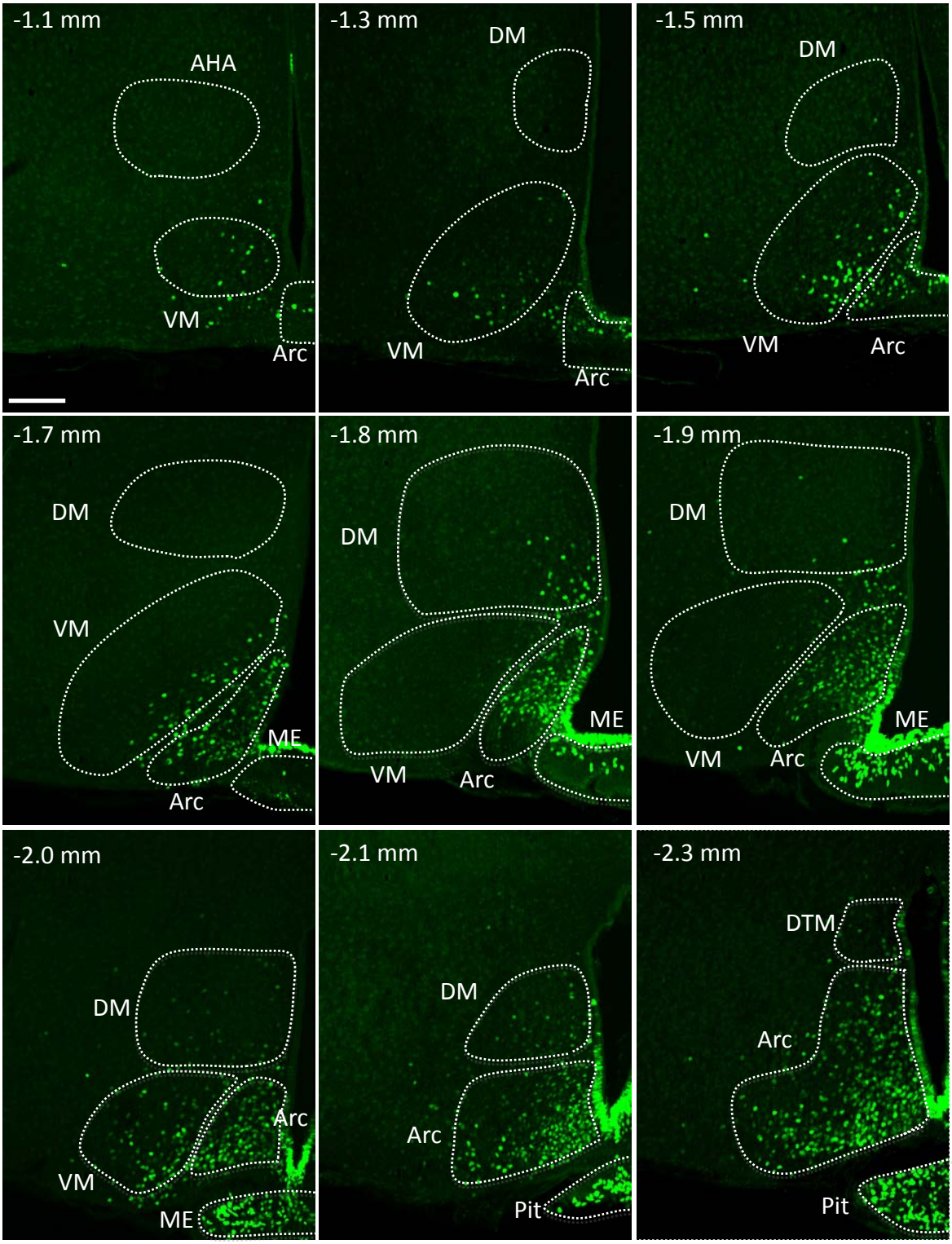

Figure 4.4 – Distribution of Fgf10-lacZ expression in different hypothalamic nuclei at P60. The outlines of the different hypothalamic nuclei are indicated by dotted lines. Expression of Fgf10-lacZ is strong in the arcuate nucleus and median eminence. Some expression is also located in the ventromedial and dorsomedial nuclei. Abbreviations: AHA: anterior hypothalamic area, VM: ventromedial nucleus, Arc: arcuate nucleus, DM: dorsomedial nucleus, ME: median eminence, Pit: pituitary gland, DTM: dorsal tuberomammillary nucleus. Scalebar represents 25 µm. Areas based on Paxinos and Franklin, 2004

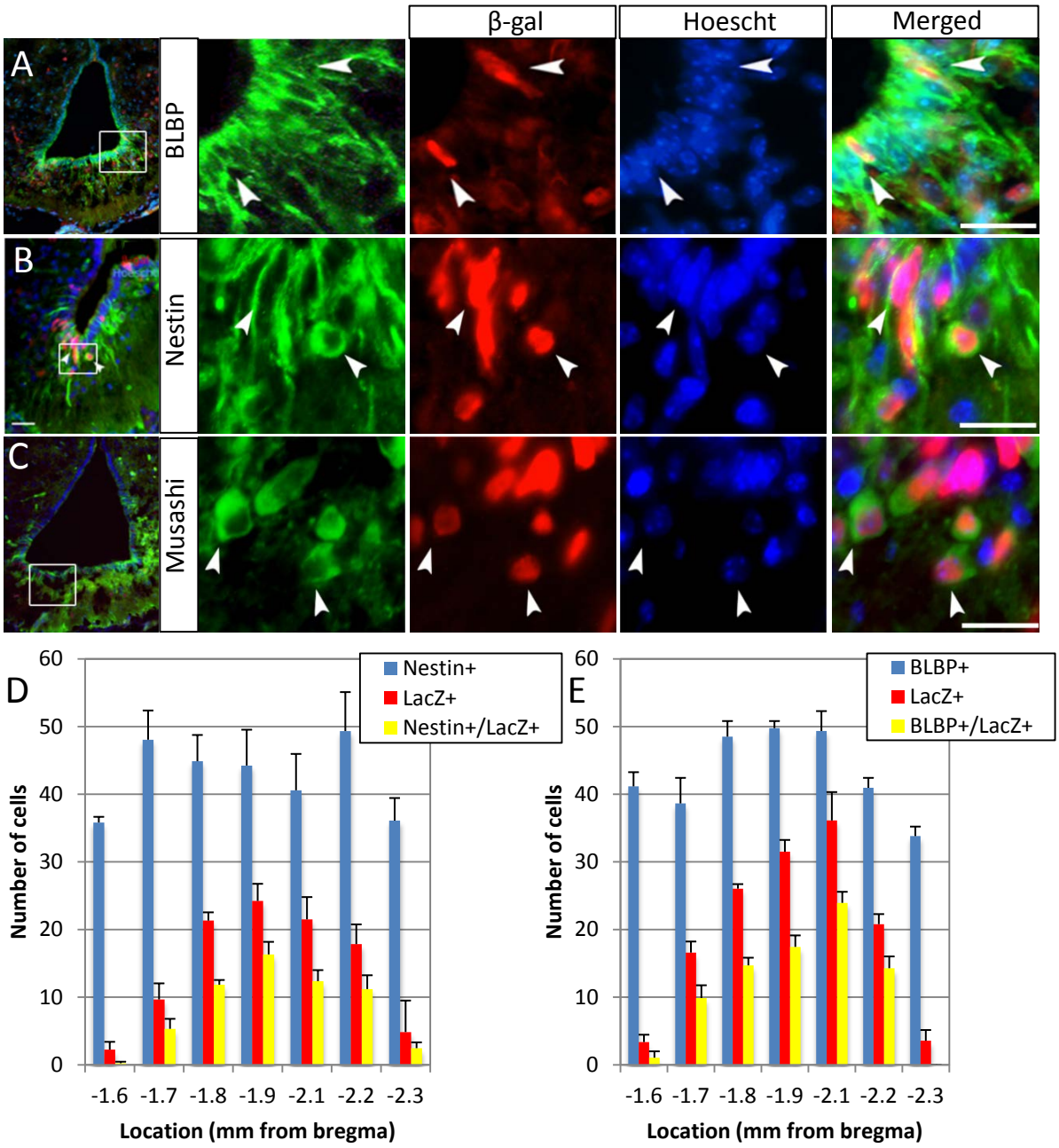

Figure 4.5 – Neural stem cell markers in the adult (P60-P90) hypothalamus. Double immunohistochemistry on cryostat sections with neural stem cell markers and β-galactosidase allows for the characterisation of the phenotype of tanycytes. (A) Radial glial marker BLBP is expressed throughout the ventral ependyma of the hypothalamus, a number of which also express Fgf10-lacZ (arrowheads) (B) The expression pattern of nestin is similar, but more widespread than that of BLBP, as apart from cells with a glial morphology, also abutting rounded cells are labeled. Examples of both types co-label with β-gal (arrowheads). Expression of musashi is found around much of the ventral ependyma, but is restricted to rounded cells abutting the ependyma, the majority of which are also β-gal$^+$. Scalebars for A-C represent 20 µm. (D) Quantification of nestin expression in the median eminence, the number of nestin expression cells is comparable over the examined area, but the number of lacZ$^+$ and double$^+$ cells peaks around -2.0 mm from bregma. A constant fraction of lacZ$^+$ cells also express nestin. (E) both the distribution of BLBP and double positive cells closely mimics that of nestin.

When the distribution and number of cells expression both neural stem cell markers (nestin or BLBP) and β-gal is investigated by immunohistochemistry on serial cryostat sections, it becomes clear that these cells are not uniformly distributed across the hypothalamus (4.5). The number of cells expressing BLBP or nestin is comparable over the range of the hypothalamus studied, but the number of these expressing β-gal shows a clear peak at the central median eminence, around bregma –1.9 mm. Also obvious from these studies is that the proportion of β-gal positive cells also expressing nestin of BLBP is a constant fraction of 50-70%. It should be noted that due to technical limitations it was not possible to study these markers at the same time, but it is likely the nestin^{+}/β-gal^{+} and BLBP^{+}/β-gal^{+} populations are in fact largely overlapping in the ependyma. It is clear that this putative progenitor/stem cell population is not a homogenous population, and is heterogeneous in both localization and immunoreactivity.

4.2.5 Fgf10-lacZ positive cells express FgfR1-IIIc and 3-IIIc, but not FgfR2 or FgfR4

In order to profile the expression of Fgf receptors in the adult hypothalamus in general and on Fgf10-lacZ positive cells in specific, a combined immunohistochemistry and RT-PCR approach was taken (Fig 4.6). The general expression pattern of the receptors was determined with immunohistochemistry, while the isoform was determined by RT-PCR. FgfRs 1, 2 and 3 were found to be expressed in the hypothalamus by immunohistochemistry. FgfR1 shows a widespread expression throughout the hypothalamus, including some of the ependymal cells. In contrast, FgfR2 is widely expressed in the cells of the hypothalamic parenchyma, but not expressed in the ependyma. FgfR3 shows an expression pattern similar to FgfR1, but shows stronger expression in the ependyma. Fgf10-lacZ^{+} cells were found to express FgfRs 1 and 3, but not 2. RT-PCR was preformed using iso-form specific primers on RNA isolated from micro-

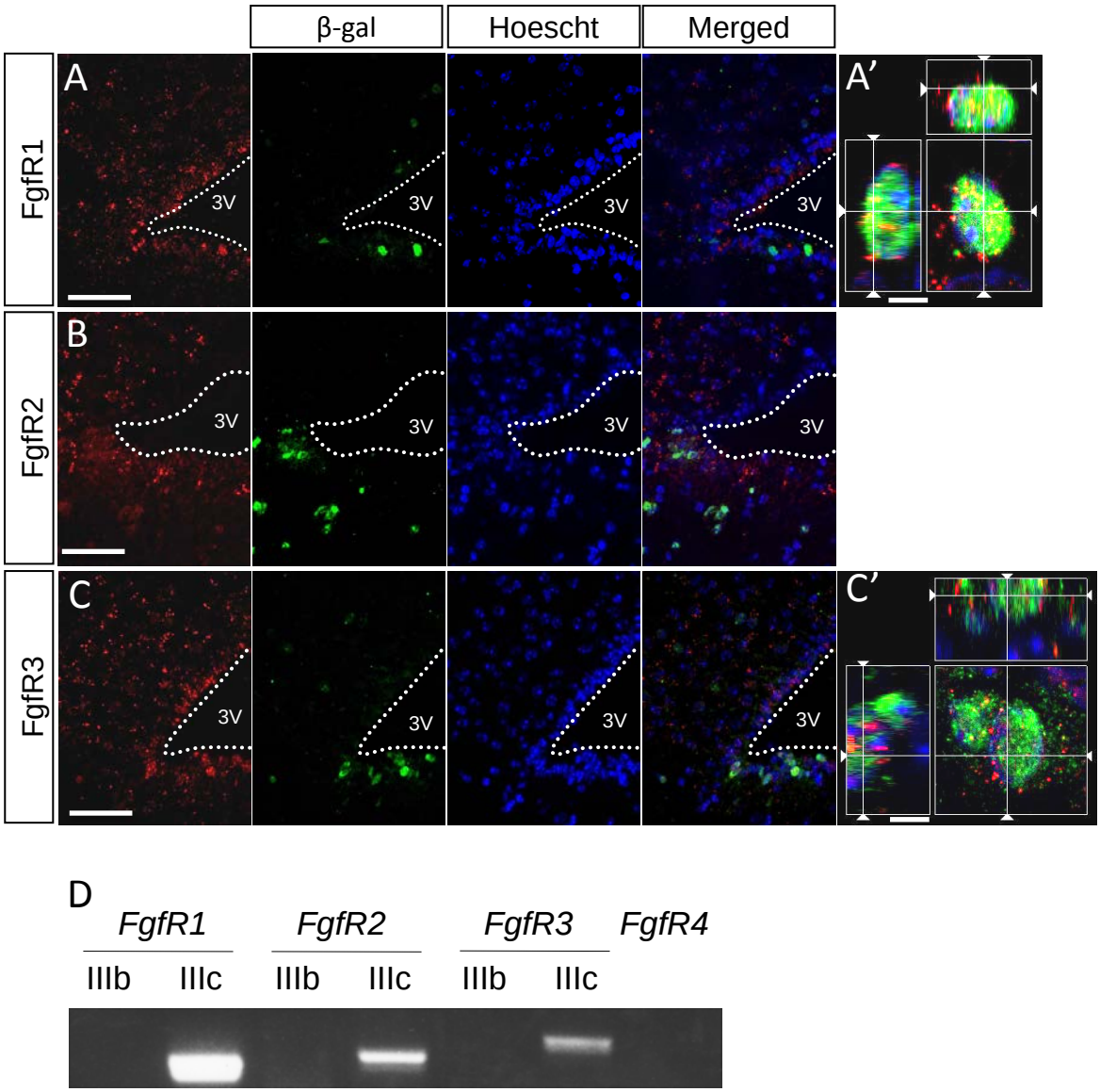

Fig 4.6 – Expression of Fgf receptors in the hypothalamus. (A) FgfR1 is expressed throughout the hypothalamus on many cells, including some in the ependyma. Fgf10-lacZ^{+} cells in the ependyma express FgfR1. (B) There is widespread expression of FgfR2 in the hypothalamus, but this is excluded form the ependyma, and no Fgf10-lacZ^{+} cells were observed to express FgfR2 (C) Expression pattern fo FfgR3 mimics that of FgFR1, again Fgf10-lacZ^{+} cells express FgfR3 (D) Using isoform specific primers in RT-PCR, it can be seen that only the IIIc isoform of Fgfrs 1, 2 and 3 are expressed in the hypothalamus. Scalebars for A-C represent 100 µm, for A' and C' this is 5 µm

dissected median eminence, showing that only the IIIc isoforms of receptors 1, 2 and 3 are expressed, and receptor 4 is absent from the hypothalamus.

4.2.6 Expression pattern of Fgf10-lacZ is largely set up before birth

To investigate the development of the Fgf10-lacZ expressing population, whole-mount Xgal staining and serial sectioning of $Fgf10^{nlacZ}$ embryonic brains of different stages was preformed (Fig 4.7). At the earliest examined stage, embryonic day 10 (E10), Fgf10-lacZ expressing cells are limited to the hypothalamic ependyma. At this stage, this is the only area of expression in the brain. At E12.5 expression is similar, and is limited to the ependyma and the developing pituitary gland, directly ventral to the hypothalamus. By E14.5, Fgf10-lacZ expressing cells in the anterior hypothalamus are found more laterally, on the ventral surface of the hypothalamus. At E16.5, expression is similar to E14.5. Shortly before birth, at E18.5, the domain of expression is extended dorsally, while in the posterior a prominent lateral streak of cells is located along the ventral surface of the hypothalamus. Additionally, further expression in other regions of the brain is seen as well. After birth, at P4 the expression pattern is essentially identical to the adult, and the prominent lateral streak seen at E18.5 is no longer present.

Shortly before birth (E18.5) the expression pattern throughout the brain has both similarities and differences with the adult pattern (Fig 4.8). The most striking difference in the hypothalamus is the prominent ventral streak of cells, which is seen throughout the anterior/rostral to posterior/caudal axis. The streak is only a few cells wide and extends up to 300 μm laterally. Additionally, a second population of cells is seen in a more dorso-lateral position, which are not present after birth.

In the neocortex at E18.5, a number of isolated Fgf10-$lacZ^{+}$ cells can be seen, with greater frequency than in the adult. Various thalamic nuclei show prominent expression, these are the paraventricular, laterodorsal and ventral lateral geniculate thalamic nuclei. Additional

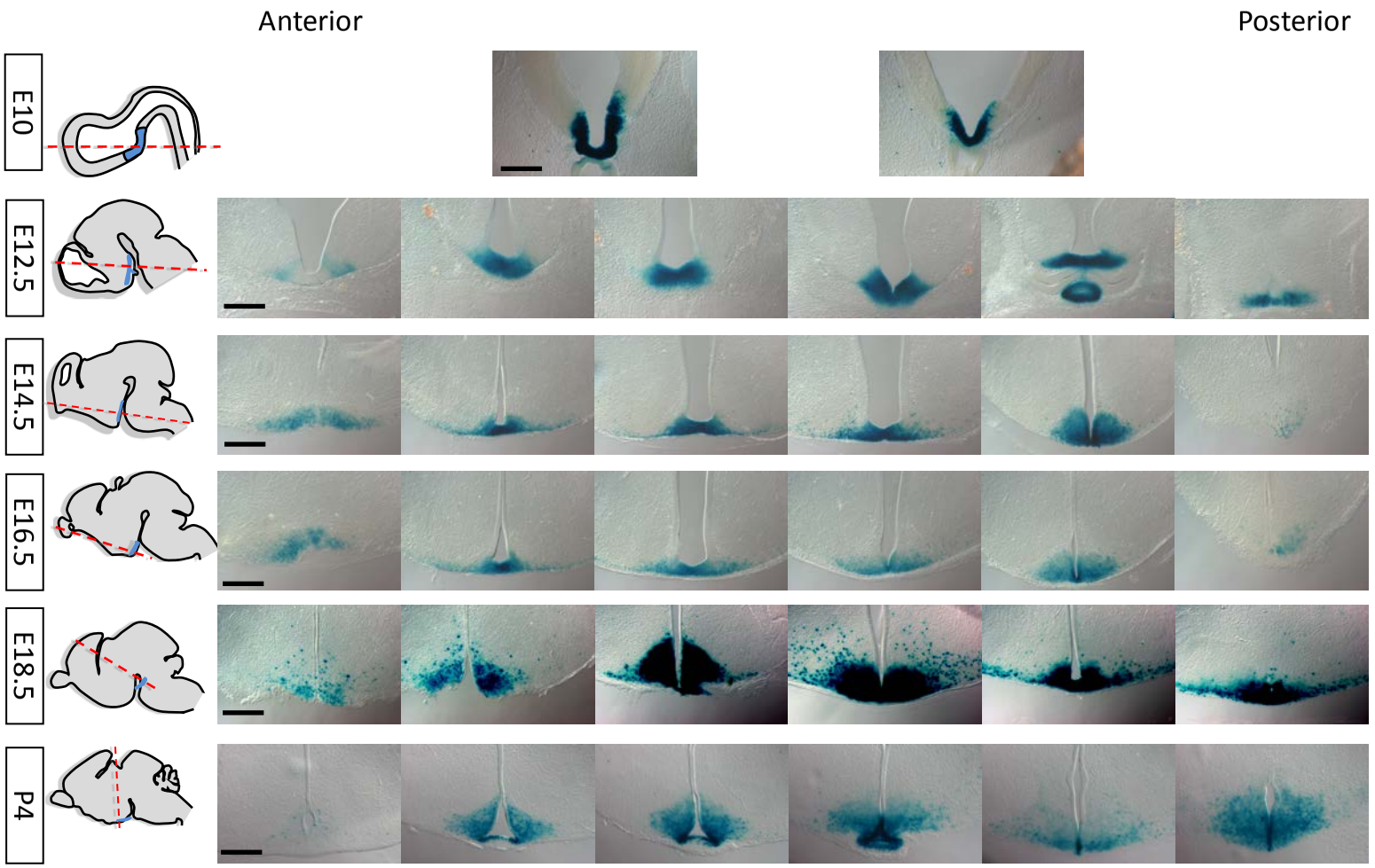

Fig 4.7 – Development of the Fgf10-lacZ expression pattern in the embryo. At E10 and 12.5, expression is limited to the ependyma. By E14.5, expression starts to be seen in the parenchyma, directly abutting the ependyma, mostly however, the cells are located near the ventral surface of the brain. At 16.5, the parenchymal expression becomes more lateral, still mostly near the ventral surface. By E18.5, dense expression in the parenchyma is seen, located further dorsal, resembling the adult expression pattern, as well as cells extending outwards laterally. After birth, at P4 the expression pattern is essentially the same as in the adult, and the prominent ventro-lateral population is gone. Scalebars: 250 µm

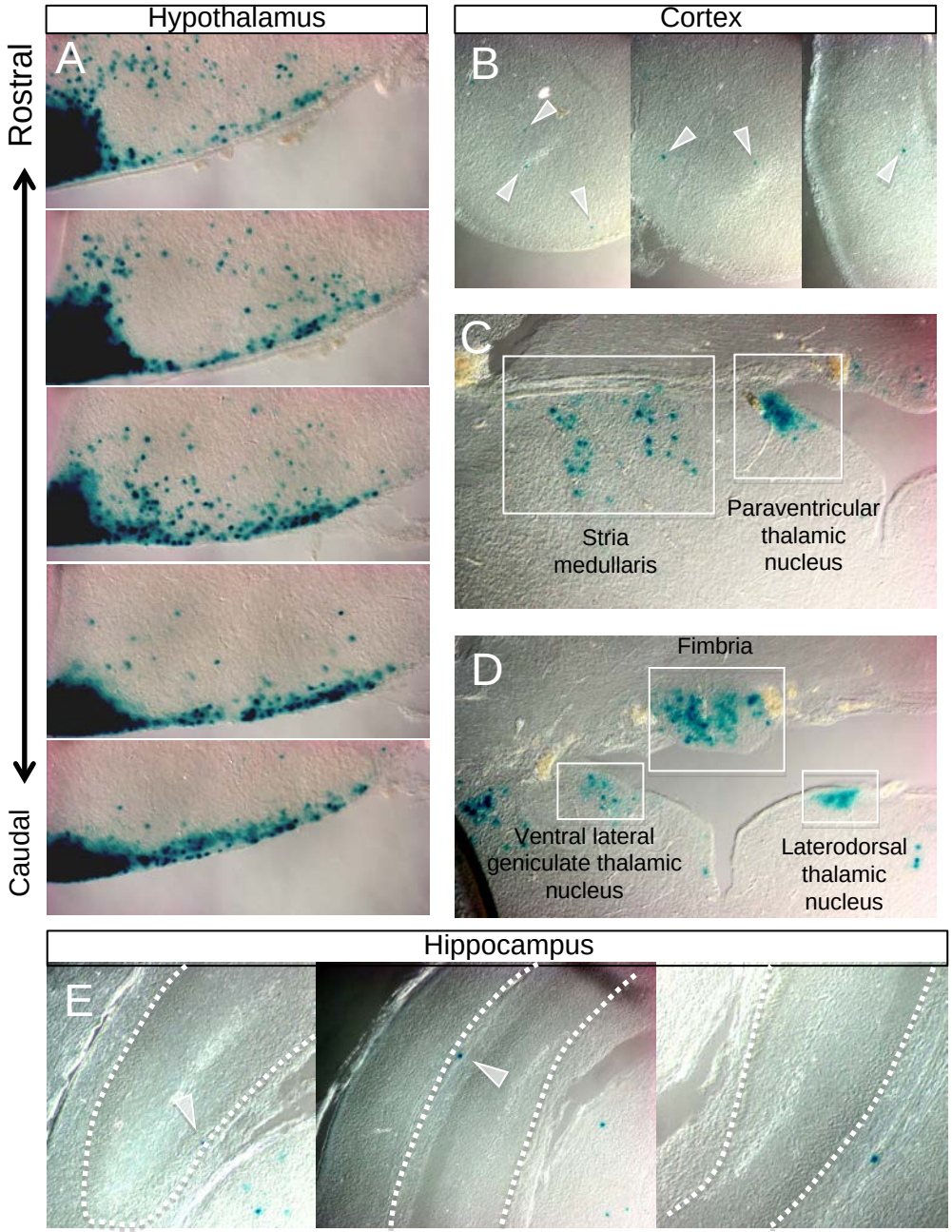

Fig 4.8 - Detailed expression pattern of Fgf10-lacZ before birth (E18.5) (A) In the hypothalamus, apart from a strong expression in the parenchyma abutting the ventricle, a population of cells on the ventral surface of the brain can be seen. (B) Expression in isolated cells throughout the neocortex (C, D) Expression is seen in a number striatal nuclei, including the stria medullaris and the paraventricular thalamic nucleus (C) and in the ventral lateral genticulate and laterodorsal thalamic nuclei and the fimbria (D). (E) Expression is seen in isolated cells in or near the hippocampus.

expression is seen in the stria medullaris and the fimbria. Lastly, some scattered cells can be observed in the hippocampus, but their number is lower than in the adult. At this stage, there is also prominent expression in various hindbrain nuclei (data no shown).

4.2.7 The Fgf10 expressing lineage contributes to embryonic hypothalamic neurogenesis.

To investigate the contribution of the Fgf10-lacZ expressing population to the development of the hypothalamus, the expression of the pan-neuronal marker Tuj1 and the postmitotic neuronal marker NeuN was examined during the embryonic neurogenesis phase, at E12.5 and E14.5. At E12.5, the peak of neurogenesis, widespread Tuj1 expression is seen (fig4.9a-d). At this stage, many Fgf10-lacZ expressing cells label with Tuj1, with the notable exception of a population in the central ependyma. During this stage, no NeuN expressing cells are found in the hypothalamus (fig4.9e). Towards the end of neurogenesis, at E14.5, expression of Tuj1 is essentially ubiquitous, with the notable exception of the ependyma (fig4.9f). Two distinct Fgf10-lacZ expressing populations are seen, a Tuj1 negative ependymal population and a Tuj1 positive parenchymal population (fig4.9g,h). NeuN expression at E14.5 is widespread, but Fgf10-lacZ expressing cells do not express this post-mitotic marker at this stage(Fig 4.9i).

4.2.8 Fgf10 expressing lineage contributes neurons and glia to the hypothalamic parenchyma

β-gal^{+} cells in the hypothalamic parenchyma do not express neural stem cell markers, and the assumption is that these cells are derived from the tanycytes. Immunohistochemistry for markers of mature neurons (NeuN) and glial cells (GFAP) was performed on sections of Fgf10^{nlacZ} mice (Fig 4.10). NeuN is widely expressed in the hypothalamic parenchyma, and at early post-natal ages (P4), many Fgf10-lacZ^{+} cells express NeuN. By P60 however, only a small fraction of Fgf10-lacZ^{+} cells continue to express NeuN. At P60, only rare Fgf10-lacZ expressing

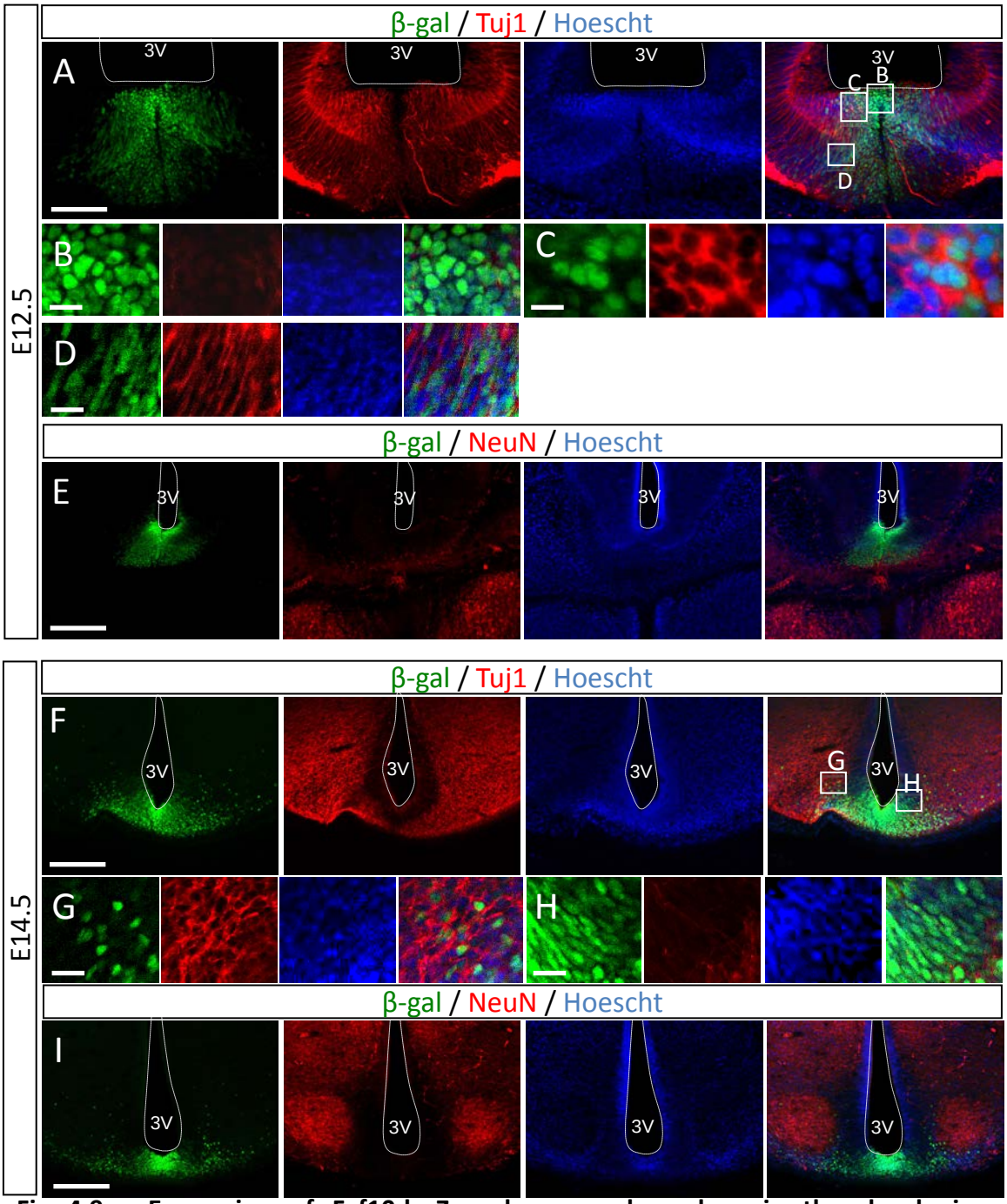

Fig 4.9 - Expression of Fgf10-lacZ and neuronal markers in the developing hypothalamus. (A) The immature marker Tuj1 is widely expressed in the E12.5 hypothalamus, boxes indicate location of images B, C and D. (B) A population of cell in the central ependyma expresses high levels of β-gal, but no Tuj1. (C) A more lateral population of cells expressed high levels of β-gal, the majority of which also express Tuj1. (D) Cells located more ventrally express low levels of β-gal, and are interspersed with Tuj1 positive fibers, but only a minority of cell themselves express Tuj1. (E) The mature neuronal marker NeuN is not expressed in the hypothalamus at E12.5. (F) At E14.5, Tuj1 expression is limited to the parenchyma, and is excluded from the ependymal zone, boxes indicate location of images G and H. (G) In the parenchyma, β-gal colocalises with Tuj1. (H) The strong expression of β-gal in the ependyma does not overlap with Tuj1 (I) At 14.5, NeuN is expressed in certain populations of the hypothalamus, but not in the β-gal expressing population. Scalebars in A, E, F, I: 250 µm, in B, C, D, G, H: 10 µm.

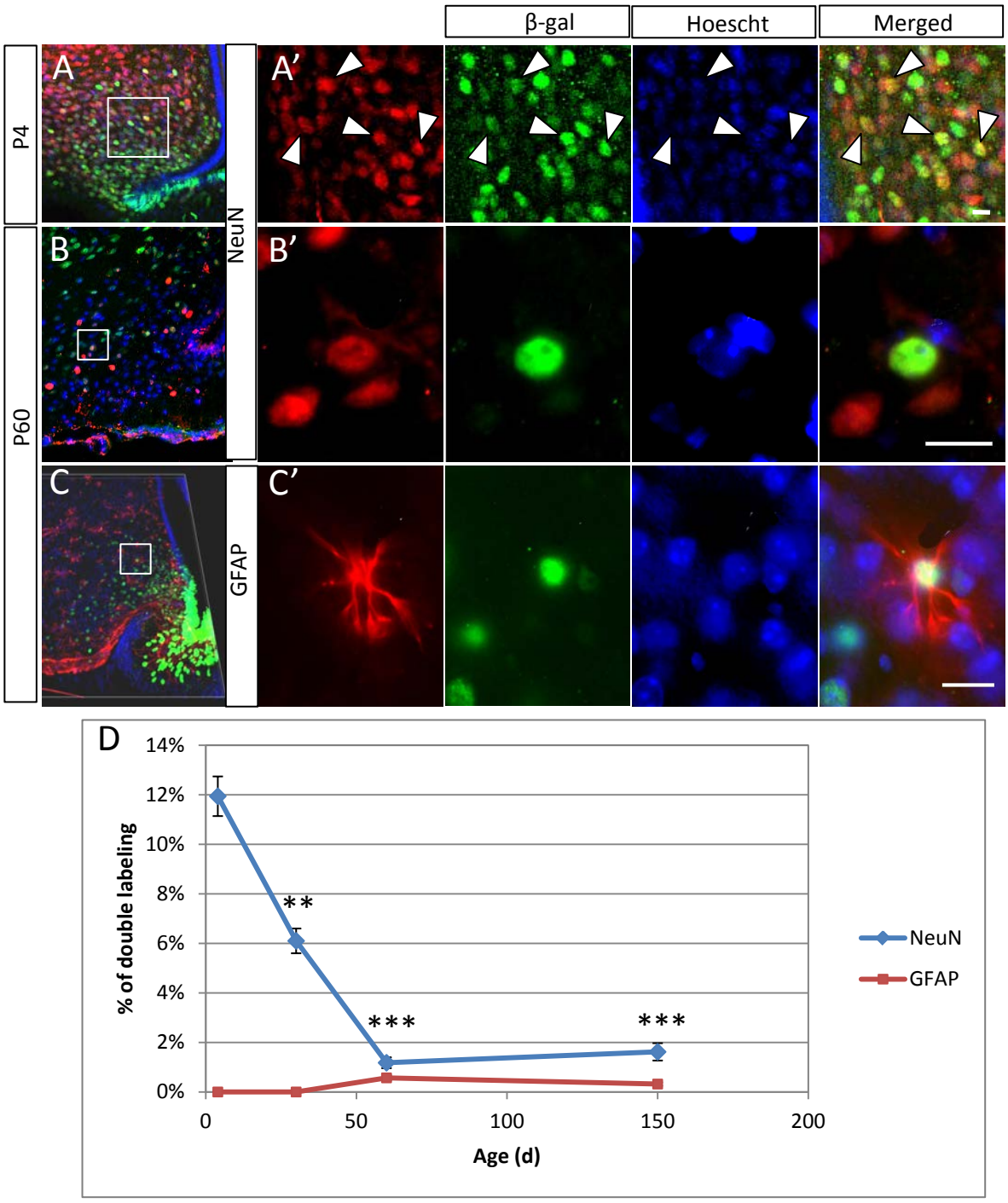

Fig 4.10 – Expression of neural makers on Fgf10-lacZ expressing cells in the post-natal hypothalamic parenchyma. (A,A') At P4, the mature marker NeuN is expressed throughout the hypothalamic parenchyma, and a significant fraction of Fgf10-lacZ$^+$ cells co-label. (B, B') At P60, NeuN expression in the parenchyma is relatively weaker, and only a small minority of Fgf10-lacZ$^+$ cells co-label. (C,C') Astrocyte marker GFAP is widely expressed, but only a few of these also express Fgf10-lacZ. Scalebars in all represent 10 µm. (D) The percentage co-localisation with both NeuN and GFAP varies over the age of the animals. At P4, and P30, a significant fraction of Fgf10-lacZ$^+$ cells express NeuN, while none express GFAP. At P60 and P150 however, both NeuN and GFAP are expressed by a small minority of Fgf10-lacZ+ cells. Scalebars: 10 µm

GFAP$^+$ glia are seen. When the degree of colabeling is quantified in different ages, the dynamics of this system become obvious. Shortly after birth, up to 12% of Fgf10-lacZ$^+$ cells label with NeuN but this percentage rapidly drops to 6% at P30 before stabilising at between 1 and 2% at later ages. In contrast, no GFAP$^+$/lacZ$^+$ cells were observed at P4 or P30, but a small (0.5-1%) fraction was seen at later ages.

4.3 - Discussion

The Fgf10 expressing tanycytes of the hypothalamus represent a possible neural progenitor or stem cell population. The identities and number of both these tanycytes and their putative descendants were determined via immunohistochemistry. Investigating the dynamics of the number of Fgf10-lacZ expressing cells in different areas of the hypothalamus is illustrative of the different properties of these populations. The expansion of the ependymal population between P4 and P60 shows the continued expansion of this population, suggesting these cells are dividing. The fact that this is mostly a selective amplification of the ependymal population, rather than a generalised expansion of Fgf10-lacZ expression is evidenced by the increase in the ependymal population as a fraction of total cell number. However, after P60 their number declines, indicating a likely decrease of mitotic activity. In contrast, the parenchymal population, which has been generated from a Fgf10 expressing population, but no longer expresses Fgf10, seems be largely generated by birth, and only declines after that. Between P4 and P60, the parenchymal domain of expression becomes larger, which together with a decrease in cell number leads to a lower cell density. The further decrease in cell number after P60 is accompanied by a shrinking of the expression domain. These morphological changes indicate a degree of plasticity in this population.

Expression of Fgf10-lacZ in the adult is not uniform over the hypothalamus, but is clustered in a number of areas. In the ependyma, the highest cell number seen in the widest extent of the ventricle, with the median eminence expression largely mirroring this. Expression in the parenchyma is more interesting, and is located mostly, but not exclusively in the arcuate, dorsomedial and ventromedial nuclei. This localisation may give hints about the function of Fgf10-lacZ expressing cells, the arcuate and ventromedial nuclei are strongly linked to energy balance and feeding behaviour (Louis-Sylvestre et al., 1980; Meister, 2007), while the dorsomedial nucleus has also been linked to the control of circadian rhythms, including

that of feeding (Chou et al., 2003; Meister, 2007), hinting to some form of homeostatic role for these cells.

The expression patterns of the neural stem cell markers used provide information about the exact cytoarchitecture of the putative neural stem cell niche of the adult hypothalamus. The expression of BLBP is limited to the tanycytes, and clearly shows their radial morphology, highly reminiscent of embryonic cortical or adult hippocampal radial glia. The expression pattern of nestin is wider, apart from labelling a similar population as BLBP, a population of rounded cells abutting the radial cells is also labelled. It is very likely that the nestin positive tanycytes and BLBP positive tanycytes in fact represent the same population of cells, but due to technical limitations a double or triple labelling for both was not possible. It is known that nestin is expressed in transit amplifying cells ('A'-cells) of the SVZ (Mignone et al., 2004), and it is likely the nestin expressing cells of a rounded morphology in the hypothalamus represent a similar population. Expression of musashi, known in the SVZ to label both stem cells and transit amplifying cells (Obermair et al., 2010), is restricted to the rounded cells, and is absent from the radial glia like cells. In this niche, musashi expression seems to be limited to a putative transit amplifying cell population, in contrast to the SVZ. Also in contract to the SVZ, the radial glial cells do not express GFAP, expression of which is limited to the dorsal half of the ependyma. Throughout the ventral hypothalamus, there is a heterogeneous expression of Fgf10, approximately 60% of cells expressing the β-gal reporter also express nestin or BLBP. The fraction of β-gal positive cells expressing nestin or BLBP is constant over the hypothalamus, but their absolute number peaks around the central median emenince, at -2.0 mm from bregma. All observed musahi expressing cells were also β-gal positive. The heterogeneous nature of the potential stem cell niche is no surprise, it is known that the subventricular niche is also highly heterogeneous, and has a mosaical organisation (Merkle et al., 2007).

The fact that β-gal positive cells only express FgfR1IIIc and FgfR3IIIc means only Fgfs 1, 2, 4, 5, 8, 9, 16, 17, 18, and 20 can signal to these cells, the absence of any FgfR2 expression on these cells excludes the entire Fgf7 family, 3, 7, 10 and 22. This also excludes the possibility of autocrine or paracrine signalling of β-gal^{+} tanycytes.

During development, the initial focus of Fgf10-lacZ expression is in the ependyma, before the onset of neurogenesis, but it is only after E14.5 that the first Fgf10-lacZ expressing mature neurons are seen, suggesting the Fgf10-lacZ positive population is involved in the late generation of hypothalamic neurons. Initial appearance of Tuj1^{+} / Ffg10-lacZ^{+} cells is at E12.5, but these are located in what will become the median eminence, rather than the parenchyma. This likely indicates a migration of neuronal precursors in the E12.5 to E14.5 timeframe. By E14.5 the population has segregated in Tuj1^{+} parenchymal neuronal precursors and Tuj1^{-} cells in the ependyma, the putative continued stem cell population. As the number of Fgf10-lacZ expressing cells in the parenchyma continues to increase up to birth, this population must continue to generate new cells even after the bulk of neurogenesis has been completed and represents a late developmental contribution to the hypothalamus. This can be addressed using inducible genetic lineage tracing during late gestation. This is also reflected by the fact that none of the Fgf10-lacZ^{+} cells at E14.5 double-label with NeuN, indicating they have not yet fully matured as neurons. At early postnatal timepoints, there is considerable expression of NeuN in the Fgf10-lacZ population, but this rapidly decreases as animals mature. Combined, these observations show that the Fgf10-lacZ^{+} population is formed very early on during development as a hypothalamic precursor population, which then contributes neurons the late developing hypothalamus that mature close to or around birth. Although a small fraction of Fgf10-lacZ^{+} cells in the mature animal continue to express mature neuronal markers, the vast majority do not. This does not have to mean that the perinatal LacZ^{+}/Neun^{+} cells are lost from the hypothalamus but may represent the turn-over of reporter protein, as these cells no longer express Fgf10. The differences between the embryonic and adult Fgf10-lacZ^{+}

populations are also illustrated by the fact that the embryonic population does not seem to generate any glia, whereas $lacZ^+/GFAP^+$ glia can been seen from P60 onwards. However, the biggest remaining question is what the majority of Fgf10-$lacZ^+$ cells in the adult hypothalamus are, as these are neither neurons nor glia. At least some of these can represent an immature population of neuronal precursors, which do not express NeuN. Immunohistochemistry for the early neuronal marker Tuj1 in the adult is impractical as the ubiquitous expression of this marker in all neuronal fibres makes distinguishing individual cells impossible, but it may be possible to use other immature neuronal markers, such as HuC, which also stains nuclei, making distinguishing individual cells possible

If migration from the ependymal zone into the surrounding parenchyma does take place as would be required for adult cell contribution, expression of migratory markers such as PSA-NCAM or doublecortin would be expected. However, no immunoreactivity for either of these markers was found anywhere in the hypothalamus (data not shown). It may be that expression levels are too low to be detected by immunohistochemistry, as genetic reporting for doublecortin has seen recombination in the adult hypothalamus, in cells surrounding the ventricle (Zhang et al., 2010).

In summary, the contribution of the $Fgf10^+$ lineage to the hypothalamus is twofold, an initial wave of neurons during late embryonic development, and a continued low-level contribution in the adult, capable generating both neurons and glia. The lineage seems have an important role in generating the various hypothalamic nuclei during development, and may represent a source for maintaining the population in the adult. Given the crucial homeostatic functions of the hypothalamus, one like function of this population may be providing for plasticity in response to environmental factors affecting homeostasis.

Chapter 5

In vivo analysis of cell proliferation and genetic lineage tracing in the hypothalamus

5.1 – Introduction

The tanycytes of the hypothalamus have long been suggested to be a potential population of progenitor or neural stem cells. In order to investigate this is vivo, detection of cell division is required, as the only dividing neural cells are the adult neural stem cells and their immediate progeny. Detection of division can be done by immunohistochemistry for markers expressed only in actively cycling cells, such as Ki67 (Gerdes et al., 1983), PCNA (Miyachi et al., 1978) or phospho-histone H3 (Hans and Dimitrov, 2001). Ki67 is expressed thoughout the cell cycle, whereas PCNA is expressed during S-phase and phospho-histone H3 mainly during M-phase. However, these markers can only provide a snapshot of cell division in a given tissue at the time of death of the animal. A different, and sometimes more informative way of detecting cell division relies on the incorporation of a labelled nucleotide into the DNA of a dividing cell during DNA replication, labelling cells during S-phase. The traditional, though now largely superseded, method used radioactively tagged thymidine (^{3}H-thymidine) as the marker, detecting any dividing cells by autoradiography (Firket and Verly, 1958).

Currently the nucleotide of choice is 5'-bromo-2'-deoxyuridine (BrdU), which can be detected by immunohistochemistry. Any dividing cell will incorporate the marker and retain it in its genetic structure. In theory, any labelled cell will retain incorporated BrdU, although subsequent rounds of division may dilute the labelling. By sacrificing BrdU treated animals immediately or shortly following administration, a snapshot of the actively dividing population can be obtained. If animals are sacrificed longer after administration, survival of cells born during the period of administration can be assessed. There are a number of routes for BrdU administration, the most common of which is intraperitoneal injection. However, this is inconvenient for longer administration times, as it requires a daily injection. Additionally, this leads to fluctuating BrdU levels, as the biological halflife of BrdU is short. A different approach is to use a micro-osmotic pump for direct intra-cerebroventricular infusion, delivering the BrdU

directly into the brain. This is amenable to long-term experiments and will give high local BrdU doses, but requires stereotactic surgery to emplace. Both these methods have been used in the adult hypothalamus before, with several studies showing dividing cells are present in the adult hypothalamus in mice (Bennett et al., 2009; Kokoeva et al., 2005; Kokoeva et al., 2007; Pierce and Xu, 2010; Yamauchi et al., 2010), rats (Perez-Martin et al., 2010; Xu et al., 2005) and voles (Fowler et al., 2002). However, most of these studies used short-term labelling, and the phenotype of these cells was generally not fully characterised.

Simply detecting cell division is not always informative of the fate of newly generated cells. In order to do in vivo lineage tracing on potential neural stem cells, the Cre-lox system can be used, originally developed in vitro by Brain Sauer (Sauer and Henderson, 1988). The Cre recombinase protein, originally isolated from a P1 bacteriophage, is capable of targeted site-specific recombination of DNA at sites flanked by specific short sequences known as loxP sites. The Cre recombinase was first introduced into a transgenic mouse line in 1992 (Orban et al., 1992) allowing targeted in vivo mutation of the mouse genome. When used for lineage tracing, it requires the use of a cross of two mouse lines. The first line, usually referred to as the 'driver', has the sequence for Cre recombinase inserted downstream of the promoter of the gene of interest causing Cre expression in any cells expressing this gene. By limiting the expression of Cre to cells expressing a specific gene, spatially restricted activation is achieved. This line can then be crossed with a reporter strain, in which a specific gene is transcribed upon Cre activation.

As the conventional Cre recombinase is constitutively active, it is not possible to control the timing of its expression. In order to overcome this limitation, novel variants of Cre were developed that consisted of fusion proteins of Cre with a different regulatory protein that allow activation of Cre by administration of an exogenous chemical. This was first achieved by a Cre recombinase fusion with the human estrogen receptor (CreER) (Metzger et al., 1995), which was later improved by use of a mutated estrogen receptor (the $CreER^{T}$) (Feil

et al., 1996). The estrogen receptor is normally sequestered in the cytoplasm, excluding the fused Cre from the nucleus. When the synthetic receptor agonist tamoxifen is administered, the complex translocates to the nucleus, and recombination can take place. A further mutation of this fusion protein, the CreER(T2), shows higher ligand specificity and is now commonly used (Feil et al., 1997). An alternative is a fusion with a mutated progesterone receptor (Kellendonk et al., 1996), which was successfully used for recombination in the mouse brain (Kellendonk et al., 1999).

The activation of Cre recombinase leads to the homologous recombination of genomic DNA flanked by the loxP recognition site (usually known as a floxed allele). The loxP sites are directional, when both loxP sites are in the same direction, the flanked sequence is excised from the genome, while if they are opposed, the sequence is reinserted into the genome in the opposite direction. Cre activity can be used both to stop gene expression and to activate it, depending on the specific genomic construct. If the loxP sites flank a gene of interest (or required portion thereof), recombination will cause the excision of the gene, in effect creating a knockout. In contrast, when Cre recombinase is used for lineage tracing, an inducible reporter gene can be activated by including a floxed stop codon upstream of the reporter gene, which is removed upon recombination, allowing for transcription of the reporter gene. Commonly used reporter genes are lacZ (producing the β-galactoside protein) and GFP or any of its variants such as YFP, RFP or Tomato. In order to accurately report Cre activity anywhere, the reporter gene must be capable of being expressed in any tissue, and thus should be driven by a ubiquitously active promoter. Generally, the promoter of choice for these reporters is the ROSA26 locus, which was initially found to drive generalised expression of a retrovirally introduced gene trapping construct carrying a lacZ gene (Zambrowicz et al., 1997). This locus was modified by introduction of a floxed transcriptional termination signal, usually in the form of a neomycin resistance cassette, to form a Cre reporter allele, initially driving lacZ (Mao et al., 1999; Soriano, 1999), and later driving fluorescent reporters (Mao et al., 2001; Srinivas et

al., 2001). Using Cre mediated recombination is the most reliable manner of lineage tracing available today for a number of reasons. Firstly, recombination will only take place in cells expressing the gene of interest, in contrast to dye labelling or retroviral labelling, which labels cells based on location. Furthermore, due to the genomic rearrangement by the Cre recombinase, reporter expression is continued indefinitely, regardless of cell division.

Aims

In order to determine the mitotic potential of Fgf10-lacZ expressing cells in the adult brain, a combination immunohistochemistry and long-term BrdU administrations was used. The long term fate of newly generated cells was investigated using genetic lineage tracing combined with immunohistochemistry.

5.2 - Results

5.2.1 Ki67 labelling shows limited cell proliferation in the adult hypothalamus

Labelling of Ki67 in the adult hypothalamus shows only a small number of cells which are proliferating (fig 5.1). Only a small portion of the Fgf10-lacZ positive cells, located in the ependyma, also express Ki67.

5.2.2 Cumulative BrdU administration shows widespread proliferation, including a subset of Fgf10-lacZ^{+} cells

Long term drinking water administration of BrdU was compared to a more traditional administration protocol, consisting of daily intraperitoneal injections of 100 mg BrdU per kg bodyweight over 5 days. When compared in both a traditional neurogenic niche, the dentate gyrus of the hippocampus, and the hypothalamus, it is clear that a 21d drinking water administration labels more cells that the short term injection regime (fig 5.2), thus showing this method is more sensitive.

After 21d of cumulative BrdU administration , the hypothalamus shows widespread BrdU incorporation, with substantial amounts of cells in the parenchyma. However, despite both being widespread, only a small number of β-gal^{+} cells incorporate BrdU. The double-positive cells were located exclusively in, or were abutting the ventral ependyma, and frequently appeared as doublets, indicating a recent division (fig 5.3).

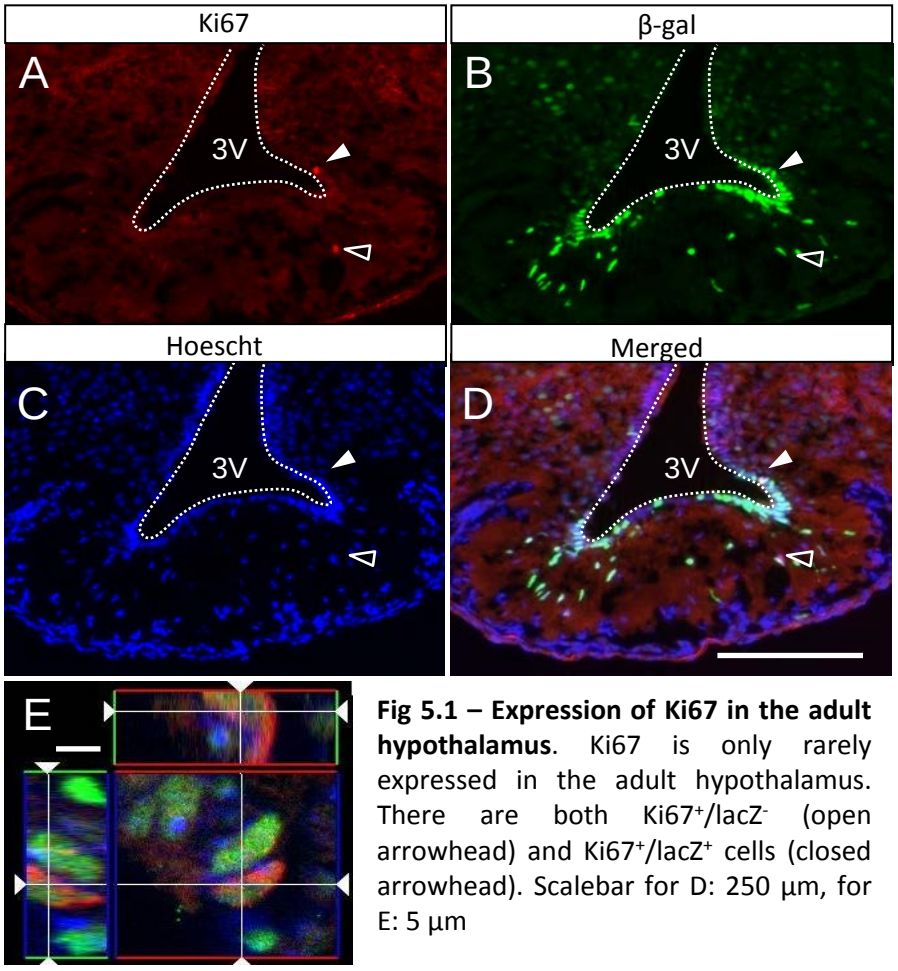

Fig 5.1 – Expression of Ki67 in the adult hypothalamus. Ki67 is only rarely expressed in the adult hypothalamus. There are both Ki67^{+}/lacZ^{-} (open arrowhead) and Ki67^{+}/lacZ^{+} cells (closed arrowhead). Scalebar for D: 250 µm, for E: 5 µm

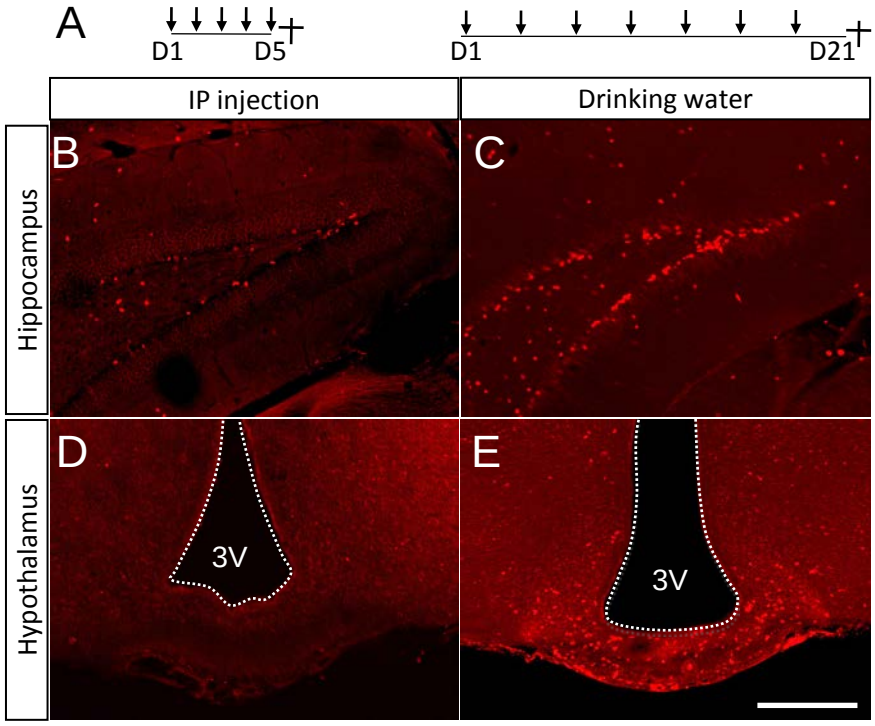

Fig 5.2 - Comparison of different administration routes for BrdU. (A) Schematic administration regimes for both. In both the hippocampus (B,C) and the hypothalamus (D,E) it is clear that a long term cumulative labeling protocol labels more cells than a traditional administration regime. Scalebar: 250 µm

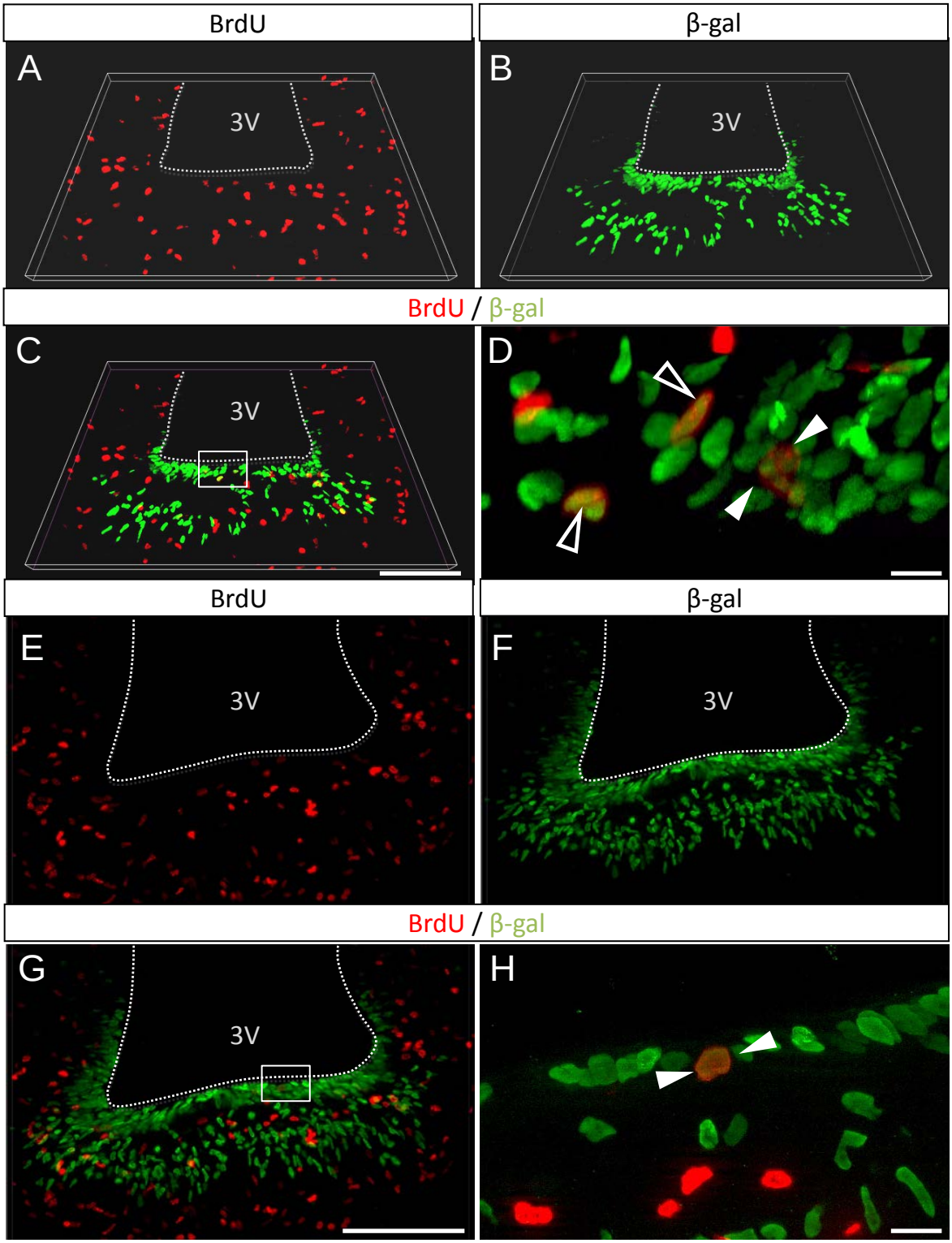

Fig 5.3 – BrdU incorporation after 21 days of administration. After immunohistochemistry for BrdU and β-gal, it can be seen that the expression patterns are not similar, and there is little overlap in expression. However, double-positive cells are present, both as single cells (open arrowheads) and doublets (filled arrowheads), likely indicating a recent mitotic event. Scalebars for C, G: 250 µm, D, H: 10 µm

5.2.3 Both total and Fgf10-lacZ expressing BrdU incorporating populations decrease with age

As it is known from other stem cell niches the number of proliferating cells decreases with age, animals of different ages were administered BrdU to asses the temporal dynamics of hypothalamic cell division (fig 5.4). Animals used were at P28-35 (n=3), P70 (n=3) and P438 (n=3). Basal levels of BrdU incorporation is at 400±1 cells per hypothalamus at the earliest timepoint, and drops steadily throughout age before reaching an average of 116±7 at P438, a significant ($p=0.02$) decrease. The vast majority of these cells are in the parenchyma, at P28-32 the ependyma contains just 12±1 BrdU incorporating cells, again this population decreases significantly ($P<0.004$), to 3±0.3 at P438. The number of BrdU incorporating cells that also expresses Fgf10-lacZ is low, with a base-line population at P28-35 of 12±4 cells. As is seen in the general BrdU incorporating population, the β-gal^{+}/BrdU^{+} population also decrease with age, staring of at 12±4 cells at P28-32, before completely disappearing by P438.

5.2.4 Majority of Fgf10-lacZ$^{\pm}$ cells do not divide after cessation of embryonic neurogenesis

To asses the mitotic potential of the Fgf10-lacZ lineage to the hypothalamus after the end of embryonic neurogenesis, BrdU was administered by daily IP injections to time-mated mothers at E15.5 and E16.5. This led to widespread BrdU incorporation in the hypotahalmus, noticeably more numerous than in the adult (fig 5.5) However, as in the adult, the portion of these that also express Fgf10-lacZ is small, and limited to the ependyma.

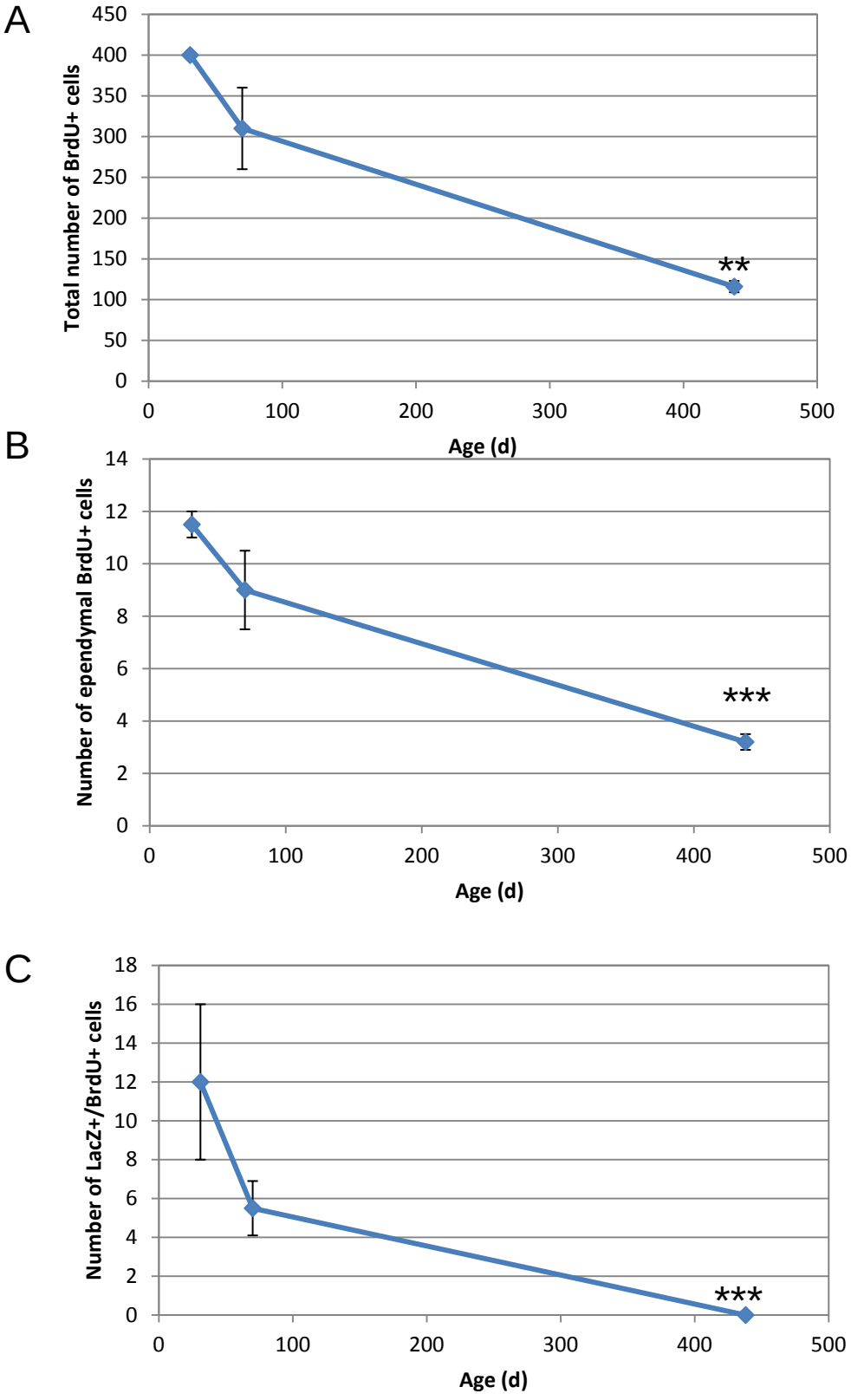

Fig 5.4 – BrdU incorporation and double-labeling with Fgf10-lacZ in young and aged Fgf10^{nlacZ} animals. (A) The hypothalamic population of BrdU decreases with aging, reaching a significantly lower level by P430. (B) In the ependymal tanycyte population, a similar decrease is observed(C) The number of BrdU incorporating Fgf10-lacZ cells also decreases with aging to an extent that none can be observed at P430.

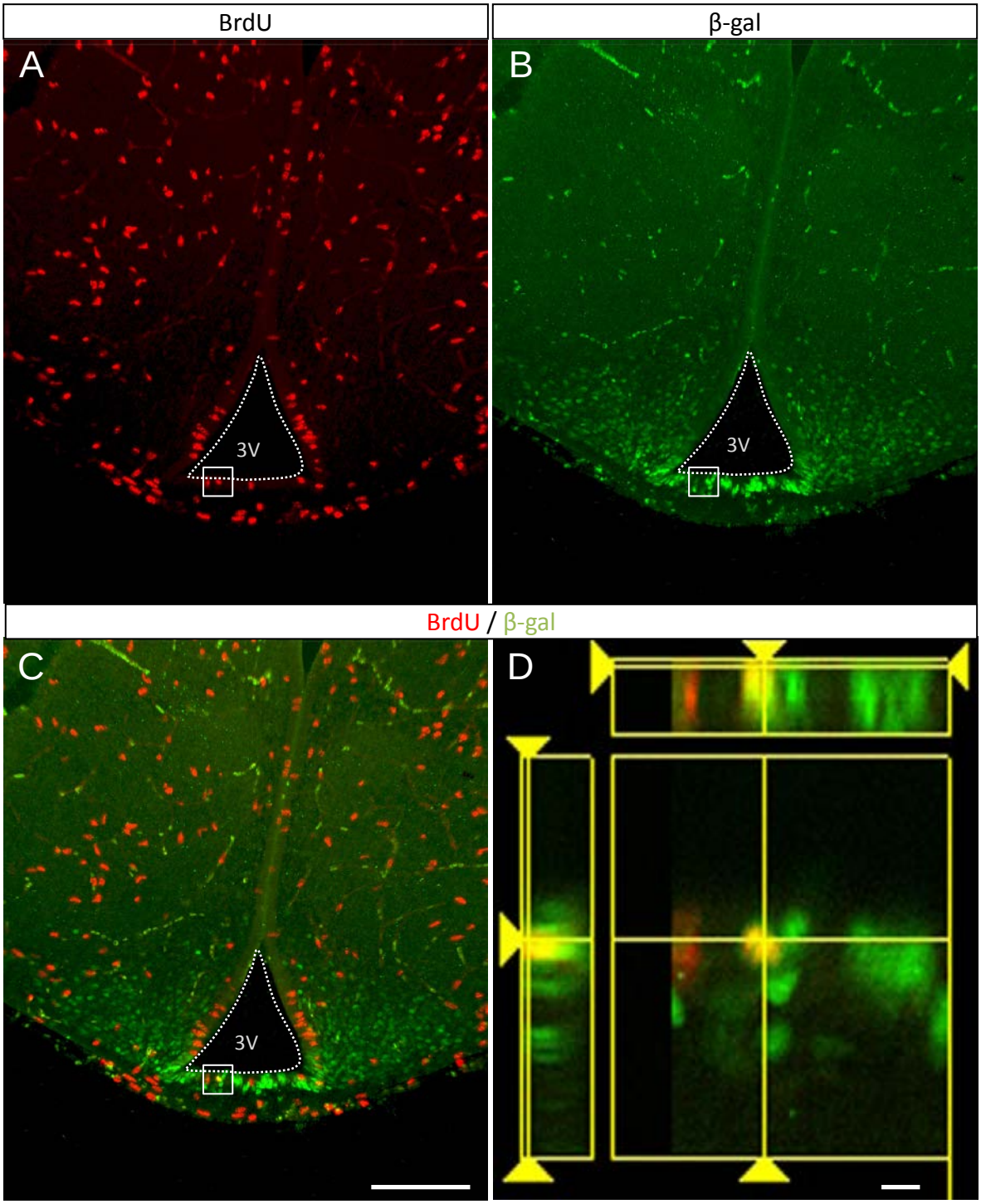

Fig 5.5 – BrdU incorporation in the hypothalamus at E16.5. Neurogenesis in the hypothalamus is finished by E16.5, but there is still significant cell proliferation, as evidenced by widespread BrdU incorporation. A fraction of ependymal Fgf10-lacZ^{+} cells incorporates BrdU. Scalebars in C: 100 µm, in D: 10 µm

3.2.5 Inducible nestin^{CreERT2} animals are not suitable for adult lineage tracing

In order to fate-map the descendents of hypothalamic tanycytes, Nestin^{CreERT2} were crossed with ROSA26^{YFP} or ROSA26^{RFP} reporter animals, generating nestin^{CreERT2}::ROSA26^{YFP} and nestin^{CreERT2}::ROSA26^{RFP} double transgenic animals. The reporter alleles were used both heterozygously and homozygously. A number of induction protocols were used, including daily IP injections of tamoxifen for 7 days, twice daily injections for 5 days, or food pellets for 14 days. At no time in either the YFP or RFP reporter animals was any recombination seen by native fluorescence, in either the hypothalamus or known neural stem cell niches. In order to increase the detection sensitivity for YFP, two different anti-GFP antibodies were used (see table 2.3), which haven been described to detect YFP. However, no staining was ever observed. With the current protocols, no detectable recombination was ever detected.

5.2.6 Inducible genetic lineage tracing confirms Fgf10 expression in the hypothalamus

An inducible lineage tracing system was set up using Fgf10^{CreERT2}::Rosa26^{lacZ} mice. A number of administration regimes were tried, the details for the mice used, treatments applied and recombination rates seen are in tables 5.1.

Table 5.1 – Optimisation of tamoxifen administration

Animals		**Treatments**			**Recombination rates**		
Age	Sex	Inj (d)	Tamox diet (d)	Normal diet (d)	No of cells	% Ependymal/ME	% Parenchyma
44	M		14	10	29	89.7	10.3
57	M	5 (2x/d)	10	8	77	64.9	35.1
57	M	5 (2x/d)	10	38	37	59.5	40.5
61	M	7	6	5	49	34.7	65.3
83	F	5	5		5	80.0	20.0
83	F	6	7	5	81	80.2	19.8

Recombined cells were observed throughout the hypothalamus (fig 5.6), with the most recombination being observed in the ependyma, although there was large inter-animal

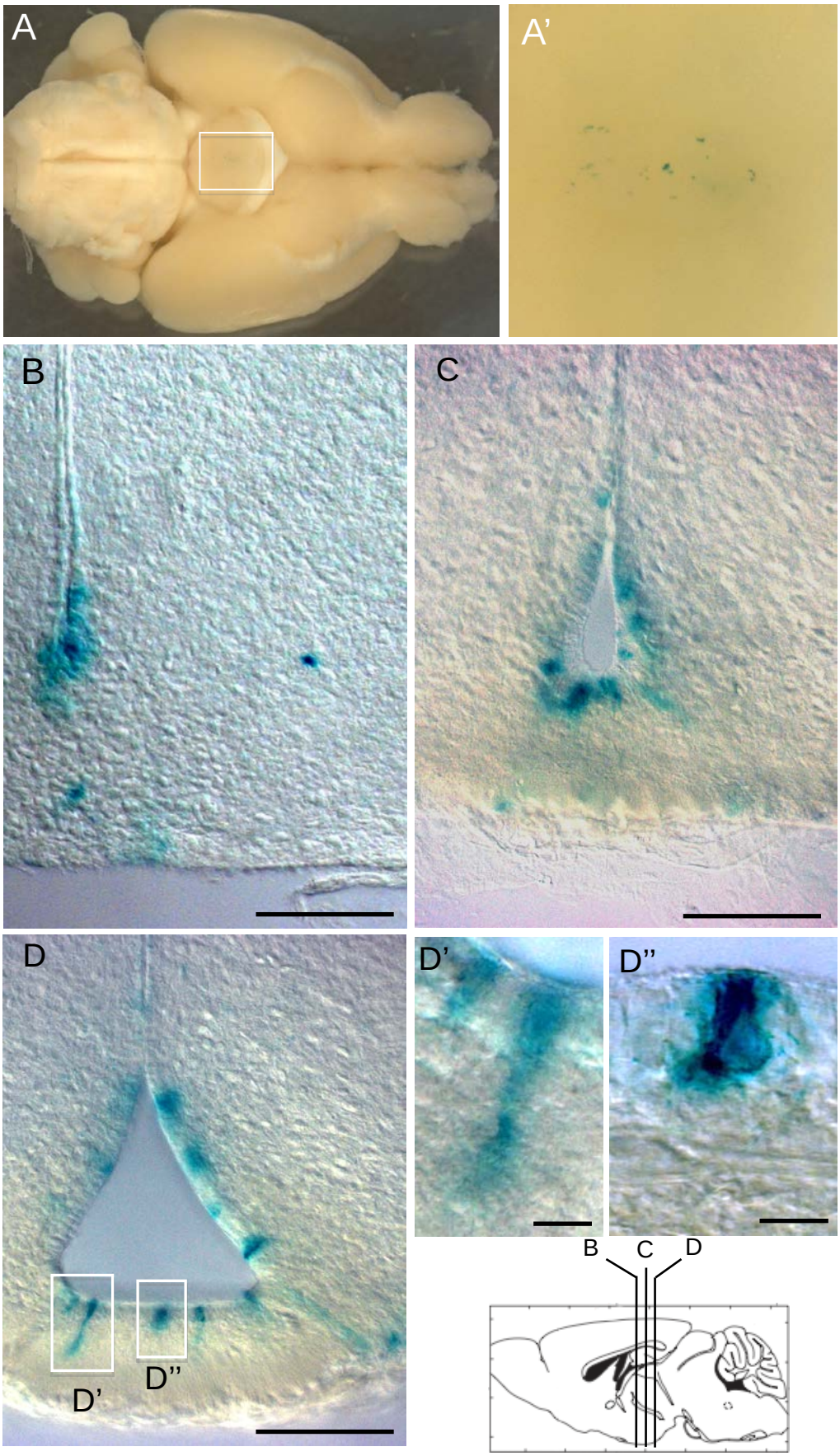

Fig 5.6 – Recombination in Fgf10^{CreERT2}::ROSA26^{lacZ} mice induced with tamoxifen. (A,A') Wholemount Xgal staining reveals successful recombination in the hypothalamus.(B-D) Recombined cells are found over the rostral-caudal axis, and in both ependyma and parenchyma . Scalebars: B-D: 250 µm, D',D'': 10 µm (E) Location of B-D

variability in both numbers and localisation of recombined cells. Expression in the ependyma is strongly clustered around -2 mm from bregma, whereas recombination in the ME is further caudal, with the majority of expression between -2.1 and -2.4 mm from bregma. In contrast, in the parenchyma recombination takes place over a much wider range, with recombined cells observed from -1.0 to -2.6 mm from bregma. A peak of expression is reached around -1.7 mm from bregma, but this is not a distinct as that of the ependyma or ME. The details of the animals used for quantification of recombination dynamics are in table 5.2

Table 5.2 – Animals used for assessing recombination dynamics. (Light gray is short treatments, dark gray long treatments)

Animals		**Treatments**			**Recombination rates**			
Age	Sex	Inj (d)	Tamox Diet (d)	Normal diet	No of cells	% Ependymal/ME	% Parenchyma	
28	F	7	10	7	53	47.2	52.8	**P28-32**
28	F	7	10		48	66.7	33.3	
28	F	7	10	36	159	42.8	57.2	
28	F	7	10	48	96	47.9	52.1	
32	F	7	10	22	129	55.0	45.0	
32	F	7	10	22	199	57.3	42.7	
42	F	7	10	12	124	59.7	40.3	**P40-42**
42	F	7	10	12	57	59.6	40.4	
40	F	7	10	36	112	57.1	42.9	
42	F	7	10	24	100	58.0	42.0	
42	F	7	10	24	87	58.6	41.1	
57	M	7	9	8	68	36.8	63.2	**P53-60**
57	M	7	9	8	87	65.6	34.4	
60	F	7	10	9	90	65.6	34.4	
60	F	7	10	9	110	61.8	38.2	
53	M	7	10	32	54	68.5	31.5	
53	M	7	10	32	59	74.6	25.4	
68	F	7	10	7	50	96.0	4.0	**P68-70**
68	F	7	10	13	60	88.3	11.7	
70	M	7	10	7	23	65.2	34.8	
70	F	7	10	9	105	70.5	29.5	
70	F	7	10	27	56	69.6	30.4	
70	F	7	10	39	69	42.0	58.0	

After 7 days of tamoxifen, 10 days of tamoxifen containing diet and approx 10 days of normal food, the baseline level of recombination in variable between animals, but averages between 60 and 90 cells per animal, depending on the age (fig 5.7). No significant effect of

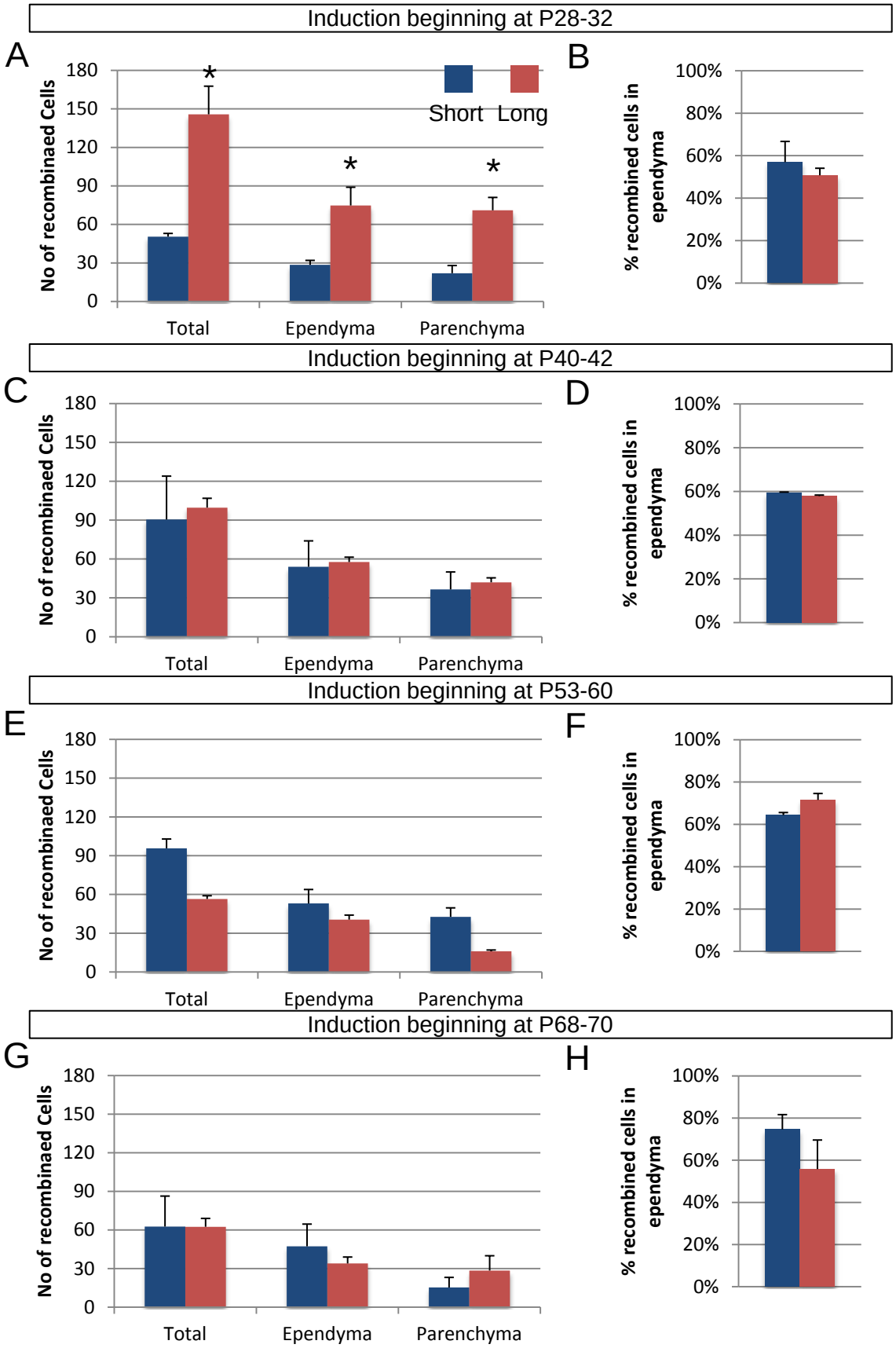

Fig 5.7 – Recombination dynamics in Fgf10^{CreERT2}::ROSA^{lacZ} mice over age. (A) At young ages (P28-P32), a significant increase in cell number is seen with longer times post-induction , in both ependyma and parenchyma. (B) This increase does not result in a greater proportion of ependyma cells. (C-H) At later ages, this effect is no longer seen.

starting age is seen on baseline levels of recombination. With longer post-induction intervals (14 to 40 days after last tamoxifen), to asses any expansion of this population over times, difference can be seen. When induction is started at young ages (P28-P32) longer post-induction intervals reveal a significantly expanded recombined total population (p=0.02), with both ependyma and parenchyma showing expansion (p=0.04 and p=0.01 respectively). This expansion does not affect the distribution of the recombined cells, as no significant difference can be seen in the fraction of cells that is located in the ependyma. At later ages (P40-42, P53-60 or P68-70) no significant differences are seen between short and long post-induction intervals.

5.2.7 Recombined cells do not express glial markers

The phenotype of recombined cells was investigated by immunohistochemistry. No recombined cells express the glial marker GFAP. In the ependymal layer, the domain of GFAP expression and the area of recombination are mutually exclusive (fig 5.8a).

5.2.8 Direct lineage tracing shows Fgf10 expressing cells generate hypothalamic neurons

To directly asses the neuronal contribution of the $Fgf10^{+}$ lineage, NeuN labelling was performed on recombined brains. Double positive cells were observed in both young adult (P28) and at later ages (P40 and P60) (fig 5.8 b-d)

5.2.9 Embryonic induction of $Fgf10^{CreERT2}$::$ROSA26^{lacZ}$ animals shows Fgf10 distribution

To investigate the activity of Fgf10 after embryonic neurogenesis, time-mated mothers received daily IP injections of tamoxifen at E15.5, E16.5 and E17.5 before being sacrificed at E18.5. At this time, few recombined cells can be seen in the hypothalamic ependyma (fig 5.9a-c). In addition, sparse recombination can be seen in the cortex (fig 5.9d) hippocampus (fig 5.9e), hindbrain (fig5.10a,b) and olfactory bulb (fig 5.10d). Interestingly, a dense cluster of

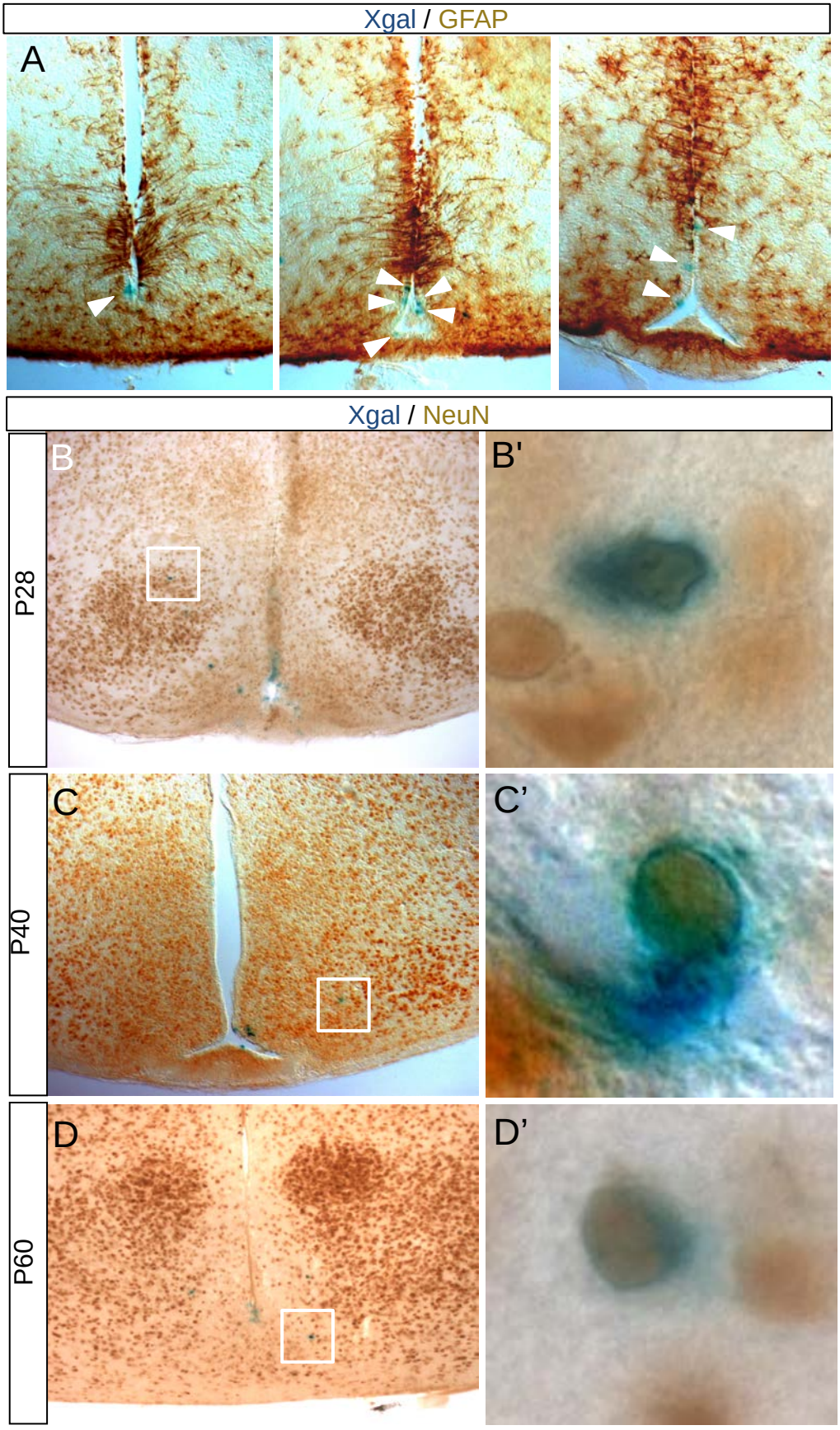

Fig 5.8 – Fate of recombined cells in Fgf10^{CreERT2}::ROSA26^{lacZ} mice. (A) The domain of ependyamal recombination (cells indicated by arrowheads) is mutually exclusive with GFAP expression. (B,C,D) Throughout early adulthood (P28, P40 and P60) a subset of recombined cells in the parenchyma express the neuronal marker NeuN

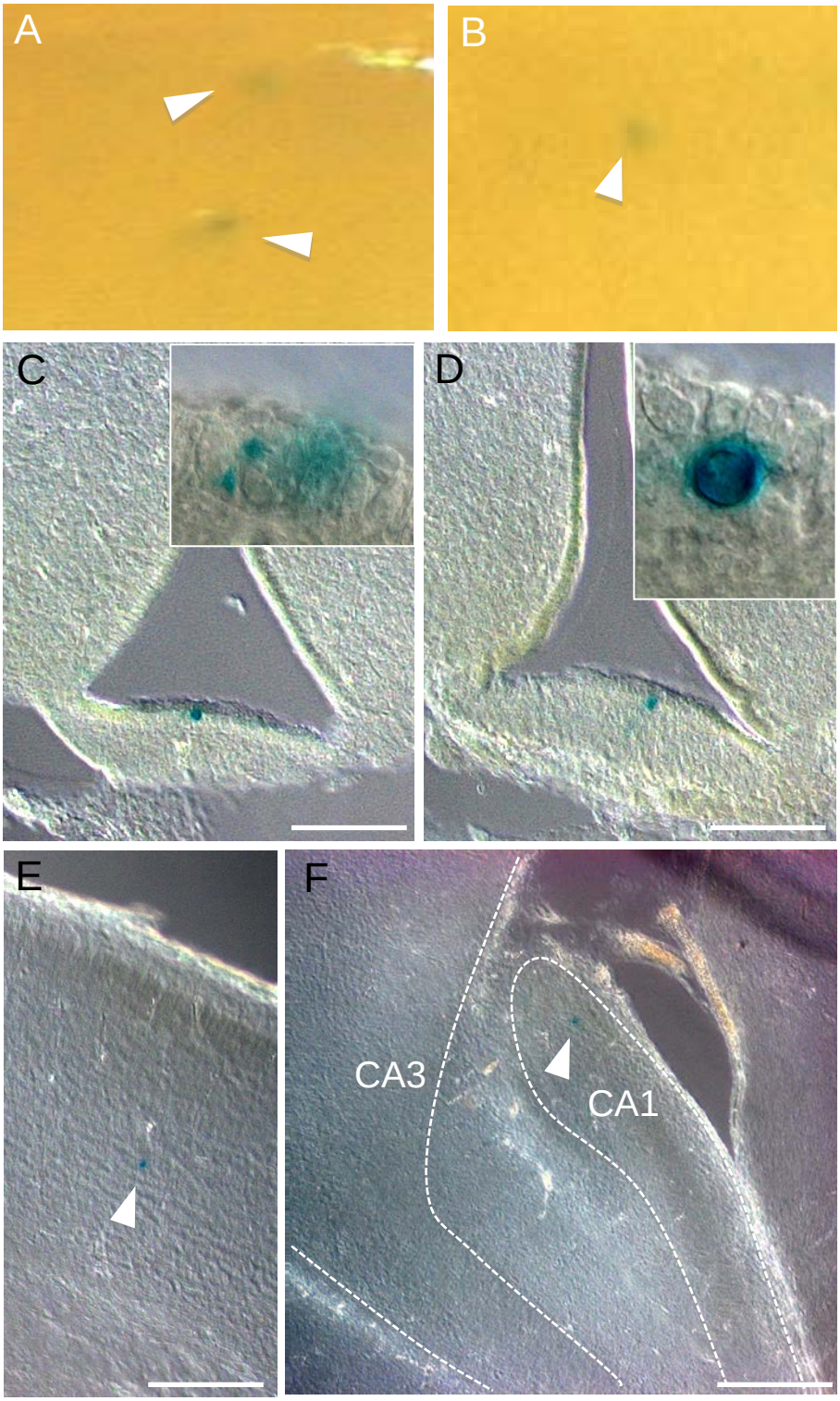

Fig 5.9 – Recombination in Fgf10^{CreERT2}::ROSA^{lacZ} mice at E18.5. Late during development, sparse recombination is seen in the hypothalamus, in both wholemount (A,B) and sections (C-D). Further recombination is occasionally seen in the neocortex (E) and hippocampus (F). Scalebars C-F: 250 µm

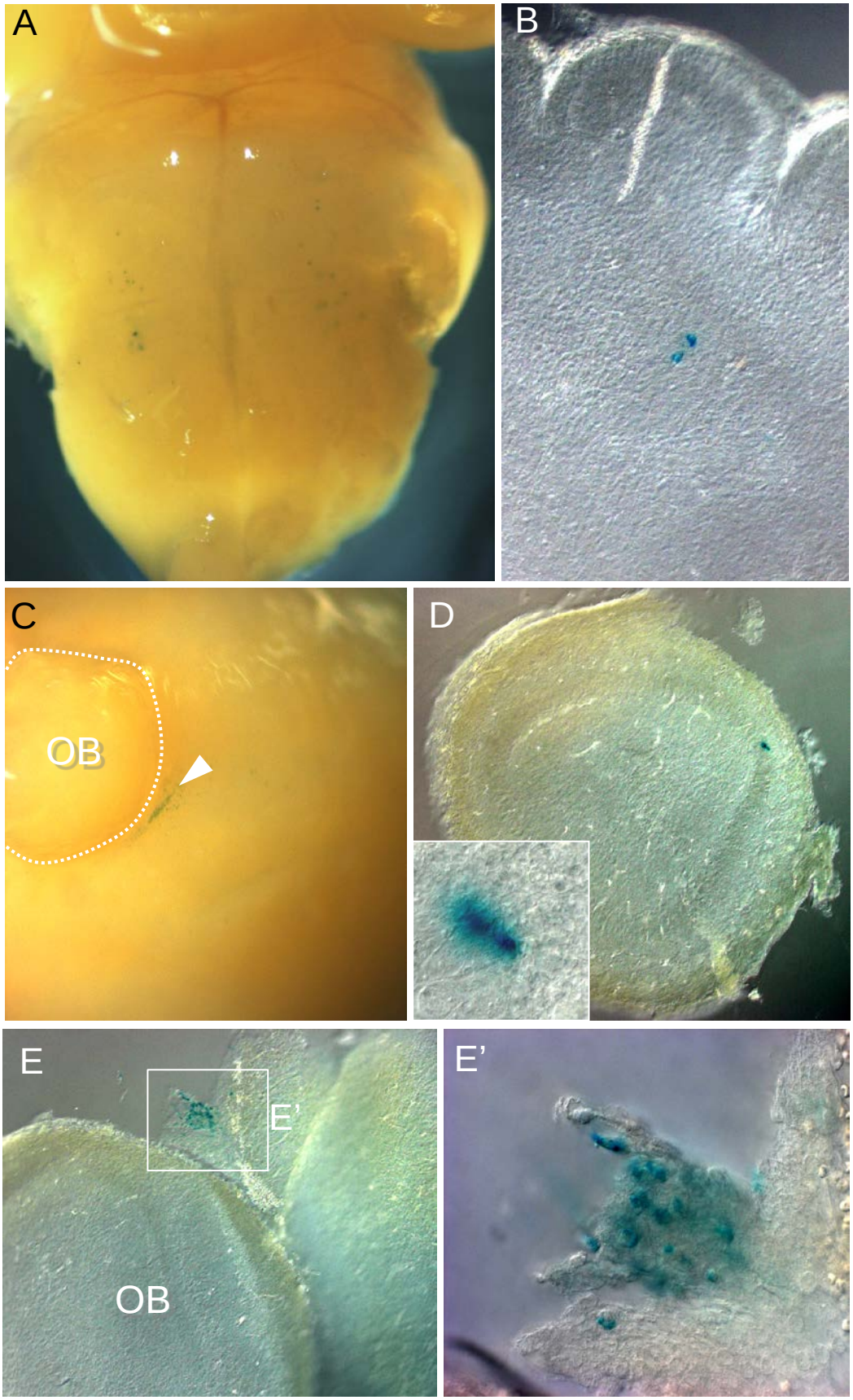

Fig 5.10 – Recombination in Fgf10^{CreERT2}::ROSA^{lacZ} mice at E18.5. (A,B) Recombination is see throughout the hindbrain. (C) View towards caudal of the olfactory bulb (OB). Recombination in the frontal brain is seen in the frontal cortex adjacent to the OB. (D) Rare recombination event in the OB proper. (E, E') Cluster of recombined cells in between the frontal cortex and the olfactory bulb.

recombined cells can be observed on the surface of the fontal cortex, directly adjacent to the olfactory bulb (fig 5.10c,e).

5.2.10 Fgf10^{CreERT2}::Rosa26^{Tomato} mice confirms lineage tracing results

Use of a fluorescent reporter strain with the Fgf10^{CreERT2} mice allows for more convenient double-labelling for lineage tracing purposes. When induced at P60 with the same administration regime as for Fgf10^{CreERT2}::Rosa26^{lacZ} mice, these mice shows extensive recombination in the hypothalamus (Fig 5.11). The Tomato reporter protein fills up the entire cytoplasm, highlighting the radial processes of the tanycytes (Fig 5.11a). Double-labelling with GFAP shows the recombined tanycytes do not express this astrocytic marker, confirming what was seen with the Rosa26^{lacZ} reporter. In the parenchyma, recombined cells show a clear neuronal morphology, with axonal networks highlighted by the fluorescent reporter (Fig 5.11b,c). The majority of these cells also express NeuN.

5.2.11 Fgf10^{CreERT2}::Rosa26^{Tomato} mice show more widespread recombination

In the rest of the brain, the Fgf10^{CreERT2}::Rosa26^{Tomato} mice show recombination in areas where the Rosa26l^{acZ} mice do not. Apart from the hypothalamus, recombination is seen in the amygdala (see Chapter 6), hippocampus (Fig 5.12a) and cortex (Fig 5.12b). In the hippocampus, very sparse labelling is seen in NeuN expressing neurons in the CA1 region, with axons projection deeper into the hippocampus towards the dentate gyrus. In the cortex, several neurons in the deeper cortical layers are labelled, showing long axons projecting towards the pial surface of the brain.

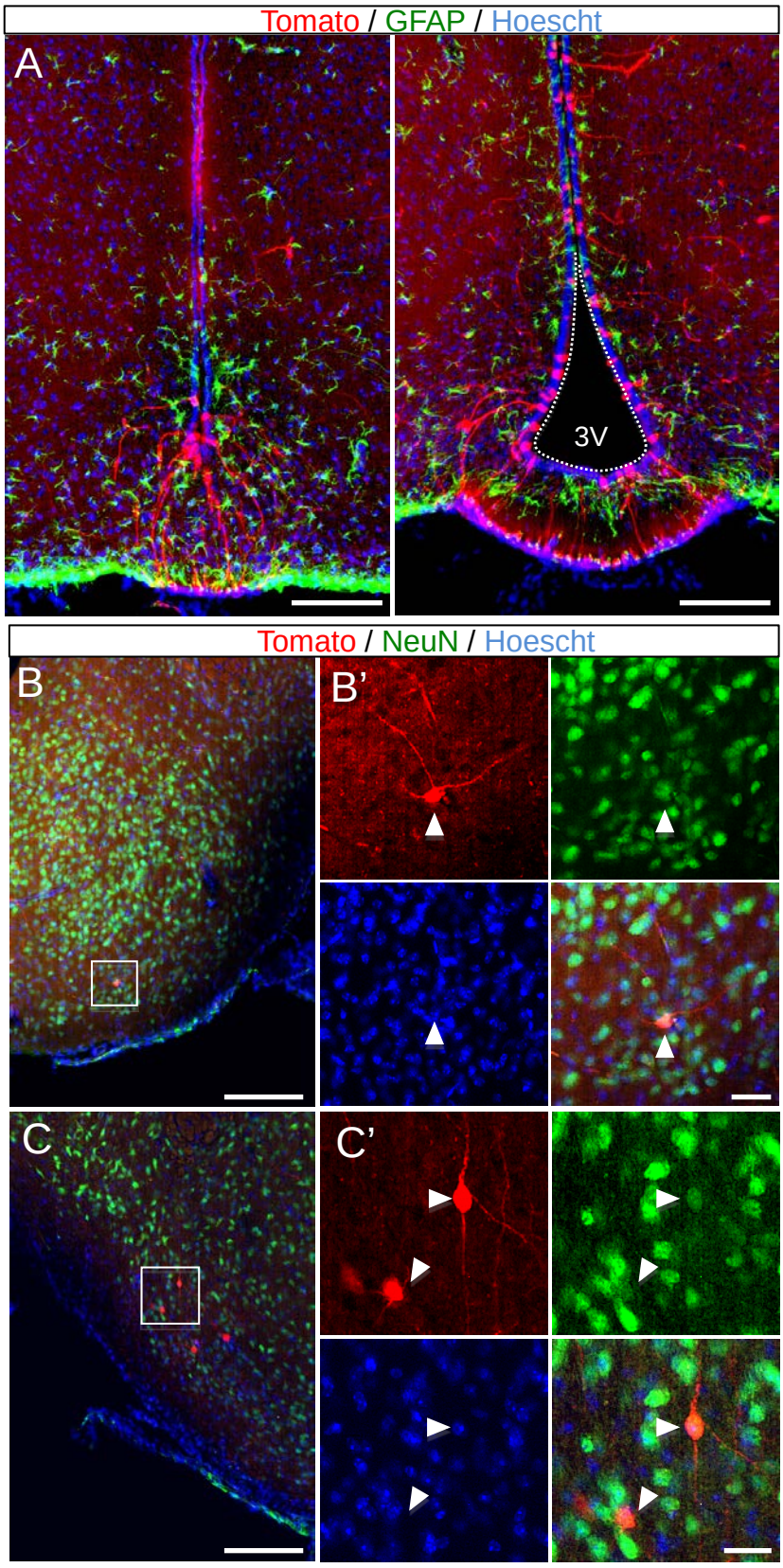

Fig 5.11 – Recombination in hypothalamus in Fgf10^{CreERT2}::ROSA26^{Tomato} mice copies that in ROSA26^{lacZ} mice. (A) Using a fluorescent Tomato reporter, recombination mimicked that of the LacZ reporter. The Tomato fills up to cells, highlighting the tanycyte processes Recombination does not colocalise with GFAP expression (B,C) Many recombined cells in the parenchyma have both neuronal morphology and express NeuN. Scalebars: A,B,C: 250 µm, B',C': 10 µm

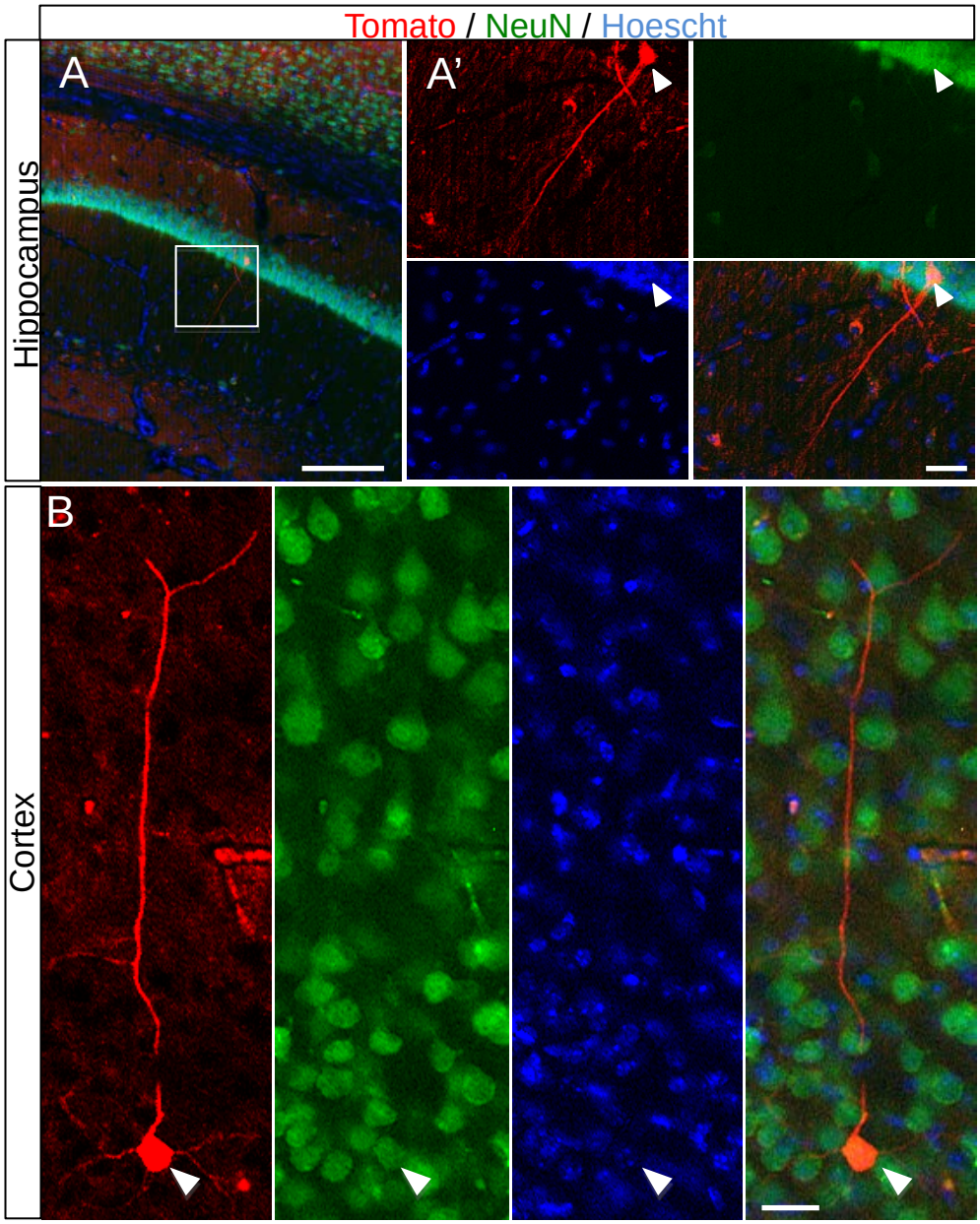

Fig 5.12 – Widespread recombination in Fgf10^{CreERT2}::ROSA26^{Tomato} mice (A) Recombined hippocampal NeuN+ in the CA1 region neuron projecting an axon deeper into the hippocampus. (B) Recombined cortical pyramidal neuron, the reporter highlights both the axonal and dendritic networks of this neuron. Scalebars: A: 250 µm, A', B: 10 µm

5.3 Discussion

If a stem or progenitor cell population is present in the hypothalamus, cell division would take place. Labelling with the proliferation associated protein Ki67 shows sparse immunoreactivity in the hypothalamus, with some of the $Ki67^{+}$ ependymal cells also labelling with β-gal. A more complete picture of cell division is achieved using BrdU administration. Given the low rates of baseline BrdU incorporation seen in previous studies, a novel protocol using a long-term cumulative BrdU administration via the drinking water was used. This labelled substantially more cells than traditional short-term IP injection protocols, in both traditional neurogenic niches (dentate gyrus) and the hypothalamus.

Although long term BrdU administration is more sensitive than traditional short-term IP injections, it also increases the total dose received. This present a potential confounding factor in that there may be significant cytotoxicity of the BrdU, disturbing the normal proliferation in the hypothalamus and leading to cell death. Immunohistochemisty for marker of apoptosis such as activated caspase 3 would need to be undertaken in BrdU treated animals to exclude this possibility.

BrdU incorporation in the hypothalamus is throughout the ependyma and parenchyma. Only a minority of tanycytes incorporate BrdU during 21 days, indicating not all Fgf10 expressing cells actively divide. Some cells in the hypothalamus do express β-gal and incorporate BrdU, these are located exclusively in the ependyma or directly adjacent to it, further strengthening the notion that this is the location of the actual dividing stem cells.

Many of the double-positive cells are located just adjacent, but not in, the ependymal layer. Two factors may affect this localisation. It is known from the embryonic neural tube and early postnatal SVZ that the nucleus of radial glia is mobile during the cell cycle, as it displays interkinetic nuclear migration (Tramontin et al., 2003). During the G1 phase, the cell nucleus moves outward into the radial fibre, where S phase takes place. During G2 phase, the nucleus

moves back to the ventricular surface, where mitosis takes place. BrdU will be incorporated during S-phase and retained during the rest of the cell cycle, leading to labelled nuclei being located throughout the radial extent of the cell. Alternatively, the relative localisation of labelled cell may represent two different populations. The most mitotic cells in other neurogenic niches are known to be the transit amplifying cells, rather than the radial glial stem cells. AraC infusion into the SVZ ablates the population of transit amplifying cells, but leaves the radial glia population largely intact, indicating these are not highly mitotic (Doetsch et al., 1999). In analogy to the to the SVZ, the resident stem cells would be the radial $BLBP^{+}/nestin^{+}/musahi^{-}$ cells, which rarely incorporate BrdU, while a population of transit amplifying $BLBP^{-}/nestin^{+}/musashi^{+}$ cells, which have a rounded morphology reminiscent of transit amplifying cells, divide more frequently. The majority of BrdU incorporating cells in the hypothalamus do not express Fgf10-lacZ. At this time it is unknown what these cells are, it is likely many of these are of a non-neural lineage, which may include blood vessel endothelial cells and resident microglia. Further immunohistochemistry will shed light on this.

During the lifetime, the number of dividing cells detected in the hypothalamus at any given time decreases. This can be due to either a lengthening of the cell cycle, causing fewer cells to be in S-phase at any given time, due to cells entering quiescence in G_0 or due to a loss of cells altogether. The decrease of mitotic activity correlates with the decrease in total Fgf10-$lacZ^{+}$ cell number seen, and would suggest a turn-over of cells, with a reduced replacement capacity as the animals age.

BrdU incorporation during late embryonic neurogenesis (E14.5 to E16.5) shows that by this stage the Fgf10-lacZ population is already largely quiescent, as double-positive cells are rare. This correlates with the expression of Tuj1 on the majority of parenchymal Fgf10-$lacZ^{+}$ cells by E12.5, showing that most of the proliferation is over by this stage, and cells are maturing. The main embryonic contribution of the Fgf10 expressing lineage to the

hypothalamus thus corresponds with the timing of wider neurogenesis in the hypothalamus, with a small population remaining mitotically active in late gestation and into adulthood.

Both the dynamics and progeny of these dividing cells were investigated through genetic lineage tracing. Tamoxifen induced recombination in $Fgf10^{CreERT2}$::$ROSA26^{LacZ}$ adults shows a far more limited expression pattern than is seen in $Fgf10^{nlacZ}$ animals. Recombination is limited to the hypothalamus, and is low efficiency. From in situ data it is known that Fgf10 is expressed throughout the ventricle floor, but only a fraction of these cells actually recombine. In other regions known to actively express Fgf10 in the adult, such as the hippocampus, no recombination is seen at all. The preferential recombination in the hypothalamus may reflect higher activity of the Fgf10 promoter in this area compared to others. A different fact to take into account is the highly vascularised nature of the hypothalamus, potentially leading to locally high doses of tamoxifen. Excision efficiency of Cre recombinase is known to be tamoxifen dose-dependant (Hayashi and McMahon, 2002). It may be possible to obtain a more complete recombination in the hypothalamus and other areas by using higher tamoxifen doses, but the dose used in the current experiments (80-100 mg/kg) is already at the high end of the commonly used doses in literature, so complete recombination in this particular mouse line will likely be impossible to achieve.

The temporal dynamics of expression were studied by inducing recombination at different ages, and assessing the recombined population at different times after induction. When young animals (P28-P30 at start of induction) are sacrificed 14 days or more after the cessation of tamoxifen administation, the recombined population significantly expands compared to shortly after administration. This increase in cell number clearly illustrates the proliferative capacity of the Fgf10 expressing population at this stage, as any more cells formed after the cessation of tamixofen administration must be solely due to cell division. In approximately 21 days, the Fgf10 population more than doubles, showing an approximate cell cycle time of 14 to 21 days, which is similar to that indicated by BrdU incorporation rates. In

contrast, when recombination is induced at later ages, the proliferation effect is no longer seen, which correlates with a decreased mitotic activity seen with BrdU incorporations.

Since in general approximately half of recombined cells at any time are in the parenchyma, where according to in situ data Fgf10 is not expressed, it is likely considerable migration takes place during the three or more weeks after the start of tamoxifen administration. The neuronal identity of these cells is evidenced by NeuN expression, and their clearly neuronal morphology as seen in the $Rosa26^{Tomato}$ reporter. The fact that recombined cells express NeuN unequivocally shows that the Fgf10 expressing lineage continues to contribute neurons to the hypothalamus post-natally. Since recombined NeuN expressing cells are seen up to P60, the $Fgf10^{+}$ tanycyte population is clearly continuing to supply new cells to the hypothalamus, although at a low level as no overall increase in cell number can be seen at this age. Although no GFAP expressing recombined glia were seen in the parenchyma, the relative rarity of Fgf10 expressing glia in general (see chapter 3) combined with the observed recombination efficiency makes detection of any recombined glia unlikely.

Induction of recombination during late gestation shows the continued expression of Fgf10 in the hypothalamus after embryonic neurogenesis. Only few cells recombine, but given the shorter administration times and the lower doses likely to be achieved in utero, this is not surprising. It is interesting to note that embryonic recombination takes place in several areas that show expression in the adult in the $Fgf10^{nlacZ}$ line, but do not show recombination in the $Fgf10^{CreERT2}$::$ROSA26^{lacZ}$ line in the adult. This includes prominent recombination in hindbrain nuclei and scattered recombination in the cortex, hippocampus and olfactory bulb. This points to the possibility that these only have low-level or indeed no active Fgf10 expression in the adult, and what is seen in the $Fgf10^{nlacZ}$ line is solely retained reporter protein from promoter activity during late gestation.

The combination of BrdU incorporation assays and genetic lineage tracing clearly shows that a continued population of Fgf10-lacZ positive cells continues to exist after the

cessation of embryonic neurogenesis and into adulthood. This population contributes neurons during embryonic neurogenesis, and continues to contribute small numbers of neurons and glia into adulthood. Although the population may be largely quiescent by P40, it still has the potential to divide and to contribute new cells to the parenchyma up to P60. In aged animals however, this population may be terminally post-mitotic.

Chapter 6

In vitro culture and characterisation of Fgf10-lacZ expressing primary cells

6.1 – Introduction

While cells can be readily studied post-mortem in fixed tissue, some properties can only be examined in living cells. This necessitates setting up a primary culture system to isolate and grow these cells in vitro. The different cell types in the adult brain require different isolation protocols and culture conditions to survive in vitro, with astrocytes being readily culturable, and neurons and neural stem cells far more difficult to grow from the adult brain.

The long-standing culture system for neural stem cells is the neurosphere assay. Here, the tissue of interest is dissected out, digested to a single cell solution, and cultured in a defined serum-free medium containing EGF and FGF2. Unless a suitable adhesion factor is provided, these cells remain non-adherent, and will divide to form clonal clusters of neural stem cells, termed neurospheres. This was first shown in a landmark paper by Reynolds and Weiss (Reynolds and Weiss, 1992), where the striatum was isolated, suggesting a probable SVZ origin for these neurospheres. They also showed these cells were capable of generating neurons. Later it was shown that neurospheres can also give rise to astrocytes and oligodendrocytes (Vescovi et al., 1993).

Neurospheres have also been isolated from the hippocampus (Gage et al., 1995), spinal cord (Weiss et al., 1996), amygdala (Arsenijevic et al., 2001) and hypothalamus (Xu et al., 2005). The fact that cells in neurospheres maintain their neurogenic potential even after long term (>1 year) culture was shown by transplanting these cells into the rat brain and showing they generate mature hippocampal granular neurons (Gage et al., 1995)

Primary neurons have been grown from many areas in the embryonic brain, including cortex (Yavin and Menkes, 1973), hippocampus (Walicke et al., 1986), spinal cord (Deloulme et al., 1991), striatum and substantia nigra (Brewer, 1995). However, culturing viable neurons from the adult brain is more difficult. From the adult, hippocampal neurons have been

cultured (Brewer, 1997). Primary neurons have been isolated from the embryonic (Lui et al., 1990), newborn (Lolait et al., 1983) and adult (Yamashita et al., 1992) hypothalamus. More recently, immortalised cell lines have been derived from primary hypothalamic neurons (Dalvi et al., 2011; Gingerich et al., 2009).

Primary astrocytes, first cultured in the early 70s (Booher and Sensenbrenner, 1972), represent a good model of astrocyte function in vivo. They maintain similar electrical properties to their in vivo counterparts (Kimelberg, 1983) and express similar proteins to in vivo astrocytes, including markers such as GFAP, S100β, receptors for glutamate (Bowman and Kimelberg, 1984) and GABA (Kettenmann and Schachner, 1985), and glutamate transporters (Swanson et al., 1997). Primary astrocytes have also been cultured from embryonic (Garcia-Segura et al., 1989) and neonatal (Ernsberger et al., 1990) hypothalamus.

Although neural stem cells, neurons and astrocytes have been cultured from the adult hypothalamus, these cells have not been studied much in vitro. Establishing reliable protocols to culture these different cell types from the adult hypothalamus will allow for detailed study of their properties, and to asses the function of Fgf10 in these cells.

Aims

In order to investigate the properties of hypothalamic Fgf10-lacZ expressing neural cells in vitro, culture protocols for these cell types were established, and the phenotype and proliferative capacity of the Fgf10-lacZ^{+} cells examined. Additionally, the potential of using FACS to enrich Fgf10-lacZ expressing cells was assessed.

6.2 – Results

6.2.1 The adult mouse hypothalamus is capable of generating neurospheres

In order to confirm that the hypothalamus contains stem cells that can form neurospheres in vitro, a number of different combinations were tried to find an optimal protocol. The protocols tried and results found are details in table 6.1. It was found that the hypothalamus is capable of generating neurospheres under a number of conditionss.

Table 6.1 Protocols used for neurosphere generation and their efficacy

Dissociation	**Culture medium**	**Percoll**	Results			
			SVZ		**ME**	
			Typical yield	Growth	Typical yield	Growth
Accutase	Neurobasal + B27	n/a	$1.5x10^6$	+/-	$1.2x10^6$	+/-
Mechanical	Neurobasal + B27	n/a	$1.4x10^6$	-	$1.1x10^6$	-
	DMEM/F12 + B27	n/a	$1.4x10^6$	++	$1.1x10^6$	++
Trypsin	DMEM/F12 + B27	n/a	$1.3x10^6$	-	$1.0x10^6$	-
Papain	DMEM/F12 + B27	n/a	$1.5x10^6$	-	$1.2x10^6$	-
	DMEM/F12 (mod) + B27	22%	$0.8x10^6$	-	$0.5x10^6$	-
	DMEM/F12 (mod) + B27	11%	$0.9x10^6$	+	$0 .6x10^6$	+/-

The efficacies of different protocol are variable. Mechanical dissociation in combination with culturing in a DMEM/F12 based medium gives the most reliable generation of neurospheres. Accutase dissociation and culture in Neurobasal medium also works, as does papain dissociation with Percoll purification and culture in modified DMEM/F12, however these are not as efficient. ++, +, +/- represent high, medium and low efficiency, respectively. – indicates no successful culture.

Hypothalamic neurospheres were found to be comparable to SVZ derived ones in size and morphology (Fig 6.1a), although fewer were initially generated for comparable amounts of tissue digested. Hypothalamic neurospheres were found to be capable of efficient regrowth after passaging for up to 5 passages. When comparing average diameter of neurospheres over time between hypothalamus and SVZ, no significant difference was found over the first three passages (Fig 6.1b. Growth rates over the different passages were found to be identical as well (Fig 6.1c).

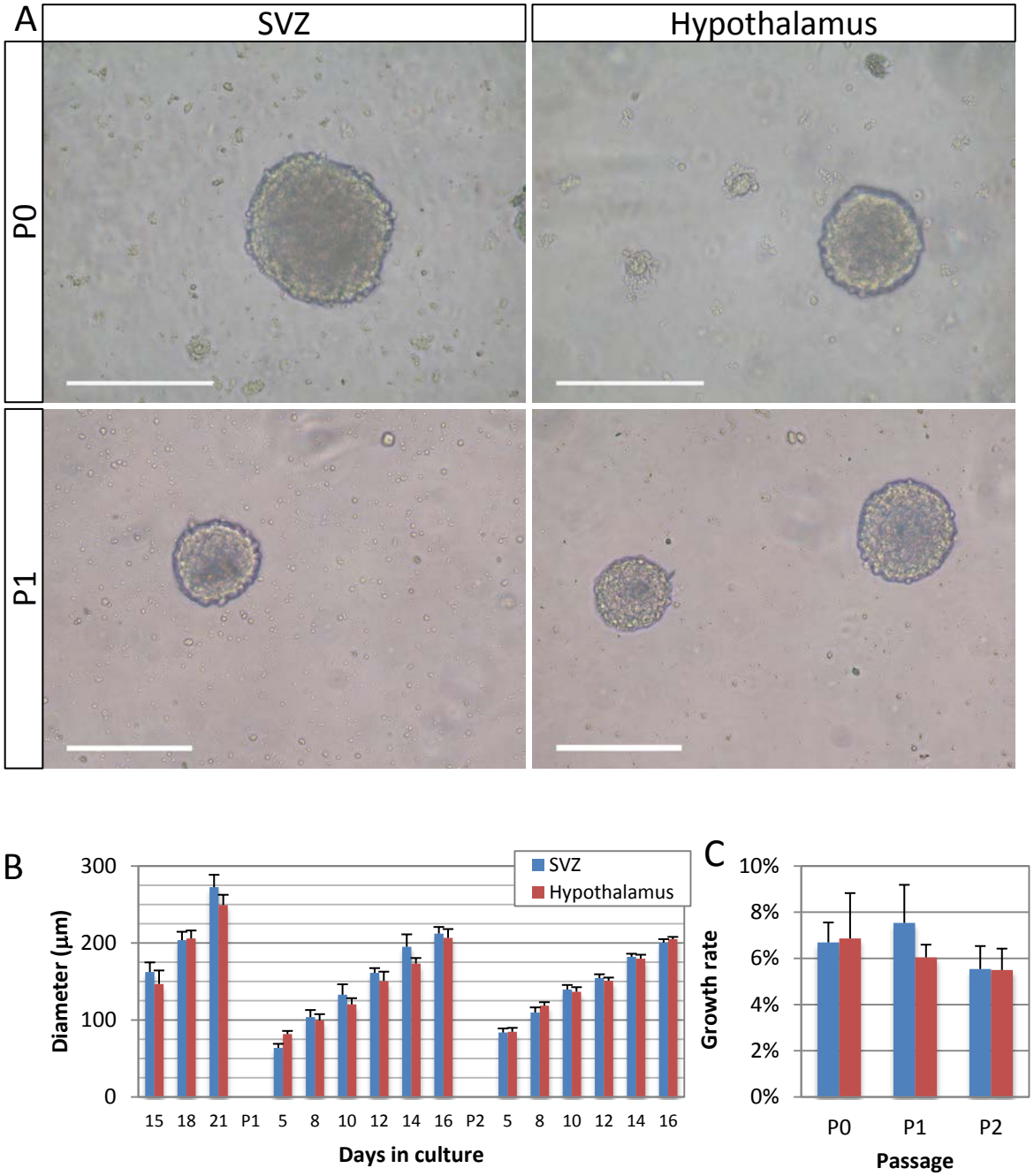

Fig 6.1 – Neurosphere formation from the adult hypothalamus (A) Neurospheres of comparable size and morphology of those from the SVZ can be grown from the hypothalamus, and are capable of regrowth after passaging. (B) The average diameter of neurospheres over time is not significantly different between SVZ and hypothalamus derived culture. (C) Average growth rates for different passages are the same between SVZ and hypothalamus cultures. Scalebars represent 100 µm

6.2.2 Hypothalamic neurospheres differentiate readily on a number of substrates

Individual neurospheres were placed onto glass coverslips coated with a variety of substrate concentrations, single or double coatings of poly-D-lysine (PDL) at 20 μg/ml or coatings of poly-D-ornithine (PORN) at 40, 100 or 250 μg/ml were used. Cells were cultured without growth factor, in the presence of 2 or 10% added fetal bovine serum to promote differentiation. Under all conditions, spheres attached and cells were observed migrating outwards after 24 to 48 hours (Fig 6.2). No appreciable difference was seen between conditions.

6.2.3 Hypothalamic neurospheres are multipotent

When induced to differentiate by withdrawal of growth factors and addition of serum, single hypothalamic neurospheres can form all three neural lineages (Fig 6.3), $Tuj1^+$ neurons, $GFAP^+$ astrocytes and $Olig2^+$ oligodendrocytes. A small number of cells express both Tuj1 and GFAP.

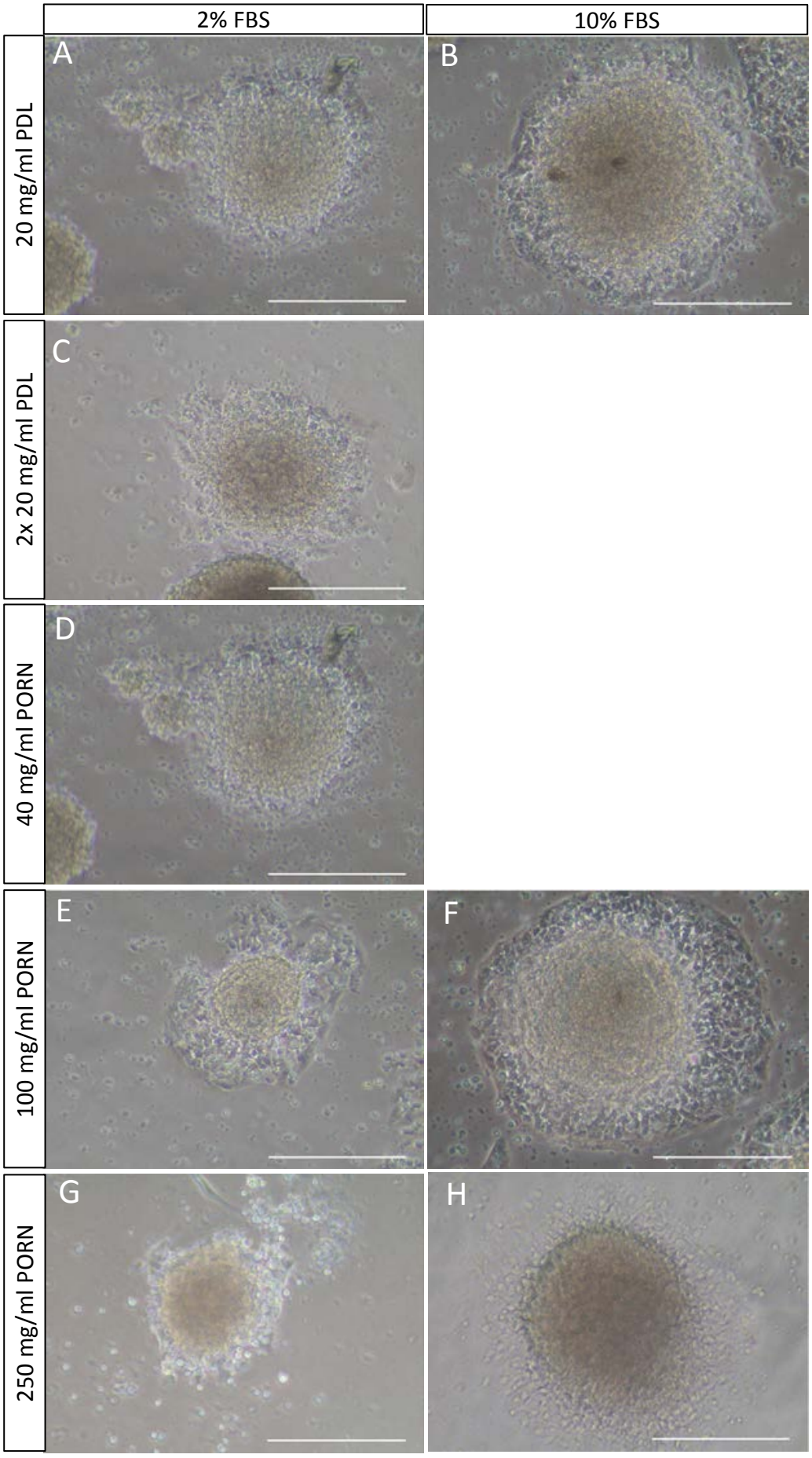

Fig 6.2 – Substrate dependency of neurosphere differentiation. Neurospheres readily differentiate on a range on substrates and with different concentrations of serum. Scale bars represent 100 µm

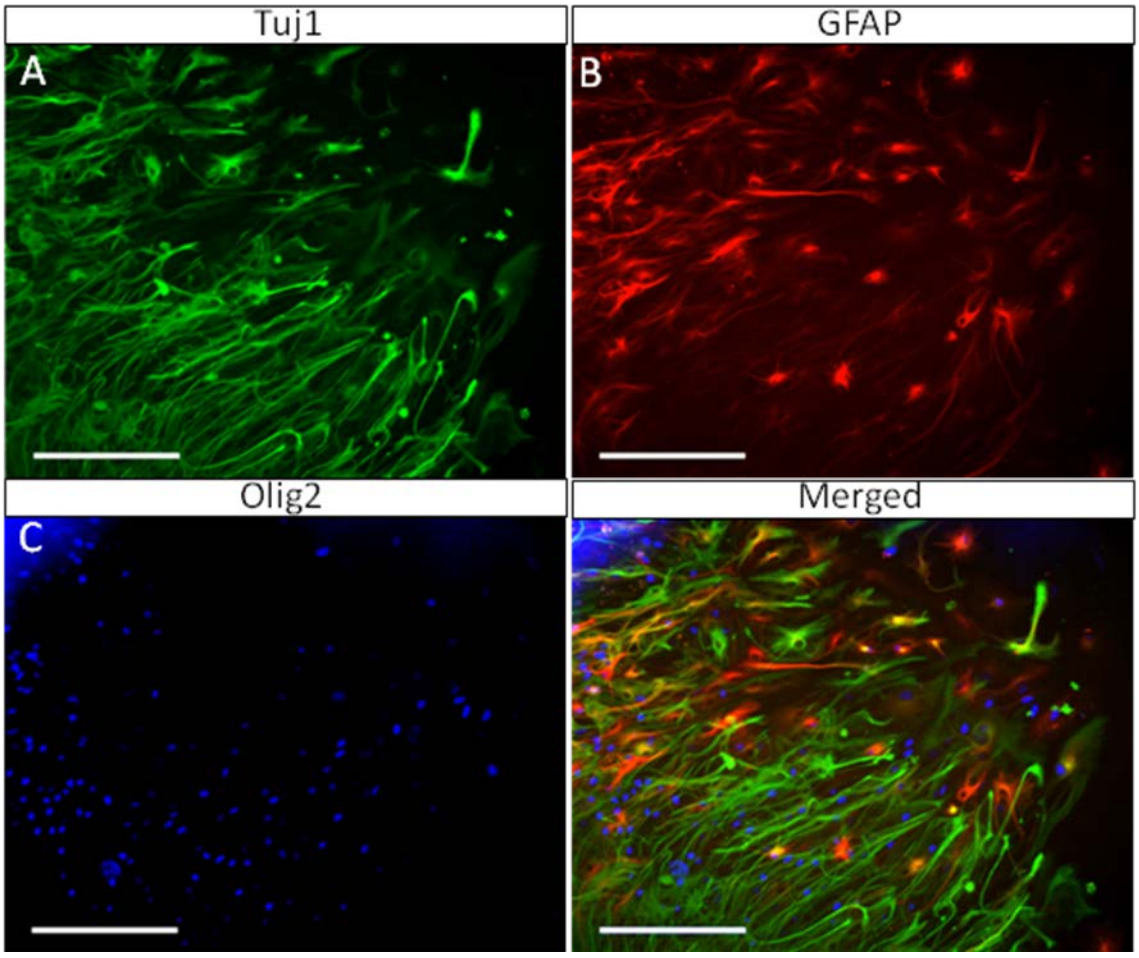

Fig 6.3 – Differentiation of hypothalamus derived neurospheres. Single neurospheres can form all three lineages, neurons (Tuj1^{+}), astrocytes (GFAP^{+}) and oligodendrocytes (Olig2^{+}). Some cells express both Tuj1 and GFAP. Scale bars represent 100 µm

6.2.4 The Fgf10-lacZ^{+} lineage readily forms astrocytes in vitro

Dissociated newborn brains from Fgf10^{nlacZ} animals were plated under astrocyte growth promoting conditions, resulting in many astrocytes at 3 to 4 DIV. Xgal staining reveals many of these are lacZ positive, and have a characteristic astrocyte morphology (Fig 6.4a,b). Some Xgal positive cells in these cultures can be observed to divide (Fig 6.4c), and many Xgal positive cells were observed in small clusters. Immunohistochemistry for GFAP confirmed that these cells are indeed astrocytes (Fig 6.4d)

In some instances, spherical cell masses were observed, surrounded by a dense patch of cells. Many of these were Xgal positive and of these, many were surrounded by a halo of Xgal positive cells (Fig 6.5). Some Xgal negative spheres were observed, but were a minority and of a smaller size than the Xgal positive one.

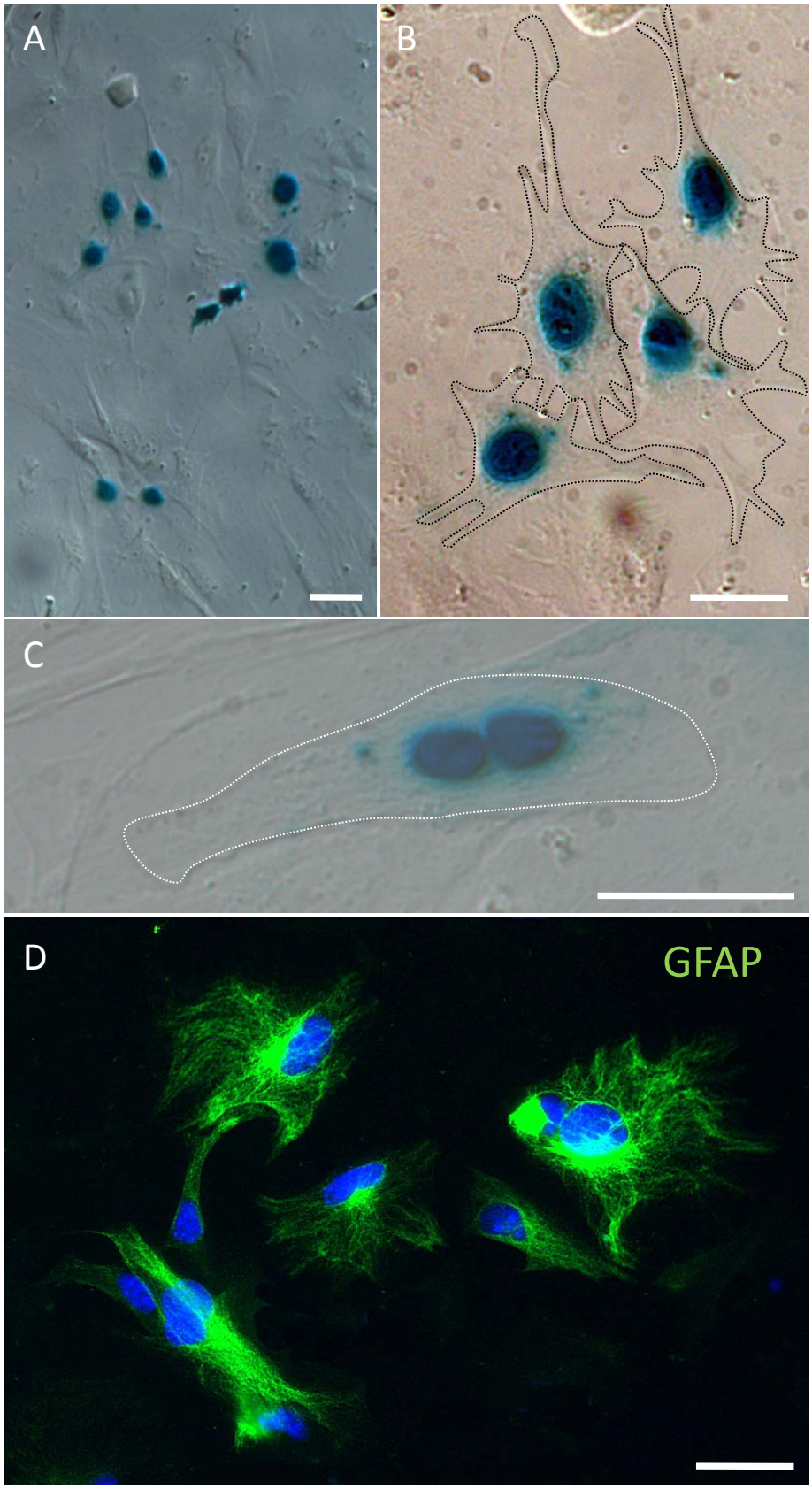

Fig 6.4 – Fgf10-lacZ expressing primary astrocyte cultures. (A) Primary astrocytes isolated from $Fgf10^{nlacZ}$ animals readily produce Xgal positive astrocytes. (B) The morphology of these cells is characteristic of astrocytes (C) In some instances, dividing Xgal positive cells can be observed. (D) immunohistochemistry for GFAP in parallel cultures confirms this population as astrocytes. Scale bars represent 10 µm

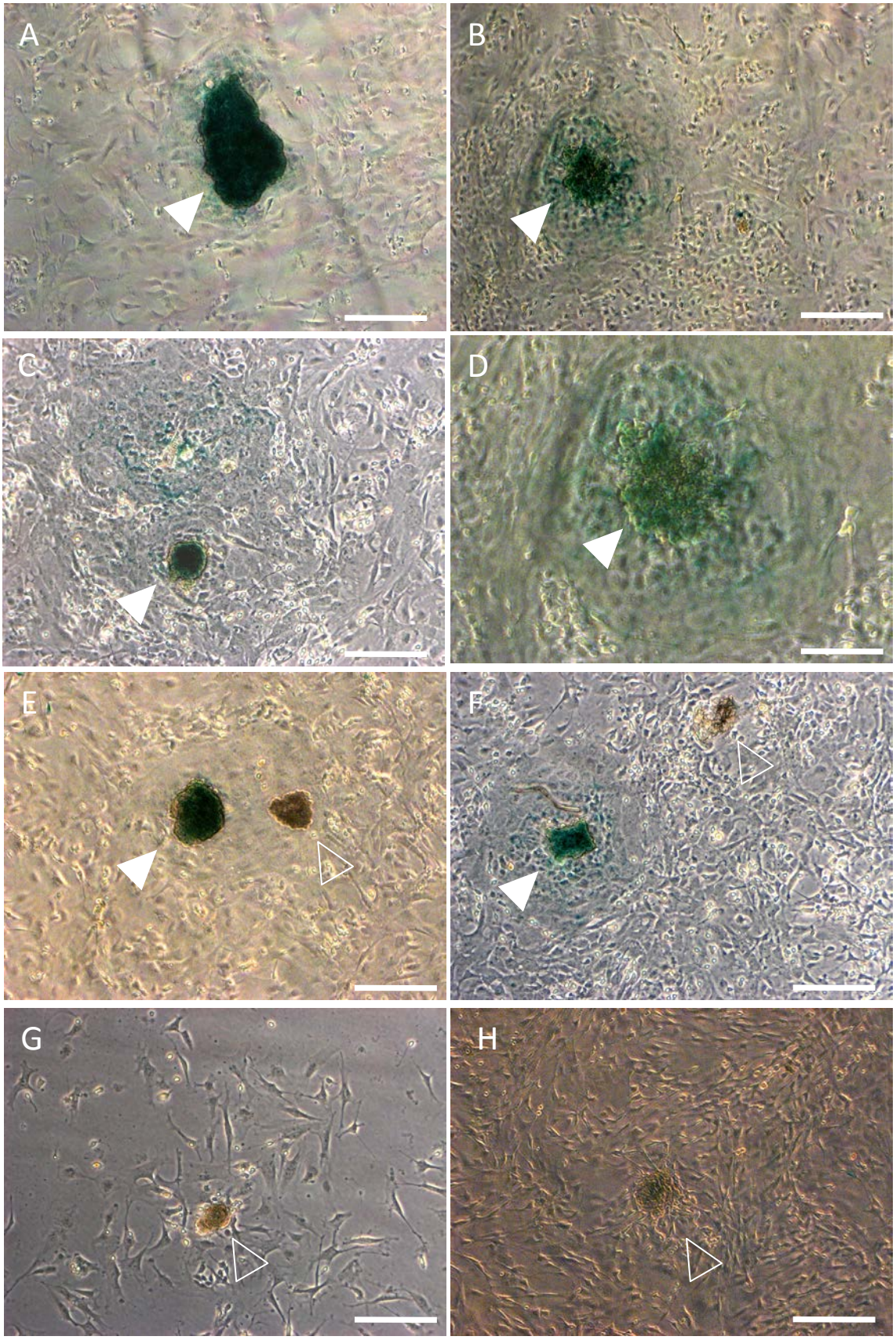

Fig 6.5 – Formation of spherical cell structures in astrocycte cultures. Several Xgal positive spheres of cells can be seen, which are commonly surrounded by a halo of positive cells in a monolayer (A-C) Heterogeneous $Xgal^{+}$ and $Xgal^{-}$ spheres were also observed (D). Occasionally, positive (closed arrowheads) and negative spheres (open arrowheads) form in close proximity (E,F). Isolated negative spheres are observed, but are generally rare and smaller than positive spheres. Scale bars represent 50 µm

6.2.5 A subset of hypothalamic primary neurons express Fgf10-lacZ in vitro

Primary neurons isolated from the adult hypothalamus were plated onto either glass coverslips coated with PDL or PDL and laminin, or directly into 24 well plates coated with PDL or PDL and laminin. Negligible adherence and growth was found on the glass substrates, these were not further used (data not shown). When cultured onto coated tissue culture plastics, some cell survival was seen on PDL-only coatings, but PDL/laminin was far more efficient. Both Xgal positive and Xgal negative cells were observed, the negative cells only appeared as single cells, or at most 2 or 3 cells together, whereas the positive cells appeared as anything from single cells to clusters of upwards of 25 cells (Fig 6.6a-c). These cells show a neuronal morphology (Fig 6.6d,e), and express Tuj1 (Fig 6.6f), confirming their neuronal identity. Cells were plated at $2.5x10^5$ cells per well of a 24 well plate, average cell number after 4 DIV was 141±20, or 0.06±0.01% of the initial population indicating the low survival rate of these cells. A majority of cells (71.3±3.5%) expressed lacZ (Fig 6.7b). When the size of cell clusters was analysed, all Xgal negative cells were found to exist in clusters of 5 cells or less, whereas of the Xgal positive cells, 19.5±3.1% had a clustersize of 5-10 cells, 4.2±5.1% 10-15 cells, and 31.1±4.9% had a clustersize of 15 cells or more (Fig 6.7c)

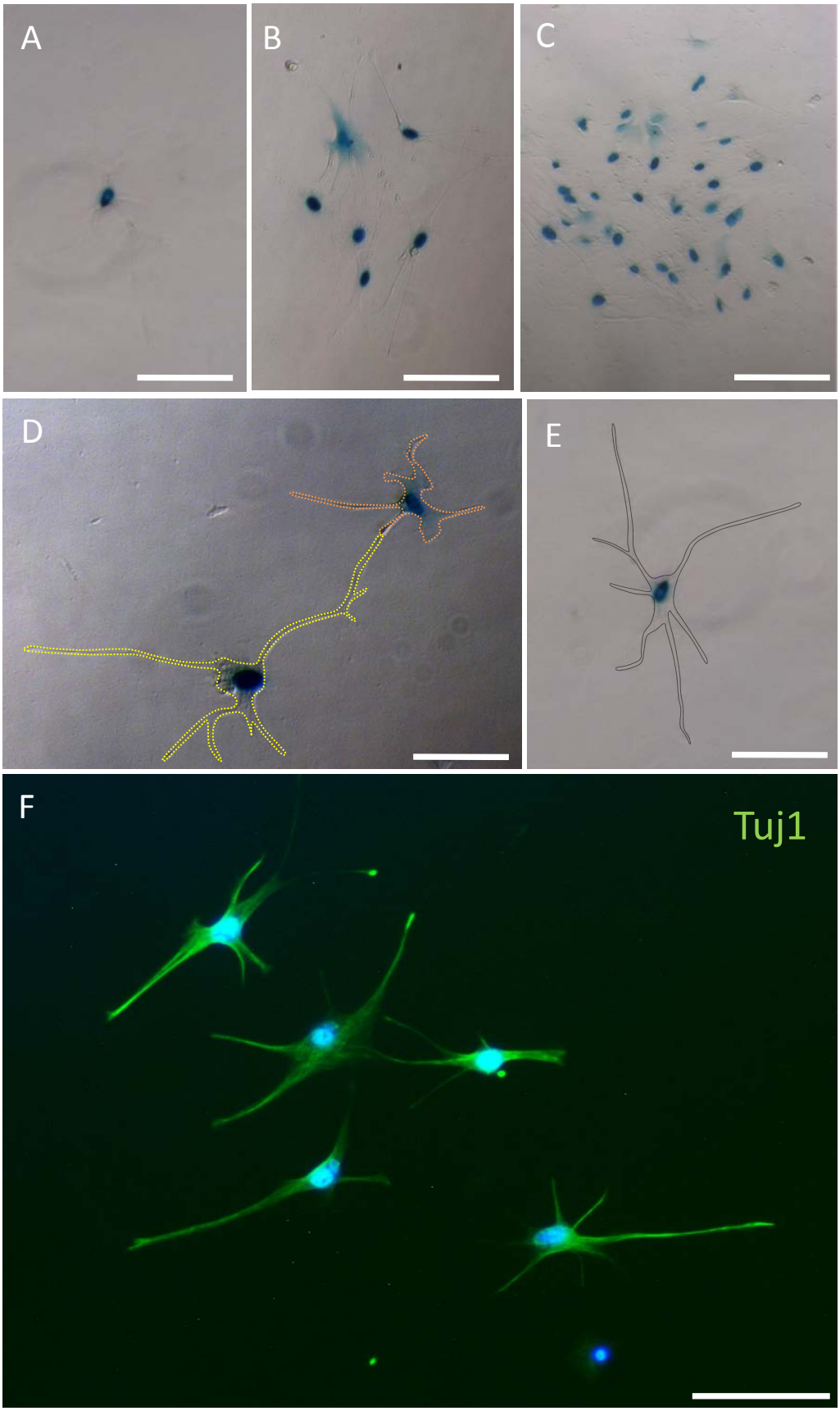

Fig 6.6 – Culture of Fgf10-lacZ^{+} primary hypothalamic neurons. Within a neuron culture, single Xgal positive cells, small clusters and large clusters of cells can be seen (A-C). These cells show a characteristic complex neuronal morphology (D, E). (F) immunohistochemistry for Tuj1 in parralel cultures confirms the neuronal identity of these cells. Scale bars represent 25 µm

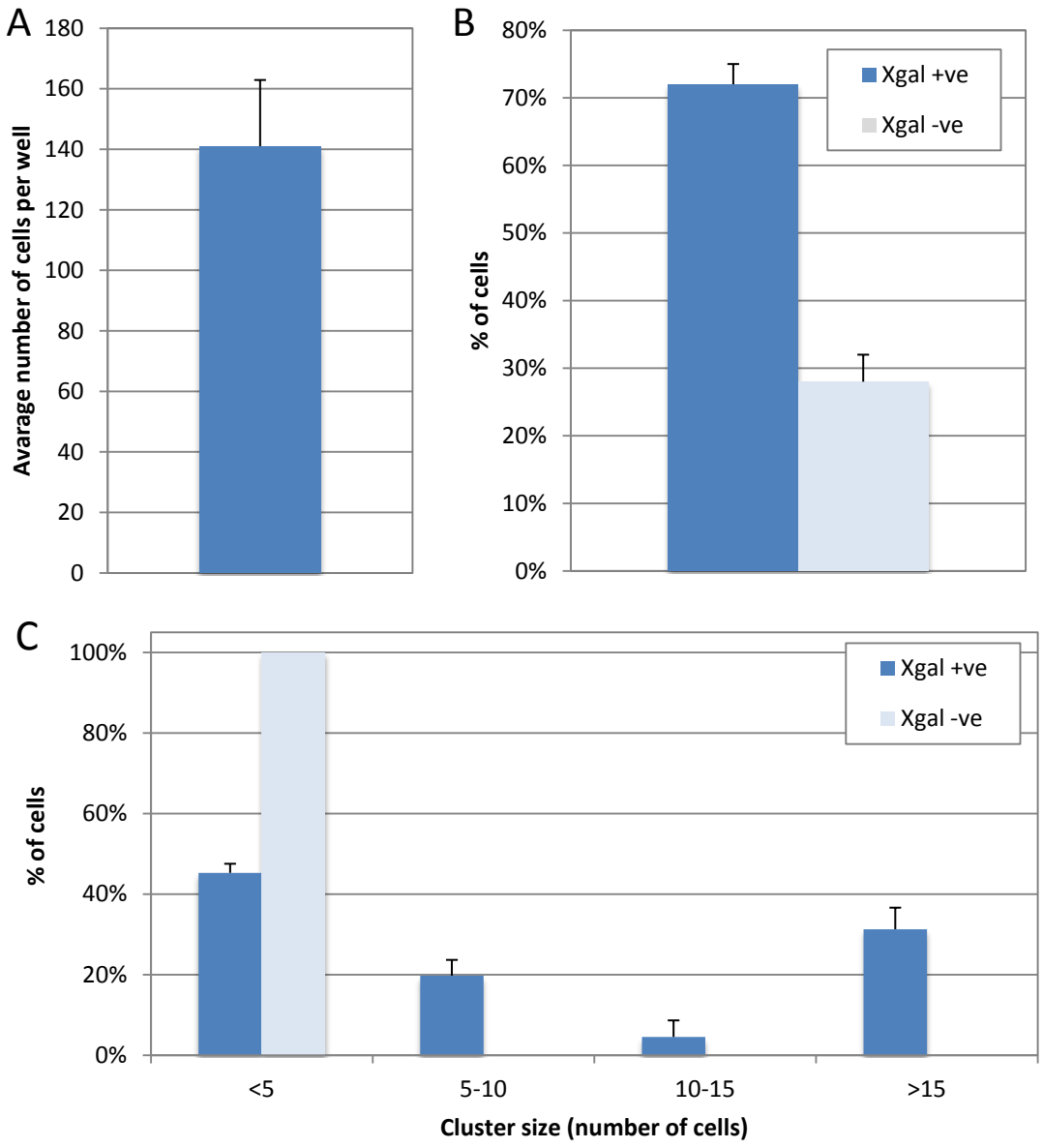

Fig 6.7 - Quantitative differences between Xgal$^+$ and Xgal$^-$ cells in neuronal culture. (A) Survival of hypothalamic cells under neruonal culture condition is low. (B) The majority of cells in neuronal cultures are Xgal positive. (C) Xgal positive cells readily from large clusters of cells, whereas Xgal negative cells do not.

6.2.6 Flow cytometry as a method of purifying lacZ expresssing cells

In order to set up a protocol to purify lacZ expressing cells by FACS, the ψ2 cell line was used as a model. This embryonic fibroblast cell line has stable expression of a cytoplasmic β-gal in approximately 30% of its cells (Fig 6.8a). ψ2 cells were loaded with either 40 or 200 μM FDG and incubated for 15 or 30 minutes afterwards to allow the substrate to be metabolised into fluorescein. FDG loaded 3T3 fibroblasts, which do not express lacZ, were used as a negative control. When assessed by flow cytometry, all β-gal expressing samples show a fluorescence of at least an order of magnitude higher than the negative control. The fluorescence is more dependent on time of incubation than initial concentration, as both the 40 μM and 200 μM samples with 30 minutes of incubation show higher fluorescence than their 15 minutes counterparts (Fig 6.8b). When cells are grown on PDL coated glass coverslips and loaded with FDG according to identical protocols, the FDG labelling can be seen to be cytoplasmic as expected, and labels the expected 30 to 35% of cells (Fig 6.8b). When the fluorescence of an ungated sample was quantified, the expected 30% of events is positive (Fig 6.8e). However, when the forward and side-scatter of this sample is examined, it is clear that is contains large amounts of cell debris. When the sample is gated to remove this debris from the analysis, all remaining events, the actual cells, have a high fluorescence, with no negative cells (Fig 6.8g,h). When a cell suspension of loaded cells was examined microscopically, all cells showed fluorescence (Fig 6.8i), indicating specificity of FDP loading is lost via an unknown mechanism during trypsinisation of cells and subsequent analysis, meaning this method currently is unsuitable for isolationg lacZ expressing cells

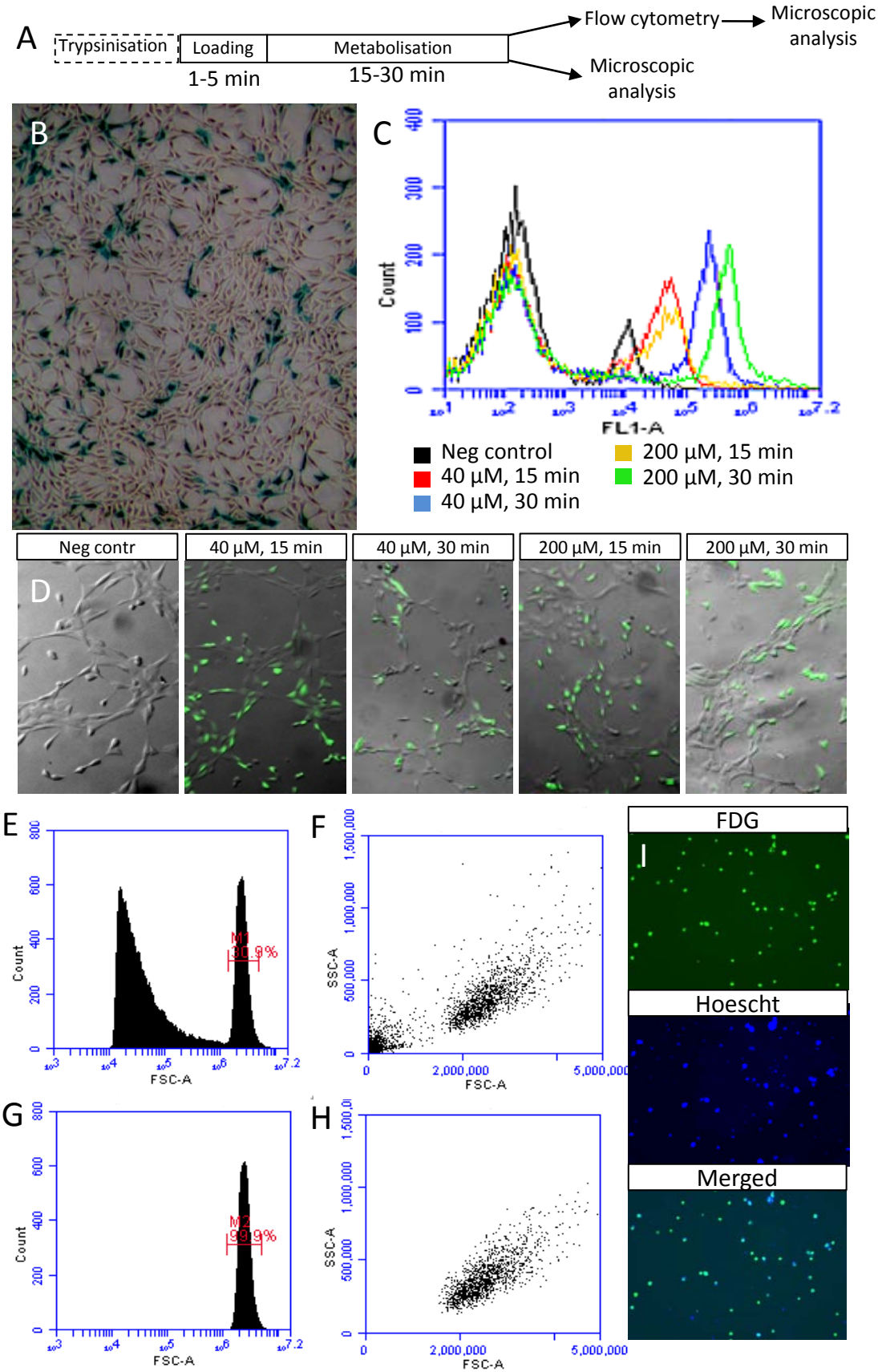

Fig 6.8 - Use of FDG for cell sorting of β-gal expressing cells. (A) Flow diagram for a typical flow cytometry experiment using FDG. (B) Xgal expression in the model cells used, ψ2. (C) Flow cytometry data for 4 different conditions of FDG staining, the fluoresence intensity is more dependant on incubation time than concentration. (D) Parallel coverslips confirm the specificity and of FDG loading compared to Xgal staining. (E, F) Scatterplot and fluorescence intensity for an ungated positive sample. (G, H) Scatterplot and fluorescence intensity for the same sample gated to remove cell debris from the data shows that according to flow cytometry all cells are positive. (I) After trypsinasation of cells and flow cytometry, the FDG loses specificity and labels all cells.

6.3 Discussion

Culture of primary cells from the post-natal brain allows for the properties of these to be examined readily. Here, primary cultures of neurospheres, astrocytes and neurons were established from the post-natal hypothalamus. Results from all primary cultures indicate the proliferative capacity of Fgf10-lacZ hypothalamic progenitors. The hypothalamus is capable of generating multipotent neurospheres, which are comparable to those derived from the SVZ However, the fact that neurospheres can be grown from the hypothalamus is by itself not firm evidence for the presence of a stem cell. There has been debate in the literature about the specific neurosphere-forming cell type isolated from different areas of the brain, and whether these represent true stem cells or progenitor cells. Although it is generally accepted that SVZ derived populations are capable of forming all three lineages, whether these cells exist in the hippocampus is less clear. Earlier in vitro work suggested the presence of separate populations of neuronal and glial restricted progenitors (Bull and Bartlett, 2005; Seaberg and van der Kooy, 2002), whereas in vivo lineage tracing more recently showed that although the majority of hippocampal radial glia form either glia or neurons, but a minority form both (Bonaguidi et al., 2011).

Analysis of single differentiated hypothalamic neurospheres shows these are multipotent and capable of forming neurons, astrocytes and oligodendrocytes. A small number of cells express both astrocytic marker GFAP and neuronal marker Tuj1. It has previously been describes that some neurons in Alzheimer's patients express GFAP (Hol et al., 2003), but this has not been described in baseline conditions. The identity and functions of these $GFAP^{+}/Tuj^{+}$ cells is unknown at present.

While these results suggest hypothalamic stem cells are mutlpoptent, it is known from the literature that neurospheres can merge and fuse into chimeric spheres (Singec et al., 2006; Singec and Quinones-Hinojosa, 2008), thus it is possible that what appears to be a single

multipotent sphere is actually comprised of previously fused neuronal-restricted and glial-respected spheres. The only way to resolve this in vitro is to culture neurospheres form isolated single cells.

The degree of mitotic activity seen in hypothalamic neurospheres is not representative of the in vivo situation as evidenced by BrdU administration experiments, as in culture the cells are activated by the Fgf2 and EGF required to maintain them in an undifferentiated state. The main receptors for Fgf2, FgfR1IIIc and FgfR3IIIc, are widely expressed in the hypothalamus (see Chapter 3), so isolated cells would be able to show a response to an Fgf2 stimulus, which includes stimulation of mitosis (Gensburger et al., 1987). Likewise, there is strong EGFR expression in the hypothalamus (Ma et al., 1994). It is known from earlier studies that cells that are quiescent or divide rarely in vivo can be induced to divide more frequently, for instance when the SVZ niche is depopulated of fast dividing cells by cytotoxic agents, it is rapidly repopulated by a population of previously quiescent cells (Doetsch et al., 1999; Morshead et al., 1994). Also, administration of exogenous EGF can cause transit amplifying cells to regress into a multipotent state (Doetsch et al., 2002). Thus, the use of growth factor will likely skew the mitotic activity of the cells in vitro compared to the in vivo situation.

Apart from neurospheres, differentiated cell types can also be cultured from the adult hypothalamus. When culturing astrocytes from early postnatal brain, apart from the normal monolayers, occasionally spherical cell masses were seen adhering to the astrocytes monolayer. The majority of these were found to express lacZ, and included a halo of lacZ positive cells in the monolayer directly surrounding the sphere. Their morphology and organisation is reminiscent of a progenitor population. These spherical assemblies could be classical neurospheres, however this is unlikely given the culture conditions. The astrocyte medium did not contain EGF or Fgf2, normally required to maintain neurospheres, and the medium was augmented with 10% fetal bovine serum, which normally promotes differentiation. Although the surrounding halo of lacZ expressing cells with an astrocytic

morphology does indicate probable differentiation, a neurosphere under the given conditions and culture times would most likely have completely differentiated. Some reports in the literature have described spherical assemblies of glial progenitors derived from human glioblastomas, these have been termed gliospheres (Chakraborty et al., 2011; Chearwae and Bright, 2008). The glial assemblies seen here may be similar to these.

When dissociated adult hypothalamus tissue was cultured under conditions promoting neuronal survival, large clusters of lacZ expressing neuronal cells were observed, with the neuronal phenotype being confirmed by immunoreactivity for Tuj1. As mature neurons rarely if ever divide in culture, this must indicate cell division by some other cell type concurrently isolated, most likely either a neural stem cell or a transit amplifying cell followed by in situ generation of neurons. This provides further evidence for the presence of a mitotic Fgf10 expressing progenitor in the adult hypothalamus.

In situ division is also evidenced by the total numbers of lacZ expressing cells versus the number of negative cells, while only a minority of all hypothalamic cells in vivo express lacZ, the majority of cells in vitro do express the reporter. This effect could be due to a preferential survival of lacZ expressing cells, but given the observed clustering, expansion of the population through division is more likely. Further examination of these types of cultures with Ki67 labelling or BrdU incorporation assays would confirm division is taking place. Some larger clusters, reaching up to 25 or 30 cells in numbers indicate multiple division events during the 5 DIV. The presence of Fgf2 in the medium, used to promote neuronal survival, would be more than adequate to stimulate cell division from responsive progenitor cells. In contrast, lacZ negative cells were ever only observed as single cells, most likely genuine primary neurons, rather than being generated in the culture. This contrast clearly illustrates the difference between lacZ expressing progenitors and lacZ negative neurons in the hypothalamus.

Although the use of FDG to sort these cells by flow cytometry has not been successful, the possibility of using FACS to enrich Fgf10 expressing populations remains. Instead of using FDG, the bright fluorescence seen in $Fgf10^{CreERT2}$::$Rosa^{Tomato}$ could be used as an alternative sorting marker. This could then be used for a number experiments, for instance to easily set up clonal cultures of Fgf10 expressing neurospheres and dissect out the neurogenic potential of ependymal versus parancymal cells by co-sorting for the ependymal marker CD133.

The ability to culture these different lacZ expressing cell types will provide a useful in vitro model system in which the function of Fgf10 in these cells can be evaluated though loss- and gain-of-function.

Chapter 7

Characterisation of Fgf10-lacZ expressing cells in olfactory bulb and amygdala

7.1 – Introduction

The olfactory bulbs (OB), located at the rostral end of the rodent brain, are the areas crucial for the sense of smell. It is here where the projections of olfactory neurons of the nasal cavity project to in order to transmit the information they sense from the environment. The OB is a privileged brain area that is continually supplied with new neurons by the rostral migratory stream during adulthood. The OB has a characteristic layered structure. On the outside surface (but not part) of the OB the olfactory nerve layer (ONL), which contains the projections of the olfactory neurons in the nasal cavity. The OB proper contains, from the outside in, the glomerular layer (GL), external plexiform layer (EPL), mitral cell layer (MCL), internal plexiform layer (IPL) and the granular cell layer (GCL), see Fig 7.1.

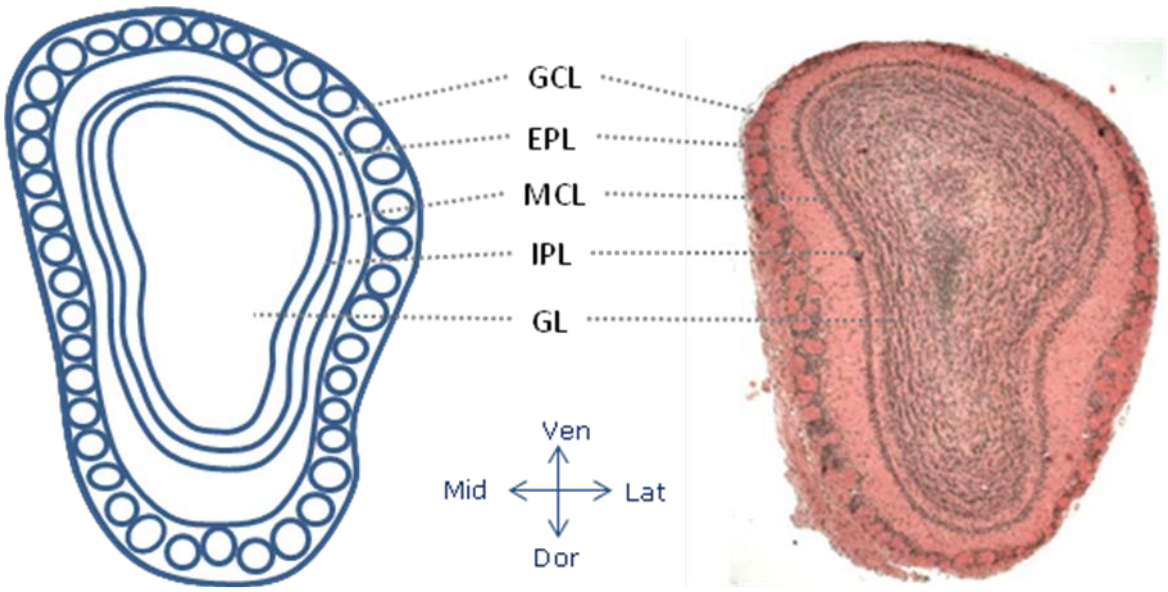

Fig 7.1 – Structure of the olfactory bulb. A coronal section and schematic of the adult mouse olfactory bulb, showing the layered structure. Layers are the granular cell layer (GCL), external plexiform layer (EPL), mitral cell layer (MCL), internal plexiform layer (IPL) and granular layer (GL)

The GL, which shows characteristic rounded structures called glomeruli, is where the olfactory neurons synapse onto local interneurons (Mombaerts, 2006). The EPL contains mainly interneuron dendrites, as well as dendrites arising from deeper granular cells, modulating the activity of the interneurons via inhibitory synapses (Hamilton et al., 2005). The MCL contain the cell bodies of the mitral cells, the interneurons that receive their information from the olfactory neurons in the glomeruli, and then send it on to different brain areas including several cortical areas and the amygdala (Shipley and Adamek, 1984). The thin IPL contain dendrites form the GSL. The GCL contains large numbers of inhibitory granular cells, mediating activity of the mitral cells (Shepherd et al., 2007).

The OB is continually supplied with new neurons via the rostral migratory stream. Neuroblasts arrive at the olfactory bulb at between day 2 and 7 after starting migration, they then migrate radially within the olfactory bulbs at days 5 to 9, during days 9 to 13 cells have reached their final position and start sending out dendrites, which by day 20 have formed into a complete dendritic network, and fully functionally integrated by day 30 (Mizrahi, 2007). Of the newly generated cells that reach the olfactory bulbs, approximately 50% will eventually fail to fully integrate into the local circuitry and will die (Petreanu and Alvarez-Buylla, 2002; Winner et al., 2002).

Interneurons are contributed to three layers during adulthood, the glomerular, external plexiform and granular layers (Lledo et al., 2008; Yang, 2008). Different areas of the SVZ produce distinct populations of adult neurons, in a cell-intrinsic manner (Merkle et al., 2007). These distict SVZ populations have different embryonic origins (Young et al., 2007). Most new neurons assume a GABAergic fate, expressing markers such as GAD67, GAD67, calbindin, calretinin or parvalbumin, and a second group assumes a dopaminergic fate, expressing tyrosine hydroxylase (TH) (Panzanelli et al., 2007; Parrish-Aungst et al., 2007).

The function of newly generated neurons is unclear. Olfactory enrichment stimulates survival of newly generated neurons (Rochefort et al., 2002), but conflicting results following ablation or reduction of neurogenesis show impaired (Gheusi et al., 2000; Sakamoto et al., 2011) or normal olfactory discrimination (Imayoshi et al., 2008).

During development, cells migrate from the amygdala to the olfactory bulb (Xu et al., 2008). Recently, it has been suggested that this contribution may continue into adulthood (Hajihosseini et al., 2008). Using the $Fgf10^{nlacZ}$ reporter mouse, a population of Fgf10 expressing cells have been found in the amygdala and the olfactory bulb, as well as a trail of Fgf10-lacZ positive cells linking these areas. In order for the amygdala to be the source of this putative migratory trail, a type of progenitor cell should be present. Whether the amygdala contains a resident stem cell population is not definitively known, but neurogenic potential for the amygdala has been noted. In several species of lower primates, BrdU incorporation in the amygdala was noted, but only double-labeling with neuronal markers was undertaken, showing that at least neurogenesis takes place in the adult (Bernier et al., 2002). In two different species of voles, a constitutive level of BrdU incorporation and formation of neurons and glia was noted, that increased in response to social housing (Fowler et al., 2002) and sex hormone levels (Fowler et al., 2003; Fowler et al., 2005). In the rat, a population of BrdU incorporating gliogenic cells has been described, which also generate neurons in response to a neuropathic pain stimulus (Goncalves et al., 2008). Repeated chemically induced seizures also induced a neurogenic population in the rat amygdala (Park et al., 2006). EGF/FGF2 responsive cells were able to be cultured from amygdalar tissue from human patients suffering from epilepsy, and were multipotent and selfrenewing (Arsenijevic et al., 2001). A stem cell population has as yet not been described in the mouse, but the cluster of Fgf10 expression previously seen in the mouse amygdala provides a hint for a possible local progenitor population, that may serve as a source for a putative migratory stream to the olfactory bulb.

Aims

At this time, nothing is known about the identity or function of these Fgf10 expressing cells in amygdala or olfactory bulb. Here, using immunohistochemistry, BrdU incorporation assays and genetic lineage tracing, the properties of Fgf10 expressing cells in the amygdala are investigated. The fate of Fgf10 expressing cells in the olfactory bulb is examined using immunohistochemistry.

7.2 – Results

7.2.1 Distribution of Fgf10-lacZ positive cells in the OB is suggestive of a migrational behaviour

Through serial sectioning of Xgal-stained brains, the distribution of Fgf10-lacZ$^+$ cells in the OB was studied. In adult animals (P60, male: n=11, female: n=3), a low, but reproducible number of 30±2 cells per pair of olfactory bulbs were found (fig 7.2a). There was no sexual dimorphism in this number. In aged animals (P200, male: n=3, female: n=3), the number of cells drops to 19±1, representing a significant decrease ($p=0.002$) compared to P60, again without any significant sexual dimorphism. In order to examine the rostral-caudal distribution of the Fgf10-lacZ$^+$ cells, the olfactory bulb was divided into 5 equal areas, designated 1/5 to 5/5, rostral to caudal (fig 7.2b). The majority of the cells are in the caudal-most segments of the OB (fig 7.2c). An ANOVA with Tukey post-hoc tests shows areas 4 and 5 contain significantly more cells than area 1 ($p<0.05$). This difference is not longer visible in aged animals (fig 7.2d).

The distribution of Fgf10-lacZ$^+$ cells amongst the different layers of the OB was also examined, with cells being found in all layers (fig 7.3), with the relative proportions not differing significantly between sex or age. However, an interesting pattern emerges when the distribution of cells over the different layers is split up in the different rostral-caudal areas. In the caudal-most segment, the majority of cells reside in the granular layer, but further caudally this peak shift outwards towards the mitral layer, before finally peaking in the glomerular layer in the rostral-most segment. The combination of the distribution over the rostral-caudal axis, and the shifting distribution pattern over the different layers, is highly suggestive of a migrational stream entering the granular layer, and gradually undergoing radial migration outwards towards the glomerular layer.

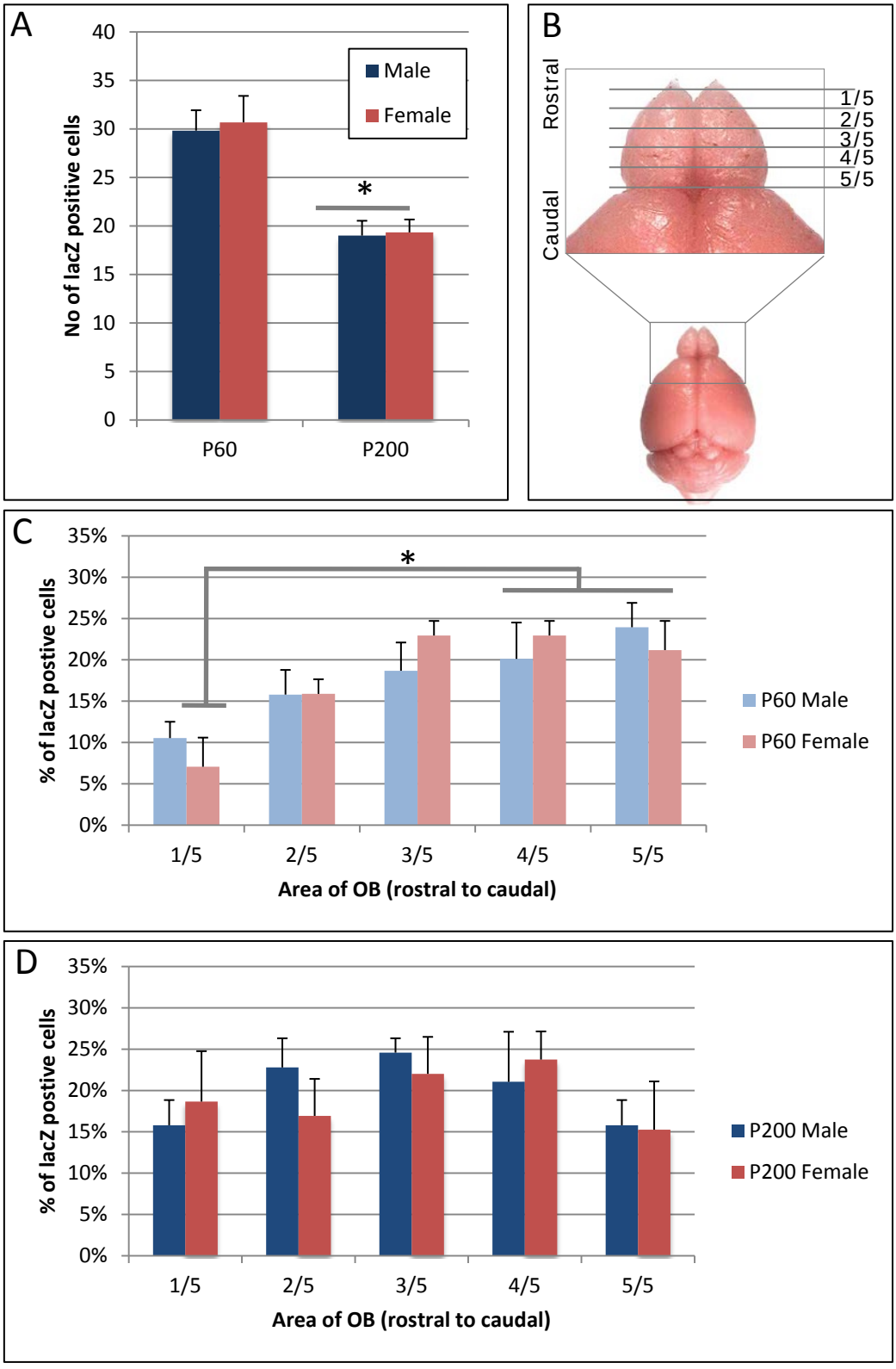

Fig 7.2 – Quantification and distribution of Fgf10-lacZ^{+} cells in the olfactory bulb. (A) At P60, the olfactory bulbs contain approximate 30 positive cells, whereas at P200 this has dropped significantly to approximately 19. There is no sexual dimorphism. (B) Areas defined for rostral-caudal distribution studies. (C) When analysing the rostral-caudal distribution of the Fgf10-lacZ expressing cells, significantly more cells can be seen in the caudal parts of the OB, again with no sexual dimorphism. (D) At P200, this rostral-caudal gradient is no longer observed.

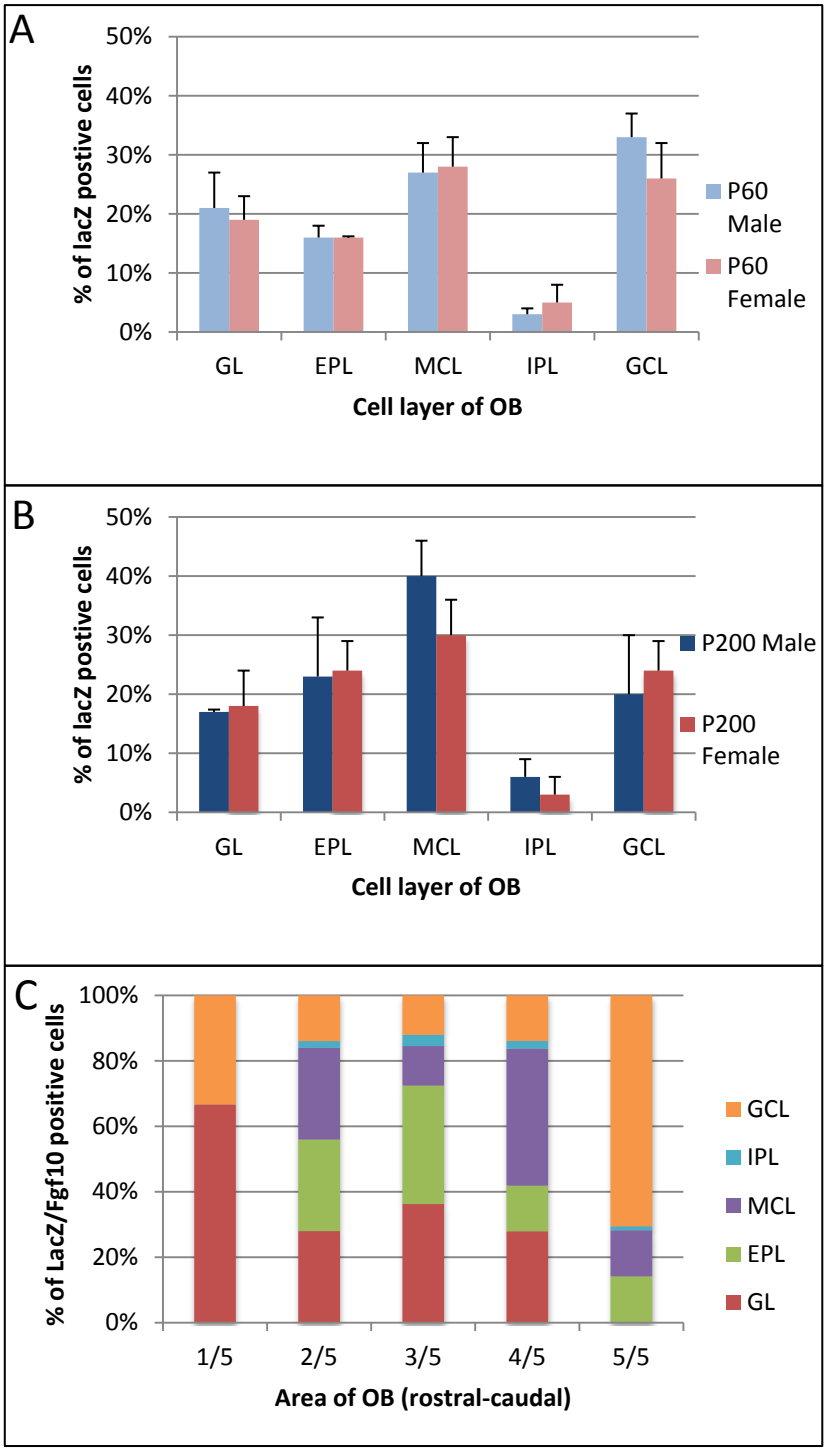

Fig 7.3 – Distribution of Fgf10-lacZ⁺ cells over the layers of the OB. (A) At P60, positive cells are spread throughout the layers of the OB, with the thin IPL having fewer cell than other layers in both males and females (B) At P200 this distribution remains unchanged. (C) Distribution over layers is dependant on rostral-caudal position. A shift from GCL to GL is seen towards rostral. GL:glomerular layer, EPL:external plexiform layer, MCL: mitral cell layer, EPL: external plexiform layer, GCL: granular cell layer.

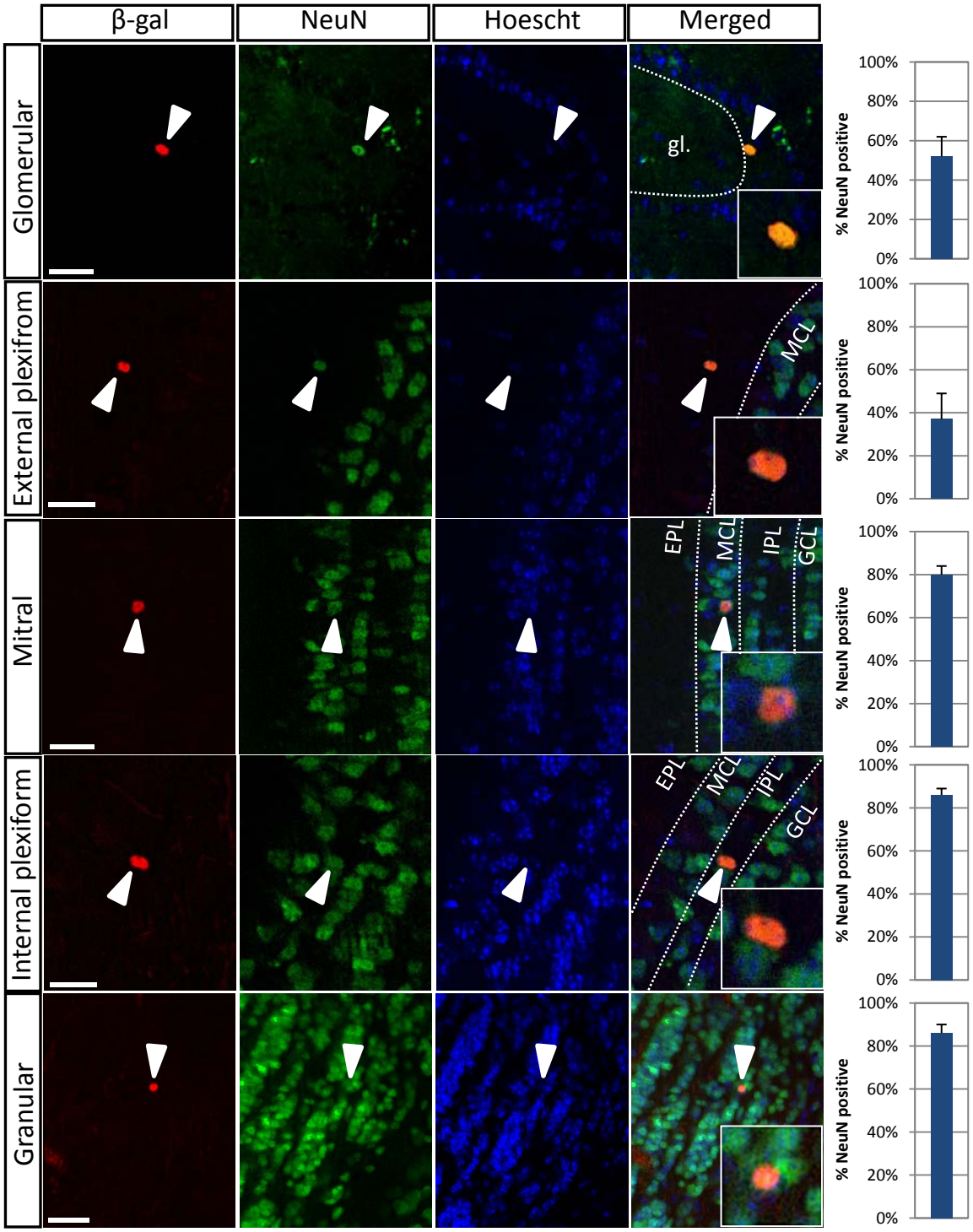

Fig 7.4 – Expression of NeuN in Fgf10-lacZ⁺ cells throughout the olfactory bulb. Fgf10-lacZ expressing cells in all layers of the OB also express the mature neuronal marker NeuN. The proportion of Fgf10-lacZ⁺ cells labelling with NeuN varies between layers. Scalebars represent 25 µm

7.2.2 The majority of Fgf10-lacZ positive cells in the OB differentiate into neurons

It is known that the fate of newgly generated neurons in the OB is to form interneurons, the proportion of Fgf10-lacZ$^+$ cells forming mature neurons was investigated by double-labeling with β-gal and NeuN. Double-positive cells were found in all layers of the OB (fig 7.4), but the exact proportion is different in each layer. The vast majority of cells in the granular, internal plexiform and mitral layers are NeuN$^+$, while only a minority of cells in the external plexiform and glomerular layer are.

7.2.3 Fgf10-lacZ positive cells in the OB form both dopaminergic and GABAergic neurons

As the most common types of interneurons in the OB are dopaminergic (excitatory) and GABAergic (inhibitory), double labelling of β-gal with tyrosine hydroxylase (rate limiting synthesis enzyme for dopamine) and GAD67 (producing enzyme of GABA) was preformed. A subset of the Fgf10-lacZ$^+$ cells in the glomerular layers (to which TH expression is limited) were found to be dopaminergic neurons (fig 7.5a). Similarly, only a subset of the glomerular GAD67$^+$ cells were also Fgf10-lacZ$^+$ (fig 7.5b), while none of the scattered GAD67$^+$ cells in deeper layers of the OB were double-positive. In both instances, low number of double-positive cells prevented any meaningful quantification based on location.

7.2.4 Fgf10-lacZ positive astrocytes are rare in the OB

The proportion of Fgf10-lacZ$^+$ cells that form astrocytes was examined by double-labeling of β-gal and GFAP. Only rare examples of double-positive cells were found (fig 7.6), with some brains not showing any examples at all, indicating glial formation is only a minor differentiation branch for Fgf10-lacZ+ cells in the OB.

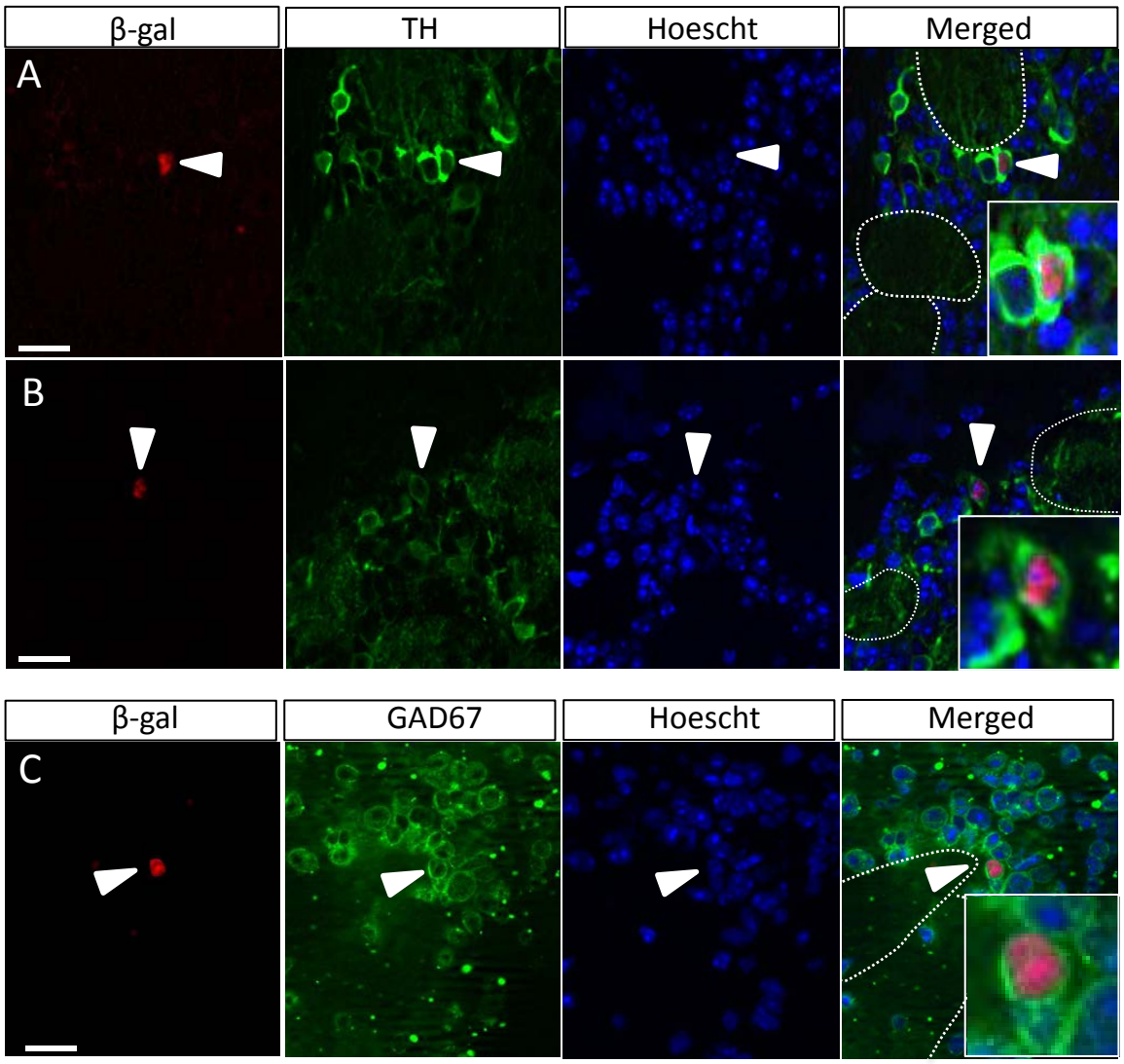

Fig 7.5 – Fgf10-lacZ expressing cells form both dopaminergic and GABAergic neurons. (A,B) Expression of tyrosine hydroxilase marks several periglomerular Fgf10-lacZ positive cells as dopaminergic neurons. (C) More rarely, Fgf10-lacZ cells express GAD67, indicating a GABAergic facte. In all, dotted lines indicate the local glomeruli. Scalebars represent 25 µm

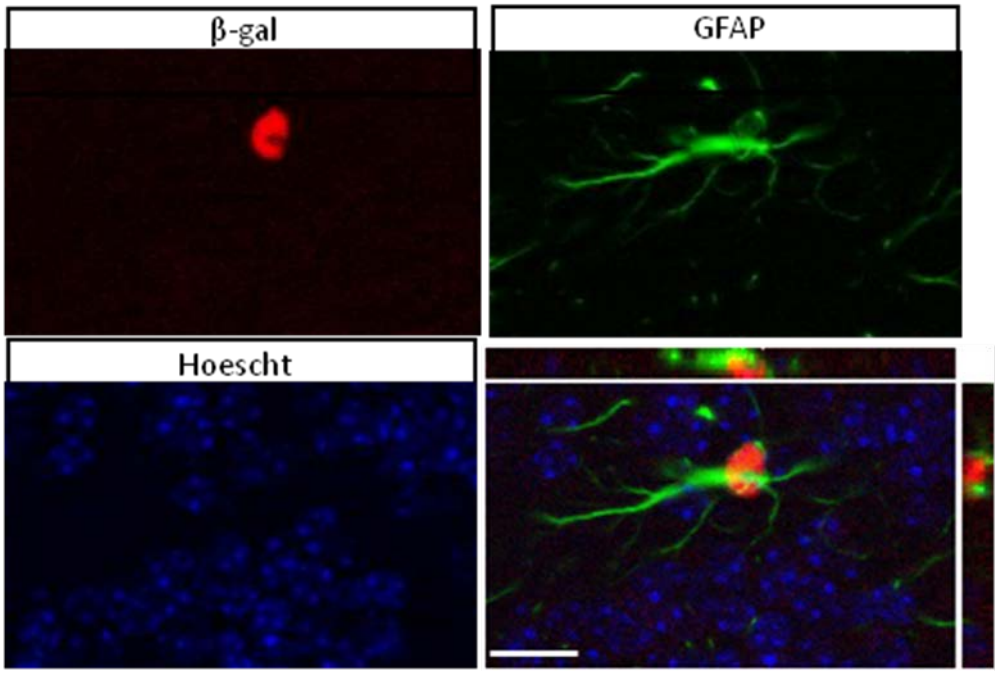

Fig 7.6 – Fgf10-lacZ expressing astrocyte in the OB. GFAP positive Fgf10-lacZ expressing astrocytes were only rarely observed in the OB. Scalebar represents 25 μm

7.2.5 Fgf10-lacZ expression in amygdala is limited mostly, but not exclusively, to neurons

Anti β-gal immunohistochemistry reveals the extent of Fgf10-lacZ expression in the amygdala at various ages. At both P30 and P60 widespread, but sparse labeling with anti β-gal is observed. Upon double-labeling with NeuN, most Fgf10-lacZ positive cells also express NeuN, although a minority do not (fig 7.7).

7.2.6 Neural stem cell markers are not expressed in the amygdala

Immunohistochemistry for NSC markers nestin, musashi and BLBP showed no expression of these markers in the amygdala.

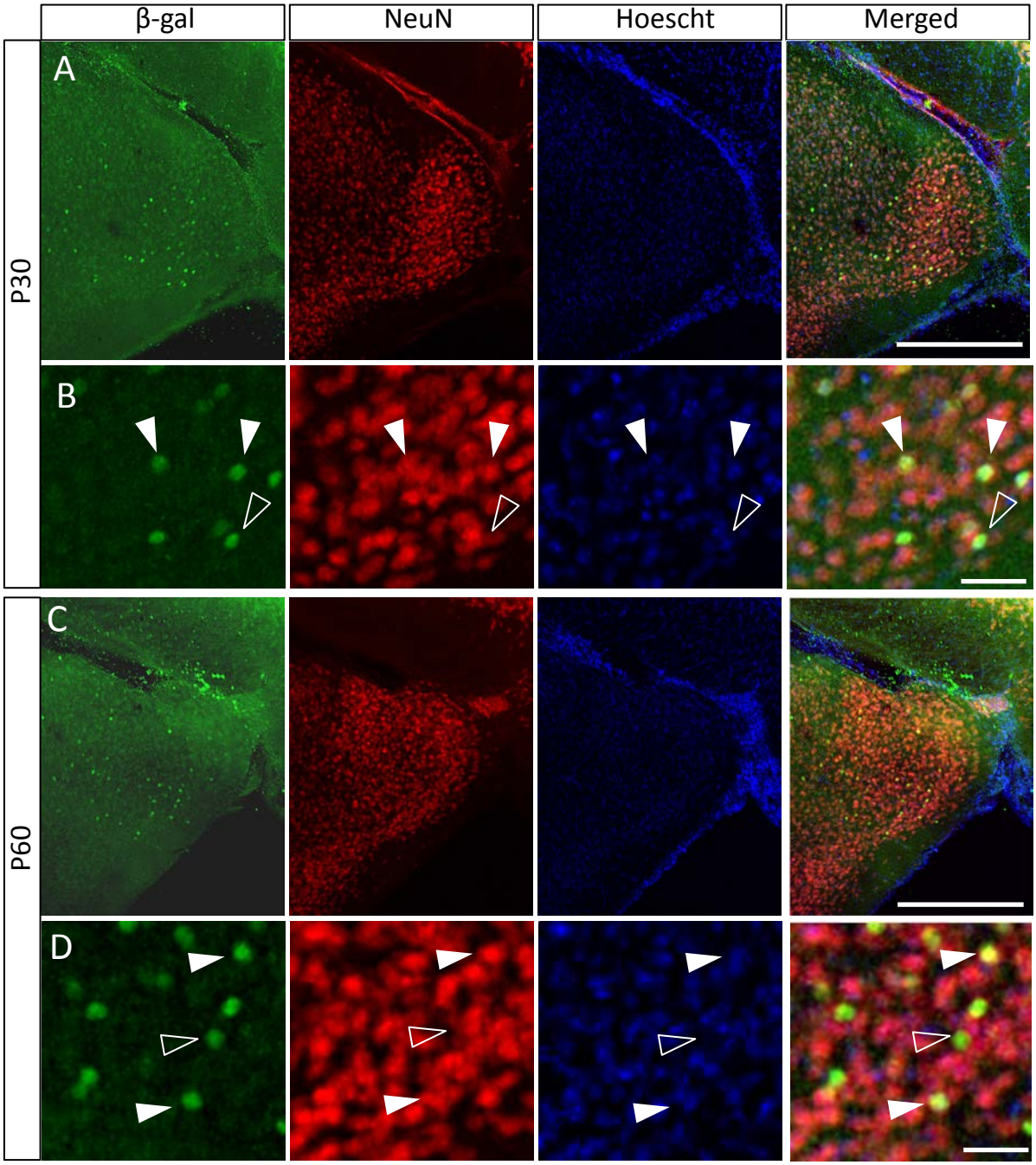

Fig 7.7 – Expression of Fgf10-lacZ and NeuN in the amygdala at different ages. (A) By P30, widespread expression of Fgf10-lacZ can be observed. (B) The majority of Fgf10-lacZ positive cells express NeuN (closed arrowheads), but some do not (open arrowhead). (C) Expression patterns at P60 are similar to P30 (D) Again, although the majority of Fgf10-lacZ expressing cells express NeuN, not all do. Scalebars: A, C: 250 µm, C,D: 25 µm

7.2.7 Active Fgf10 expression is maintained into adulthood in some amygdala cells.

In order to study whether active Fgf10 expression is maintained in the adult, $Fgf10^{CreET2}$::$Rosa26^{lacZ}$ inducible reporter mice were induced at postnatal day 40, and $Fgf10^{CreERT2}$::$Rosa26^{Tomato}$ mice at P60. Occasional low-level recombination, far sparser than the expression in $Fgf10^{nlacZ}$ mice, is seen was the amygdala (fig 7.8). Double-labeling with NeuN showed that some, but not all, recombined cells express this neuronal marker.

7.2.8 Constitutive cell division in the adult amygdala, but not by Fgf10-lacZ positive cells.

Long-term cumulative BrdU labeling via the drinking water of $Fgf10^{nlacZ}$ mice over 21 days shows widespread incorporation throughout the amygdala (fig 7.9). However, none of these BrdU incorporating cells also express Fgf10-lacZ.

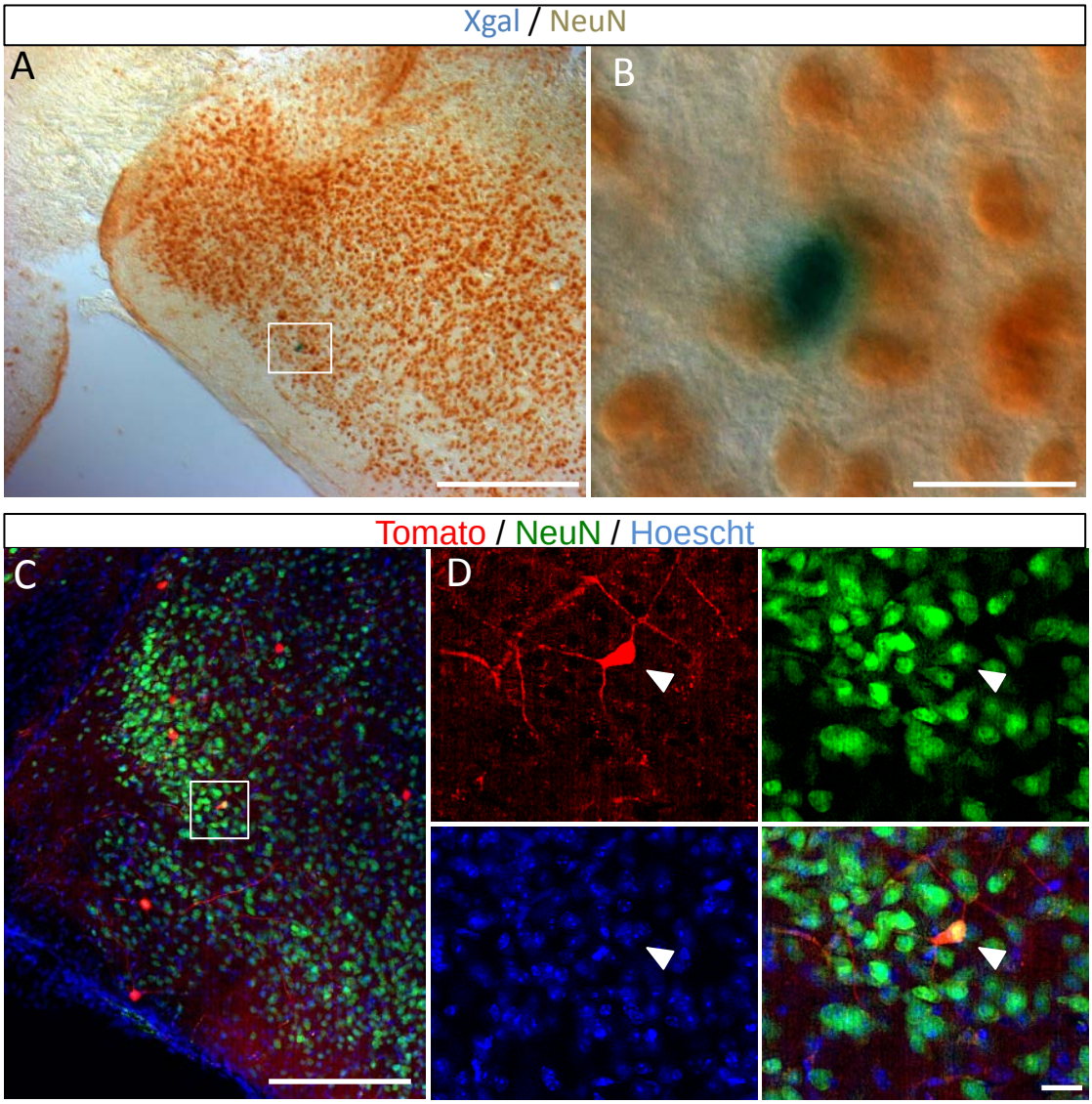

Fig 7.8 – Genetic lineage tracing in amygdala. Recombination can seen be with the Fgf10^{CreERT2} driver using both ROSA^{lacZ} (A) and ROSA^{Tomato} (C) reporters. Both NeuN^{+} (B) and NeuN^{-} recombined cells (D) are seen. Scalebars: A,C: 250 µm, B,D: 10 µm

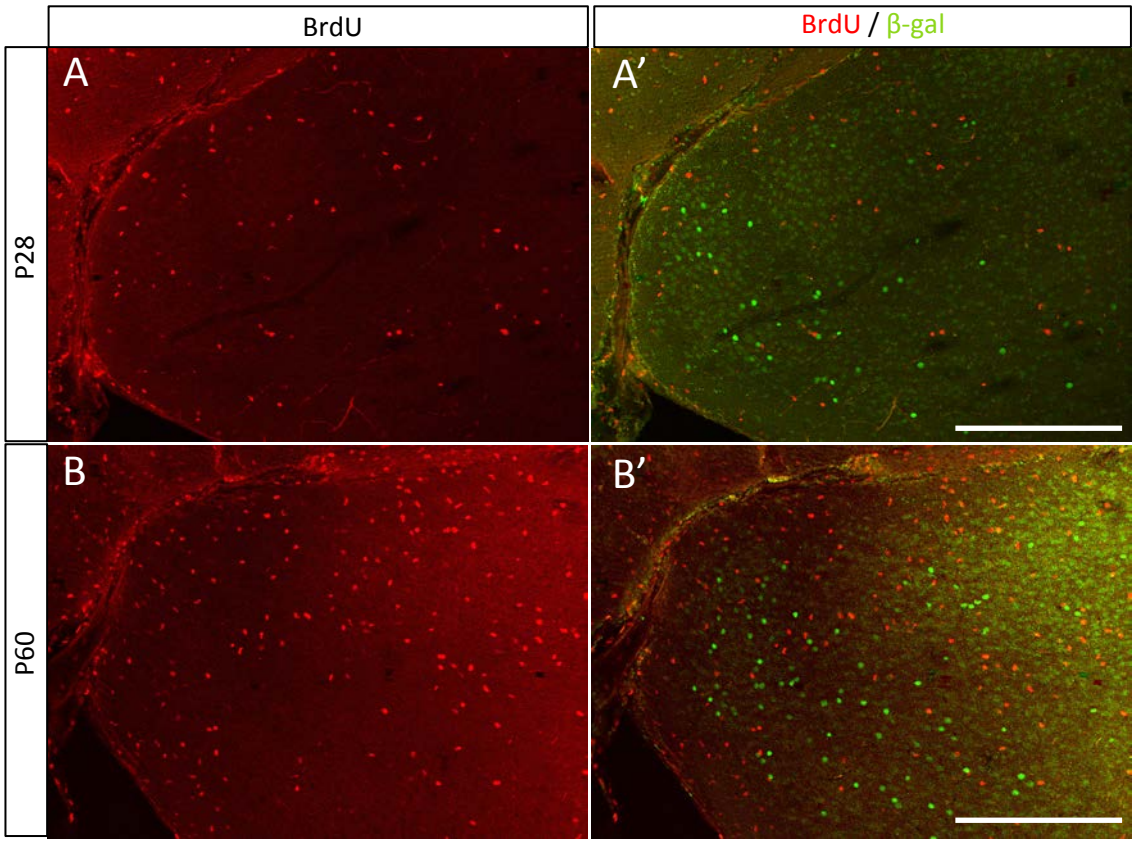

Fig 7.9 – Constitutive cell division in the amygdala. Cumulative BrdU labelling shows constitutive cell division in the amygdala at both the P28 (A) and P60 (B). At P60, proliferation seems increased However, no double-labelling with β-gal is seen (A',B'). Scalebars for all : 250 µm

7.3 Discussion

The OB has a privileged position within the adult brain, as it is continuously replenished with new neurons throughout adulthood by the rostral migratory stream (RMS). Although the major source for these, the subventricular zone of the lateral ventricle, has been well characterised (Luskin 1993), it is possible that other sources for new OB neurons exist. Indeed, the future amygdala served as a source of cells for the OB during development (Xu et al., 2008). Previously, a putative Fgf10 expressing migratory stream connecting the amygdala and the OB has been described (Hajihosseini et al 2008). This represents a potential novel source of new neurons for the OB during adulthood.

The distribution pattern of Fgf10-lacZ positive cells, with cell numbers tapering off toward the rostral end of the OB, is suggestive of migration into the OB from elsewhere. In the RMS, retroviral lineage tracing has shown that cells migrating into the OB enter though the granular zone, before moving radially into the glomerular layer (Luskin 1993). If Fgf10-lacZ positive cells do enter the OB from outside, a concentration of cells at the caudal end would be expected. This is backed up by the fact that in the caudal-most areas cells are predominantly in the granular zone, whereas further rostral, cells are found more in the glomerular zone, mimicking the pattern seen in the well characterised RMS.

It has been well characterised that the SVZ generates fewer neuroblasts, and fewer new neurons are contributed to the OB in aged animals (Bouab et al 2011, Ahlenius et al 2009, Luo et al 2006). This is mirrored by the Fgf10-lacZ^{+} cells in the OB, which show a significant decrease of up to 40% between P60 and P200. However, the fact that these cells can still be observed at P200 suggests they are continually generated during adulthood, rather than during embryonic or early postnatal timeframes, as it is unlikely the lacZ reporter would be stable in the absence of expression for this length of time. Previously, it has been shown that the OB already contains a few Fgf10-lacZ expressing cells as early as P5 (Hajihosseini et al.,

2008), showing that although numbers may change, the Fgf10-lacZ population is present in the OB throughout life.

Even if the distribution pattern of Fgf10-lacZ$^+$ cells over the OB is highly reminiscent of that seen by newly formed cells from the RMS, that in itself cannot be taken as evidence for a migratory stream. The vast majority of Fgf10-lacZ$^+$ cells in the OB are post-mitotic neurons, suggesting that at any given time there are only a small number of migratory cells, if any. Also, it is known that NeuN does not mark all post-mitotic neurons in the olfactory bulb, with particularly poor performance in the glomerular layer (Bagley et al., 2007), meaning the actual fraction of Fgf10-lacZ$^+$ cells in the OB that are neurons is likely to be even higher than determined here. Although rare Fgf10-lacZ expressing GFAP$^+$ glia have been observed, their low frequency suggest this is not a predominant fate for this lineage. Detailed genetic lineage tracing will be required to verify the origin and timing of differentiation of these cells.

The Fgf10-lacZ expressing lineage contributes both GABAergic and dopaminergic neurons to the olfactory bulb. It has been appreciated that inhibitory GABAergic interneurons, and newly generated ones in particular, are required for modulating local neuronal activity in response to changing environmental stimuli, allowing for appropriate circuit plasticity (Gheusi et al., 2000; Lledo et al., 2006). Dopeminergic interneurons, although frequently also capable of synthesising GABA (Gall et al., 1987), represent a separate population from the main GABAergic population, with different localisation. Their function however is similar; modulation of local neuronal activity by inhibitory signalling (Cave and Baker, 2009). Although the function of the specifically Fgf10-lacZ positive population of GABAergic and dopaminergic neurons has not been assessed, based on their location a similar function could be expected. Although there are only a small number of Fgf10-lacZ expressing neurons in the OB, the fact that their number is comparable between animals and sexes does suggest a functional relevance. What this function is will have to be addressed using loss-of-function or genetic ablation experiments.

The source of these Fgf10-lacZ expressing neurons is unknown, but has been speculated to be the amygdala. A resident population of Fgf10-lacZ positive cells is found in the amygdala is present soon after birth, but not before (data not shown), and is maintained at later ages. Although most Fgf10-lacZ expressing cells are in the medial amygdala, adjacent to the hypothalamus, the domain of expression includes the basolateral amygdala and the adjacent piriform cortex, making an assessment of function based on localisation difficult if not impossible. For the amygdala to be the source for a migratory stream to the OB, a resident progenitor or stem cell population would be required, but no expression of NSC markers such as BLBP, nestin or musashi has been found. The absence of nestin expression is confirmed by the lack of observed recombination in nestin^{CreERT2} mice (Chen et al., 2009). Interestingly though, doublecortin^{CreERT2} mice show recombination in the piriform cortex, which is on the route between the amygdala and the olfactory bulb (Zhang et al., 2010). This migratory marker would be expected to be expressed by neuroblasts.

If not progenitor or neural stem cells, what is the identity of amygdalar Fgf10-lacZ^{+} cells? The majority of these cells express the post-mitotic neuronal marker NeuN, showing them to be mature neurons. A significant minority however, does not express NeuN, and represent an as yet uncharacterised population.

To ensure that the expression of Fgf10-lacZ seen in the adult Fgf10^{nlacZ} is genuine, rather than accumulated reporter protein from the perinatal period, when these cells first appear, Fgf10^{CreERT2}::ROSA26^{lacZ} and Fgf10^{CreERT2}::ROSA26^{tomato} reporter mice were used. Recombination in the amygdala in both shows the continued expression of Fgf10, and that most, but not all of these cells are in fact mature neurons. The possibility remains that the Neun^{-} recombined cells may be a progenitor population.

Long-term cumulative BrdU administration shows numerous dividing cells in the amygdala, in accordance with literature. However, none of these BrdU incorporating cells express Fgf10-lacZ. This, as well as the lack of NSC marker expression and widespread co-

localisation with Neun, makes it unlikely for the Fgf10-lacZ expressing population to be stem cells. The BrdU incorporating cells may be part of non-neural lineages such as microglia or endothelial cells, or they may be not have originated in the amygdala and migrated in from a different brain area, as has been suggested in (Bernier et al., 2002)

The current work can neither prove nor disprove the notion that the Fgf10-lacZ expressing cells in the olfactory bulb are derived from the amygdala, but with the results found here it is unlikely that the Fgf10-lacZ expression cells in the amygdala represent a stem cell population. Therefore it is unlikely that, at least in the adult, the amygdala contributes cells to the olfactory bulb. It may well be that there is a migrational stream between the amygdala and the olfactory bulb, but that this is only during late development and/or early postnatal stages. Indeed, in the developing mouse brain, a putative migratory stream of NKX2.1 expressing cells has been described between the amygdala and the olfactory bulb (Xu et al., 2008). The only way to conclusively prove the olfactory bulb Fgf10-lacZ expressing cells are produced from the amygdala in adulthood is through some from of genetic lineage tracing. The $Fgf10^{CreERT2}$ line combined with the efficient $ROSA26^{Tomato}$ reporter may be suitable for this. An alternative would be linage tracing via stereotactically injected retrovirus.

As it has previously been shown by RT-PCR that there is continued Fgf10 expression in the olfactory bulb in the adult (Hajihosseini et al., 2008), the lacZ expressing cells seen at later age could have migrated into the olfactory bulb at an earlier stage and continue to express Fgf10 and lacZ. Whatever its origin, the Fgf10-expressing lineage contributes functional neurons to the adult olfactory bulb. This population, may be required to perform a specific function, given its different origin from the vast majority of other newly generated interneurons. The exact functions and origins of this population remain to be investigated.

Chapter 8

Discussion

Formation of new cells in the adult mammalian brain, though long not believed to take place, has now been widely accepted in the neuroscience community. The classical neurogenic niches, the subventricular zone of the lateral ventricle and the subgranular zone of the hippocampus, have both been well studied and characterised. However, increasing amounts of data suggest that these are not the only areas in the adult brain capable of supporting proliferation. Amongst others, the hypothalamus and amydala have been under investigation as novel stem cell niches. Previously, these areas have been found to express Fgf10, which is known from development of many peripheral organs to be involved in stem cell maintenance. Here, the phenotype and proliferative capacity of Fgf10 expressing cells have been investigated during development and throughout adulthood in the hypothalamus, olfactory bulb and amygdala through immunohistochemistry, BrdU administration, in vitro culture of primary cells and genetic lineage tracing.

In the hypothalamus, the basis for the putative adult stem cell niche is present early during during development. There is strong Fgf10-lacZ expression even at E10, before the start of neurogenesis of the hypothalamus. This indicates this population is specified very early on during brain development, soon after neural tube closure. This early origin underlines the likely importance of the Fgf10-lacZ expression population. The Fgf10 expressing lineage contributes new neurons to the hypothalamus by the middle of the neurogenic window (E12.5), but these do not mature until after the end of the bulk of neurogenesis (>14.5). In between the end of neurogenesis and birth, a substantial number of Fgf10-lacZ expressing cells form neurons, indicating the importance of this population during late formation of the hypothalamus.

Although Fgf10-lacZ expression is maintained into adulthood, the number of expressing cells that also express neuronal markers drastically decreases during early adulthood, indicating a twofold role for Fgf10 in this system. After its role in

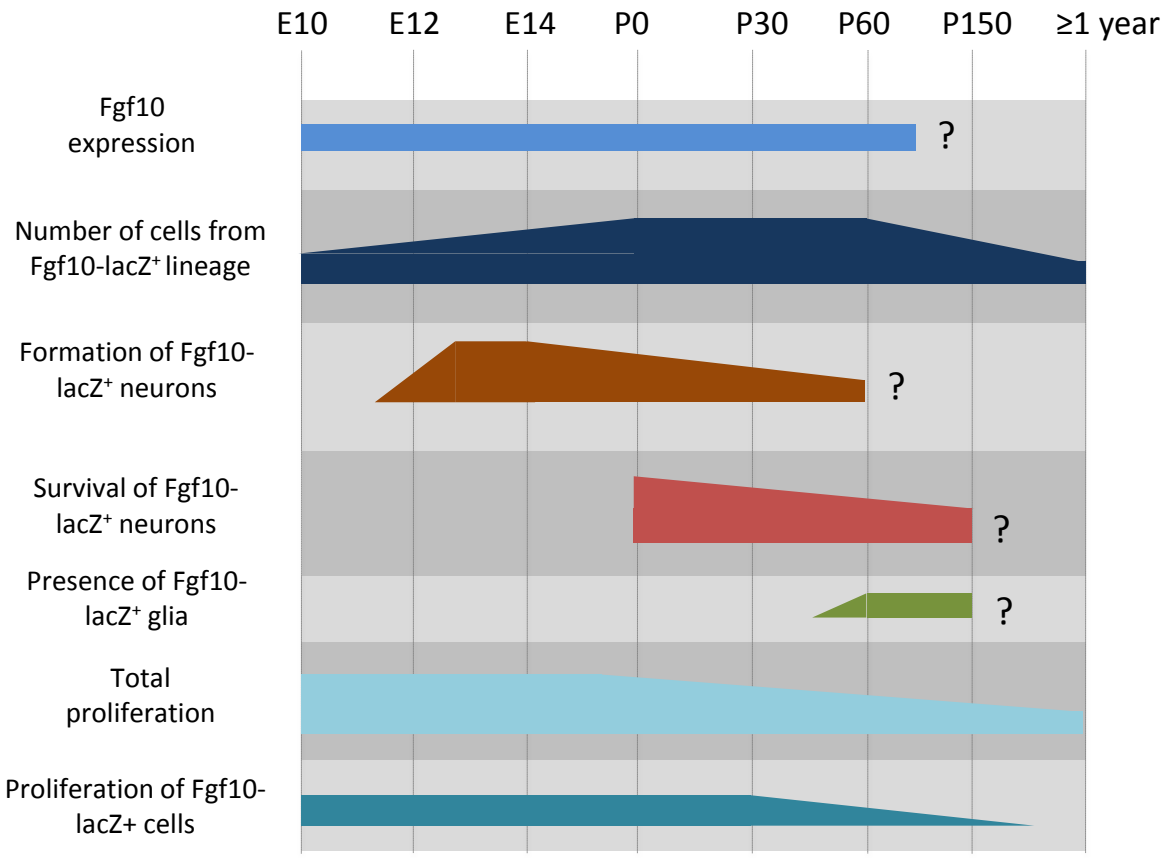

Fig 8.1 Timecourse of events in the hypothalamus. Expression of Fgf10 mRNA is present from as early as E10, and the Fgf10 promoter is still active as late as P80. The total number of Fgf10-lacZ expressing cells increases up to birth, after which it remains relatively constant for 2 months before declining over the rest of the lifetime. Formation of new Fgf10-lacZ expressing neurons are starts between E10 and E12, peaks prior to E14, and continues at much lower levels to at least P60. The neurons generated from the Fgf10-lacZ expressing lineage survive in the adult to at least P150. Fgf10-lacZ$^+$ glia start to be formed between P30 and P60, and are present till at least P150. Proliferative capacity in the hypothalamus is large during initial neurogenesis starting form E10 onwards, still considerable at E18, and decline steadily after birth. However, proliferation still takes place in animals as old as P400. The Fgf10-lacZ$^+$ expression cells proliferate continuously at low levels during late gestation and beyond, but proliferation decreases more markedly than in the general population, and has ceased prior to P400. Question marks indicate the particular property not been examined in later stages than indicated.

widespread embryonic and possibly early postnatal neurogenesis, this population continues to contribute low levels of neurons to the hypothalamus, as confirmed up to P60 with $Fgf10^{CreERT2}$ mediated lineage tracing, and up to P150 with colocalisation in $Fgf10^{nlacZ}$ mice. Additionally in the adult, glial differentiation is seen, which is a switch from the neuronal-only differentiation profile seen during development and up to P30.

Immunohistochemistry for a number of different stem cell markers has allowed for the cytoarchitecture of the neural stem cell niche of the hypothalamus to be characterised. The radial glia-like tanycytes, expressing BLBP and nestin are the resident stem cells. In both late development and in the adult, these cells only rarely divide, as they show low rates of BrdU incorporation. However, the population is capable of expansion, as evidenced by genetic lineage tracing, indicating symmetrical division of these progenitor cells. The location of $BLBP^{-}$/$nestin^{+}$/$mushashi^{+}$ rounded cells directly abutting the radial $BLBP^{+}$ fibers suggests there are transit amplifying cells, migrating along the radial fibers. Some of these cells also show BrdU incorporation, but this may be retained labelling from an asymmetric division event of a tanycyte.

The radial glial-like tanycytes likely represents a continuous progenitor population from the earliest stages of development, progressing from proliferative neuroepithelium around E10, to immature tanycytes and finally to radial tanycytes around birth and into adulthood, closely resembling the process in the developing SVZ (Merkle et al., 2004).

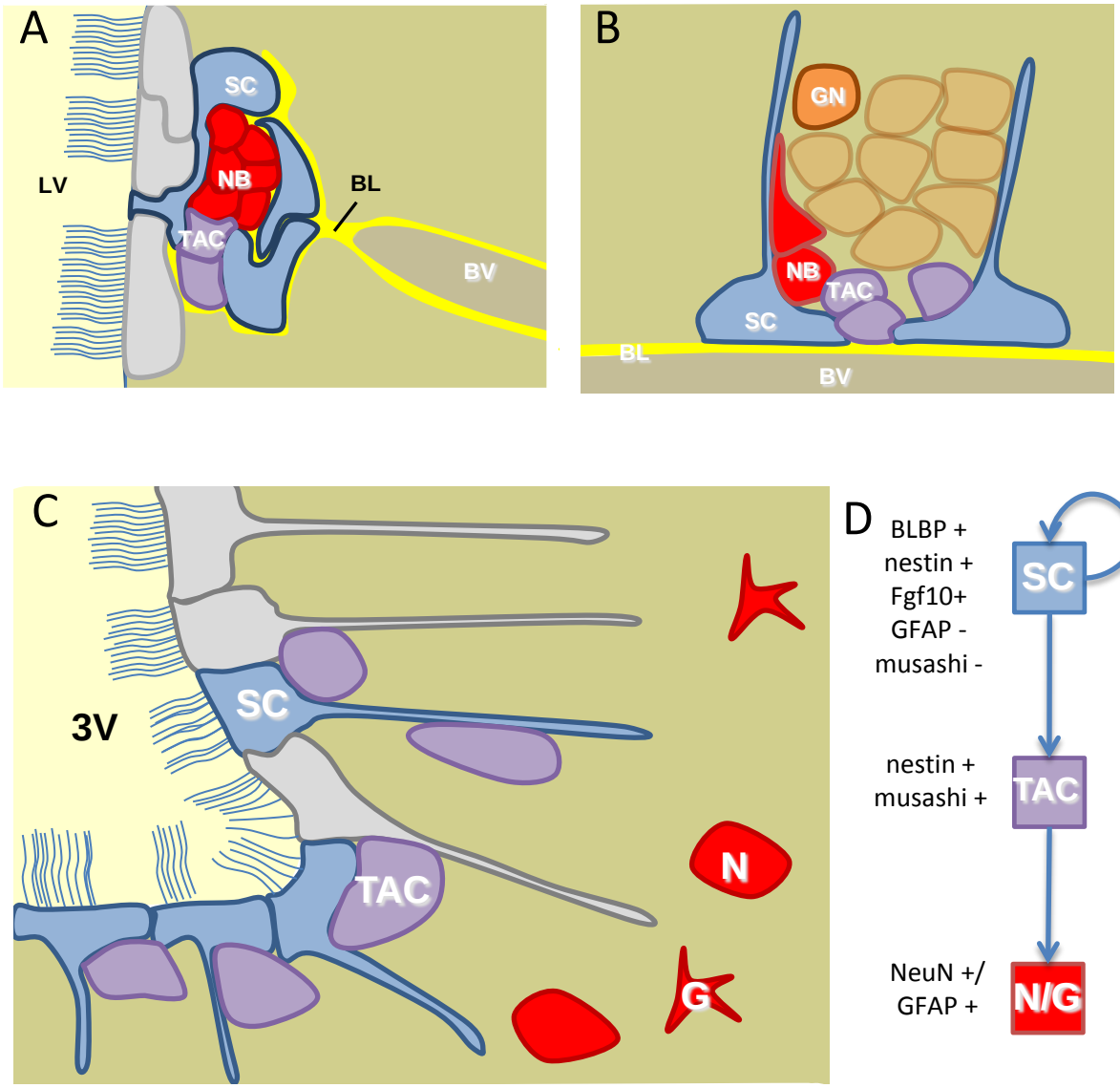

Fig 8.2 – Comparative cytoarchitecture of the classical NSC niches and the hypothalamus. (A) In the SVZ, nestin$^+$/BLBP$^+$/GFAP$^+$ stem cells (SC) are associated with the ciliated ependyma of the lateral ventricle, these produce nestin$^+$/DLX$^+$/GFAP$^+$ transit amplifying cells (TAC) that produce doublecortin$^+$ migratory neuroblasts (NB). These cells are all invested by a blood vessel (BV) derived basal lamina (BL) (B) In the hippocampus, the radial glial stem cells produce transit amplifying cells that form migratory neuroblasts that locally from granular neurons (C) The hypothalamus has properties similar to both niches, but is heterogeneous. The Fgf10 expressing stem cell is closely associated with the ventricle as in the SVZ, but the BLBP$^+$/nestin$^+$ stem cells of a radial morphology as in the hippocampus. The tanycytes seem to produce a BLBP$^-$/nestin$^+$/musashi$^+$ transit amplifying/intermediate progenitor cell that migrates along the radial fibres to produce both neurons and glia (D) Proposed lineage model for the hypothalamic stem cells. The tanycyte stem cell can either amplify through symmetric division or produce and transit amplifying cell through asymmetric division. The TAC then goes on to produce either neurons or glia. For cells that do not express Fgf10 the lineage is not know as yet.

The function of the Fgf10-lacZ^{+} lineage derived neurons in the hypothalamus is not known at this time, and will require further investigation of the exact neuronal type that these cells form. However, given the fact that the majority of cells are found in the arcuate nucleus and median eminence can give hints for their possible function. The arcuate nucleus contains many neuroendocrine neurons, including those expressing agouti-related peptide (AgRP) (Gropp et al., 2005), neuropeptide Y (NPY) (Kalra and Kalra, 2003) and proopiomelanocortin (POMC) (Millington, 2007), which are strong regulatory factors for feeding behaviour and energy balance. Apart from likely expressing many neuroendocrine substances, these hypothalamic neurons are also likely to express receptors for hormones produces elsewhere in the body that are involved in energy balance, such as leptin from fat tissue and ghrelin from the stomach. This makes it likely for the newly generated neurons to be involved in control of feeding behaviour. Indeed, this has previously been suggested (Kokoeva et al., 2005; Pierce and Xu, 2010).

The regulation of proliferation in the hypothalamus is still an unknown area, but given the crucial role of the hypothalamus in the control of feeding behaviour and homeostasis, diet and energy requirement is a tempting field to look for regulators. Indeed, it is well known that dietary factors can influence neurogenesis in the adult hippocampus (Stangl and Thuret, 2009). For instance, a high fat diet can decrease hippocampal proliferation in male rats (Lindqvist et al., 2006), while an antioxidant rich blueberry supplemented diet can increase proliferation (Casadesus et al., 2004). Interestingly, in the latter, this was associated with an increase in IGF1 levels, a factor which has also been shown to be capable of increasing hypothalamic proliferation. Hypothalamic stem cells as a method for providing plasticity in response to environmental factors such as diet is a compelling notion.

In the amygdala, in contrast to the hypothalamus, Fgf10-lacZ expressing cells do not express neural stem cell markers, and do not incorporate BrdU. They are formed around birth, somewhere between E18.5 and P4, and in adulthood most of these are NeuN expressing mature neurons. Although widespread BrdU incorporation was seen, confirming reports from the literature and suggesting the presence of stem cells in the amygdala, the Fgf10-lacZ expressing cells are likely not these stem cells. Although the subtype of neurons that express Fgf10-lacZ has not been determined, the main neuronal subtypes in the amygdala are serotonergic, glutamatergic and GABAergic and it is likely the Fgf10-lacZ expression cells are part of one or more of these populations. Although the possibility remains that some of the NeuN negative Fgf10-lacZ expressing cells represent some kind of stem cell, the complete lack of neural stem cell marker expression and BrdU incorporation makes this unlikely.

The hypothesis that the amygdala is the source of a novel migratory stream towards the olfactory bulbs, at least in the adult, seems unlikely. The possibility of a migration during late development or early life exists, but the fact that $Fgf10^{CreERT2}$ mice show sporadic recombination in the olfactory bulb at E18.5, when little or no Fgf10 expression is seen in the amygdala, makes this unlikely as well.

Regardless of their source, the cells derived from the Fgf10 expressing lineage in the olfactory bulb form the two main subtypes of inhibitory neurons, dopaminergic and GABAergic, which are also the celltypes produced from the RMS. These cells may be involved in olfactory discrimination and consolidation of olfactory memory. Whether the Fgf10 expressing cells in the OB have a similar role remains to be seen, but their phenotype and location suggest this may be the case.

In the adult brain, Fgf10 thus seems to mark two different populations of cells, both stem cells in the hypothalamus and differentiated neurons in the amygdala and

olfactory bulb. Why is this one molecule expressed in two such different populations, and does it have different functions in different cells?

The role of Fgf10 in differentiated neurons is likely to aid in synaptogenesis in these cells. FGF10, as well as the closely related FGF7 and 22, have been shown to promote formation of synapses in vitro (Umemori et al., 2004). This is also likely the case in the hippocampus, where Fgf10 is not expressed in the neural stem cell niche, but in the granular layer where newly formed neurons differentiate and mature. However, this is obviously not the case in the hypothalamus, where the Fgf10 derived differentiated neurons no longer express Fgf10 mRNA.

How these two apparently different roles for Fgf10 are regulated is unclear, but it may be related to the subcellular location of Fgf10. Although due to the lack of antibodies there is little data on the localisation of Fgf10, there is data to suggest that apart from its classical secretory signalling Fgf10 may also localise to the nucleus (Kosman et al., 2007). This is especially likely for Fgf10 in the hypothalamus, since the receptor for Fgf10 is not expressed anywhere near the cells expressing Fgf10.

The closely related Fgf3 has long been known to be both secreted and imported into the nucleus, and has both a bipartite nuclear import motif and a secretory signalling peptide (Kiefer et al., 1994). Forced nuclear expression of Fgf3 causes a decrease in proliferation of cells in vitro (Kiefer and Dickson, 1995), and this effect is regulated by an Fgf3 binding protein, NoBP (Reimers et al., 2001). On the contrary, nuclear expression of Fgf10 has been shown to have a proliferative effect, which cytoplasmic Fgf10 lacks (Kosman et al., 2007). It may be possible that in the hypothalamus, Fgf10 is located in the nucleus and its function is to maintain the proliferative capacity of progenitor cells. In areas where Fgf10 does not seem to mark neural stem cells, it may be instead preferentially secreted and have a role in synaptic organisation. This also explains the lack of FgfR2IIIb expression in the hypothalamus,

as a nuclear role for Fgf10 as a maintainer of proliferative capacity would not necessarily require the expression of the receptor on the cell surface.

The continued decrease of the Fgf10 population in total as evidenced in the $Fgf10^{nlacZ}$ mouse, and the decrease in proliferative capacity as shown in $Fgf10^{CreERT2}$::$ROSA26^{lacZ}$ mice and with BrdU incorporation assays suggests Fgf10 is not the only signal required to maintain proliferation in the hypothalamic tanycytes. Further signals must be required to maintain active proliferation, as the proliferative capacity of Fgf10 expressing cells decreases with age, while Fgf10 expression is maintained. This factor would be present in the early post-natal hypothalamus, allowing for continued proliferation, and is downregulated later in life, leading to a decrease in proliferation and cell number. A likely candidate for this proliferative factor is the classical mitogen Fgf2, which is widely expressed in the adult hypothalamus (Gonzalez et al., 1994). It's main receptors, FgfR1-IIIc and FgfR3-IIIc are also expressed throughout the hypothalamus (Chapter 4). Other interesting possibilities are IGF1, CNTF and BDNF, which have already been shown to stimulate proliferation in the hypothalamus (Kokoeva et al., 2005; Pencea et al., 2001; Perez-Martin et al., 2010). However, no data exists on whether the expression levels of these factors change as animals age, so it remains to be confirmed whether they are involved in the regulation of Fgf10 expressing progenitors.

The possible involvement of cell extrinsic growth factors and Fgf10 for proliferation in the hypothalamus suggests a two-step mechanism for initiation and maintenance of proliferation. The presence of Fgf10 in the cell, most likely the nucleus, provides for a permissive environment for proliferation, possibly through a nuclear interacting protein as is the case with Fgf3. The presence of Fgf10 may be required for, or promote the activity of transcriptional machinery involved in proliferation. This proliferation is then initiated by a second signal, likely a cell-

extrinsic growth factor activating the MAPK (Fgf2, BNDF), Jak/STAT (CNTF) or Akt (IGF1) pathway. The downstream effect of these pathways can be the transcription of genes involved in proliferation.

Indeed, it has been observed that in the developing cortex of Fgf10 knockouts, the radial glia progenitor population is decreased, and cells instead become post-mitotic neurons (Sahara and O'Leary, 2009), underscoring the putative requirement for Fgf10 to maintain proliferative capacity in at least some cells.

This possible requirement in the hypothalamus is also suggested by in vitro experiments. In neuronal cultures, cells not expressing Fgf10 were only found as single cells, or small clusters. On the other hand, Fgf10 expressing cells were seen in large clonal clusters, likely generated in situ by a precursor cell type. This illustrates that even in the presence of a powerful mitogen, Fgf2, Fgf10 negative cells from the adult hypothalamus will not show a mitotic response, whereas those expressing Fgf10 do. The Fgf10 expressing tanycytes in the hypothalamus after approximately P40 thus represents a potential source of new cells, keeping a proliferative capacity by Fgf10 expression, but requiring a further signal to actually induce proliferation. This represents a quiescent reservoir of cells which can be primed to respond to a need for new cells.

These two different putative roles for Fgf10 in the adult brain, maintenance of stem cells and promotion of synapse formation, clearly illustrate the pleiotropic nature of Fgf10 and the likely importance of this factor both during developments and adulthood.

Future work

In the hypothalamus, the phenotype of neurons derived from the Fgf10 expressing lineage can be characterised with immunohistochemistry. Likely candidates to be expressed in these cells, particularly those in the arcuate nucleus are AgRP, POMC, NPY and leptin receptors. Expression of these markers would underline the possible role for these cells in energy balance.

The genetic lineage tracing performed here can be expanded to longer timeframes to assess the long-term survival of the adult-generated Fgf10 expressing neurons. Along with this, apoptosis can be studied to determine the fraction of these cells that fail to integrate and die.

In vitro, clonal analysis of neurospheres can be undertaken, growing spheres form single isolated cells to ensure each individual neurosphere is multipotent, rather than a restricted progenitor and to study the expression of Fgf10 on a single cell level during proliferation and differentiation. Also, this system would be amenable to loss- and gain-of-function experiments, allowing for the study of the role of Fgf10 in neural progenitors.

The relative importance of the local niche environment of the hypothalamus can be assessed through grafting experiments. For instance, it is known that embryonic cortical neural progenitors, which are normally multipotent, become restricted to glial lineages once transplanted into the non-neurogenic adult spinal cord (Cao et al., 2001). Conversely, if the niche environment of the hypothalamus promotes and/or maintains multipotency, transplantation of restricted progenitors such as adult spinal cord glial progenitors into the hypothalamus may result in these regaining multipotency.

In vivo clonal analysis can be undertaken by titrating tamoxifen doses down to a level that only one or a few cells in any brain recombine, allowing for the progeny of

individual cells to be examined. This approach has been successfully used in the hippocampus (Bonaguidi et al., 2011). Alternatively, a very attractive and elegant solution would be to combine the $Fgf10^{CreERT2}$ line with the recent "Brainbow" reporter strains, in which recombined cells can assume a number of different fluorescent colours through combinatorial recombination of a number of different floxed fluorescent reporter proteins (Livet et al., 2007). This would allow for the lineage of many cells to be individually traced in a single brain.

In the amygdala, further characterisation of Fgf10 derived neurons can be undertaken, with the most likely candidate neuronal subtypes being serotonergic, glutamatergic and GABAergic.

To assess the function of Fgf10 in the brain, $Fgf10^{CreERT2}$::$Fgf10^{loxP}$ mice can be utilised. In these mice, one allele of the Fgf10 gene is knocked out by the presence of the Cre allele, whereas the other allele can be removed by activation of the Cre, thus creating an inducible knockout, and circumventing the lethality of constitutive Fgf10 knockouts. The inclusion of the $ROSA26^{lacZ}$ or $ROSA^{Tomato}$ reporter allele in these mice would allow for the detection of cells in which Cre is active and from which Fgf10 has been removed.

To take this approach one step further, Fgf10 expressing cells could be selectively ablated using inducible expression of a suicide gene. This could be done with existing mouse lines, crossing the $Fgf10^{CreERT2}$ line to an existing mouse line carrying a Cre-activatable herpes simplex thymidine kinase (Chen et al., 2004). This would result in expression of thymidine kinase in Fgf10 expressing cells following tamoxifen administration, which can then be selectively ablated using ganciclovir. This model could be used to asses the function of the cells generated by the Fgf10 expressing lineage.

In order to validate the potential two-role model of Fgf10 function in the adult brain and its mechanism, more data on the subcellular localisation of Fgf10 is required. In vitro experiments with fluorescently tagged fusion proteins and mutagenesis, currently ongoing, will provide information. In vivo, the most convenient way of determining subcellular localisation this would be with immunohistochemistry, but as no antibodies are available, this remains impossible. Generation of an Fgf10 reporter mouse carrying an Fgf10 fusion protein with a fluorescent or different tag would currently be the only option for these investigations. A different intriguing possibility to asses the importance of nuclear Fgf10 localisation would be a the generation of a mouse in which the nuclear localisation site of Fgf10 is disrupted, or, if this gives a non-viable phenotype, a line where a floxed wt Fgf10 is upstream of the mutant Fgf10, allowing for inducible replacement of the wt with the mutant.

Although this work here presented has started the characterisation of the Fgf10 expressing lineage in the brain, future work will determine its function and importance of Fgf10 and the cells in which it is expressed.

List of abbreviations

AER	Apical ectodermal ridge
aFGF	acidic fibroblast growth factor (Fgf1)
ALSG	aplasia of lacrimal and salivary glands
ANOVA	analysis of variance
AraC	cytarabine
BDNF	brain derived neurotrophic factor
bFGF	basic fibroblast growth factor (Fgf2)
BLBP	brain lipid binding protein
BMP	bone morphogenic factor
BrdU	5-bromo-2'-deoxiuridine
C/EBPβ	ccaat-enhancer-binding proteins
cDNA	complementary DNA
CFA	complete Freund's adjuvans
CNTF	ciliary neurotrophic factor
CreER	Cre recombinase - estrogen receptor fusion protein
CSF	Cerebrospinal fluid
Dll4	delta-like 4
DLX	distal-less
DMEM	Dulbecco's modified Eagle's medium
DTT	dithiothreitol
ECL	Enhanced chemoluminescence
EDTA	ethylenediaminotetra-acetic acid
EGF	epidermal growth factor
E*n*	Embryonic day *n*
EPL	External plexiform layer
Erk	extracellular signal-activated kinase
FACS	fluorescence activated cell sorting
FDG	fluoresceine-di-β-D-galactopyranoside
Fgf	fibroblast growth factor
FgfR	Fgf receptor
FLAG	NDYDDDDKC peptide tag
FRS2	FgfR substrate 2
Gab1	GRB2-associated-binding protein
GABA	γ-aminobutyric acid
GCK3β	germinal centre kinase 3β
GCL	granular cell layer
GFAP	glial fibrilary acidic protein
GL	glomerular layer
GLAST	glutamate aspartate transporter
Grb2	growth factor receptor bound protein 2
Gt	goat
HA	heamaglutinin
HCl	Hydrochloric acid
HEK	human embryonic kidney
Hes	hairey and enhancer of split
hFgf	hormonal Fgf
HRP	horseradish peroxidase
Hu	human
IFA	incomplete Freund's adjuvans
iFgf	intracellular Fgf

Ig	immunoglobulin
IHC	immunohistochemistry
IPL	internal plexiform layer
IRES	independent ribosomal entry site
JAK/STAT	Janus activated kinase / signal transducer and activator of transciption
kDA	kiloDalton
KO	knockout
L-glut	L-glutamine
LADD	lacrimo-auriculo-dento-digital syndrome
Lif	leukaemia inhibitory factor
MAPK	mitogen activated protein kinase
Mash1	mammalian achaete homolog
MCL	mitral cell layer
MeOH	methanol
MMP	matrix metaloprotease
Ms	mouse
NeuN	neuronal nuclei
NeuroD	neuronal differentiation
Neurog2	neurogenin 2
NGS	normal goat serum
NSC	neural stem cell
OB	olfactory bulb
Olig2	oligodendrocyte transcription factor 2
ONL	olfactory nerve layer
PAGE	polyacrylamide gel electrophoresis
Pax6	transcription factorpaired box 6
PCNA	proliferating cell nuclear antigen
PDL	poly-D-lysine
PEDF	pigment epithelium-derived growth factor
Pen/strep	penicillin/ streptomycin
PFA	paraformaldehyde
PI3	phosphoinositide 3-kinase
PIPES	piperazine-N,N'bis(2-ethanesulfonic acid)
PKCζ	protein kinase ζ
P*n*	Post-natal day *n*
PORN	poly-L-ornithin
PPARγ	peroxisome proliferator-activated receptor γ
RFP	red fluorescent portein
RIPA	radio immunoprecipitation assay
RMS	rostral migratory stream
ROBO	roundabout
rpm	revolutions per minute
RT-PCR	reverse transcriptase polymerase chain reaction
Sal3	saccaromyces cerevisiae allosuppressor
SDS	sodium dodecyl sulphate
SGZ	subgranular zone
Shh	sonic hedgehog homolog
Shp2	Src homology phosphatase 2
SOS	son of sevenless homolog
SOX	Sry-related HMG box

Sp8	specificiy protein 8
SVZ	subventricular zone
Tbr2	T-box brain gene
TCEP	tris(2-carboxyethyl) phosphine
TE	Tris-EDTA
TESPA	3-aminopropyl-triethoxy silane
TLX	tailless
Tris	tris(hydroxymethyl)amino methane
Tuj1	neurons-specific class II β-tubulin
Tx red	Texas Red
Wnt	Int1 and wingless
YFP	yellow fluorescent protein

References

Abler, L. L., S. L. Mansour, and X. Sun. (2009). Conditional gene inactivation reveals roles for Fgf10 and Fgfr2 in establishing a normal pattern of epithelial branching in the mouse lung. *Dev Dyn* 238 (8):1999-2013.

Ables, J. L., N. A. Decarolis, M. A. Johnson, P. D. Rivera, Z. Gao, D. C. Cooper, F. Radtke, J. Hsieh, and A. J. Eisch. 2010. Notch1 is required for maintenance of the reservoir of adult hippocampal stem cells. *J Neurosci* 30 (31):10484-92.

Aguirre, A., M. E. Rubio, and V. Gallo. (2010). Notch and EGFR pathway interaction regulates neural stem cell number and self-renewal. *Nature* 467 (7313):323-7.

Altman, J. 1962. Are new neurons formed in the brains of adult mammals? *Science* 135:1127-8.

Altman, J., and S. A. Bayer. (1978). Development of the diencephalon in the rat. III. Ontogeny of the specialized ventricular linings of the hypothalamic third ventricle. *J Comp Neurol* 182 (4 Pt 2):995-1015.

Altman, J., and S. A. Bayer. (1995). *Atlas of prenatal rat brain development*: CRC Press Inc.

Altman, J., and G. D. Das. (1965). Autoradiographic and histological evidence of postnatal hippocampal neurogenesis in rats. *J Comp Neurol* 124 (3):319-35.

Altman, J., and G. D. Das. (1966). Autoradiographic and histological studies of postnatal neurogenesis. I. A longitudinal investigation of the kinetics, migration and transformation of cells incorporating tritiated thymidine in neonate rats, with special reference to postnatal neurogenesis in some brain regions. *J Comp Neurol* 126 (3):337-89.

Alvarez-Buylla, A., and J. M. Garcia-Verdugo. (2002). Neurogenesis in adult subventricular zone. *J Neurosci* 22 (3):629-34.

Alvarez-Buylla, A., and D. A. Lim. (2004). For the long run: maintaining germinal niches in the adult brain. *Neuron* 41 (5):683-6.

Alvarez-Buylla, A., M. Theelen, and F. Nottebohm. (1988). Birth of projection neurons in the higher vocal center of the canary forebrain before, during, and after song learning. *Proc Natl Acad Sci U S A* 85 (22):8722-6.

Andreu-Agullo, C., J. M. Morante-Redolat, A. C. Delgado, and I. Farinas. (2009). Vascular niche factor PEDF modulates Notch-dependent stemness in the adult subependymal zone. *Nat Neurosci* 12 (12):1514-23.

Androutsellis-Theotokis, A., R. R. Leker, F. Soldner, D. J. Hoeppner, R. Ravin, S. W. Poser, M. A. Rueger, S. K. Bae, R. Kittappa, and R. D. McKay. (2006). Notch signalling regulates stem cell

numbers in vitro and in vivo. *Nature* 442 (7104):823-6.
Anton, E. S., H. T. Ghashghaei, J. L. Weber, C. McCann, T. M. Fischer, I. D. Cheung, M. Gassmann, A. Messing, R. Klein, M. H. Schwab, K. C. Lloyd, and C. Lai. (2004). Receptor tyrosine kinase ErbB4 modulates neuroblast migration and placement in the adult forebrain. *Nat Neurosci* 7 (12):1319-28.

Arsenijevic, Y., J. G. Villemure, J. F. Brunet, J. J. Bloch, N. Deglon, C. Kostic, A. Zurn, and P. Aebischer. (2001). Isolation of multipotent neural precursors residing in the cortex of the adult human brain. *Exp Neurol* 170 (1):48-62.

Asaki, T., M. Konishi, A. Miyake, S. Kato, M. Tomizawa, and N. Itoh. (2004). Roles of fibroblast growth factor 10 (Fgf10) in adipogenesis in vivo. *Mol Cell Endocrinol* 218 (1-2):119-28.

Bagley, J., G. LaRocca, D. A. Jimenez, and N. N. Urban. (2007). Adult neurogenesis and specific replacement of interneuron subtypes in the mouse main olfactory bulb. *BMC Neurosci* 8:92.

Barnea, A., and F. Nottebohm. (1994). Seasonal recruitment of hippocampal neurons in adult free-ranging black-capped chickadees. *Proc Natl Acad Sci U S A* 91 (23):11217-21.

Battista, D., and U. Rutishauser. (2010). Removal of polysialic acid triggers dispersion of subventricularly derived neuroblasts into surrounding CNS tissues. *J Neurosci* 30 (11):3995-4003.

Bauer, S. (2009). Cytokine control of adult neural stem cells. *Ann N Y Acad Sci* 1153:48-56.

Bedard, A., C. Gravel, and A. Parent. (2006.) Chemical characterization of newly generated neurons in the striatum of adult primates. *Exp Brain Res* 170 (4):501-12.

Bedard, A., M. Levesque, P. J. Bernier, and A. Parent. (2002). The rostral migratory stream in adult squirrel monkeys: contribution of new neurons to the olfactory tubercle and involvement of the antiapoptotic protein Bcl-2. *Eur J Neurosci* 16 (10):1917-24.

Beer, H. D., C. Florence, J. Dammeier, L. McGuire, S. Werner, and D. R. Duan. (1997). Mouse fibroblast growth factor 10: cDNA cloning, protein characterization, and regulation of mRNA expression. *Oncogene* 15 (18):2211-8.

Bellusci, S., J. Grindley, H. Emoto, N. Itoh, and B. L. Hogan. (1997). Fibroblast growth factor 10 (FGF10) and branching morphogenesis in the embryonic mouse lung. *Development* 124 (23):4867-78.

Belvindrah, R., S. Hankel, J. Walker, B. L. Patton, and U. Muller. (2007). Beta1 integrins control the formation of cell chains in the adult rostral migratory stream. *J Neurosci* 27 (10):2704-17.

Bennett, L., M. Yang, G. Enikolopov, and L. Iacovitti. (2009). Circumventricular organs: a novel site of neural stem cells in the adult brain. *Mol Cell Neurosci* 41 (3):337-47.

Berg, T., C. B. Rountree, L. Lee, J. Estrada, F. G. Sala, A. Choe, J. M. Veltmaat, S. De Langhe, R. Lee, H. Tsukamoto, G. M. Crooks, S. Bellusci, and K. S. Wang. (2007). Fibroblast growth factor 10 is critical for liver growth during embryogenesis and controls hepatoblast survival via beta-catenin activation. *Hepatology* 46 (4):1187-97.

Bergami, M., R. Rimondini, S. Santi, R. Blum, M. Gotz, and M. Canossa. (2008). Deletion of TrkB in adult progenitors alters newborn neuron integration into hippocampal circuits and increases anxiety-like behavior. *Proc Natl Acad Sci U S A* 105 (40):15570-5.

Bernier, P. J., A. Bedard, J. Vinet, M. Levesque, and A. Parent. (2002). Newly generated neurons in the amygdala and adjoining cortex of adult primates. *Proc Natl Acad Sci U S A* 99 (17):11464-9.

Bhushan, A., N. Itoh, S. Kato, J. P. Thiery, P. Czernichow, S. Bellusci, and R. Scharfmann. (2001). Fgf10 is essential for maintaining the proliferative capacity of epithelial progenitor cells during early pancreatic organogenesis. *Development* 128 (24):5109-17.

Bohlen, P., A. Baird, F. Esch, N. Ling, and D. Gospodarowicz. (1984). Isolation and partial molecular characterization of pituitary fibroblast growth factor. *Proc Natl Acad Sci U S A* 81 (17):5364-8.

Bonaguidi, M. A., T. McGuire, M. Hu, L. Kan, J. Samanta, and J. A. Kessler. (2005). LIF and BMP signaling generate separate and discrete types of GFAP-expressing cells. *Development* 132 (24):5503-14.

Bonaguidi, M. A., M. A. Wheeler, J. S. Shapiro, R. P. Stadel, G. J. Sun, G. L. Ming, and H. Song. (2011). In vivo clonal analysis reveals self-renewing and multipotent adult neural stem cell characteristics. *Cell* 145 (7):1142-55.

Booher, J., and M. Sensenbrenner. (1972). Growth and cultivation of dissociated neurons and glial cells from embryonic chick, rat and human brain in flask cultures. *Neurobiology* 2 (3):97-105.

Boutin, C., O. Hardt, A. de Chevigny, N. Core, S. Goebbels, R. Seidenfaden, A. Bosio, and H. Cremer. (2010). NeuroD1 induces terminal neuronal differentiation in olfactory neurogenesis. *Proc Natl Acad Sci U S A* 107 (3):1201-6.

Bovetti, S., P. Bovolin, I. Perroteau, and A. C. Puche. (2007). Subventricular zone-derived neuroblast migration to the olfactory bulb is modulated by matrix remodelling. *Eur J Neurosci* 25 (7):2021-33.

Bowman, C. L., and H. K. Kimelberg. (1984). Excitatory amino acids directly depolarize rat brain astrocytes in primary culture. *Nature* 311 (5987):656-9.

Brewer, G. J. (1995). Serum-free B27/neurobasal medium supports differentiated growth of neurons from the striatum, substantia nigra, septum, cerebral cortex, cerebellum, and dentate gyrus. *J Neurosci Res* 42 (5):674-83.

Brewer, G. J. (1997). Isolation and culture of adult rat hippocampal neurons. *J Neurosci Methods* 71 (2):143-55.

Brill, M. S., J. Ninkovic, E. Winpenny, R. D. Hodge, I. Ozen, R. Yang, A. Lepier, S. Gascon, F. Erdelyi, G. Szabo, C. Parras, F. Guillemot, M. Frotscher, B. Berninger, R. F. Hevner, O. Raineteau, and M. Gotz. (2009). Adult generation of glutamatergic olfactory bulb interneurons. *Nat Neurosci* 12 (12):1524-33.

Bull, N. D., and P. F. Bartlett. (2005). The adult mouse hippocampal progenitor is neurogenic but not a stem cell. *J Neurosci* 25 (47):10815-21.

Casadesus, G., B. Shukitt-Hale, H. M. Stellwagen, X. Zhu, H. G. Lee, M. A. Smith, and J. A. Joseph. (2004). Modulation of hippocampal plasticity and cognitive behavior by short-term blueberry supplementation in aged rats. *Nutr Neurosci* 7 (5-6):309-16.

Cave, J. W., and H. Baker. (2009). Dopamine systems in the forebrain. *Adv Exp Med Biol* 651:15-35.

Chakraborty, S., S. Kanakasabai, and J. J. Bright. (2011). Constitutive androstane receptor agonist CITCO inhibits growth and expansion of brain tumour stem cells. *Br J Cancer* 104 (3):448-59.

Charrier, C., V. Coronas, J. Fombonne, M. Roger, A. Jean, S. Krantic, and E. Moyse. (2006). Characterization of neural stem cells in the dorsal vagal complex of adult rat by in vivo proliferation labeling and in vitro neurosphere assay. *Neuroscience* 138 (1):5-16.

Chearwae, W., and J. J. Bright. (2008). PPARgamma agonists inhibit growth and expansion of CD133+ brain tumour stem cells. *Br J Cancer* 99 (12):2044-53.

Chen, C. W., C. S. Liu, I. M. Chiu, S. C. Shen, H. C. Pan, K. H. Lee, S. Z. Lin, and H. L. Su. (2010). The signals of FGFs on the neurogenesis of embryonic stem cells. *J Biomed Sci* 17:33.

Chen, J., C. H. Kwon, L. Lin, Y. Li, and L. F. Parada. (2009). Inducible site-specific recombination in neural stem/progenitor cells. *Genesis* 47 (2):122-31.

Chen, Y. T., R. Levasseur, S. Vaishnav, G. Karsenty, and A. Bradley. (2004). Bigenic Cre/loxP, puDeltatk conditional genetic ablation. *Nucleic Acids Res* 32 (20):e161.

Cholfin, J. A., and J. L. Rubenstein. (2008). Frontal cortex subdivision patterning is coordinately regulated by Fgf8, Fgf17, and Emx2. *J Comp Neurol* 509 (2):144-55.

Chou, T. C., T. E. Scammell, J. J. Gooley, S. E. Gaus, C. B. Saper, and J. Lu. (2003). Critical role of dorsomedial hypothalamic nucleus in a wide range of behavioral circadian rhythms. *J Neurosci* 23 (33):10691-702.

Courtes, S., J. Vernerey, L. Pujadas, K. Magalon, H. Cremer, E. Soriano, P. Durbec, and M. Cayre. (2010). Reelin controls progenitor cell migration in the healthy and pathological adult

mouse brain. *PLoS One* 6 (5):e20430.

Dalvi, P. S., A. Nazarians-Armavil, S. Tung, and D. D. Belsham. (2011. Immortalized neurons for the study of hypothalamic function. *Am J Physiol Regul Integr Comp Physiol* 300 (5):R1030-52.

Das, A. V., K. B. Mallya, X. Zhao, F. Ahmad, S. Bhattacharya, W. B. Thoreson, G. V. Hegde, and I. Ahmad. (2006). Neural stem cell properties of Muller glia in the mammalian retina: regulation by Notch and Wnt signaling. *Dev Biol* 299 (1):283-302.

De Moerlooze, L., B. Spencer-Dene, J. M. Revest, M. Hajihosseini, I. Rosewell, and C. Dickson. (2000). An important role for the IIIb isoform of fibroblast growth factor receptor 2 (FGFR2) in mesenchymal-epithelial signalling during mouse organogenesis. *Development* 127 (3):483-92.

Deloulme, J. C., J. Baudier, and M. Sensenbrenner. (1991). Establishment of pure neuronal cultures from fetal rat spinal cord and proliferation of the neuronal precursor cells in the presence of fibroblast growth factor. *J Neurosci Res* 29 (4):499-509.

Deng, W., J. B. Aimone, and F. H. Gage. (2010). New neurons and new memories: how does adult hippocampal neurogenesis affect learning and memory? *Nat Rev Neurosci* 11 (5):339-50.

Doetsch, F., J. M. Garcia-Verdugo, and A. Alvarez-Buylla. 1999. Regeneration of a germinal layer in the adult mammalian brain. *Proc Natl Acad Sci U S A* 96 (20):11619-24.

Doetsch, F., L. Petreanu, I. Caille, J. M. Garcia-Verdugo, and A. Alvarez-Buylla. (2002). EGF converts transit-amplifying neurogenic precursors in the adult brain into multipotent stem cells. *Neuron* 36 (6):1021-34.

Emoto, H., S. Tagashira, M. G. Mattei, M. Yamasaki, G. Hashimoto, T. Katsumata, T. Negoro, M. Nakatsuka, D. Birnbaum, F. Coulier, and N. Itoh. (1997). Structure and expression of human fibroblast growth factor-10. *J Biol Chem* 272 (37):23191-4.

Entesarian, M., H. Matsson, J. Klar, B. Bergendal, L. Olson, R. Arakaki, Y. Hayashi, H. Ohuchi, B. Falahat, A. I. Bolstad, R. Jonsson, M. Wahren-Herlenius, and N. Dahl. (2005). Mutations in the gene encoding fibroblast growth factor 10 are associated with aplasia of lacrimal and salivary glands. *Nat Genet* 37 (2):125-7.

Ernsberger, P., L. Iacovitti, and D. J. Reis. (1990). Astrocytes cultured from specific brain regions differ in their expression of adrenergic binding sites. *Brain Res* 517 (1-2):202-8.

Eswarakumar, V. P., I. Lax, and J. Schlessinger. (2005). Cellular signaling by fibroblast growth factor receptors. *Cytokine Growth Factor Rev* 16 (2):139-49.

Favaro, R., M. Valotta, A. L. Ferri, E. Latorre, J. Mariani, C. Giachino, C. Lancini, V. Tosetti, S. Ottolenghi, V. Taylor, and S. K. Nicolis. (2009). Hippocampal development and neural stem cell maintenance require Sox2-dependent regulation of Shh. *Nat Neurosci* 12 (10):1248-56.

Feil, R., J. Brocard, B. Mascrez, M. LeMeur, D. Metzger, and P. Chambon. (1996). Ligand-activated site-specific recombination in mice. *Proc Natl Acad Sci U S A* 93 (20):10887-90.

Feil, R., J. Wagner, D. Metzger, and P. Chambon. (1997). Regulation of Cre recombinase activity by mutated estrogen receptor ligand-binding domains. *Biochem Biophys Res Commun* 237 (3):752-7.

Ferri, A. L., M. Cavallaro, D. Braida, A. Di Cristofano, A. Canta, A. Vezzani, S. Ottolenghi, P. P. Pandolfi, M. Sala, S. DeBiasi, and S. K. Nicolis. (2004). Sox2 deficiency causes neurodegeneration and impaired neurogenesis in the adult mouse brain. *Development* 131 (15):3805-19.

Firket, H., and W. G. Verly. (1958). Autoradiographic visualization of synthesis of deoxyribonucleic acid in tissue culture with tritium-labelled thymidine. *Nature* 181 (4604):274-5.

Fischer, T., T. Faus-Kessler, G. Welzl, A. Simeone, W. Wurst, and N. Prakash. (2011). Fgf15-mediated control of neurogenic and proneural gene expression regulates dorsal midbrain neurogenesis. *Dev Biol* 350 (2):496-510.

Fowler, C. D., M. E. Freeman, and Z. Wang. (2003). Newly proliferated cells in the adult male amygdala are affected by gonadal steroid hormones. *J Neurobiol* 57 (3):257-69.

Fowler, C. D., F. Johnson, and Z. Wang. (2005). Estrogen regulation of cell proliferation and distribution of estrogen receptor-alpha in the brains of adult female prairie and meadow voles. *J Comp Neurol* 489 (2):166-79.

Fowler, C. D., Y. Liu, C. Ouimet, and Z. Wang. (2002). The effects of social environment on adult neurogenesis in the female prairie vole. *J Neurobiol* 51 (2):115-28.

Franklin, KBJ., and G. Paxinos. (2008). *The mouse brain in stereotxic coordinates*. 3rd ed: Academic Press.

Frosch, M. P., and M. A. Dichter. (1984). Physiology and pharmacology of olfactory bulb neurons in dissociated cell culture. *Brain Res* 290 (2):321-32.

Gage, F. H., P. W. Coates, T. D. Palmer, H. G. Kuhn, L. J. Fisher, J. O. Suhonen, D. A. Peterson, S. T. Suhr, and J. Ray. (1995). Survival and differentiation of adult neuronal progenitor cells transplanted to the adult brain. *Proc Natl Acad Sci U S A* 92 (25):11879-83.

Gall, C. M., S. H. Hendry, K. B. Seroogy, E. G. Jones, and J. W. Haycock. (1987). Evidence for coexistence of GABA and dopamine in neurons of the rat olfactory bulb. *J Comp Neurol* 266 (3):307-18.

Garcia, M. A., C. Millan, C. Balmaceda-Aguilera, T. Castro, P. Pastor, H. Montecinos, K. Reinicke, F. Zuniga, J. C. Vera, S. A. Onate, and F. Nualart. (2003). Hypothalamic

ependymal-glial cells express the glucose transporter GLUT2, a protein involved in glucose sensing. *J Neurochem* 86 (3):709-24.

Garcia-Segura, L. M., I. Torres-Aleman, and F. Naftolin. (1989). Astrocytic shape and glial fibrillary acidic protein immunoreactivity are modified by estradiol in primary rat hypothalamic cultures. *Brain Res Dev Brain Res* 47 (2):298-302.

Gascon, E., A. G. Dayer, M. O. Sauvain, G. Potter, B. Jenny, M. De Roo, E. Zgraggen, N. Demaurex, D. Muller, and J. Z. Kiss. (2006). GABA regulates dendritic growth by stabilizing lamellipodia in newly generated interneurons of the olfactory bulb. *J Neurosci* 26 (50):12956-66.

Gensburger, C., G. Labourdette, and M. Sensenbrenner. (1987). Brain basic fibroblast growth factor stimulates the proliferation of rat neuronal precursor cells in vitro. *FEBS Lett* 217 (1):1-5.

Gerdes, J., U. Schwab, H. Lemke, and H. Stein. (1983). Production of a mouse monoclonal antibody reactive with a human nuclear antigen associated with cell proliferation. *Int J Cancer* 31 (1):13-20.

Ghashghaei, H. T., C. Lai, and E. S. Anton. (2007). Neuronal migration in the adult brain: are we there yet? *Nat Rev Neurosci* 8 (2):141-51.

Gheusi, G., H. Cremer, H. McLean, G. Chazal, J. D. Vincent, and P. M. Lledo. (2000). Importance of newly generated neurons in the adult olfactory bulb for odor discrimination. *Proc Natl Acad Sci U S A* 97 (4):1823-8.

Giaume, C., and L. Venance. (1998). Intercellular calcium signaling and gap junctional communication in astrocytes. *Glia* 24 (1):50-64.

Gimeno, L., P. Brulet, and S. Martinez. (2003). Study of Fgf15 gene expression in developing mouse brain. *Gene Expr Patterns* 3 (4):473-81.

Gimeno, L., and S. Martinez. (2007). Expression of chick Fgf19 and mouse Fgf15 orthologs is regulated in the developing brain by Fgf8 and Shh. *Dev Dyn* 236 (8):2285-97.

Gingerich, S., X. Wang, P. K. Lee, S. S. Dhillon, J. A. Chalmers, M. M. Koletar, and D. D. Belsham. (2009). The generation of an array of clonal, immortalized cell models from the rat hypothalamus: analysis of melatonin effects on kisspeptin and gonadotropin-inhibitory hormone neurons. *Neuroscience* 162 (4):1134-40.

Goldfarb, M. (2005). Fibroblast growth factor homologous factors: evolution, structure, and function. *Cytokine Growth Factor Rev* 16 (2):215-20.

Goldfarb, M., B. Bates, B. Drucker, J. Hardin, and O. Haub. (1991). Expression and possible functions of the FGF-5 gene. *Ann N Y Acad Sci* 638:38-52.

Gomez-Pinilla, F., J. W. Lee, and C. W. Cotman. (1992). Basic FGF in adult rat brain: cellular distribution and response to entorhinal lesion and fimbria-fornix transection. *J Neurosci* 12

(1):345-55.

Goncalves, L., R. Silva, F. Pinto-Ribeiro, J. M. Pego, J. M. Bessa, A. Pertovaara, N. Sousa, and A. Almeida. (2008). Neuropathic pain is associated with depressive behaviour and induces neuroplasticity in the amygdala of the rat. *Exp Neurol* 213 (1):48-56.

Gotoh, N., K. Manova, S. Tanaka, M. Murohashi, Y. Hadari, A. Lee, Y. Hamada, T. Hiroe, M. Ito, T. Kurihara, H. Nakazato, M. Shibuya, I. Lax, E. Lacy, and J. Schlessinger. (2005). The docking protein FRS2alpha is an essential component of multiple fibroblast growth factor responses during early mouse development. *Mol Cell Biol* 25 (10):4105-16.

Gould, E. (2007). How widespread is adult neurogenesis in mammals? *Nat Rev Neurosci* 8 (6):481-8.

Gould, E., A. J. Reeves, M. S. Graziano, and C. G. Gross. (1999). Neurogenesis in the neocortex of adult primates. *Science* 286 (5439):548-52.

Gropp, E., M. Shanabrough, E. Borok, A. W. Xu, R. Janoschek, T. Buch, L. Plum, N. Balthasar, B. Hampel, A. Waisman, G. S. Barsh, T. L. Horvath, and J. C. Bruning. (2005). Agouti-related peptide-expressing neurons are mandatory for feeding. *Nat Neurosci* 8 (10):1289-91.

Grothe, C., M. Timmer, T. Scholz, C. Winkler, G. Nikkhah, P. Claus, N. Itoh, and E. Arenas. (2004). Fibroblast growth factor-20 promotes the differentiation of Nurr1-overexpressing neural stem cells into tyrosine hydroxylase-positive neurons. *Neurobiol Dis* 17 (2):163-70.

Guo, Q., K. Li, N. A. Sunmonu, and J. Y. Li. (2010). Fgf8b-containing spliceforms, but not Fgf8a, are essential for Fgf8 function during development of the midbrain and cerebellum. *Dev Biol* 338 (2):183-92.

Hack, I., M. Bancila, K. Loulier, P. Carroll, and H. Cremer. (2002). Reelin is a detachment signal in tangential chain-migration during postnatal neurogenesis. *Nat Neurosci* 5 (10):939-45.

Hack, M. A., A. Saghatelyan, A. de Chevigny, A. Pfeifer, R. Ashery-Padan, P. M. Lledo, and M. Gotz. 2005. Neuronal fate determinants of adult olfactory bulb neurogenesis. *Nat Neurosci* 8 (7):865-72.

Hadari, Y. R., H. Kouhara, I. Lax, and J. Schlessinger. (1998). Binding of Shp2 tyrosine phosphatase to FRS2 is essential for fibroblast growth factor-induced PC12 cell differentiation. *Mol Cell Biol* 18 (7):3966-73.

Hajihosseini, M. K., S. De Langhe, E. Lana-Elola, H. Morrison, N. Sparshott, R. Kelly, J. Sharpe, D. Rice, and S. Bellusci. (2008). Localization and fate of Fgf10-expressing cells in the adult mouse brain implicate Fgf10 in control of neurogenesis. *Mol Cell Neurosci* 37 (4):857-68.

Hamilton, K. A., T. Heinbockel, M. Ennis, G. Szabo, F. Erdelyi, and A. Hayar. (2005). Properties of external plexiform layer interneurons in mouse olfactory bulb slices. *Neuroscience* 133 (3):819-29.

Hans, F., and S. Dimitrov. (2001). Histone H3 phosphorylation and cell division. *Oncogene* 20 (24):3021-7.

Harada, H., T. Toyono, K. Toyoshima, M. Yamasaki, N. Itoh, S. Kato, K. Sekine, and H. Ohuchi. (2002). FGF10 maintains stem cell compartment in developing mouse incisors. *Development* 129 (6):1533-41.

Harrison, S. J., M. Parrish, and A. P. Monaghan. (2008). Sall3 is required for the terminal maturation of olfactory glomerular interneurons. *J Comp Neurol* 507 (5):1780-94.

Hart, A., S. Papadopoulou, and H. Edlund. (2003). Fgf10 maintains notch activation, stimulates proliferation, and blocks differentiation of pancreatic epithelial cells. *Dev Dyn* 228 (2):185-93.

Hatakeyama, J., Y. Bessho, K. Katoh, S. Ookawara, M. Fujioka, F. Guillemot, and R. Kageyama. (2004). Hes genes regulate size, shape and histogenesis of the nervous system by control of the timing of neural stem cell differentiation. *Development* 131 (22):5539-50.

Hattori, Y., M. Yamasaki, M. Konishi, and N. Itoh. (1997). Spatially restricted expression of fibroblast growth factor-10 mRNA in the rat brain. *Brain Res Mol Brain Res* 47 (1-2):139-46.

Haub, O., B. Drucker, and M. Goldfarb. (1990). Expression of the murine fibroblast growth factor 5 gene in the adult central nervous system. *Proc Natl Acad Sci U S A* 87 (20):8022-6.

Hayamizu, T. F., P. T. Chan, and C. E. Johanson. (2001). FGF-2 immunoreactivity in adult rat ependyma and choroid plexus: responses to global forebrain ischemia and intraventricular FGF-2. *Neurol Res* 23 (4):353-8.

Hayashi, S., and A. P. McMahon. (2002). Efficient recombination in diverse tissues by a tamoxifen-inducible form of Cre: a tool for temporally regulated gene activation/inactivation in the mouse. *Dev Biol* 244 (2):305-18.

Higginbotham, H., T. Tanaka, B. C. Brinkman, and J. G. Gleeson. (2006). GSK3beta and PKCzeta function in centrosome localization and process stabilization during Slit-mediated neuronal repolarization. *Mol Cell Neurosci* 32 (1-2):118-32.

Horstman, E. (1954). Die Faserglia der Selachiergehirns. *Z. Zellforsch* 39:588-617.

Hsuchou, H., W. Pan, and A. J. Kastin. (2007). The fasting polypeptide FGF21 can enter brain from blood. *Peptides* 28 (12):2382-6.

Ifft, J. D. (1972). An autoradiographic study of the time of final division of neurons in rat hypothalamic nuclei. *J Comp Neurol* 144 (2):193-204.

Ihrie, R. A., J. K. Shah, C. C. Harwell, J. H. Levine, C. D. Guinto, M. Lezameta, A. R. Kriegstein, and A. Alvarez-Buylla. (2011). Persistent sonic hedgehog signaling in adult brain determines neural stem cell positional identity. *Neuron* 71 (2):250-62.

Imayoshi, I., T. Ohtsuka, D. Metzger, P. Chambon, and R. Kageyama. (2006). Temporal regulation of Cre recombinase activity in neural stem cells. *Genesis* 44 (5):233-8.

Imayoshi, I., M. Sakamoto, T. Ohtsuka, K. Takao, T. Miyakawa, M. Yamaguchi, K. Mori, T. Ikeda, S. Itohara, and R. Kageyama. (2008). Roles of continuous neurogenesis in the structural and functional integrity of the adult forebrain. *Nat Neurosci* 11 (10):1153-61.

Imayoshi, I., M. Sakamoto, M. Yamaguchi, K. Mori, and R. Kageyama. (2010). Essential roles of Notch signaling in maintenance of neural stem cells in developing and adult brains. *J Neurosci* 30 (9):3489-98.

Jacques, T. S., J. B. Relvas, S. Nishimura, R. Pytela, G. M. Edwards, C. H. Streuli, and C. ffrench-Constant. (1998). Neural precursor cell chain migration and division are regulated through different beta1 integrins. *Development* 125 (16):3167-77.

Johansson, C. B., S. Momma, D. L. Clarke, M. Risling, U. Lendahl, and J. Frisen. (1999). Identification of a neural stem cell in the adult mammalian central nervous system. *Cell* 96 (1):25-34.

Kageyama, R., T. Ohtsuka, J. Hatakeyama, and R. Ohsawa. (2005). Roles of bHLH genes in neural stem cell differentiation. *Exp Cell Res* 306 (2):343-8.

Kalra, S. P., and P. S. Kalra. (2003). Neuropeptide Y: a physiological orexigen modulated by the feedback action of ghrelin and leptin. *Endocrine* 22 (1):49-56.

Kanard, R. C., T. J. Fairbanks, S. P. De Langhe, F. G. Sala, P. M. Del Moral, C. A. Lopez, D. Warburton, K. D. Anderson, S. Bellusci, and R. C. Burns. (2005). Fibroblast growth factor-10 serves a regulatory role in duodenal development. *J Pediatr Surg* 40 (2):313-6.

Kanda, T., T. Iwasaki, S. Nakamura, T. Kurokawa, K. Ikeda, and H. Mizusawa. (2000). Self-secretion of fibroblast growth factor-9 supports basal forebrain cholinergic neurons in an autocrine/paracrine manner. *Brain Res* 876 (1-2):22-30.

Kaplan, M. S., and J. W. Hinds. (1977). Neurogenesis in the adult rat: electron microscopic analysis of light radioautographs. *Science* 197 (4308):1092-4.

Karpowicz, P., S. Willaime-Morawek, L. Balenci, B. DeVeale, T. Inoue, and D. van der Kooy. (2009). E-Cadherin regulates neural stem cell self-renewal. *J Neurosci* 29 (12):3885-96.

Kellendonk, C., F. Tronche, E. Casanova, K. Anlag, C. Opherk, and G. Schutz. (1999). Inducible site-specific recombination in the brain. *J Mol Biol* 285 (1):175-82.

Kellendonk, C., F. Tronche, A. P. Monaghan, P. O. Angrand, F. Stewart, and G. Schutz. (1996). Regulation of Cre recombinase activity by the synthetic steroid RU 486. *Nucleic Acids Res* 24 (8):1404-11.

Kelly, R. G., N. A. Brown, and M. E. Buckingham. (2001). The arterial pole of the mouse heart forms from Fgf10-expressing cells in pharyngeal mesoderm. *Dev Cell* 1 (3):435-40.

Kerever, A., J. Schnack, D. Vellinga, N. Ichikawa, C. Moon, E. Arikawa-Hirasawa, J. T. Efird, and F. Mercier. (2007). Novel extracellular matrix structures in the neural stem cell niche capture the neurogenic factor fibroblast growth factor 2 from the extracellular milieu. *Stem Cells* 25 (9):2146-57.

Kettenmann, H., and M. Schachner. (1985). Pharmacological properties of gamma-aminobutyric acid-, glutamate-, and aspartate-induced depolarizations in cultured astrocytes. *J Neurosci* 5 (12):3295-301.

Kiefer, P., P. Acland, D. Pappin, G. Peters, and C. Dickson. (1994). Competition between nuclear localization and secretory signals determines the subcellular fate of a single CUG-initiated form of FGF3. *EMBO J* 13 (17):4126-36.

Kiefer, P., and C. Dickson. (1995). Nucleolar association of fibroblast growth factor 3 via specific sequence motifs has inhibitory effects on cell growth. *Mol Cell Biol* 15 (8):4364-74.

Kimelberg, H. K. (1983). Primary astrocyte cultures--a key to astrocyte function. *Cell Mol Neurobiol* 3 (1):1-16.

Koizumi, H., H. Higginbotham, T. Poon, T. Tanaka, B. C. Brinkman, and J. G. Gleeson. (2006). Doublecortin maintains bipolar shape and nuclear translocation during migration in the adult forebrain. *Nat Neurosci* 9 (6):779-86.

Kokoeva, M. V., H. Yin, and J. S. Flier. (2005). Neurogenesis in the hypothalamus of adult mice: potential role in energy balance. *Science* 310 (5748):679-83.

Kokoeva, M. V., H. Yin, and J. S. Flier. (2007). Evidence for constitutive neural cell proliferation in the adult murine hypothalamus. *J Comp Neurol* 505 (2):209-20.

Kokovay, E., S. Goderie, Y. Wang, S. Lotz, G. Lin, Y. Sun, B. Roysam, Q. Shen, and S. Temple. (2010). Adult SVZ lineage cells home to and leave the vascular niche via differential responses to SDF1/CXCR4 signaling. *Cell Stem Cell* 7 (2):163-73.

Konishi, M., T. Asaki, N. Koike, H. Miwa, A. Miyake, and N. Itoh. (2006). Role of Fgf10 in cell proliferation in white adipose tissue. *Mol Cell Endocrinol* 249 (1-2):71-7.

Kornack, D. R., and P. Rakic. (2001). Cell proliferation without neurogenesis in adult primate neocortex. *Science* 294 (5549):2127-30.

Kosaka, N., M. Kodama, H. Sasaki, Y. Yamamoto, F. Takeshita, Y. Takahama, H. Sakamoto, T. Kato, M. Terada, and T. Ochiya. (2006). FGF-4 regulates neural progenitor cell proliferation and neuronal differentiation. *FASEB J* 20 (9):1484-5.

Kosman, J., N. Carmean, E. M. Leaf, K. Dyamenahalli, and J. A. Bassuk. (2007. Translocation of

fibroblast growth factor-10 and its receptor into nuclei of human urothelial cells. *J Cell Biochem* 102 (3):769-85.

Koutcherov, Y., J. K. Mai, K. W. Ashwell, and G. Paxinos. (2002. Organization of human hypothalamus in fetal development. *J Comp Neurol* 446 (4):301-24.

Kriegstein, A., and A. Alvarez-Buylla. (2009. The glial nature of embryonic and adult neural stem cells. *Annu Rev Neurosci* 32:149-84.

Langub, M. C., Jr., and R. E. Watson, Jr. (1992). Estrogen receptor-immunoreactive glia, endothelia, and ependyma in guinea pig preoptic area and median eminence: electron microscopy. *Endocrinology* 130 (1):364-72.

Lemaitre, H., V. S. Mattay, F. Sambataro, B. Verchinski, R. E. Straub, J. H. Callicott, R. Kittappa, T. M. Hyde, B. K. Lipska, J. E. Kleinman, R. McKay, and D. R. Weinberger. (2010). Genetic variation in FGF20 modulates hippocampal biology. *J Neurosci* 30 (17):5992-7.

Lerant, A., and M. E. Freeman. (1998). Ovarian steroids differentially regulate the expression of PRL-R in neuroendocrine dopaminergic neuron populations: a double label confocal microscopic study. *Brain Res* 802 (1-2):141-54.

Li, A. J., K. Ozawa, H. Tsuboyama, and T. Imamura. (1999). Distribution of fibroblast growth factor-5 in rat hypothalamus, and its possible role as a regulator of feeding behaviour. *Eur J Neurosci* 11 (4):1362-8.

Lie, D. C., S. A. Colamarino, H. J. Song, L. Desire, H. Mira, A. Consiglio, E. S. Lein, S. Jessberger, H. Lansford, A. R. Dearie, and F. H. Gage. (2005). Wnt signalling regulates adult hippocampal neurogenesis. *Nature* 437 (7063):1370-5.

Lim, D. A., and A. Alvarez-Buylla. (1999). Interaction between astrocytes and adult subventricular zone precursors stimulates neurogenesis. *Proc Natl Acad Sci U S A* 96 (13):7526-31.

Lin, Y., L. Chen, C. Lin, Y. Luo, R. Y. Tsai, and F. Wang. (2009). Neuron-derived FGF9 is essential for scaffold formation of Bergmann radial fibers and migration of granule neurons in the cerebellum. *Dev Biol* 329 (1):44-54.

Lindqvist, A., P. Mohapel, B. Bouter, H. Frielingsdorf, D. Pizzo, P. Brundin, and C. Erlanson-Albertsson. (2006). High-fat diet impairs hippocampal neurogenesis in male rats. *Eur J Neurol* 13 (12):1385-8.

Liu, A., J. Y. Li, C. Bromleigh, Z. Lao, L. A. Niswander, and A. L. Joyner. (2003). FGF17b and FGF18 have different midbrain regulatory properties from FGF8b or activated FGF receptors. *Development* 130 (25):6175-85.

Liu, H. K., T. Belz, D. Bock, A. Takacs, H. Wu, P. Lichter, M. Chai, and G. Schutz. (2008). The nuclear receptor tailless is required for neurogenesis in the adult subventricular zone. *Genes*

Dev 22 (18):2473-8.

Livet, J., T. A. Weissman, H. Kang, R. W. Draft, J. Lu, R. A. Bennis, J. R. Sanes, and J. W. Lichtman. (2007). Transgenic strategies for combinatorial expression of fluorescent proteins in the nervous system. *Nature* 450 (7166):56-62.

Lledo, P. M., M. Alonso, and M. S. Grubb. (2006). Adult neurogenesis and functional plasticity in neuronal circuits. *Nat Rev Neurosci* 7 (3):179-93.

Lledo, P. M., F. T. Merkle, and A. Alvarez-Buylla. (2008). Origin and function of olfactory bulb interneuron diversity. *Trends Neurosci* 31 (8):392-400.

Lois, C., and A. Alvarez-Buylla. (1994). Long-distance neuronal migration in the adult mammalian brain. *Science* 264 (5162):1145-8.

Lolait, S. J., A. T. Lim, D. Dahl, B. A. Khalid, B. H. Toh, and J. W. Funder. (1983). Neonatal rat hypothalamus cell culture: neuron subpopulations secrete immunoreactive beta-endorphin but not immunoreactive ACTH. *Neuroendocrinology* 37 (2):111-6.

Louis-Sylvestre, J., C. Larue-Achagiotis, and J. Le Magnen. (1980). Oral induction of the insulin hyper-responsiveness in rats with ventromedial hypothalamic lesions. *Horm Metab Res* 12 (12):671-6.

Lu, J., K. I. Izvolsky, J. Qian, and W. V. Cardoso. (2005). Identification of FGF10 targets in the embryonic lung epithelium during bud morphogenesis. *J Biol Chem* 280 (6):4834-41.

Lui, E. Y., S. L. Asa, D. J. Drucker, Y. C. Lee, and P. L. Brubaker. (1990). Glucagon and related peptides in fetal rat hypothalamus in vivo and in vitro. *Endocrinology* 126 (1):110-7.

Lum, M., A. Turbic, B. Mitrovic, and A. M. Turnley. (2009). Fibroblast growth factor-9 inhibits astrocyte differentiation of adult mouse neural progenitor cells. *J Neurosci Res* 87 (10):2201-10.

Luskin, M. B. (1993). Restricted proliferation and migration of postnatally generated neurons derived from the forebrain subventricular zone. *Neuron* 11 (1):173-89.

Luzzati, F., S. De Marchis, A. Fasolo, and P. Peretto. (2006). Neurogenesis in the caudate nucleus of the adult rabbit. *J Neurosci* 26 (2):609-21.

Ma, Y. J., D. F. Hill, M. P. Junier, M. E. Costa, S. E. Felder, and S. R. Ojeda. (1994). Expression of epidermal growth factor receptor changes in the hypothalamus during the onset of female puberty. *Mol Cell Neurosci* 5 (3):246-62.

Mahmood, R., I. J. Mason, and G. M. Morriss-Kay. (1996). Expression of Fgf-3 in relation to hindbrain segmentation, otic pit position and pharyngeal arch morphology in normal and retinoic acid-exposed mouse embryos. *Anat Embryol (Berl)* 194 (1):13-22.

Mailleux, A. A., R. Kelly, J. M. Veltmaat, S. P. De Langhe, S. Zaffran, J. P. Thiery, and S. Bellusci. (2005). Fgf10 expression identifies parabronchial smooth muscle cell progenitors and is required for their entry into the smooth muscle cell lineage. *Development* 132 (9):2157-66.

Mains, R. E., and P. H. Patterson. (1973). Primary cultures of dissociated sympathetic neurons. I. Establishment of long-term growth in culture and studies of differentiated properties. *J Cell Biol* 59 (2 Pt 1):329-45.

Mann, R., R. C. Mulligan, and D. Baltimore. (1983). Construction of a retrovirus packaging mutant and its use to produce helper-free defective retrovirus. *Cell* 33 (1):153-9.

Mao, X., Y. Fujiwara, A. Chapdelaine, H. Yang, and S. H. Orkin. (2001). Activation of EGFP expression by Cre-mediated excision in a new ROSA26 reporter mouse strain. *Blood* 97 (1):324-6.

Mao, X., Y. Fujiwara, and S. H. Orkin. (1999). Improved reporter strain for monitoring Cre recombinase-mediated DNA excisions in mice. *Proc Natl Acad Sci U S A* 96 (9):5037-42.

Marins, M., A. L. Xavier, N. B. Viana, F. S. Fortes, M. M. Froes, and J. R. Menezes. (2009). Gap junctions are involved in cell migration in the early postnatal subventricular zone. *Dev Neurobiol* 69 (11):715-30.

Mason, I. J., F. Fuller-Pace, R. Smith, and C. Dickson. (1994). FGF-7 (keratinocyte growth factor) expression during mouse development suggests roles in myogenesis, forebrain regionalisation and epithelial-mesenchymal interactions. *Mech Dev* 45 (1):15-30.

Meister, B. (2007). Neurotransmitters in key neurons of the hypothalamus that regulate feeding behavior and body weight. *Physiol Behav* 92 (1-2):263-71.

Menn, B., J. M. Garcia-Verdugo, C. Yaschine, O. Gonzalez-Perez, D. Rowitch, and A. Alvarez-Buylla. (2006). Origin of oligodendrocytes in the subventricular zone of the adult brain. *J Neurosci* 26 (30):7907-18.

Merkle, F. T., Z. Mirzadeh, and A. Alvarez-Buylla. (2007). Mosaic organization of neural stem cells in the adult brain. *Science* 317 (5836):381-4.

Merkle, F. T., A. D. Tramontin, J. M. Garcia-Verdugo, and A. Alvarez-Buylla. (2004). Radial glia give rise to adult neural stem cells in the subventricular zone. *Proc Natl Acad Sci U S A* 101 (50):17528-32.

Metzger, D., J. Clifford, H. Chiba, and P. Chambon. (1995). Conditional site-specific recombination in mammalian cells using a ligand-dependent chimeric Cre recombinase. *Proc Natl Acad Sci U S A* 92 (15):6991-5.

Mignone, J. L., V. Kukekov, A. S. Chiang, D. Steindler, and G. Enikolopov. (2004). Neural stem and progenitor cells in nestin-GFP transgenic mice. *J Comp Neurol* 469 (3):311-24.

Millington, G. W. (2007). The role of proopiomelanocortin (POMC) neurones in feeding behaviour. *Nutr Metab (Lond)* 4:18.

Milunsky, J. M., G. Zhao, T. A. Maher, R. Colby, and D. B. Everman. (2006). LADD syndrome is caused by FGF10 mutations. *Clin Genet* 69 (4):349-54.

Min, H., D. M. Danilenko, S. A. Scully, B. Bolon, B. D. Ring, J. E. Tarpley, M. DeRose, and W. S. Simonet. (1998). Fgf-10 is required for both limb and lung development and exhibits striking functional similarity to Drosophila branchless. *Genes Dev* 12 (20):3156-61.

Miralles, F., P. Czernichow, K. Ozaki, N. Itoh, and R. Scharfmann. (1999). Signaling through fibroblast growth factor receptor 2b plays a key role in the development of the exocrine pancreas. *Proc Natl Acad Sci U S A* 96 (11):6267-72.

Miralles, F., L. Lamotte, D. Couton, and R. L. Joshi. (2006). Interplay between FGF10 and Notch signalling is required for the self-renewal of pancreatic progenitors. *Int J Dev Biol* 50 (1):17-26.

Miyachi, K., M. J. Fritzler, and E. M. Tan. (1978). Autoantibody to a nuclear antigen in proliferating cells. *J Immunol* 121 (6):2228-34.

Miyake, A., M. Konishi, F. H. Martin, N. A. Hernday, K. Ozaki, S. Yamamoto, T. Mikami, T. Arakawa, and N. Itoh. (1998). Structure and expression of a novel member, FGF-16, on the fibroblast growth factor family. *Biochem Biophys Res Commun* 243 (1):148-52.

Miyamoto, M., K. Naruo, C. Seko, S. Matsumoto, T. Kondo, and T. Kurokawa. (1993). Molecular cloning of a novel cytokine cDNA encoding the ninth member of the fibroblast growth factor family, which has a unique secretion property. *Mol Cell Biol* 13 (7):4251-9.

Mizrahi, A. (2007). Dendritic development and plasticity of adult-born neurons in the mouse olfactory bulb. *Nat Neurosci* 10 (4):444-52.

Mohammadi, M., S. K. Olsen, and O. A. Ibrahimi. (2005). Structural basis for fibroblast growth factor receptor activation. *Cytokine Growth Factor Rev* 16 (2):107-37.

Mombaerts, P. (2006). Axonal wiring in the mouse olfactory system. *Annu Rev Cell Dev Biol* 22:713-37.

Morshead, C. M., B. A. Reynolds, C. G. Craig, M. W. McBurney, W. A. Staines, D. Morassutti, S. Weiss, and D. van der Kooy. (1994). Neural stem cells in the adult mammalian forebrain: a relatively quiescent subpopulation of subependymal cells. *Neuron* 13 (5):1071-82.

Mu, Y., S.W. Lee, and F. H. Gage. (2010). Signaling in adult neurogenesis. *Curr Opin Neurobiol* 20 (4):416-23.

Murase, S., and A. F. Horwitz. (2002). Deleted in colorectal carcinoma and differentially expressed integrins mediate the directional migration of neural precursors in the rostral

migratory stream. *J Neurosci* 22 (9):3568-79.

Nait-Oumesmar, B., N. Picard-Riera, C. Kerninon, L. Decker, D. Seilhean, G. U. Hoglinger, E. C. Hirsch, R. Reynolds, and A. Baron-Van Evercooren. (2007). Activation of the subventricular zone in multiple sclerosis: evidence for early glial progenitors. *Proc Natl Acad Sci U S A* 104 (11):4694-9.

Nam, S. C., Y. Kim, D. Dryanovski, A. Walker, G. Goings, K. Woolfrey, S. S. Kang, C. Chu, A. Chenn, F. Erdelyi, G. Szabo, P. Hockberger, and F. G. Szele. (2007). Dynamic features of postnatal subventricular zone cell motility: a two-photon time-lapse study. *J Comp Neurol* 505 (2):190-208.

Nguyen-Ba-Charvet, K. T., N. Picard-Riera, M. Tessier-Lavigne, A. Baron-Van Evercooren, C. Sotelo, and A. Chedotal. (2004). Multiple roles for slits in the control of cell migration in the rostral migratory stream. *J Neurosci* 24 (6):1497-506.

Norgaard, G. A., J. N. Jensen, and J. Jensen. (2003). FGF10 signaling maintains the pancreatic progenitor cell state revealing a novel role of Notch in organ development. *Dev Biol* 264 (2):323-38.

Nyeng, P., M. A. Bjerke, G. A. Norgaard, X. Qu, S. Kobberup, and J. Jensen. (2011). Fibroblast growth factor 10 represses premature cell differentiation during establishment of the intestinal progenitor niche. *Dev Biol* 349 (1):20-34.

Nyeng, P., G. A. Norgaard, S. Kobberup, and J. Jensen. (2007). FGF10 signaling controls stomach morphogenesis. *Dev Biol* 303 (1):295-310.

Nyeng, P., G. A. Norgaards, S. Kobberup and J. Jensen. (2008). FGF10 maintains distal lung bud epithelium and excessive signaling leads to progenitor state arrest, distalization, and goblet cell metaplasia. *BMC Dev Biol* 8:2.

Obermair, F. J., R. Fiorelli, A. Schroeter, S. Beyeler, C. Blatti, B. Zoerner, and M. Thallmair. (2010). A novel classification of quiescent and transit amplifying adult neural stem cells by surface and metabolic markers permits a defined simultaneous isolation. *Stem Cell Res* 5 (2):131-43.

O'Brien, R. J., and G. D. Fischbach. (1986). Excitatory synaptic transmission between interneurons and motoneurons in chick spinal cord cell cultures. *J Neurosci* 6 (11):3284-9.

Ohmachi, S., Y. Watanabe, T. Mikami, N. Kusu, T. Ibi, A. Akaike, and N. Itoh. (2000). FGF-20, a novel neurotrophic factor, preferentially expressed in the substantia nigra pars compacta of rat brain. *Biochem Biophys Res Commun* 277 (2):355-60.

Ohuchi, H., Y. Hori, M. Yamasaki, H. Harada, K. Sekine, S. Kato, and N. Itoh. (2000). FGF10 acts as a major ligand for FGF receptor 2 IIIb in mouse multi-organ development. *Biochem Biophys Res Commun* 277 (3):643-9.

Ohuchi, H., T. Nakagawa, A. Yamamoto, A. Araga, T. Ohata, Y. Ishimaru, H. Yoshioka, T.

Kuwana, T. Nohno, M. Yamasaki, N. Itoh, and S. Noji. (1997). The mesenchymal factor, FGF10, initiates and maintains the outgrowth of the chick limb bud through interaction with FGF8, an apical ectodermal factor. *Development* 124 (11):2235-44.

Olsen, S. K., M. Garbi, N. Zampieri, A. V. Eliseenkova, D. M. Ornitz, M. Goldfarb, and M. Mohammadi. (2003). Fibroblast growth factor (FGF) homologous factors share structural but not functional homology with FGFs. *J Biol Chem* 278 (36):34226-36.

Ong, S. H., Y. R. Hadari, N. Gotoh, G. R. Guy, J. Schlessinger, and I. Lax. (2001). Stimulation of phosphatidylinositol 3-kinase by fibroblast growth factor receptors is mediated by coordinated recruitment of multiple docking proteins. *Proc Natl Acad Sci U S A* 98 (11):6074-9.

Orban, P. C., D. Chui, and J. D. Marth. (1992). Tissue- and site-specific DNA recombination in transgenic mice. *Proc Natl Acad Sci U S A* 89 (15):6861-5.

Ornitz, D. M., and N. Itoh. (2001). Fibroblast growth factors. *Genome Biol* 2 (3):REVIEWS3005.

Ornitz, D. M., J. Xu, J. S. Colvin, D. G. McEwen, C. A. MacArthur, F. Coulier, G. Gao, and M. Goldfarb. (1996). Receptor specificity of the fibroblast growth factor family. *J Biol Chem* 271 (25):15292-7.

Ozawa, K., S. Suzuki, M. Asada, Y. Tomooka, A. J. Li, A. Yoneda, A. Komi, and T. Imamura. (1998). An alternatively spliced fibroblast growth factor (FGF)-5 mRNA is abundant in brain and translates into a partial agonist/antagonist for FGF-5 neurotrophic activity. *J Biol Chem* 273 (44):29262-71.

Palma, V., D. A. Lim, N. Dahmane, P. Sanchez, T. C. Brionne, C. D. Herzberg, Y. Gitton, A. Carleton, A. Alvarez-Buylla, and A. Ruiz i Altaba. (2005). Sonic hedgehog controls stem cell behavior in the postnatal and adult brain. *Development* 132 (2):335-44.

Panzanelli, P., J. M. Fritschy, Y. Yanagawa, K. Obata, and M. Sassoe-Pognetto. (2007). GABAergic phenotype of periglomerular cells in the rodent olfactory bulb. *J Comp Neurol* 502 (6):990-1002.

Park, J. H., H. Cho, H. Kim, and K. Kim. (2006). Repeated brief epileptic seizures by pentylenetetrazole cause neurodegeneration and promote neurogenesis in discrete brain regions of freely moving adult rats. *Neuroscience* 140 (2):673-84.

Park, W. Y., B. Miranda, D. Lebeche, G. Hashimoto, and W. V. Cardoso. (1998). FGF-10 is a chemotactic factor for distal epithelial buds during lung development. *Dev Biol* 201 (2):125-34.

Parras, C. M., R. Galli, O. Britz, S. Soares, C. Galichet, J. Battiste, J. E. Johnson, M. Nakafuku, A. Vescovi, and F. Guillemot. (2004). Mash1 specifies neurons and oligodendrocytes in the postnatal brain. *EMBO J* 23 (22):4495-505.

Parrish-Aungst, S., M. T. Shipley, F. Erdelyi, G. Szabo, and A. C. Puche. (2007). Quantitative analysis of neuronal diversity in the mouse olfactory bulb. *J Comp Neurol* 501 (6):825-36.

Paterson, J. A., A. Privat, E. A. Ling, and C. P. Leblond. (1973). Investigation of glial cells in semithin sections. 3. Transformation of subependymal cells into glial cells, as shown by radioautography after 3 H-thymidine injection into the lateral ventricle of the brain of young rats. *J Comp Neurol* 149 (1):83-102.

Pencea, V., K. D. Bingaman, S. J. Wiegand, and M. B. Luskin. (2001). Infusion of brain-derived neurotrophic factor into the lateral ventricle of the adult rat leads to new neurons in the parenchyma of the striatum, septum, thalamus, and hypothalamus. *J Neurosci* 21 (17):6706-17.

Peretto, P., C. Dati, S. De Marchis, H. H. Kim, M. Ukhanova, A. Fasolo, and F. L. Margolis. (2004). Expression of the secreted factors noggin and bone morphogenetic proteins in the subependymal layer and olfactory bulb of the adult mouse brain. *Neuroscience* 128 (4):685-96.

Perez-Martin, M., M. Cifuentes, J. M. Grondona, M. D. Lopez-Avalos, U. Gomez-Pinedo, J. M. Garcia-Verdugo, and P. Fernandez-Llebrez. (2010). IGF-I stimulates neurogenesis in the hypothalamus of adult rats. *Eur J Neurosci* 31 (9):1533-48.

Petreanu, L., and A. Alvarez-Buylla. (2002). Maturation and death of adult-born olfactory bulb granule neurons: role of olfaction. *J Neurosci* 22 (14):6106-13.

Piccin, D., and C. M. Morshead. (2010). Wnt Signaling Regulates Symmetry of Division of Neural Stem Cells in the Adult Brain and in Response to Injury. *Stem Cells*.

Pierce, A. A., and A. W. Xu. (2010). De novo neurogenesis in adult hypothalamus as a compensatory mechanism to regulate energy balance. *J Neurosci* 30 (2):723-30.

Qu, Q., G. Sun, W. Li, S. Yang, P. Ye, C. Zhao, R. T. Yu, F. H. Gage, R. M. Evans, and Y. Shi. (2010). Orphan nuclear receptor TLX activates Wnt/beta-catenin signalling to stimulate neural stem cell proliferation and self-renewal. *Nat Cell Biol* 12 (1):31-40; sup pp 1-9.

Ramasamy, S. K., A. A. Mailleux, V. V. Gupte, F. Mata, F. G. Sala, J. M. Veltmaat, P. M. Del Moral, S. De Langhe, S. Parsa, L. K. Kelly, R. Kelly, W. Shia, E. Keshet, P. Minoo, D. Warburton, and S. Bellusci. (2007). Fgf10 dosage is critical for the amplification of epithelial cell progenitors and for the formation of multiple mesenchymal lineages during lung development. *Dev Biol* 307 (2):237-47.

Raponi, E., F. Agenes, C. Delphin, N. Assard, J. Baudier, C. Legraverend, and J. C. Deloulme. (2007). S100B expression defines a state in which GFAP-expressing cells lose their neural stem cell potential and acquire a more mature developmental stage. *Glia* 55 (2):165-77.

Reimers, K., M. Antoine, M. Zapatka, V. Blecken, C. Dickson, and P. Kiefer. (2001). NoBP, a nuclear fibroblast growth factor 3 binding protein, is cell cycle regulated and promotes cell growth. *Mol Cell Biol* 21 (15):4996-5007.

Reuss, B., R. Dono, and K. Unsicker. (2003). Functions of fibroblast growth factor (FGF)-2 and

FGF-5 in astroglial differentiation and blood-brain barrier permeability: evidence from mouse mutants. *J Neurosci* 23 (16):6404-12.

Reynolds, B. A., and S. Weiss. (1992). Generation of neurons and astrocytes from isolated cells of the adult mammalian central nervous system. *Science* 255 (5052):1707-10.

Richards, L. J., T. J. Kilpatrick, and P. F. Bartlett. (1992). De novo generation of neuronal cells from the adult mouse brain. *Proc Natl Acad Sci U S A* 89 (18):8591-5.

Rochefort, C., G. Gheusi, J. D. Vincent, and P. M. Lledo. (2002). Enriched odor exposure increases the number of newborn neurons in the adult olfactory bulb and improves odor memory. *J Neurosci* 22 (7):2679-89.

Rodriguez, E. M., J. L. Blazquez, F. E. Pastor, B. Pelaez, P. Pena, B. Peruzzo, and P. Amat. (2005). Hypothalamic tanycytes: a key component of brain-endocrine interaction. *Int Rev Cytol* 247:89-164.

Rutzel, H., and T. H. Schiebler. (1980). Prenatal and early postnatal development of the glial cells in the median eminence of the rat. *Cell Tissue Res* 211 (1):117-37.

Sahara, S., and D. D. O'Leary. (2009). Fgf10 regulates transition period of cortical stem cell differentiation to radial glia controlling generation of neurons and basal progenitors. *Neuron* 63 (1):48-62.

Sakamoto, M., I. Imayoshi, T. Ohtsuka, M. Yamaguchi, K. Mori, and R. Kageyama. (2011). Continuous neurogenesis in the adult forebrain is required for innate olfactory responses. *Proc Natl Acad Sci U S A* 108 (20):8479-84.

Sakaue, H., M. Konishi, W. Ogawa, T. Asaki, T. Mori, M. Yamasaki, M. Takata, H. Ueno, S. Kato, M. Kasuga, and N. Itoh. (2002). Requirement of fibroblast growth factor 10 in development of white adipose tissue. *Genes Dev* 16 (8):908-12.

Sarruf, D. A., J. P. Thaler, G. J. Morton, J. German, J. D. Fischer, K. Ogimoto, and M. W. Schwartz. (2010). Fibroblast growth factor 21 action in the brain increases energy expenditure and insulin sensitivity in obese rats. *Diabetes* 59 (7):1817-24.

Sauer, B., and N. Henderson. (1988). Site-specific DNA recombination in mammalian cells by the Cre recombinase of bacteriophage P1. *Proc Natl Acad Sci U S A* 85 (14):5166-70.

Scheckenbach, K., V. Balz, M. Wagenmann, and T. K. Hoffmann. (2008). An intronic alteration of the fibroblast growth factor 10 gene causing ALSG-(aplasia of lacrimal and salivary glands) syndrome. *BMC Med Genet* 9:114.

Schmechel, D. E., and P. Rakic. (1979). A Golgi study of radial glial cells in developing monkey telencephalon: morphogenesis and transformation into astrocytes. *Anat Embryol (Berl)* 156 (2):115-52.

Seaberg, R. M., and D. van der Kooy. (2002). Adult rodent neurogenic regions: the ventricular subependyma contains neural stem cells, but the dentate gyrus contains restricted progenitors. *J Neurosci* 22 (5):1784-93.

Sekine, K., H. Ohuchi, M. Fujiwara, M. Yamasaki, T. Yoshizawa, T. Sato, N. Yagishita, D. Matsui, Y. Koga, N. Itoh, and S. Kato. (1999). Fgf10 is essential for limb and lung formation. *Nat Genet* 21 (1):138-41.

Seri, B., J. M. Garcia-Verdugo, L. Collado-Morente, B. S. McEwen, and A. Alvarez-Buylla. (2004). Cell types, lineage, and architecture of the germinal zone in the adult dentate gyrus. *J Comp Neurol* 478 (4):359-78.

Shamim, H., R. Mahmood, C. Logan, P. Doherty, A. Lumsden, and I. Mason. (1999). Sequential roles for Fgf4, En1 and Fgf8 in specification and regionalisation of the midbrain. *Development* 126 (5):945-59.

Shams, I., E. Rohmann, V. P. Eswarakumar, E. D. Lew, S. Yuzawa, B. Wollnik, J. Schlessinger, and I. Lax. (2007). Lacrimo-auriculo-dento-digital syndrome is caused by reduced activity of the fibroblast growth factor 10 (FGF10)-FGF receptor 2 signaling pathway. *Mol Cell Biol* 27 (19):6903-12.

Shen, Q., Y. Wang, E. Kokovay, G. Lin, S. M. Chuang, S. K. Goderie, B. Roysam, and S. Temple. (2008). Adult SVZ stem cells lie in a vascular niche: a quantitative analysis of niche cell-cell interactions. *Cell Stem Cell* 3 (3):289-300.

Shepherd, G. M., W. R. Chen, D. Willhite, M. Migliore, and C. A. Greer. (2007). The olfactory granule cell: from classical enigma to central role in olfactory processing. *Brain Res Rev* 55 (2):373-82.

Shi, Y., D. Chichung Lie, P. Taupin, K. Nakashima, J. Ray, R. T. Yu, F. H. Gage, and R. M. Evans. (2004). Expression and function of orphan nuclear receptor TLX in adult neural stem cells. *Nature* 427 (6969):78-83.

Shimada, M., and T. Nakamura. (1973). Time of neuron origin in mouse hypothalamic nuclei. *Exp Neurol* 41 (1):163-73.

Shipley, M. T., and G. D. Adamek. (1984). The connections of the mouse olfactory bulb: a study using orthograde and retrograde transport of wheat germ agglutinin conjugated to horseradish peroxidase. *Brain Res Bull* 12 (6):669-88.

Singec, I., R. Knoth, R. P. Meyer, J. Maciaczyk, B. Volk, G. Nikkhah, M. Frotscher, and E. Y. Snyder. (2006). Defining the actual sensitivity and specificity of the neurosphere assay in stem cell biology. *Nat Methods* 3 (10):801-6.

Singec, I., and A. Quinones-Hinojosa. (2008). Neurospheres. In *Adult Neurogenesis*, edited by G. Kemperman and H. Song: Cold Sping Harbor Laboratory.

Sleeman, M., J. Fraser, M. McDonald, S. Yuan, D. White, P. Grandison, K. Kumble, J. D. Watson, and J. G. Murison. (2001). Identification of a new fibroblast growth factor receptor, FGFR5. *Gene* 271 (2):171-82.

Snapyan, M., M. Lemasson, M. S. Brill, M. Blais, M. Massouh, J. Ninkovic, C. Gravel, F. Berthod, M. Gotz, P. A. Barker, A. Parent, and A. Saghatelyan. (2009). Vasculature guides migrating neuronal precursors in the adult mammalian forebrain via brain-derived neurotrophic factor signaling. *J Neurosci* 29 (13):4172-88.

Solberg, N., O. Machon, and S. Krauss. (2008). Effect of canonical Wnt inhibition in the neurogenic cortex, hippocampus, and premigratory dentate gyrus progenitor pool. *Dev Dyn* 237 (7):1799-811.

Soriano, P. (1999). Generalized lacZ expression with the ROSA26 Cre reporter strain. *Nat Genet* 21 (1):70-1.

Sottile, V., M. Li, and P. J. Scotting. (2006). Stem cell marker expression in the Bergmann glia population of the adult mouse brain. *Brain Res* 1099 (1):8-17.

Spencer-Dene, B., F. G. Sala, S. Bellusci, S. Gschmeissner, G. Stamp, and C. Dickson. (2006). Stomach development is dependent on fibroblast growth factor 10/fibroblast growth factor receptor 2b-mediated signaling. *Gastroenterology* 130 (4):1233-44.

Srinivas, S., T. Watanabe, C. S. Lin, C. M. William, Y. Tanabe, T. M. Jessell, and F. Costantini. (2001). Cre reporter strains produced by targeted insertion of EYFP and ECFP into the ROSA26 locus. *BMC Dev Biol* 1:4.

Stangl, D., and S. Thuret. (2009). Impact of diet on adult hippocampal neurogenesis. *Genes Nutr* 4 (4):271-82.

Sun, G., R. T. Yu, R. M. Evans, and Y. Shi. (2007). Orphan nuclear receptor TLX recruits histone deacetylases to repress transcription and regulate neural stem cell proliferation. *Proc Natl Acad Sci U S A* 104 (39):15282-7.

Sun, W., A. Winseck, S. Vinsant, O. H. Park, H. Kim, and R. W. Oppenheim. (2004). Programmed cell death of adult-generated hippocampal neurons is mediated by the proapoptotic gene Bax. *J Neurosci* 24 (49):11205-13.

Swanson, R. A., J. Liu, J. W. Miller, J. D. Rothstein, K. Farrell, B. A. Stein, and M. C. Longuemare. (1997). Neuronal regulation of glutamate transporter subtype expression in astrocytes. *J Neurosci* 17 (3):932-40.

Tagashira, S., H. Harada, T. Katsumata, N. Itoh, and M. Nakatsuka. (1997). Cloning of mouse FGF10 and up-regulation of its gene expression during wound healing. *Gene* 197 (1-2):399-404.

Tashiro, A., V. M. Sandler, N. Toni, C. Zhao, and F. H. Gage. (2006). NMDA-receptor-mediated, cell-specific integration of new neurons in adult dentate gyrus. *Nature* 442 (7105):929-33.

Terauchi, A., E. M. Johnson-Venkatesh, A. B. Toth, D. Javed, M. A. Sutton, and H. Umemori. (2010). Distinct FGFs promote differentiation of excitatory and inhibitory synapses. *Nature* 465 (7299):783-7.

Theil, T., E. Dominguez-Frutos, and T. Schimmang. (2008). Differential requirements for Fgf3 and Fgf8 during mouse forebrain development. *Dev Dyn* 237 (11):3417-23.

Thomas, K. A., M. Rios-Candelore, and S. Fitzpatrick. (1984). Purification and characterization of acidic fibroblast growth factor from bovine brain. *Proc Natl Acad Sci U S A* 81 (2):357-61.

Tomasiewicz, H., K. Ono, D. Yee, C. Thompson, C. Goridis, U. Rutishauser, and T. Magnuson. (1993). Genetic deletion of a neural cell adhesion molecule variant (N-CAM-180) produces distinct defects in the central nervous system. *Neuron* 11 (6):1163-74.

Tramontin, A. D., J. M. Garcia-Verdugo, D. A. Lim, and A. Alvarez-Buylla. (2003). Postnatal development of radial glia and the ventricular zone (VZ): a continuum of the neural stem cell compartment. *Cereb Cortex* 13 (6):580-7.

Umemori, H., M. W. Linhoff, D. M. Ornitz, and J. R. Sanes. (2004). FGF22 and its close relatives are presynaptic organizing molecules in the mammalian brain. *Cell* 118 (2):257-70.

Veeraraghavalu, K., S. H. Choi, X. Zhang, and S. S. Sisodia. (2010). Presenilin 1 mutants impair the self-renewal and differentiation of adult murine subventricular zone-neuronal progenitors via cell-autonomous mechanisms involving notch signaling. *J Neurosci* 30 (20):6903-15.

Vescovi, A. L., B. A. Reynolds, D. D. Fraser, and S. Weiss. (1993). bFGF regulates the proliferative fate of unipotent (neuronal) and bipotent (neuronal/astroglial) EGF-generated CNS progenitor cells. *Neuron* 11 (5):951-66.

Waclaw, R. R., Z. J. Allen, 2nd, S. M. Bell, F. Erdelyi, G. Szabo, S. S. Potter, and K. Campbell. (2006). The zinc finger transcription factor Sp8 regulates the generation and diversity of olfactory bulb interneurons. *Neuron* 49 (4):503-16.

Walicke, P., W. M. Cowan, N. Ueno, A. Baird, and R. Guillemin. (1986). Fibroblast growth factor promotes survival of dissociated hippocampal neurons and enhances neurite extension. *Proc Natl Acad Sci U S A* 83 (9):3012-6.

Wang, Q., M. E. Bardgett, M. Wong, D. F. Wozniak, J. Lou, B. D. McNeil, C. Chen, A. Nardi, D. C. Reid, K. Yamada, and D. M. Ornitz. (2002). Ataxia and paroxysmal dyskinesia in mice lacking axonally transported FGF14. *Neuron* 35 (1):25-38.

Weaver, M., N. R. Dunn, and B. L. Hogan. (2000). Bmp4 and Fgf10 play opposing roles during lung bud morphogenesis. *Development* 127 (12):2695-704.

Weiss, S., C. Dunne, J. Hewson, C. Wohl, M. Wheatley, A. C. Peterson, and B. A. Reynolds. (1996). Multipotent CNS stem cells are present in the adult mammalian spinal cord and

ventricular neuroaxis. *J Neurosci* 16 (23):7599-609.

Weiss, S., J. P. Pin, M. Sebben, D. E. Kemp, F. Sladeczek, J. Gabrion, and J. Bockaert. (1986). Synaptogenesis of cultured striatal neurons in serum-free medium: a morphological and biochemical study. *Proc Natl Acad Sci U S A* 83 (7):2238-42.

Wexler, E. M., A. Paucer, H. I. Kornblum, T. D. Palmer, and D. H. Geschwind. (2009). Endogenous Wnt signaling maintains neural progenitor cell potency. *Stem Cells* 27 (5):1130-41.

Whitman, M. C., W. Fan, L. Rela, D. J. Rodriguez-Gil, and C. A. Greer. (2009). Blood vessels form a migratory scaffold in the rostral migratory stream. *J Comp Neurol* 516 (2):94-104.

Winner, B., C. M. Cooper-Kuhn, R. Aigner, J. Winkler, and H. G. Kuhn. (2002). Long-term survival and cell death of newly generated neurons in the adult rat olfactory bulb. *Eur J Neurosci* 16 (9):1681-9.

Wu, W., K. Wong, J. Chen, Z. Jiang, S. Dupuis, J. Y. Wu, and Y. Rao. (1999). Directional guidance of neuronal migration in the olfactory system by the protein Slit. *Nature* 400 (6742):331-6.

Xu, J., Z. Liu, and D. M. Ornitz. (2000). Temporal and spatial gradients of Fgf8 and Fgf17 regulate proliferation and differentiation of midline cerebellar structures. *Development* 127 (9):1833-43.

Xu, Q., M. Tam, and S. A. Anderson. (2008). Fate mapping Nkx2.1-lineage cells in the mouse telencephalon. *J Comp Neurol* 506 (1):16-29.

Xu, Y., N. Tamamaki, T. Noda, K. Kimura, Y. Itokazu, N. Matsumoto, M. Dezawa, and C. Ide. (2005). Neurogenesis in the ependymal layer of the adult rat 3rd ventricle. *Exp Neurol* 192 (2):251-64.

Yadirgi, G., V. Leinster, S. Acquati, H. Bhagat, O. Shakhova, and S. Marino. (2011). Conditional activation of Bmi1 expression regulates self-renewal, apoptosis, and differentiation of neural stem/progenitor cells in vitro and in vivo. *Stem Cells* 29 (4):700-12.

Yamasaki, M., H. Emoto, M. Konishi, T. Mikami, H. Ohuchi, K. Nakao, and N. Itoh. (1999). FGF-10 is a growth factor for preadipocytes in white adipose tissue. *Biochem Biophys Res Commun* 258 (1):109-12.

Yamasaki, M., A. Miyake, S. Tagashira, and N. Itoh. (1996). Structure and expression of the rat mRNA encoding a novel member of the fibroblast growth factor family. *J Biol Chem* 271 (27):15918-21.

Yamashita, N., N. Nishiyama, K. Abe, H. Saito, and J. Fukuda. (1992). Primary culture of postnatal rat hypothalamic neurons in astrocyte-conditioned medium. *Brain Res* 594 (2):215-20.

Yamashita, T., M. Yoshioka, and N. Itoh. (2000). Identification of a novel fibroblast growth factor, FGF-23, preferentially expressed in the ventrolateral thalamic nucleus of the brain. *Biochem Biophys Res Commun* 277 (2):494-8.

Yamauchi, T., K. Tatsumi, M. Makinodan, S. Kimoto, M. Toritsuka, H. Okuda, T. Kishimoto, and A. Wanaka. (2010). Olanzapine increases cell mitotic activity and oligodendrocyte-lineage cells in the hypothalamus. *Neurochem Int* 57 (5):565-71.

Yang, Z. (2008). Postnatal subventricular zone progenitors give rise not only to granular and periglomerular interneurons but also to interneurons in the external plexiform layer of the rat olfactory bulb. *J Comp Neurol* 506 (2):347-58.

Yavin, E., and J. H. Menkes. (1973). The culture of dissociated cells from rat cerebral cortex. *J Cell Biol* 57 (1):232-7.

Young, K. M., M. Fogarty, N. Kessaris, and W. D. Richardson. (2007). Subventricular zone stem cells are heterogeneous with respect to their embryonic origins and neurogenic fates in the adult olfactory bulb. *J Neurosci* 27 (31):8286-96.

Zambrowicz, B. P., A. Imamoto, S. Fiering, L. A. Herzenberg, W. G. Kerr, and P. Soriano. (1997). Disruption of overlapping transcripts in the ROSA beta geo 26 gene trap strain leads to widespread expression of beta-galactosidase in mouse embryos and hematopoietic cells. *Proc Natl Acad Sci U S A* 94 (8):3789-94.

Zhang, C. L., Y. Zou, W. He, F. H. Gage, and R. M. Evans. (2008). A role for adult TLX-positive neural stem cells in learning and behaviour. *Nature* 451 (7181):1004-7.

Zhang, J., F. Giesert, K. Kloos, D. M. Vogt Weisenhorn, L. Aigner, W. Wurst, and S. Couillard-Despres. (2010). A powerful transgenic tool for fate mapping and functional analysis of newly generated neurons. *BMC Neurosci* 11:158.

Zhang, X., O. A. Ibrahimi, S. K. Olsen, H. Umemori, M. Mohammadi, and D. M. Ornitz. (2006). Receptor specificity of the fibroblast growth factor family. The complete mammalian FGF family. *J Biol Chem* 281 (23):15694-700.

Zhao, C., G. Sun, S. Li, M. F. Lang, S. Yang, W. Li, and Y. Shi. (2010). MicroRNA let-7b regulates neural stem cell proliferation and differentiation by targeting nuclear receptor TLX signaling. *Proc Natl Acad Sci U S A* 107 (5):1876-81.

Zhao, C., G. Sun, S. Li, and Y. Shi. (2009). A feedback regulatory loop involving microRNA-9 and nuclear receptor TLX in neural stem cell fate determination. *Nat Struct Mol Biol* 16 (4):365-71.

Zhao, M., S. Momma, K. Delfani, M. Carlen, R. M. Cassidy, C. B. Johansson, H. Brismar, O. Shupliakov, J. Frisen, and A. M. Janson. (2003). Evidence for neurogenesis in the adult mammalian substantia nigra. *Proc Natl Acad Sci U S A* 100 (13):7925-30.